Department of Natural Resources
Resource Assessment Service
MARYLAND GEOLOGICAL SURVEY
Richard A. Ortt, Jr., Director

REPORT OF INVESTIGATIONS 86

GEOLOGY AND KARST DEVELOPMENT OF THE HAGERSTOWN VALLEY (GREAT VALLEY) OF MARYLAND

by

David K. Brezinski

Report of research conducted in cooperation with
the Maryland State Highway Administration

DNR Publication No. 12-053118-73

2018

EXECUTIVE SUMMARY

- This report summarizes findings of a multi-year study, conducted by the Maryland Geological Survey and sponsored by the Maryland State Highway Administration Office of Materials Technology, on the relationship between geology and sinkhole development in the Hagerstown Valley.

- Approximately 3,800 karst features were identified and located using a Global Positioning System (GPS).

- Active sinkholes make up 20% of the total number of features, while depressions and springs comprise 66% and 9%, respectively.

- There is an identifiable relationship between the types of karst features and the bedrock units in which they occur; this relationship allowed development of a karst susceptibility index (KSI) for rocks of the Hagerstown Valley.

- High KSI rock units include the Stonehenge Limestone, St. Paul Group, Rockdale Run Formation, and the Chambersburg Formation. The Tomstown, Waynesboro, and Elbrook formations, and Pinesburg Station Dolomite had low KSI numbers.

- The impact humans have on karst development are substantially less than that observed in the Frederick Valley of Maryland.

- With this understanding of the relationship between geologic variables and karst development, an *a priori* knowledge about areas that pose a high risk for sinkhole potential can be utilized as a foundation on which any future site-specific study can be built.

TABLE OF CONTENTS

Page

LIST OF ILLUSTRATIONS

ABSTRACT

The Hagerstown Valley is Maryland's part of the Great Valley section of the Ridge and Valley Physiographic Province. The valley is a highly folded, fault-bounded synclinorium, bordered on the east by the Blue Ridge Physiographic Province and on the west by the folded mountains section of the Ridge and Valley Province. The valley bedrock consists of primarily carbonate rocks of Cambrian and Ordovician age and Ordovician clastics. Detailed study of these rocks has allowed recognition of 3,801 karst features that are distributed unequally among the bedrock formations. This uneven distribution has led to the interpretation that geologic and topographic factors substantially control their distribution and frequency.

Folds, faults, and joints are shown to play locally important roles in the number, type, and density of active sinkholes, depressions, and springs. Thick Quaternary deposits along the eastern and western borders of the valley tend to stifle active sinkhole and spring development, and promote depression or doline formation.

Topography is recognized as an important factor in karst feature distribution. Areas where substantial topographic changes exist tend to display large numbers and high density of active sinkholes, depressions, and caves. This is interpreted as being related to a strong hydrologic gradient between the land surface and the local water table level.

The karst features and their distribution relative to bedrock units allow recognition of a relative scale of karst development known as a Karst Susceptibility Index (KSI). This numeric characterization of karst susceptibility can be utilized by land-use planners, developers, and the public as a first approximation of the susceptibility for an area, and can be interpreted as a baseline from which site-specific studies can be initiated. The KSI indicates that the Stonehenge Limestone and Rockdale Run Formation and the St. Paul Group have very high karst susceptibility (KSI), with a rating of more than 0.30. Slightly lesser karst susceptibilities are recognized for the Conococheague Formation (KSI 0.25) and Chambersburg Formation (KSI 0.28). The Tomstown, Waynesboro, and Elbrook formations and the Pinesburg Station Dolomite have relatively low KSI's of 0.11, 0.05, 0.13, and 0.16, respectively.

Human factors also can be shown to play locally important roles in the creation of active sinkholes. Storm water retention ponds, unlined drainage, and depressed water tables associated with quarry dewatering can promote soil-cover collapse sinkholes.

INTRODUCTION

In April 1994, a Maryland motorist was killed when he drove his vehicle into a sinkhole that had opened in Maryland State Route 31 near Westminster, Maryland. Two years later another motorist was injured when he drove into a collapsed sinkhole that had catastrophically formed in South Street, within the boundaries of Frederick City, Frederick County, Maryland. These two events brought to the attention of State officials that there was a need for determining and delineating Maryland's sinkhole-prone regions, and that it was necessary to demarcate areas that were most susceptible to catastrophic sinkhole collapses. This precipitated a cooperative study between the Maryland State Highway Administration and the Maryland Geological Survey to examine sinkhole development in the State's second largest karst terrain, the Frederick Valley (Figure 1). That study, completed in 2004, is summarized in Maryland Geological Survey Report of Investigations 75 (Brezinski, 2004a). This report follows the ensuing karst research and summarizes findings of a decade-long investigation of Maryland's largest contiguous karst region, the Great Valley, locally termed the Hagerstown Valley.

Areas underlain by carbonate rocks such as limestone, marble, and dolomite are prone to dissolution by groundwater. Such solution of bedrock produces distinctive topographic features that characterize what is known as *karst terrain*. While karst terrains are present to some degree in all areas underlain by carbonate rocks, they develop to varying extents based on changes in the chemical makeup and geologic structure of the bedrock. Thus, there is no *typical karst* terrain. It is therefore impossible to *a priori* characterize or predict the distribution, type, abundance, or size of karst features in any particular terrain without first assembling data and evaluating the arrangement of the features with respect to the distribution of mapped bedrock units, their intrinsic geologic structure, and proximity to major hydrologic features such as streams or rivers.

The Frederick Valley study (Brezinski, 2004a) demonstrated that modern geologic and karst mapping techniques and data analysis allow characterization of rocks within a region by utilizing a *Karst Susceptibility Index* (KSI). The KSI gives engineers, developers, planners, and homeowners a first approximation of how susceptible individual rock units are to sinkhole development. Unfortunately, the KSI values for the Frederick Valley units are only applicable to those units, inasmuch as differing compositions elsewhere would produce different KSI values. In order to develop a KSI for other karst areas of the State, it is necessary to undertake a similar comprehensive mapping program of both the rock units and the karst features developed within those units.

The findings of the Frederick Valley study demonstrated that differing compositions of limestone layers produce different karst susceptibilities. Additionally, and when area data obtained from detailed GIS-based geologic maps are merged with karst feature data, the empirical KSI can give an initial picture of the sinkhole potential for a region.

The methods utilized in the Frederick Valley study also were employed during the current study of the Hagerstown Valley. Field work for the current investigation was divided into two phases. Phase I, completed in 2009, covered the eastern half of the valley and encompassed the Keedysville, Funkstown, Shepherdstown, Myersville, and Smithsburg 7.5´quadrangles (Figure 2). The second phase dealt with the remaining quadrangles in the Hagerstown Valley-Hagerstown, Mason-Dixon, Williamsport, Clear Spring and Hedgesville. This report will discuss the findings of both phases of the investigation.

Setting

The Hagerstown Valley, also known as the Great Valley (Cumberland or Lehigh Valley in Pennsylvania and Shenandoah Valley in Virginia), is a continuous geologic structure that stretches from New Jersey to Georgia (Figure 1). This nearly 800-mile long valley is underlain by easily erodible shale and dissolvable carbonate rocks (limestone and dolomite). These rocks were formed in shallow marine waters on an ancient carbonate platform, similar to today's Bahama Banks. During the Cambrian and Ordovician Periods (540 to 450 million years ago=Mya), these rocks were deposited near the southern edge of the ancient Laurentian paleocontinent. Mountain-building episodes during the late Paleozoic (350-250 Mya) configured these rock layers into tight folds that have been partially eroded into the landforms seen today. The Great Valley is the eastern section of the Ridge and Valley Physiographic Province in Maryland (Reger and Cleaves, 2008). It represents a broad down warp or fold in the Earth's crust known as the Massanutten Synclinorium. It is bordered on the east and in fault contact with, a large up-fold known as the South Mountain Anticlinorium (Cloos, 1947, 1971; Brezinski, 1992) (Figure 3). The South Mountain Anticlinorium comprises the northern part of the Blue Ridge Physiographic Province. To the west,

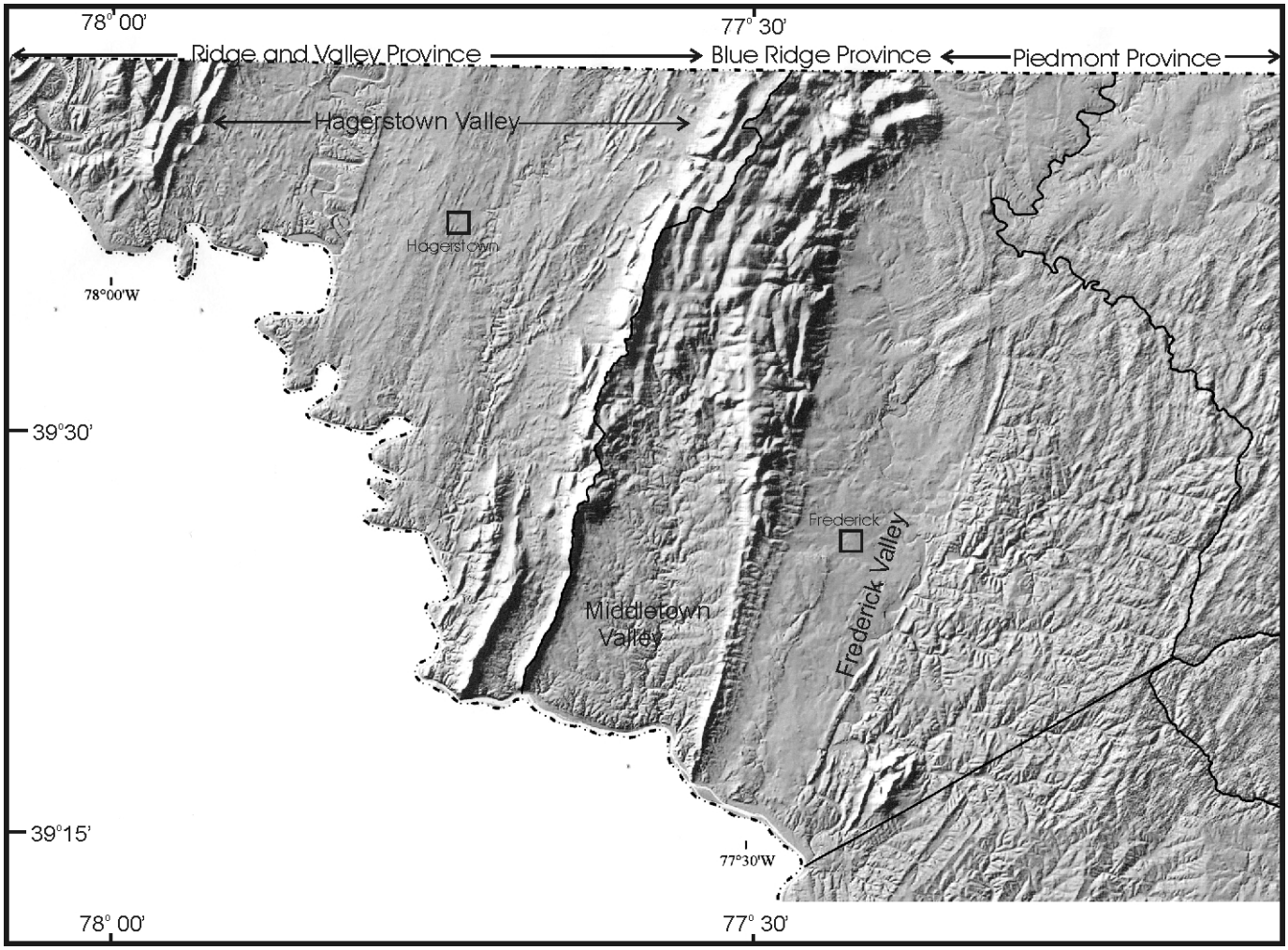

Figure 1.– Shaded relief map of eastern Washington County and Frederick County Maryland, illustrating the location of the Hagerstown Valley with respect to the eastern Ridge and Valley, Blue Ridge, and western Piedmont Physiographic Provinces.

the Great Valley is in fault contact with the folded Appalachian mountain section of the Ridge and Valley Physiographic Province (Reger and Cleaves, 2008).

History of Investigation

Keith (1893, 1894) presented the first description of the rocks of the western Blue Ridge and eastern Great Valley. Much of his work was summarized and repeated by Bassler (1919). The stratigraphy of the Upper Cambrian through Lower Ordovician carbonate rocks of the Hagerstown Valley was thoroughly discussed and summarized by Sando (1956, 1957, 1958). Demicco and Mitchell (1982), Demicco (1985), and Brezinski (1996b) presented a discussion about the genesis and depositional environments of the Conococheague Formation (Upper Cambrian) and St. Paul Group (Middle Ordovician). The first detailed descriptions of the stratigraphy of the Tomstown and Waynesboro formations of the Great Valley of Maryland and Pennsylvania were published by Brezinski (1992). Brezinski (1996a) later described the character and origin of the overlying Elbrook Formation. The stratigraphy and depositional history of the Stonehenge Limestone were delineated by Taylor et al. (1992). The overlying Rockdale Run Formation was discussed by Sando (1957) and Brezinski et al. (1999). The depositional history of the entire Great Valley carbonate succession was summarized by Brezinski et al. (2012).

Hydrologic study of the carbonate rocks of the Great Valley of Maryland was first conducted by Nutter (1973). Duigon (2001) investigated the karst hydrogeology of the Hagerstown Valley through examination of a water well inventory.

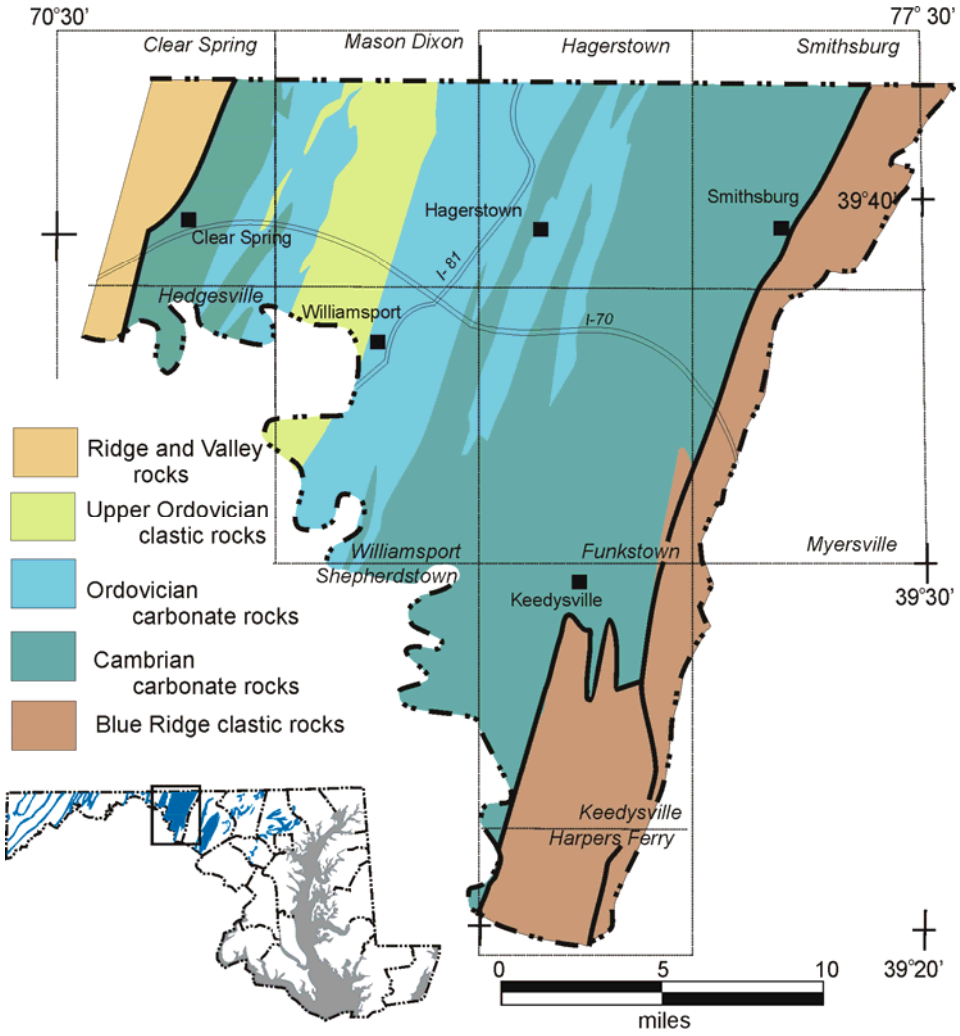

Figure 2.– Generalized geologic map of the Hagerstown Valley and its location with respect to other areas of Maryland containing karstic conditions.

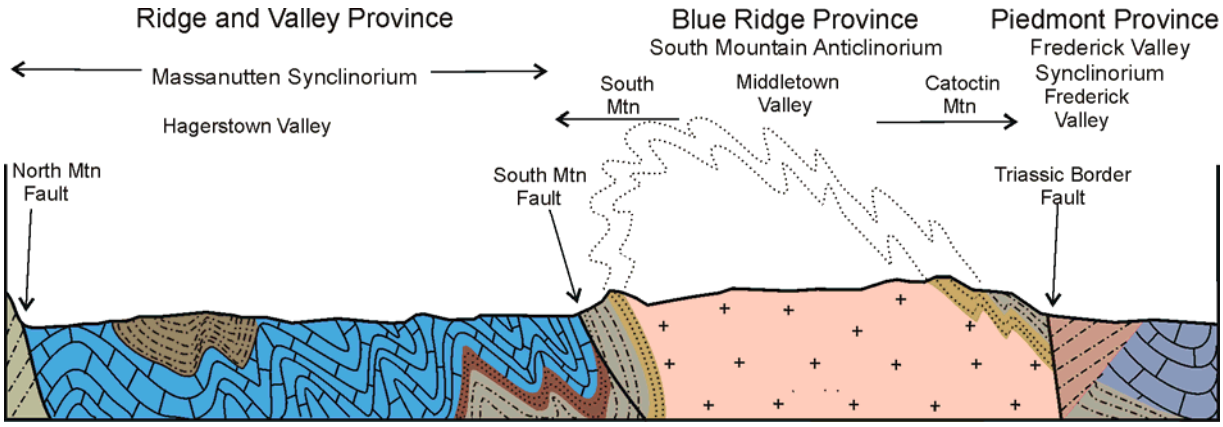

Figure 3.– Simplified geologic cross-section from Maryland's western Piedmont (right) to Fairview Mountain at the eastern edge of the folded Appalachian Mountain Section of the Ridge and Valley Physiographic Province. (Redrawn and modified from Cloos, 1947).

LITHOSTRATIGRAPHY

Rocks of the Hagerstown Valley range from late Precambrian to Late Ordovician in age. Carbonate deposition began during the Early Cambrian and continued for nearly 90 million years. The total thickness of this succession of carbonate rocks is more than 12,000 feet (3,650 m).

Chilhowee Group

Strata older than, and originally lying beneath, the carbonate rocks of the Hagerstown Valley succession are assigned to the Late Proterozoic to Lower Cambrian Chilhowee Group. These strata originally covered the basement rocks of the Blue Ridge and are commonly termed the Blue Ridge cover sequence (Brezinski, 1992). The Chilhowee strata are folded into the Blue Ridge anticlinorium and faulted against the Tomstown Formation along the eastern edge of the Hagerstown Valley.

The basal unit of the Chilhowee Group is the Loudoun Formation. The Loudoun consists primarily of grayish black to brownish black phyllite and medium to dark gray, tuffaceous, phyllitic conglomerate. While phyllite makes up most of the formation, the dark gray, quartz-pebble conglomerate is its most distinctive lithologic characteristic. Such conglomerate intervals are very useful in marking the approximate base of the Chilhowee Group throughout the Blue Ridge Physiographic Province of Maryland (Brezinski, 1992). The Loudoun Formation varies from 0 to 200 feet (0-60 m) in thickness.

Keith (1894) named the main ridge-forming unit of the Blue Ridge of Maryland the Weverton Formation, which overlies the Loudoun Formation. Brezinski (1992) subdivided the Weverton Formation into three members. The lowest member, the Buzzard Knob Member, is the principal unit underlying the ridges in the Maryland Blue Ridge. This member consists of approximately 150 to 200 feet of very light gray to yellowish gray, medium-bedded, medium- to coarse-grained, well-sorted quartzite.

The middle member of the Weverton Formation is composed of alternating layers of medium gray quartzite, medium dark gray, conglomeratic graywacke, dark gray phyllite, and metasiltstone. Named the Maryland Heights Member by Brezinski (1992), this member is approximately 300 feet thick.

The upper part of the Weverton Formation consists of a ledge-forming quartzite named the Owens Creek Member by Brezinski (1992). This member consists of interbedded, dark gray phyllite; thin-bedded, coarse-grained, dark gray metagraywacke; and interbedded, medium to dark gray, thin-bedded, coarse-grained greywacke; dark gray, quartz-pebble conglomerate; and a few intervals of greenish gray, quartzose, ferruginous siltstone.

Overlying the coarse-grained, ridge-forming quartzites of the Weverton Formation is a thick interval of metamorphosed shale, siltstone, and sandstone of the Harpers Formation. At its base, the Harpers Formation is characterized by several hundred feet of dark gray to olive-black, medium-grained sandstone and siltstone with thin beds (1 to 4 inches thick) of medium gray, fine-grained sandstone. This part of the formation is overlain by 700 to 1,000 feet of greenish black to brownish black, highly cleaved siltstone, fine-grained sandstone, and some silty shale. The uppermost part of the Harpers Formation consists of up to 1,000 feet of interbedded dark greenish gray to olive black, sandy siltstone and shales, and light gray to medium light gray, fine-grained sandstone, with beds 2 to 6 inches thick. These beds contain very abundant *Skolithos* burrows.

The uppermost formation of the Chilhowee Group is the Antietam Sandstone (Keith, 1894). The Antietam Sandstone consists of light gray to light brown, medium-bedded, medium- to fine-grained sandstone. These strata typically weather to angular cobbles of cross-bedded, *Skolithus*-bearing sandstone. The Antietam Sandstone has been shown to be Early Cambrian in age through the presence of the trilobite *Olenellus* (Nickelson, 1956; Brezinski, 1992).

Great Valley Succession

The Late Proterozoic to Lower Cambrian Blue Ridge cover rocks of the Chilhowee Group are overlain by a thick succession of carbonate rocks known as the Great Valley succession. This episode of deposition of carbonate strata began during the early Cambrian with the Tomstown Formation and persisted nearly continuously for 90 million years until the Late Ordovician. This prolonged period of carbonate deposition resulted in the accumulation of more than 12,000 feet (3,650 m) of largely shallow water carbonate rocks (Figure 4). This carbonate depositional episode ended with the formation of the Taconic Mountains of New York, near the end of the Ordovician Period.

Keith, 1894	Stose, 1906, 1908	Sando, 1956, 1957	Brezinski, 1992, 1996	This Report
Martinsburg Shale	Martinsburg Shale			Martinsburg Fm (upper mbr / lower mbr)
Shenandoah Limestone	Chambersburg Ls			Chambersburg Fm
	Stones River Formation	St. Paul Group		St. Paul Gp: New Market Ls / Row Park Ls
	Beekmantown Group: Stonehenge Ls	Beekmantown Group: Pinesburg Station Dol		Pinesburg Station Dol
		Rockdale Run Fm		Rockdale Run Fm
		Stonehenge Ls		Stonehenge Ls: Dam Five Mbr / Funkstown Mbr / Stoufferstown Mbr
	Conococheague Ls	Conococheague Ls	Conococheague Fm	Conococheague Fm: Shady Grove Mbr / Zullinger Mbr / Big Spring Station Mbr
	Elbrook Limestone	Elbrook Fm	Elbrook Fm	Elbrook Fm
	Waynesboro Formation		Waynesboro Fm: Chewsville Mbr / CavetownMbr / Red Run Mbr	Waynesboro Fm: Chewsville Mbr / Cavetown Mbr / Red Run Mbr
	Tomstown Dolomite		Tomstown Fm: Dargan Mbr / Benevola Mbr / Ft. Duncan Mbr / Bolivar Heights Mbr	Tomstown Fm: Dargan Mbr / Benevola Mbr / Ft. Duncan Mbr / Bolivar Heights Mbr
Antietam Sandstone	Antietam Sandstone		Antietam Formation	Antietam Formation

Figure 4.– Nomenclatural history and derivation for the stratigraphic units of the Great Valley succession in the Hagerstown Valley of Maryland.

Tomstown Formation

The oldest carbonate unit of Maryland's Great Valley is the Tomstown Formation. Stose (1908) applied the name Tomstown Dolomite to this poorly exposed interval that occurs directly above the Antietam Sandstone and below the shales of the Waynesboro Formation. The Tomstown Formation is only exposed along the eastern margin of the Hagerstown Valley, where it is in fault contact with the Harpers Formation and Antietam Sandstones (Brezinski, 2009; Brezinski and Fauth, 2009). This fault contact represents the boundary between the Ridge and Valley and Blue Ridge physiographic provinces.

Brezinski (1992) subdivided the Tomstown Formation into four laterally continuous and mappable members. These are, in ascending order, the Bolivar Heights, Fort Duncan, Benevola, and Dargan members.

Stose (1910) estimated that the Tomstown Formation is approximately 1,000 feet thick in the type area, but measurements provided by Brezinski (1992) (Appendix I, Sections 1, 2) suggest that the formation is nearly 1,200 feet in thickness. This is consistent with estimates of Woodward (1949) for the formation in West Virginia.

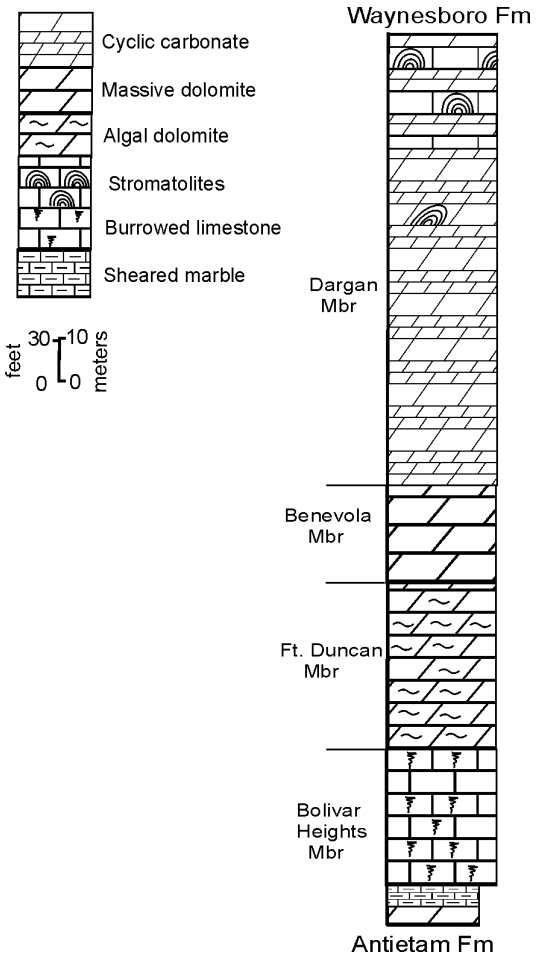

Figure 5.– Generalized stratigraphic column of the Tomstown Formation in the eastern part of the Hagerstown Valley.

Bolivar Heights Member: The basal member of the Tomstown Formation is the Bolivar Heights Member. The Bolivar Heights is characterized by a tan, vuggy dolomite at its contact with the underlying Antietam Sandstone. This dolomite ranges from 10 to 40 feet in thickness. Overlying the basal dolomite is an interval, 40 to 50 feet thick, composed of very light gray, sheared, laminated, dolomitic marble that Brezinski (1992) termed the Keedysville Marble Bed. Brezinski et al. (1996) proposed that the Keedysville Marble Bed was a stratotectonic unit formed either during the Late Ordovician or early in the Late Paleozoic Alleghenian orogeny.

Above the Keedysville Marble Bed the Bolivar Heights Member consists of 200 to 250 feet of thin- to medium-bedded, dark gray, argillaceous, ribbony, burrow-mottled, lime mudstone that weathers buff to light gray in color. The amount and density of bioturbation generally tend to increase upsection. In many exposures the burrows have been distorted by Alleghenian deformation.

The Bolivar Heights Member is completely exposed at several locations in the region (Brezinski, 1992). At these locations the member varies from 180 to 220 feet thick. Perhaps the best exposure of this member is at its type section along the CSXT railroad tracks in Jefferson County, West Virginia (Appendix I, Section 1), where 218 feet of the member are exposed.

The contact between the Bolivar Heights and overlying Fort Duncan members is distinctly gradational and conformable. This contact is exposed along the CSXT railroad tracks at Section 1 (Appendix I), where the intensely bioturbated limestone of the upper Bolivar Heights Member transitions into the knotty dolomite of the Fort Duncan Member over a stratigraphic interval of 3 feet.

Fort Duncan Member: Overlying the limestone strata of the Bolivar Heights Member is an interval, ranging in thickness from 200 to 250 feet thick, of dark gray, medium- to thick-bedded, knotty dolomite that Brezinski (1992) named the Fort Duncan Member. The Fort Duncan Member consists of burrow-mottled to knotty dolomite that weathers to an irregular, rough surface (Figure 6B). In polished slabs the knotty or burrowed areas appear to be represented by dark gray, rounded clots of fine-grained dolomite with white, void-filling, crystalline dolomite. Individual clots show no internal structure, but this appears to be largely the result of the destruction of the original fabric by dolomitization.

The contact of the Fort Duncan Member with the overlying Benevola Member is characterized by an intertonguing gradation that takes place over approximately 15 feet. The boundary is represented by a gradual decrease in strata with the knotty appearance as well as a gradual lightening of color from dark gray to very light gray dolomite. This decrease in knotty strata is paralleled upsection with an increase in beds of light gray, fractured dolomite.

Benevola Member: Overlying the dark gray, knotty dolomite of the Fort Duncan Member is an interval of light gray to white, massive dolomite that Brezinski (1992) named the Benevola Member. The Benevola Member is a white to very light gray, sugary dolomite both on fresh and weathered surfaces varies from 70 to 140 feet in thickness (Figure 6C). The Benevola Member also has a tendency to be highly fractured. Bedding is rarely evident within the Benevola Member, but polished slabs of the unit commonly display faint ghosts of cross-bedding. The type section the Benevola Member consists of two massive, light gray dolomite units separated by an interval 17 feet thick, comprised of laminated and bioturbated, gray dolomite. However, at most locations the unit occurs as a single, massive, white dolomite interval.

The contact between the Benevola Member and the overlying Dargan Member of the Tomstown consists of an intercalated succession of light gray, thick-bedded to massive dolomite, alternating with thinly laminated dolomite.

Dargan Member: The uppermost member of the Tomstown Formation is the Dargan Member (Brezinski, 1992). This unit is the thickest member of the formation and locally exceeds 700 feet. The Dargan Member consists of interbedded dark gray, bioturbated dolomite and gray laminated dolomite. The dark gray, bioturbated dolomite intervals range from 3 to 9 feet in thickness and alternate with intervals of medium to dark gray, laminated dolomite, 1 to 6 feet thick (Figure 6D). The upper 300 to 400 feet of the member consist of interbedded, dark gray, bioturbated and oolitic dolomite; dark gray, laminated limestone; tan, laminated, silty dolomite; mudcracked, laminated, cryptalgal and domal stromatolites. Near the top of the member numerous thinly laminated, algal limestone strata are interbedded with the laminated dolomite.

Contact Between the Tomstown and Waynesboro Formations: The contact between the Dargan Member of the Tomstown and the overlying basal Waynesboro Formation is relatively sharp. It is represented by the rapid replacement of alternating stromatolitic limestone and tan dolomite cyclic carbonates with a greenish gray to tan, calcareous shale and tan dolomite of the overlying Waynesboro Formation. Because both formations contain Early Cambrian fossils, the contact is believed to be conformable (Brezinski et al., 2012).

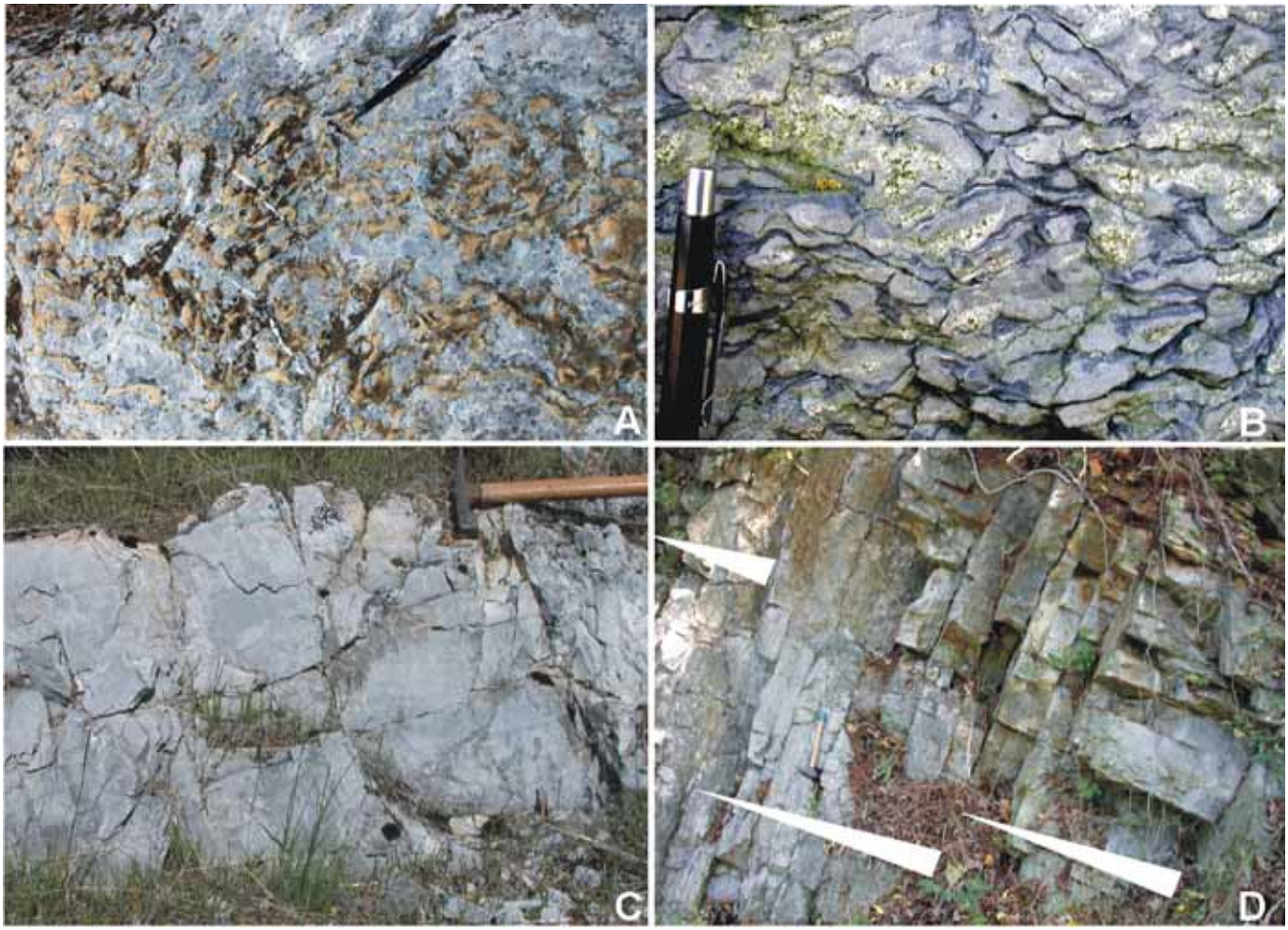

Figure 6.– Lithologic character of the Tomstown Formation. A, Burrowed fabric of the Bolivar Heights. B, Weathered knotty fabric of the Fort Duncan Member. C, Massive sugary dolomite of the Benevola Member. D, Cyclic bedded Dargan Member exhibiting shallowing cycles (arrows).

Karst Tendencies in the Tomstown Formation: The Tomstown Formation has lithologies that vary vertically through its stratigraphic succession. Because of this, the relative solubility of the four members of the formation differs vertically. The Bolivar Heights Member tends to exhibit a greater incidence of karst feature development within its outcrop belt than do the other three members. This apparent increase in solubility can be attributed to the preponderance of limestone strata within the Bolivar Heights as compared to the dolomite that characterizes the overlying Fort Duncan, Benevola, and Dargan members. An example of this increased solubility is the most prominent cave in the Great Valley of Maryland, Crystal Grottoes, which is confined to the Bolivar Heights Member of the Tomstown Formation.

Waynesboro Formation

Overlying the Tomstown Formation is an interval of interbedded carbonates and clastics known as the Waynesboro Formation. This formation was named by Stose (1908) for exposures surrounding the town of Waynesboro, Franklin County, Pennsylvania. Traditionally, the Waynesboro has been characterized as red shale and sandstone, but several authors (Bassler, 1919; Root, 1968) recognized a three-fold subdivision of the formation. This led Brezinski (1992) to subdivide the formation into three named members. In ascending order they are the Red Run, Cavetown, and Chewsville members (Figure 7). Like the Tomstown Formation, the Waynesboro Formation is confined to the eastern outcrop belt of the Great Valley in Maryland.

Red Run Member: The base of the Waynesboro Formation marks a discrete change from the pure carbonate deposition of the Tomstown Formation. The basal Waynesboro Formation, named the Red Run Member by Brezinski (1992) consists of interbedded, gray, calcareous, bioturbated, dolomitic sandstones, laminated and ribbony,

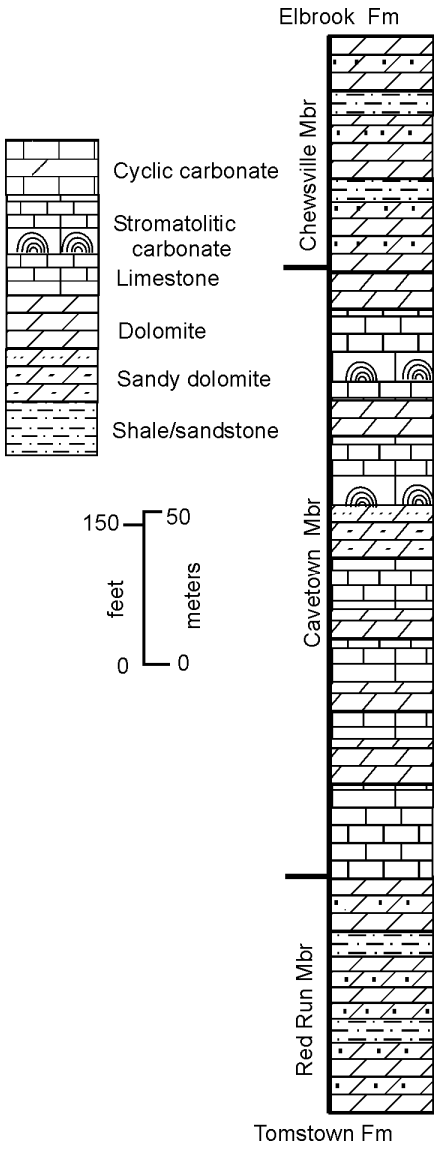

Figure 7.– Generalized stratigraphic column of the Waynesboro Formation in the eastern part of the Hagerstown Valley.

sandy dolomite, and olive-gray, silty, mudcracked, calcareous shale (Figure 8A). Sandstone layers vary from 0.5 to 3.0 feet thick and are commonly separated from one another by thin (0.5 to 1 foot thick), red-brown to greenish gray shale and shaly stringers, and tan ribbony to laminated, silty dolomite. This member weathers to blocks of calcareous sandstone and tan, sandy dolomite chips.

The Red Run Member varies between 150 and 200 feet in thickness (Brezinski, 1992). It is a continuous member throughout southern Pennsylvania and extends into northern Virginia. Where exposed, the upper contact of the Red Run Member consists of interbedded shaly and sandy strata with an upward increase in laminated and bioturbated limestone and dolomite.

Cavetown Member: Overlying the shaly and sandy strata of the Red Run Member is the medial part of the Waynesboro Formation named the Cavetown Member (Brezinski, 1992). The Cavetown Member is the thickest member of the formation, but also its most poorly exposed. The Cavetown Member characteristically forms a solution valley or topographically low area between the adjacent low ridges created by the clastic-rich Red Run and Chewsville members. Because the Cavetown Member contains lithologies common to the Dargan Member of the Tomstown and the Elbrook Formation, this member has been mistaken for these two units (Cloos, 1941; Root, 1968; Edwards, 1978).

The lowest 200 feet of the Cavetown Member consist of a massive, medium gray to grayish brown, lime mudstone and bioturbated dolomite. This pure carbonate rock has been extensively quarried in the past along the Potomac River and in northern West Virginia. The middle 200 feet of this member consist of interbedded, medium to dark gray, bioturbated, ribbony, dolomitic limestone and ribbony to laminated dolomite with intervals of interbedded, tan dolomite, light gray, fine-grained, calcareous sandstone, and olive-gray, calcareous shale. Near the top of the Cavetown Member is a 75-foot interval of light gray, thick-bedded to massive, dolomitic limestone to dolomite that is bioturbated and contains intraclasts and ooids (Figure 8B). This part of the member, like the section at the base, contains relatively pure carbonate intervals, and forms the western wall of the Cavetown quarry. Above this massive interval, the Cavetown Member consists of approximately 15 feet of laminated dolomite that grades upsection into sandy and shaly dolomite of the basal strata of the overlying Chewsville Member.

Nowhere is a complete section of the Cavetown Member known, however, Brezinski (1992) estimated its thickness at 400 to 600 feet. Based on an incomplete section and outcrop width, this member appears to be as thick as 700 feet (Appendix I, Section 3). The best exposures of this member are at the type section at the Cavetown quarry (see Brezinski, 1992, Section 17), where 363 feet are exposed, and at the Beaver Creek quarry along Interstate 70 where 300 feet are exposed.

The gradational contact between the Cavetown and overlying Chewsville Member is exposed along the CSX tracks 0.25 mile west of the Cavetown quarry. This exposure illustrates how the interbedded dolomite and shaly limestone of the upper part of the Cavetown Member are abruptly replaced by the siliciclastic beds of the Chewsville Member.

Chewsville Member: The most distinctive part of the Waynesboro Formation is the uppermost 150 to 200 feet of the formation. This stratigraphic package was named the Chewsville Member by Brezinski (1992) and is characterized by a succession of interbedded dark reddish brown siltstone, sandstone, and shale similar to that of the Red Run Member (Figure 8C). At the type section, along the CSX railroad tracks east of Chewsville (Washington County, Maryland), the Chewsville Member consists of nearly 150 feet of cyclically interbedded, dusky red and dark reddish brown, sandy siltstone and shale, grayish red, grayish pink, and pinkish gray, medium- to fine-grained sandstone, and light brown to grayish orange, silty and sandy, laminated dolomite. Less common lithologies include light olive gray shale and medium gray, stromatolitic and bioturbated dolomitic limestone. The reddish brown siltstone units are commonly rippled and mudcracked, whereas the sandstone beds are pervasively cross-bedded and exhibit *Skolithos* burrows.

Like the basal Waynesboro Formation, the arrangement of repetitive lithologies in the Chewsville Member suggests that it was formed under shallow water cyclic conditions. The Chewsville cycles consist of shallow subtidal limestone shallowing into intertidal sandstone, and then into supratidal red, mudcracked siltstone and shale. This contrasts with the massive carbonate strata of the Cavetown Member, which was deposited in deeper water environments. This change in character has implications for the development of karst. Both the lower and upper members were found to be relatively devoid of karst features, while the middle member was determined to be highly susceptible to karst development.

Contact Between the Waynesboro and Elbrook Formations: Where exposed, the contact between the Waynesboro and overlying Elbrook Formation is concordant, but sharp. Paleontological analysis has shown that, even though there is no salient evidence of erosion, there exists a large gap between the deposition of the Waynesboro Formation and the Elbrook (Bassler, 1919; Brezinski, 1996a). The trilobite *Olenellus* and the hyolithid *Salterella* are known to occur within the Chewsville Member of the Waynesboro. Both of these biotic components indicate an Early Cambrian age for the upper part of the Waynesboro Formation. Conversely, the basal limestones of the Elbrook Formation contain the late Middle Cambrian trilobite *Glossopleura*. The break in deposition between these two formations has been termed

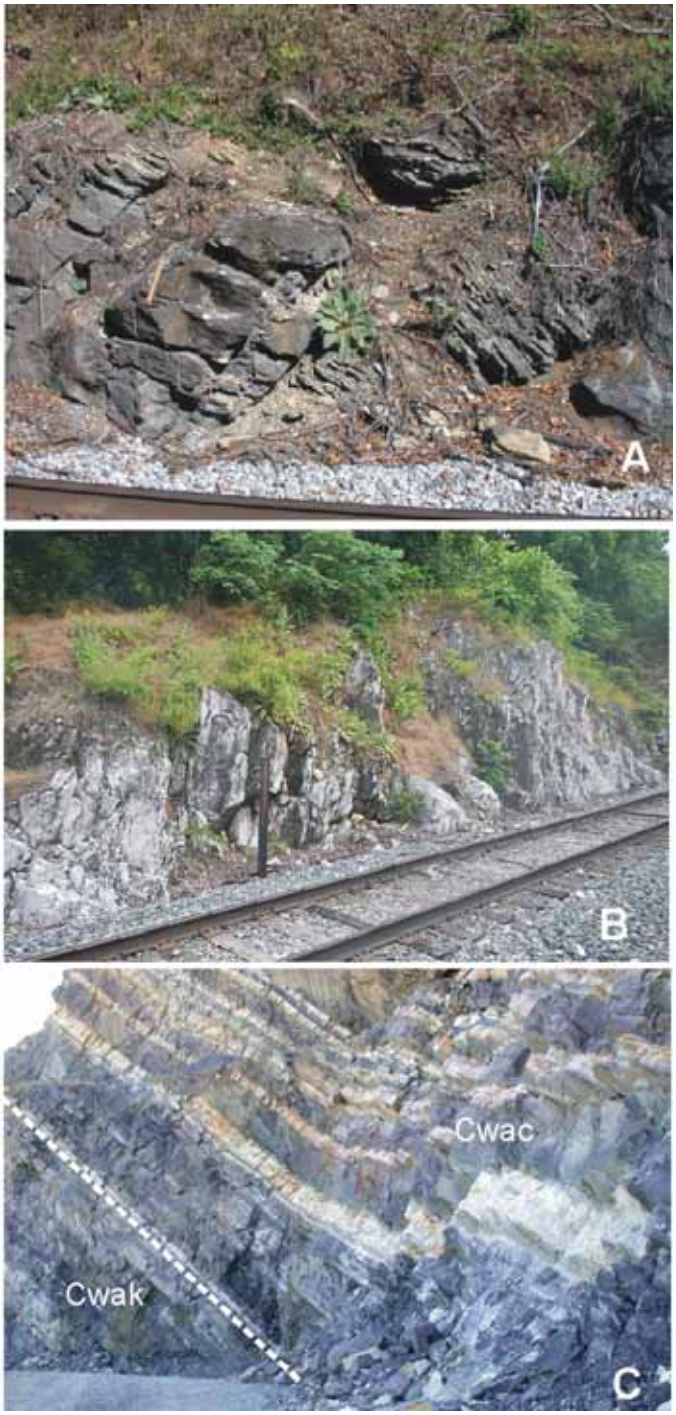

Figure 8.– Lithologic character of the Waynesboro Formation. A, Calcareous shale of the Red Run Member near Engle West Virginia. B, Massive fractured dolomite of the Cavetown Member at Cavetown, Maryland. C, Contact between the Cavetown (Cwak) and Chewsville members of the Waynesboro Formation in the Beaver Creek quarry.

the Hawke Bay Event or unconformity (Palmer and James, 1979). The magnitude of the lacuna is uncertain, but Brezinski et al. (2012) postulated it to be several million years' duration. This is consistent with the suggestions of Read (1989) who indicated that equivalent strata in southwestern Virginia contain a time gap of as much as 5 million years. Taylor et al. (1997) and Brezinski et al. (2012) have shown that the contact between these two formations is a hiatus that spans much of the Middle Cambrian, an interval of time as much as 10 million years.

Karst Tendencies in the Waynesboro Formation: The three members of the Waynesboro Formation exhibit sharp differences in karst development. The siliciclastic-rich Red Run and Chewsville members exhibit little evidence of dissolution. However, the Cavetown Member, as its name implies, is highly susceptible to the formation of karst features. This is suggested by the development of numerous caves within this member, especially those at Mt. Aetna and Cavetown. At other locations prominent sinkholes and springs tend to be concentrated within the low-lying middle member of this formation.

Elbrook Formation

Sharply overlying the mixed clastic-carbonate strata of the Chewsville Member of the Waynesboro Formation is a thick interval of cyclic limestone and dolomite that Stose (1908) named the Elbrook Limestone. Now termed the Elbrook Formation, the type section of this unit is poorly exposed near Elbrook, Franklin County, Pennsylvania. Using a partial measured section along the Potomac River (Appendix I, Section 6), Brezinski (1996a) was able to subdivide the Elbrook into three informal members. These informal subdivisions are termed the lower, middle, and upper members (Figure 9). Even though these three subdivisions were first identified along the western outcrop belt, all three can be identified in the eastern outcrop belt as well. However, because of poor exposure and cover by colluvium, the mapping of these members is difficult (Brezinski, 1996a).

The Elbrook Formation is entirely Middle Cambrian in age as suggested by trilobite faunas. Brezinski (1996a) has shown that the basal strata of this formation contain trilobites from the *Glossopleura* zone while the "middle member" contains trilobites of the *Bolaspidella* zone. The "upper member" has yielded trilobites assignable to the *Cedaria* and *Crepicephalus* zones, which suggest that this part of the formation is latest Middle Cambrian

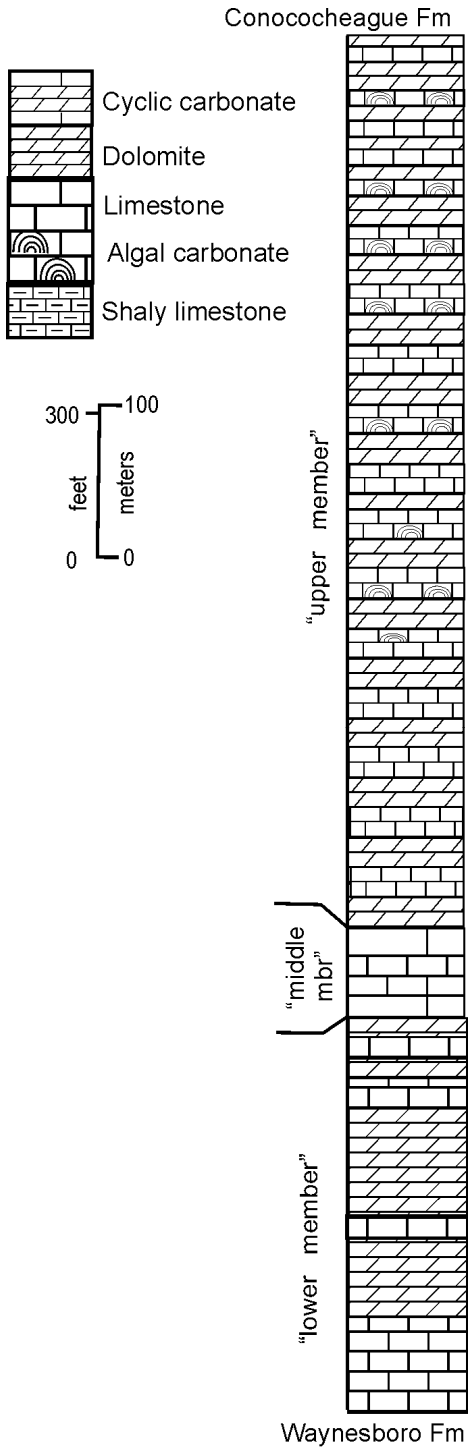

Figure 9.– Generalized stratigraphic column of the Elbrook Formation in the Hagerstown Valley illustrating vertical arrangements of lithologies and informal members.

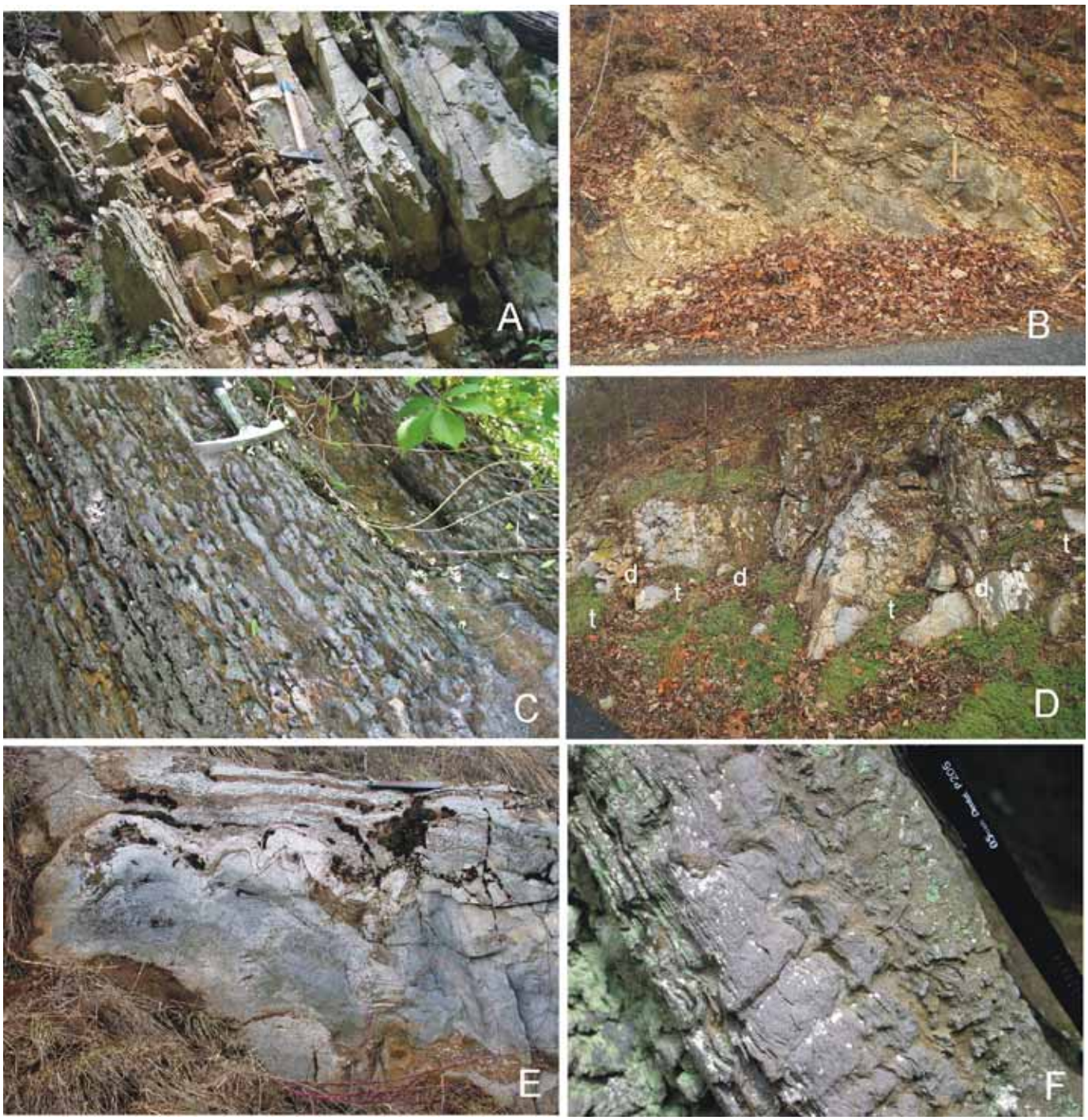

Figure 10. - Lithologic character of the Elbrook Formation. A, Close up of shaly dolomitic strata of the lower member. B, Weathered basal lower member, Monroe Chapel Road. C, Burrowed limestone of the middle member, CXST tracks, McCoys Ferry. D, Cyclic thrombolitic (t) and dolomitc (d) strata along US Alternate 40 at Cool Hollow. E, Domal thrombolites of the upper member, Maryland 68, Antietam National Battlefield. F, Digitate stromatolites at the top of a biostromal thrombolite in the upper member, C&O Canal National Historic Park, McCoys Ferry.

Lower member: The base of the Elbrook Formation throughout the central Appalachians is composed of 25 feet of medium gray, medium-bedded limestone. Above this basal limestone, the lower member is composed primarily of 700 feet of cyclic, light gray limestone, tan shale, and tan, shaly dolomite (Figure 10A). The characteristic lithologies of this interval are yellowish-weathering shale and dolomitic shale that commonly contain mudcracks. Interbedded with these yellowish dolomitic shales are white to very light gray, thinly bedded, limestone strata. In the eastern outcrop belt the interbedded tan shale and dolomitic shales, characteristic of the lower part of the Elbrook, are well-exposed at numerous small outcrops (Brezinski, 1996a), where relatively thick shaly intervals are punctuated by a medium-light gray, wavy-bedded limestone. Exposures of this member typically produce abundant chips of tan, shaly, and laminated dolomite, dolomitic silty shale, and green gray to tan, calcareous shale.

Locally, distributed within the cyclic strata are several intervals of medium to dark gray, bioturbated limestone. These dark gray limestone units range in thickness from 20 to 40 feet. The dark gray limestones can be traced locally, but cannot be correlated between the eastern and western sides of the Great Valley.

From the small and discontinuous exposures in the eastern outcrop belt, it is essentially impossible to determine the thickness of the lower member. Based upon outcrop width, the lower member on the eastern side of the valley is postulated to be at least as thick, or perhaps thicker, than the 700 feet measured at Section 6 (Appendix I)

Middle member: Unlike the shaly dolomitic lower member, the middle member is composed predominantly of limestone. This member is best exposed along the western limb of the Great Valley, but has locally been recognized on the eastern flank as well. This limestone interval is comprised primarily of argillaceous, medium gray, medium-bedded, locally lumpy- to nodular-bedded, bioturbated limestone with thin interbeds of dark gray, tan-weathering, laminated and fractured dolomite. The dolomite beds are rarely thicker than 3 feet, but the limestone intervals typically range from 15 to 30 feet in thickness. Burrow-mottling is exhibited as tan-weathering, silty, dolomitic infilling within the gray limestone (Figure 10B). Bedding is generally indicated by thin (< 0.25 in), shaly partings, and fossil fragments are present in many layers.

Although the middle member is rarely completely exposed, its thickness can be estimated at approximately 200 feet. This is consistent with thickness measurements obtained along the C&O Canal and CSXT railroad tracks east of McCoys Ferry near the western border of the Hagerstown Valley.

Upper member: Above the middle limestone member, the Elbrook Formation is a thick interval of cyclic, medium gray, medium-bedded limestone, dolomite, and dolomitic shale. This part of the formation was informally termed the upper member by Brezinski (1996a). A prominent and diagnostic lithologic package of this member is medium gray, thrombolitic limestones, 1 to 6 feet thick, interbedded with light gray to tan-weathering, laminated dolomite, 1 to 3 feet thick (Figure 10C). The thrombolites in this intervals exhibit a pinching and swelling appearance in outcrop (Brezinski et al., 2012) (Figure 10C). The tops of many of the thrombolitic intervals display digitate and laterally-linked hemispherical stromatolites. Such stromatolitic intervals are typically overlain by fractured, tan-weathering, silty dolomite, and thick-bedded, tan dolomite bearing mudcracks.

Near McCoys Ferry, over 1,400 feet of this member were measured (Appendix I, Section 6). Thus, the upper member appears to make up the greatest thickness of the Elbrook Formation, at least in the western outcrop belt. Additionally, this is also the best exposed member of the formation. The upper member can be distinguished from the lower by the well-developed stromatolitic and thrombolitic limestone in the former and the well-developed shaly intervals in the latter.

Contact between the Elbrook and Conococheague formations: Unlike the sharp basal Elbrook contact, the contact of the top of the Elbrook with the overlying Conococheague Formation is often difficult to identify. The upper part of the Elbrook Formation appears to exhibit a gradational contact with the overlying Conococheague Formation. This is because the carbonate cycles that characterize the upper member of the Elbrook Formation also are present within the overlying Conococheague Formation. In the western outcrop belt, the top of the Elbrook is placed at the base of the lowest occurring 3-foot-thick quartzarenite bed (Wilson, 1952, Brezinski, 1996a). Along the eastern outcrop belt, the contact is placed where the tan to yellowish dolomites, that Wilson (1952) considered to be the Big Spring Station Member of the Conococheague Formation, totally replace the thrombolitic limestone intervals that characterize the Elbrook Formation.

Karst Tendencies in the Elbrook Formation: The Elbrook Formation does not exhibit a strong susceptibility to karst development. This is especially true along the Elbrook's eastern outcrop belt where the formation contains numerous argillaceous interbeds and

interfingering dolomite. Although the formation contains much less clayey material along the western margin of the synclinorium, it still represents one of the least susceptible carbonate units to karst development. Where it is buried beneath thick coverings of colluvium, the Elbrook does exhibit a tendency to form broad, shallow dolines.

Conococheague Formation

The youngest Cambrian unit in the Hagerstown Valley carbonate succession consists of interbedded limestone and dolomite that Stose (1908) named the Conococheague Formation. The type area for the Conococheague Formation is along Conococheague Creek in Franklin County, Pennsylvania. Previous workers have attempted to subdivide the Conococheague Formation into members, but because the formation exhibits considerable vertical and lateral lithologic variation, recognition of these members is difficult. Moreover, lateral facies changes between the eastern and western outcrop belts further confound nomenclatural applications (Wilson, 1952; Root, 1968; Bell, 1993; Duigon, 2001).

Based upon trilobite biostratigraphy, the Conococheague Formation is Late Cambrian in age. Trilobites from the lower Zullinger Member are assignable to the *Elvinia* through *Taenacephalus* zones, while the upper Zullinger bears trilobites of the *Plethopeltis* zone (Brezinski et al., 2012).

No complete stratigraphic sections were located during this study. However, incomplete sections (Appendix I, Sections 7, 8) indicate that the Conococheague Formation is more than 2,100 feet (640 m) thick in Maryland (Figure 11). Based on measured sections, Root (1968) ascertained that the Conococheague Formation was as much as 2,200 feet thick in Franklin County, Pennsylvania.

Big Spring Station Member: Wilson (1952) named the predominately dolomitic lower strata of the Conococheague Formation the Big Spring Station Member for exposures along the CSXT railroad tracks near the town of Big Spring, Maryland on the western edge of the valley. Near the type area the Big Spring Station Member is approximately 250 feet thick and consists of tan to buff-weathering dolomites containing cross-bedded, dolomitic, calcareous sandstones up to 3 feet thick (Figure 12A). While this basal dolomitic interval is present, the characteristic sandstones near the base of the member are absent in Maryland, but are known from the eastern side of the valley in Virginia. Root (1968) lumped these dolomitic strata near the base of the Conococheague within his Zullinger Member. Bell (1993) and Duigon (2001) did employ the name, "Zullinger Member," in Maryland, but included much of this lithologic sequence within an informal "middle member." However, they segregated out the dolomitic interval near the base of the formation, and assigned it to the Big Spring Station Member. On the eastern side of the valley, the Big Spring Station Member consists of interbedded, massive, fractured, tan dolomite and thick-bedded, light gray, thrombolitic dolomite. These

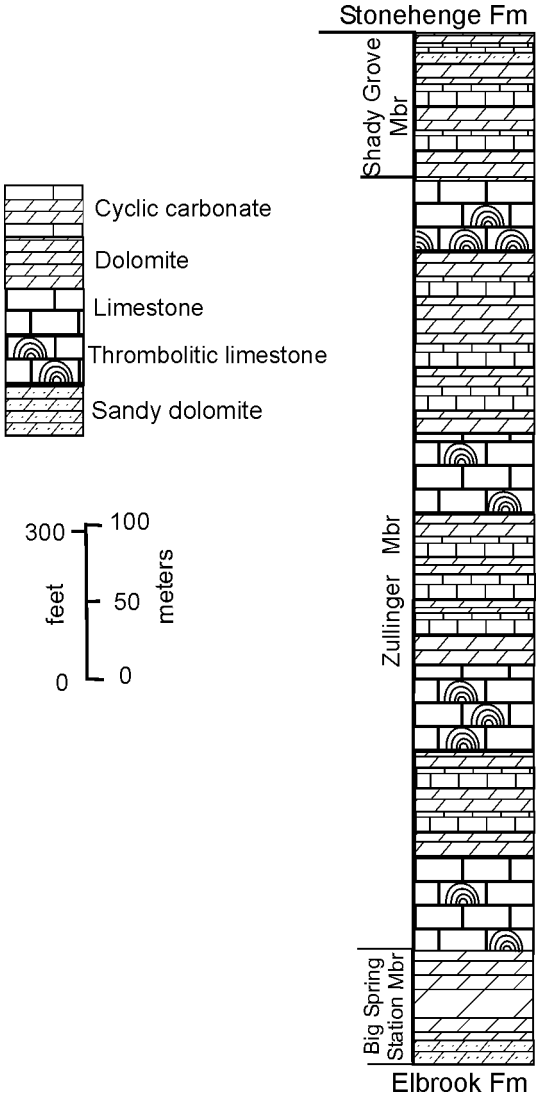

Figure 11.– Generalized stratigraphic column of lithologic character and member subdivisions of the Conococheague Formation in the Hagerstown Valley as utilized in this report.

strata tend to form a low, gentle rise adjacent to the stratigraphically subjacent Elbrook Formation and weathers to a thin soil with tan dolomite chips. On the eastern side of the valley this member may exceed 300 feet in thickness (Brezinski et al., 2015).

The contact between the Big Spring Station Member and the overlying Zullinger Member is gradational. This interval consists of interbedded light gray dolomites of the

upper part of the Big Spring Station Member and thin, ribbony, and thrombolitic strata of the lower part of the Zullinger Member.

Zullinger Member (revised): Root (1968) elevated the Conococheague from formation to group status and subdivided the group into two formations. He named the lower of the two units the Zullinger Formation and the upper the Shady Grove Formation. In this report, the Conococheague is reverted back to formation status, and as such, the Zullinger and Shady Grove are herein considered members of the Conococheague Formation. Moreover, in the current report the Big Spring Station Member is sufficiently extensive to be recognized on both the eastern and western flanks of the synclinorium below the Zullinger Member. Thus, in Maryland, the Conococheague Formation is herein subdivided into three members, the Big Spring Station, Zullinger, and Shady Grove members. The current nomenclatural subdivisions require a revision of the Zullinger from its initial designation by Root (1968).

The Zullinger Member was named by Root (1968) for exposures near Zullinger in southern Franklin County, Pennsylvania. Root (1968) proposed that this formation made up most of the Conococheague Group in southern Pennsylvania. Remeasurement of the Zullinger type section during the current study identified a 283 foot thick interval of dolomite strata at the base of the Zullinger that is herein assigned to the Big Spring Station Member. The Zullinger Member as it is currently perceived is equivalent to the informal "middle member" of the Conococheague Formation of Bell (1993), Brezinski and Bell (2009), and Brezinski and Glaser (2014).

The Zullinger Member, as recognized for this study, consists of a thick succession of interbedded, thick-bedded, medium to dark gray, thrombolitic limestone and medium to dark gray, ribbony, and tan, laminated, dolomitic limestone. The alternations between thrombolitic to ribbony limestone varies from 200 to 300 feet. Within these alternations are thinner lithologic repetitions, ranging from 3 to 15 feet thick, which appear to represent individual shallowing cycles recognized by Demicco (1985). Within the thrombolitic intervals these smaller cycles consist of thick, massive, thrombolitic strata, up to 20 feet thick, alternating with thin, ribbony limestone intervals (Figure 12 B,C). Within the predominantly ribbony intervals the alternations consist of thick, ribbony intervals containing thin (> 2 feet) thrombolitic layers alternating with tan, laminated, mudcracked dolomite and dolomitic limestone (Figure 12 D,E).

Brezinski et al. (2012) interpreted the alternating thrombolitic dominated intervals and the mudcracked laminated intervals as representing a scale of cyclicity equal to 3rd-order sea level changes. These supposed craton-wide sea level changes represent the smallest scale of cycles that could be correlated across North America with any confidence.

Root (1968) maintained that the Zullinger Member of the Conococheague Formation of Franklin County, Pennsylvania was nearly 2,000 feet thick. However, he noted that the basal 280 feet contained significant intervals of tan dolomite and several thin, sandy carbonate beds. This basal interval is herein reassigned to the Big Spring Station Member. The remainder of this part of the Zullinger of Pennsylvania is retained within the member.

Measured sections within Maryland delineate the thickness of the Zullinger Member as between 1,600 feet on the western side of the Great Valley and 1,900 feet on the eastern side. The thickness outlined by Root (1968) for the Zullinger in Pennsylvania included the 250 to 300 feet of dolomite at the base of the formation, herein considered the Big Spring Station Member. Thus, the thickness displayed by the formation in southern Pennsylvania matches those measured in Washington County, Maryland.

Shady Grove Member: Near the top of the Conococheague Formation the character of the formation recognizably changes. The thick intervals of alternating thrombolitic and laminated carbonate cycles that characterize the Zullinger Member are replaced by a succession of ribbony limestone and sandy dolomite. In this interval the cyclicity that characterizes the Zullinger Member is not clearly evident. Root (1968) termed this part of the Conococheague Formation in Franklin County Pennsylvania, the Shady Grove Member. Bell (1993), Brezinski and Bell (2013), Brezinski (2014), and Brezinski and Glaser (2014) informally termed this part of the Conococheague Formation the "upper member" in Washington County, Maryland. Because there appears to be no significant difference between the character, thickness, and distribution of this unit in Maryland and Pennsylvania, the name Shady Grove is adopted for the Hagerstown Valley. The Shady Grove Member consists of interbedded light to medium gray, sandy, intraclastic, lime grainstone, and ribbony, lime mudstone containing nodules and beds of gray chert (Figure 12E). There are a few thin thrombolitic intervals present but these rarely exceed 1 foot (30 cm) in thickness. Near the top of the member the ribbony intervals, become thicker and more prominent and are gradually replaced by the thick, ribbony layers of the overlying Stonehenge Limestone.

Root (1968) maintained that the Shady Grove had a thickness of between 350 and 500 feet. No complete sections of this member were measured in

Figure 12.– Lithologic character of the Conococheague Formation. A, Bedded and sandy dolomite of the Big Spring Station Member. B, Algal thrombolites of the Zullinger Member. C, Ribbony limestone of the Zullinger Member. D, Prism-cracked, laminated, dolomitic limestone of the Zullinger Member. E, Cyles of thrombolites, ribbony limestone, and laminated dolomites of the Zullinger Member. Triangle indicated shoaling cycles. F, Thin, cyclic facies at the top of the Shady Grove Member.

Maryland, although several partial exposures are present along the C&O Canal.

Conococheague-Stonehenge Contact: Sando (1957) placed the contact between the Conococheague Formation and Stonehenge Limestone at the base of the thick algal limestone succession that sat upon a ribbony limestone at the top of the Conococheague Formation. Sando (1958) subsequently moved the contact to the base of a thick, ribbony limestone interval, which he named the Stoufferstown Member. He then assigned that member to the Stonehenge Limestone. As a result, the contact between the two formations was lowered stratigraphically to the top of the cyclic limestone and dolomite interval at the top of the Conococheague Formation. Thus, today the base of the Stonehenge Limestone is considered the base of the ribbony and distinctly noncyclic Stoufferstown Member.

The contact between the Conococheague and overlying Stonehenge Limestone is gradational through approximately 30 feet (10 m) of strata. During the current mapping study, the contact is marked at the point where the thin (1-3 m) limestone/dolomite cycles are completely replaced by the ribbony, siliciclastic-rich Stoufferstown Member of the Stonehenge.

Karst Tendencies in the Conococheague Formation: Because of the broad areas underlain by the Conococheague Formation, many karst features were identified within this unit. However, inferences about the karst development within the Conococheague can be made based upon qualitative observations. The massive dolomites of the Big Spring Station Member tend to form a line of low hills that have a poorly developed karst surface morphology. Within the Zullinger Member the numerous alternations between thrombolite-bearing and ribbony and dolomitic intervals tends to mask any clearly recognizable solubility variations within this member. However, superficially there does appear to be an identifiable difference in the solubility of these distinct lithologies. Thrombolitic intervals tend to exhibit a greater susceptibility to dissolution than do the ribbony and dolomitic layers.

Beekmantown Group

Throughout the central Appalachian basin the Conococheague Formation is overlain by a thick interval of Lower Ordovician limestones and dolomites that were lumped together as the Beekmantown Group (Clarke and Schuchert, 1899). In Maryland, strata previously assigned to the Beekmantown Group are currently comprised of three formations, the Stonehenge Limestone, Rockdale Run Formation, and the Pinesburg Station Dolomite (Brezinski et al., 2012).

Stonehenge Limestone

The basal limestone unit of the Beekmantown Group was named the Stonehenge Limestone by Stose (1908). The type section of the Stonehenge Limestone is in Franklin County, Pennsylvania, where the formation is more than 900 feet thick (Sando, 1956). Sando (1957) subdivided the formation into two informal members, a basal algal member and an upper mechanical limestone member. Later, Sando (1958) included the upper 200 to 300 feet (70 to 100 m) of ribbony strata of the Conococheague Formation in the basal Stonehenge Limestone and named these newly reassigned basal strata, the Stoufferstown Member. He then lumped the algal and mechanical limestone members together into an upper member. Bell (1993) subdivided and mapped the

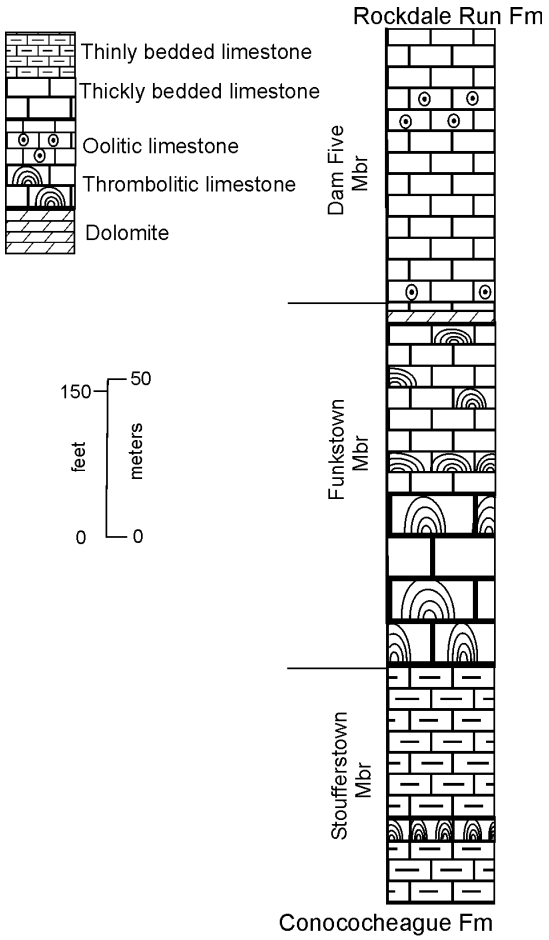

Figure 13.– Generalized stratigraphic column demonstrating member subdivisions of the Stonehenge Limestone in the Hagerstown Valley and adjacent states.

Stonehenge Limestone into four units, including the basal Stoufferstown Member. During this study, numerous stratigraphic sections of the Stonehenge Limestone were examined and measured. Evaluation of these sections suggests that the recurrent succession displayed in these exposures reflect a characteristic order of lithologies that allows subdivision of the Stonehenge Limestone into three members. These three members represent a combination from subdivisions of Sando (1957) and Sando (1958). This tripartite subdivision for the Stonehenge Limestone was utilized during geologic mapping by Brezinski and Bell (2009), Brezinski (2013a,b), and Brezinski (2014). These subdivisions include the Stoufferstown Member at the base, a middle member corresponding to the algal limestone member of Sando (1957, herein named the Funkstown Member, and an upper member equivalent to Sando's (1957) mechanical limestone, and herein named the Dam Five Member (Figure 13).

The Stonehenge Limestone was determined to be approximately 775 feet thick in southern Pennsylvania (Sando, 1958). Measurement of this unit in Maryland (Appendix I, Section 9) indicates that the formation is approximately 850 feet thick.

Stoufferstown Member: The thick, ribbony limestone interval that was recognized as the top of the Conococheague Formation by Sando (1957) was reassigned to the basal Stonehenge Limestone by Sando (1958). Named the Stoufferstown Member for exposures in Franklin County, Pennsylvania, this unit consists of dark gray, thinly bedded to ribbony, siliceous, lime mudstone. Individual limestone layers are 0.25 to 1.0 inches thick (Figure 14A). Individual ribbons are typically separated by thin, wispy, black to dark gray, argillaceous to silty layers that tend to weather out on solution surfaces. Punctuating this monotonous interval of ribbony limestone is a single interval of massive, dark gray, thrombolitic lime mudstone. This atypical lithology is only 3 feet thick in the western outcrop belt but thickens to more than 9 feet in the eastern belt. It consistently occurs approximately 30 feet above the base of the member, and appears to be continuous across both sides of the Hagerstown Valley.

The Stoufferstown Member is 220 feet thick at its type section near Chamberburg, Franklin County, Pennsylvania. In Maryland, it ranges from 175 to 275 feet in thickness.

Funkstown Member (New Name): Overlying the ribbony to thin-bedded Stoufferstown Member is an interval composed of medium gray, massive to thick-bedded, algal lime mudstone to boundstone (Figure 14B). Sando (1957) originally termed this lithology the lower member of the Stonehenge, but Sando (1958) lumped this lithology with the overlying mechanical limestone into his upper member. This unit also is equivalent to the entire lower biohermal facies and much of the middle ribbony carbonate facies as mapped by Bell (1993).

This member is well-exposed at the type section, north of Funkstown (Appendix I, Section 10 = Sando Section 12). It also is well-exposed within the Funkstown municipal park. Another excellent exposure of the Funkstown Member is along the C&O Canal National Historical Park at Two Locks.

In outcrop, Funkstown Member is readily identifiable by the massive exposure of limestone pinnacles of unbedded lime mudstone that is actually algal boundstone. In the lower part of the Funkstown Member, individual algal colonies can be as much as 12 feet thick and tend to show significant lateral variations in thickness and character within individual strata (Figure 14B). Near the top of the member, the thrombolitic layers are much thinner, rarely exceeding 3 feet in thickness, and tend to be laterally continuous biostromes. Low in the member, the thrombolites are interbedded with thin intervals of ribbony, lime mudstone and rippled, lime packstone. However, upsection, as the thrombolites become thinner, the ribbony intervals become thicker. The Funkstown Member tends to form a solution lowland between low uplands formed by the more resistant Stoufferstown Member and the somewhat more resistant Dam Five Member at the top of the Stonehenge Limestone. The top of the member can be identified by the appearance of thin dolomitic layers that serve to separate the Funkstown Member from the overlying Stonehenge Limestone.

This member ranges from 350 up to 450 feet in thickness (Sando, 1958). It is 350 feet thick at its type section (Appendix I, Section 10).

Dam Five Member (New Name): With progression upsection through the Funkstown Member, the number and thickness of thrombolitic intervals diminish. The absence of thrombolitic strata marks the transition from the Funkstown Member into the overlying Dam Five Member. Sando (1957) considered this portion of the section part of the upper member of the Stonehenge Limestone, while Sando (1958) termed it the upper mechanical limestone part of the upper member. These strata are equivalent to Bell's (1993) middle ribbony carbonate facies and upper limestone facies (Figure 14E).

The type stratigraphic section for the Dam Five Member is exposed along the C&O Canal National Historical Park towpath between the Dam Five parking area and the Two Locks area (Appendix I, Section 11). This part of the Stonehenge Limestone consists of medium to dark gray, medium-bedded, locally ribbon-bedded, intraclastic lime wackestone, packstone and grainstone (Figure 14F).

Figure 14.–Lithogies of the Stonehenge Limestone. A, Stoufferstown Member. Ribbony, and locally intraclastic limestone with argillaceous partings. B, Lenticular, thrombolitic, lime boundstone of the Funkstown Member. C, Massive, algal thrombolitic boundstone, and flanking strata of the Funkstown Member. D, Unbedded thrombolites (th) separated by lime grainstone channels (ch) deposit, Funkstown Member. E, Ribbony, intraclastic, lime packstone characteristic of the Dam Five Member. F, Thinly bedded, oolitic, lime grainstone near top of the Dam Five Member.

There also are numerous oolitic lime packstone strata, especially near the top of the member.

Sando (1958) maintained that the mechanical limestone that comprise the Dam Five Member was between 330 to 450 feet thick. At its type section, 317 feet of this member were measured (Appendix I, Section 9). The discrepancies in the thickness of this member are largely the result of accurately identifying the highest thrombolitic interval of the Funkstown Member.

Contact Between the Stonehenge Limestone and Rockdale Run Formation: The contact between the Stonehenge and overlying Rockdale Run Formation is relatively sharp and readily identifiable in the field. It can be pinpointed by the first appearance of tan, laminated dolomite upsection from the bedded intraclastic and oolitic limestone of the Dam Five Member of the Stonehenge Limestone. This first dolomitic bed signals the return to cyclic motifs that characterize the Elbrook and Conococheague formations, but are absent in the Stonehenge Limestone. This return to cyclic deposition is believed to represent the final stages of regression of the Stonehenge submergence of the platform (Brezinski et al., 1999; 2012; 2015).

Karst Tendencies in the Stonehenge Limestone: As a general statement, the Stonehenge Limestone appears to have a very high incidence of sinkhole development. However, not all of the members possess the same level of proneness to production of karst features. The Stoufferstown Member appears to have a low level of susceptibility to dissolution. This is indicated by its low incidence rate for sinkhole development, but also by the topography exhibited by this member. The low ridge typically marking the outcrop of the Stoufferstown Member's indicates a reduced level of dissolution. This is likely the result of the abundant siliceous material within the strata that reduces its susceptibility to dissolution.

In contrast to the Stoufferstown Member, the Funkstown Member displays a strong tendency toward dissolution. This member forms a solution valley on the upsection side of the Stoufferstown outcrops. This lowland typically exposes an area of well-developed limestone pinnacles and very thin soil.

The Dam Five Member of the Stonehenge Limestone also exhibits a strong tendency for sinkhole development. This propensity is notably less than that of the Funkstown Member, but is much stronger than that of the Stoufferstown Member.

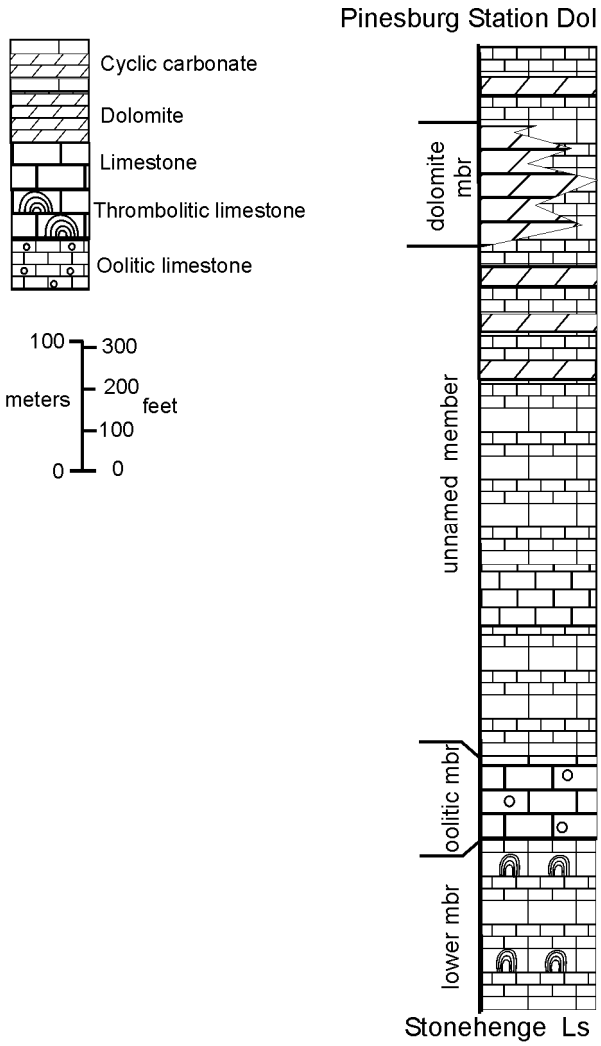

Figure 15.– Generalized stratigraphic column and vertical arrangement of lithologies and informal members of the Rockdale Run Formation in the Hagerstown Valley.

Rockdale Run Formation

Overlying the limestone strata of the Stonehenge Limestone a thick interval of cyclically bedded carbonate strata that Sando (1956) termed the Rockdale Run Formation of the Beekmantown Group. The type section of this formation is along Rockdale Run in Washington County, Maryland. Sando (1957) recognized three rock type groupings or lithologic zones within the Rockdale Run that he informally designated as members (Figure 15).

The lower 350 to 450 feet of the Rockdale Run Formation consists of cycles of interbedded thrombolitic to stromatolitic lime boundstone, ribbony limestone, and light gray to tan, laminated dolomite (Figure 16A). Many of the algal heads in this stratigraphic interval have been replaced by chert. Where this part of the formation crops out, large residual blocks of chert typically are preserved in the soil.

Bassler (1919) termed this interval the *Cryptozoan steeli* zone.

This part of the formation is well-exposed along the C&O Canal (Appendix I, Section 11) where approximately 450 feet crop out. However, in southern Pennsylvania Sando (1958) indicated that this part of the Rockdale Run Formation was only 350 feet thick.

The basal cyclic interval of the Rockdale Run Formation is overlain by approximately 200 feet of interbedded, medium gray, oolitic, lime packstone and thin, light gray to tan dolomite. Sando (1957) termed this the "oolitic member." The oolitic interval, in turn, is overlain by another interval of cyclic carbonate that is more than 1,000 feet thick (Figure 16B). Near the middle of this cyclic interval is approximately 100 feet of medium gray, thin-bedded and bioturbated, lime mudstone. This limestone interval has been correlated with the Axeman Limestone of central Pennsylvania (Brezinski et al., 2012; 2015).

Approximately 600 feet below the top of the Rockdale Run Formation there is a 200-foot-thick interval where the cyclic alternations of limestone and dolomite are replaced by a succession of light gray, medium- to thick-bedded dolomite (Appendix I, Section 11). Sando (1957) termed this the "dolomite member." Above the dolomite the Rockdale Run retains its cyclic character.

Bassler (1919) identified a distinct difference in lithologic character between the eastern and western outcrop belts of what is now termed the Rockdale Run Formation. This formation is more than 2,700 feet thick in the Hagerstown Valley. Sando (1957) was able to demonstrate that this difference could be attributed to the substantially fewer number of dolomitic interbeds within the Rockdale Run in the eastern areas. This change in lithology is depositionally important in that it suggests that the Early Ordovician carbonate platform that is now the Hagerstown Valley exhibited an eastward slope. This slope resulted in deeper water conditions that allowed deposition of more limestone strata in the eastern outcrop belt, whereas more subaerial conditions prevailed to the west and caused dolomite deposition.

At Section 11 (Appendix I), more than 2,300 feet of the Rockdale Run Formation was measured. Based on measurement of this section and several others, Sando (1957) determined that the Rockdale Run Formation was approximately 2,500 feet thick.

Contact Between the Rockdale Run Formation and Pinesburg Station Dolomite: Sando (1957) placed the contact between the Rockdale Run Formation and the Pinesburg Station Dolomite at the top of the highest limestone strata of the Rockdale Run. This contact is more readily placed where the cycles of alternating gray limestone and tan, fractured and laminated dolomite of the Rockdale Run Formation are replaced by buff-weathering, fractured dolomite of the Pinesburg Station.

Karst Tendencies in the Rockdale Run Formation: The Rockdale Run Formation exhibits a similar level of karst development to the Conococheague Formation. Both formations show a modest and very localized high level of dissolution, but there is not a particular interval that can be determined to be highly susceptible and prone to catastrophic collapse sinkhole formation.

Pinesburg Station Dolomite

The uppermost cyclic strata of the Rockdale Run Formation grade upsection into dove-weathering, medium- to thick-bedded, light gray, fractured dolomite that marks the upper unit of the Beekmantown Group, the Pinesburg Station Dolomite (Sando, 1956) (Figure 16C). The type section for the Pinesburg Station Dolomite is a discontinuous field exposure north of the CSXT tracks west of Pinesburg, Washington County, Maryland. Excellent alternate reference sections are found along the C&O Canal National Historical Park towpath at approximately milemarker 102.5 (Appendix I Section 11), and along the westbound lanes of Interstate 70 at Cedar Ridge Road (Appendix I, Section 12).

In weathered exposures the Pinesburg Station Dolomite consists of nearly white, fine-grained, medium- to thick-bedded dolomite alternating with medium beds of light gray, laminated dolomite (Figure 16C). On fresh outcrops the dolomite is medium-bedded, light gray, and locally contains thin, tan, laminated dolomite beds.

Although cyclicity within the Pinesburg Station is not easily apparent, alternations of thick-bedded dolomite with dolomite laminite attest to the cyclic nature of the depositional original sediment. Commonly, the massive to thick-bedded dolomite is highly fractured and locally brecciated (Figure 18). Much of the characteristic fracturing of this unit is attributable to tectonic deformation, but some of the brecciation of the thinner dolomite layers has been interpreted as having formed during periods of subaerial exposure and dissolution by fresh waters as paleokarst (Mussman and Read, 1986) (Figure 18).

Throughout the central Appalachian basin, the latter stages of deposition of the Beekmantown Group are characterized by the regional development of dolomite successions. The Pinesburg Station Dolomite of Maryland is coeval with thick dolomitic successions of Pennsylvania, such as the Ontelaunee and Bellefonte dolomites (Brezinski et al., 2015). These dolomites are attributable

Figure 16.– Lithologic character of the upper part of the Beekmantown Group. A, Cyclic limestone of the lower part of the Rockdale Run Formation exposed along eastbound lanes of Interstate 70. B, Dolomite member of the Rockdale Run Formation exposed along the C&O Canal towpath. C, Pinesburg Station Dolomite along the National Road, Wilson, Maryland. D, Corroded microkarstic contact between the Pinesburg Station Dolomite and St. Paul Group (Row Park Limestone) at Pinesburg, Maryland.

to a global drop in sea level and restriction of the carbonate platform during the later parts of the Early Ordovician (Morgan, 2012). This led to exposure of much of the platform and creation of a widespread lacuna manifested in the Knox unconformity (Ryder et al., 1992; Morgan, 2012; Brezinski et al., 2012). In the Hagerstown Valley the precise stratigraphic position and magnitude of the lacuna for the Knox unconformity are not well constrained. This unconformity does not, however, appear to coincide with any formational boundary, but is confined within the upper part of the Rockdale Run Formation.

Sando (1958) determined the thickness of the Pinesburg Station Dolomite at between 372 to 503 feet. Measurement for the two stratigraphic sections measured for this study range from 320 to 437 feet.

Contact Between the Pinesburg Station Dolomite and St. Paul Group: Neuman (1951) and Sando (1957) believed that the contact between the Pinesburg Station Dolomite and the overlying Row Park Limestone was gradational and interbedded over an interval of approximately 60 feet. Brezinski et al. (2012, fig. 20a) showed that the contact between these two units was sharp. This contact is well exposed in the bluffs overlooking the Potomac River southwest of Pinesburg, Maryland. At this location the dense, fine-grained, fenestral limestone of the Row Park Limestone sharply overlies an interval of approximately 2 feet of punky dolomite at the top of the Pinesburg Station (Figure 16D, 18). This punky zone is interpreted as an interval of paleokarst that separates the deposition of the two units, and represents a period of nondeposition of unknown duration.

Karst Tendencies in the Pinesburg Station Dolomite: The Pinesburg Station Dolomite does not appear to be very susceptible to dissolution. During this study, very few active sinkholes or springs were observed in its outcrop belt, and only a few depressions.

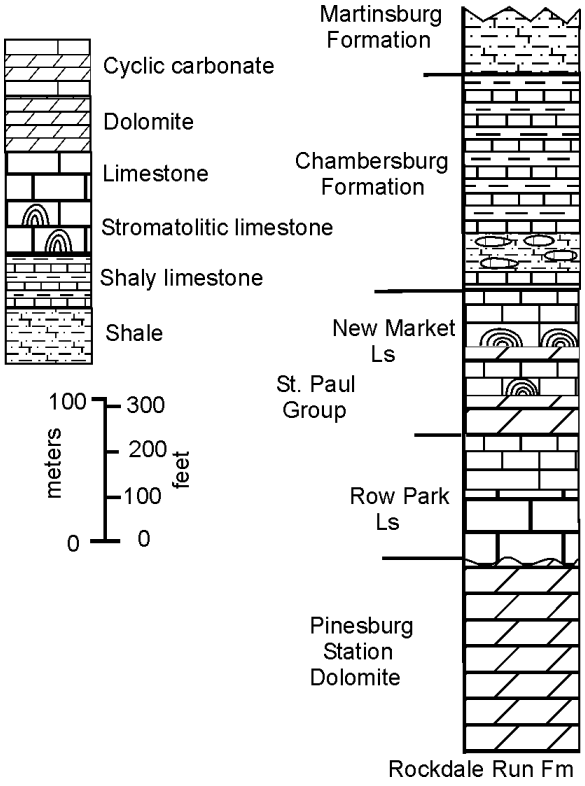

Figure 17.–Generalized stratigraphic column illustrating units of the Pinesburg Station Dolomite and Middle Ordovician strata of the Hagerstown Valley.

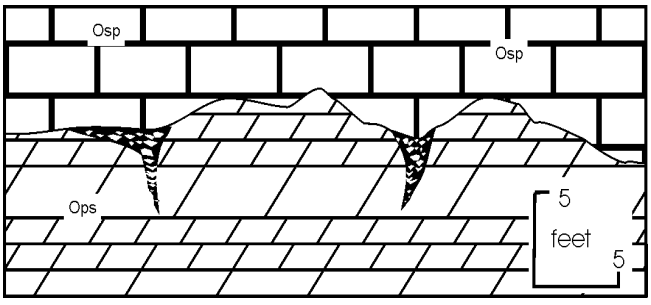

Figure 18.–Sketch of local relief created by paleokarstification along contact between the Pinesburg Station Dolomite and St. Paul Group. Diagram depicts section along C&O Canal at Pinesburg. Ops=Pinesburg Station Dolomite, Osp=St. Paul Group, Row Park Limestone.

St. Paul Group

Overlying the fractured buff dolomites of the Pinesburg Station is an interval of interbedded limestone and dolomite that Neuman (1951) termed the St. Paul Group, for exposures near St. Paul Church in Washington County, Maryland. The St. Paul Group was subdivided by Neuman into a lower formation, the Row Park Limestone, and an upper, the New Market Limestone (Figure 17). The salient lithology that allows recognition of the Row Park Limestone is a massive, light gray, dense, fine-grained lime mudstone. These massive lime mudstone intervals are up to 30 feet thick and exhibit irregularly shaped calcite-filled voids termed "bird's eye." These filled voids are believed to represent gas bubbles that were pervasive in the fine-grained lime mud during deposition. The voids were subsequently filled with crystalline carbonate (Figure 19A). These bird's eye mudstone intervals are overlain by medium-bedded, lime grainstone and then by laminated, dolomitic lime mudstone.

The Row Park Limestone is approximately 150 feet thick at Section 11 (Appendix I) and 230 feet at Section 12. Demicco and Mitchell (1982) show that this unit can range from less than 200 feet to more than 350 feet thick. The significant thickness variations exhibited by this unit are attributed to the prominence and localized distribution of the massive, bird's-eye lime mudstone units.

Grading upsection from the Row Park Limestone is an interval of interbedded, gray to grayish brown, thin-bedded, or stromatolitic lime mudstone, and light gray to tan, laminated dolomite (Figure 19B, C). This succession of interbedded limestone and dolomite is termed the New Market Limestone (Brezinski, 1996b).

The New Market Limestone varies between 230 and 270 feet thick in the two measured sections present herein (Appendix I, Sections 11, 12). These thicknesses are consistent with Demicco and Mitchell (1982) who showed that this formation varied from 200 to 300 feet in thickness.

The interbedding of limestone and dolomite that typifies the New Market Limestone is identical to that which characterizes the Rockdale Run Formation. This suggests that, following the restricted circulation and exposure of the carbonate platform during Early Ordovician deposition of the upper part of the Rockdale Run Formation and the Pinesburg Station Dolomite, the platform returned to cyclic carbonate deposition.

The combined thickness of the St. Paul Group is between 300 to 400 feet in Washington County, Maryland. Because both the Row Park and New Market limestones share so many characteristic lithologies, they were not mapped separately during the current study.

Figure 19.– Lithologic character of the St. Paul Group and the Chambersburg Formation. A, Bird's-eye limestone of the Row Park Limestone. B, Cyclic stromatolitic limestone (L) and dolomite (D) of the New Market Limestone. C, Close-up of stromatolitic, lime boundstone of the New Market Limestone. D, Sharp contact (at hammer head) between the New Market Limestone (left) and Chambersburg Formation (right) at Pinesburg quarry. E, Nodular-bedded *Echinospaerites* strata of the lower Chambersburg Formation. F, Medium-bedded, dark gray, lime mudstone of the upper Chambersburg Formation.

Contact Between the St. Paul Group and Chambersburg Formation: The contact between the New Market and Chambersburg formations appears to be conformable. This contact is exposed along the C&O Canal and the Martin Marietta quarry at Pinesburg. At this location, the sharp transition between the light gray, lime mudstone of the upper part of the New Market and the argillaceous, dark gray, lime mudstone of the basal Chambersburg Formation is exposed (Figure 19F).

Karst Tendencies in the St. Paul Group: The St. Paul Group exhibits a strong proclivity toward dissolution and sinkhole formation. This tendency is displayed in the fields on the north side of Maryland Route 68 at Cedar Ridge Road at Pinesburg, as well as at a number of other outcrop areas of the St. Paul Group.

Chambersburg Formation

Overlying the cyclically bedded, gray limestone and tan dolomite of the New Market Limestone is an interval of dark gray, argillaceous, thin- to medium-bedded, locally nodular-bedded, fossiliferous limestone termed the Chambersburg Formation for exposures near Chambersburg, Pennsylvania (Stose, 1906). This unit is the stratigraphically youngest carbonate unit of the Great Valley. In northern Virginia, the light-colored, upper limestone strata of the New Market Limestone interfinger with, and are replaced by, a dark gray, thin- to medium-bedded, siliceous, argillaceous lime wackestone termed the Lincolnshire Formation (Read, 1989; Radar and Read, 1989). However, in Maryland the thinly bedded, cherty Lincolnshire lithologies are absent, and the medium-bedded limestones of the New Market are sharply replaced by the deeper-water argillaceous and nodular-bedded lithologies of the Chambersburg Formation.

The Chambersburg Formation varies between 250 and 400 feet in thickness, and averages approximately 300 feet thick in Maryland. The thin-bedded, dark gray, argillaceous basal strata grade upsection into 80 to 100 feet of dark gray, shaly, nodular limestone that are locally termed the "*Echinosphaerites* beds" (Neuman, 1951; Brezinski, 1996b). These nodular beds, in turn, grade upwards into thin-bedded, argillaceous limestone and then into a thickly bedded, bioturbated, lime wackestone that is up to 35 feet thick (Figure 19E). The thick-bedded limestone occurs near the middle of the formation, and then is replaced by thinly bedded lithologies and by wavy- to nodular-bedded lime mudstones at the top of the formation.

Brezinski et al. (2012) interpreted the vertical arrangement of lithologies in the Chambersburg Formation as a record of two separate transgressive episodes. The earlier deepening episode was initiated within the upper part of the New Market Limestone. The upsection transition from medium-bedded, bioturbated limestone into thinly bedded and then nodular-bedded lithologies was interpreted as representing the deepening from intertidal (New Market) lithofacies into deeper ramp environments (*Echinosphaerites* interval). Shoaling shallow subtidal environments are recorded upsection in the thickly-bedded middle part of the Chambersburg Formation, followed by a return to deeper water environments at the top of the formation (Figure 19D).

Contact between the Chambersburg and Martinsburg formations: The contact between the Chambersburg and Martinsburg formations is exposed at two locations in Maryland, both along the C&O Canal. The first location is at Pinesburg where the bedded limestone of the upper part of the Chambersburg are sharply overlain by dark gray, graptolite-bearing shale of the Martinsburg Formation. The second outcrop is south of Falling Waters Road. At this second location the contact between the limestone of the Chambersburg and the overlying Martinsburg Formation is gradational over several hundred feet of stratigraphic section. The basal Martinsburg Formation consists of interbedded, calcareous shale and argillaceous limestone (Figure 20A). In Virginia, this interval and its characteristic lithology is named the Stickley Run Member (Epstein et al., 1995). Because this interval is absent at the Pinesburg location, the contact at that location is interpreted as a fault (Brezinski, 2014).

Karst Tendencies in the Chambersburg Formation: Duigon (2001) postulated that the Chambersburg Formation had one of the highest incidences of sinkhole development of all the stratigraphic units of the Hagerstown Valley. This interpretation was based upon the large number of dolines exposed along Cedar Ridge Road from Pinesburg to Wilson. However, close examination of this area suggests that the depressions exposed there are within the St. Paul Group. Since the Chambersburg Formation underlies a relatively small outcrop area in the Hagerstown Valley, it is difficult to objectively assign it a karst susceptibility value.

Martinsburg Formation

The Martinsburg Formation consists of a thick sequence of shale, siltstone, and sandstone that crops out in the center of the Hagerstown Valley and serves to separate the carbonate bedrock exposed in the valley into eastern and western belts. Brezinski (2013b; 2014) subdivided and mapped the Martinsburg Formation as two informal members, the lower and upper members. These members are consistent with similar subdivisions proposed by

McBride (1962) and Root (1968). The Martinsburg Formation of the Great Valley is equivalent to the Reedsville Formation of the Ridge and Valley Physiographic Province of central Pennsylvania.

Lower member: The "lower member" of the Martinsburg Formation as used in this report consists primarily of dark gray shale. This shale interval contains lithologies, at its base, identical to the Stickley Run Member of the Martinsburg Formation of Virginia. These Stickley Run lithologies in Maryland consist of interbedded, dark gray, medium-bedded, argillaceous lime mudstone and dark gray, brittle, calcareous, graptolite-bearing shale, but were not mapped separately in the Hagerstown Valley. Above the Stickley Run lithologies, the lower member consists of medium to dark gray to black, brittle shale. Within these shales are thin (~ 0.25 inch) siltstone to very fine-grained sandstone beds (Figure 20B). The gray shale in this part of the Martinsburg Formation weathers to olive-gray to tan. Within the upper part of this lower member, thin sandstone beds between 2 to 6 inches in thickness are present within the dark gray shale. These thin sandstone beds exhibit a fine graded bedding and sole markings. Upsection, the thickness and number of these sandstone interbeds increases. The lower member is best exposed in Maryland along the CSXT tracks east of Pinesburg. At this location the lower member is discontinuously exposed along several outcrops. Each of these outcrops expose between 300 to 500 feet of strata. Based on these discontinuous exposures, the thickness of the Lower Member can be approximated at 2,000 to 2,500 feet.

The dark gray to black shale interval that makes up the lower member of the Martinsburg Formation in Maryland is equivalent to the Utica Shale of Pennsylvania and New York. The Utica Shale is a carbonaceous and pyritic organic shale, whereas the lower member of the Martinsburg in Maryland contains a significantly higher level of siliciclastics and a lower percentage of organic matter than correlative strata deposited in areas to the north and west.

Upper member: The thin sandstone beds that characterize the upper part of the lower member increase in number and thickness upsection. These sandstone interbeds become so prominent and regularly bedded upsection that they become the dominant lithology (Figure 20C). Many of these sandstone layers exhibit graded-bedding, sole marks, and flute casts. Some of these sandstone intervals are up to 30 feet thick, and display sharp bases, with pebble basal lag conglomerates. These thicker sandstone intervals are upward fining, as they become regularly interbedded with gray, silty shale. In Franklin County, Pennsylvania, Root

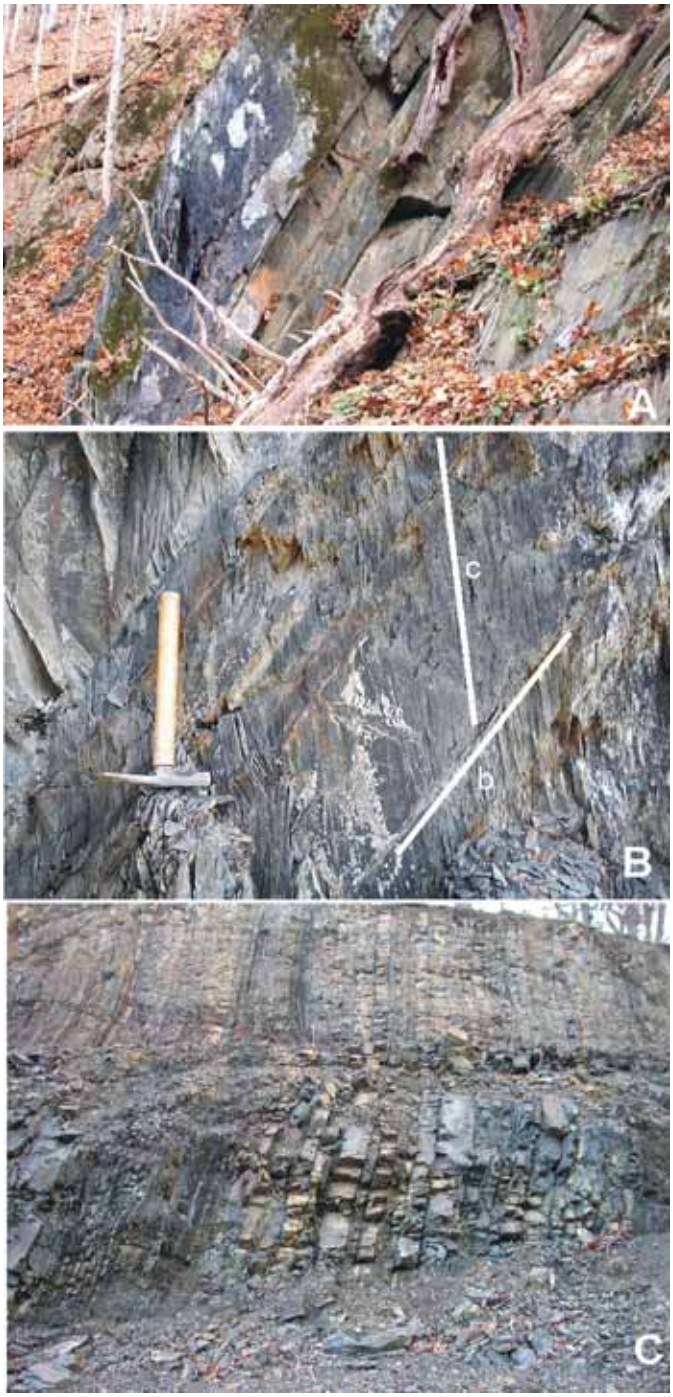

Figure 20.– Lithologic character of the Martinsburg Formation in Maryland. A, Strata of the lower member immediately above the Chambersburg Formation. These strata are similar to the Stickley Run Member of the Martinsburg Formation in Virginia. B, Dark gray silty shale of the lower member of the Martinsburg Formation. Note thin siltstone interbeds. C=cleavage, b=bedding. C, Upper member of the Martinsburg Formation. Upward fining, medium-grained sandstone.

(1968, fig. 27) called this the "sandstone member" and showed that it could be separately mapped within the Martinsburg Formation.

In Maryland, the upper member is well exposed along the CSXT tracks west of Williamsport, and along the eastern edge of the Martinsburg outcrop belt. More than 700 feet of section is exposed there. Based upon both stratigraphic position and lithologic character, the upper member can be considered equivalent to the Bald Eagle Formation of the Ridge and Valley of central Pennsylvania.

The top of the Martinsburg is not exposed within the Great Valley of Maryland. To the north and west in Pennsylvania, the upper member of the Martinsburg Formation and its equivalent, the Bald Eagle Formation of Pennsylvania, grade upsection into the Upper Ordovician Juniata Formation.

The Origin of Maryland's Great Valley Carbonate Succession

Brezinski et al. (2012) discussed the origin of the Cambrian-Ordovician carbonate succession of the central Appalachians. They described the development and persistence of the Great American Carbonate Bank in Maryland and showed how the various scales of depositional cycles produced the more than 10,000 feet of carbonate rocks that underlie today's Great Valley.

Carbonate sediment deposition in the Great Valley began during the Early Cambrian following the breakup of the supercontinent Rodinia and the formation of a deep water ramp along the eastern edge of the Laurasian continent. This carbonate ramp was interpreted as being gently inclined seaward (eastward). On this deep-water ramp the Tomstown Formation was deposited. Bioturbated sediments of the Bolivar Heights Member were laid down first followed by dolomitized microbial reefs of the Fort Duncan members. The Fort Duncan reefs formed a shelf margin and initiated platform sedimentation. Along the edge of this platform carbonate shoals produced well-winnowed sand facies of the Benevola Member. Landward of these shoals, peritidal cyclic sedimentation was initiated with the deposition of the Dargan Member of the Tomstown Formation. This initiation of shallow subtidal to supratidal deposition was coincident with the development of a rimmed platform that would persist throughout much of the Cambrian and Early Ordovician. Continued shallowing of the platform resulted in the development of subaerial facies of the Red Run and Chewsville Members of the Waynesboro Formation. The platform became completely exposed during the latest Early Cambrian with the creation of a regional unconformity known as the Hawke Bay event where upon Early Cambrian deposition ended. During the early Middle Cambrian the carbonate bank deposition resumed in the form of peritidal cyclic deposits of the Elbrook Formation. The middle member of this unit suggest that the platform was, at least infrequently, submerged by deeper water conditions. These facies can be traced into central Pennsylvania where the coeval Pleasant Hill and Warrior formations were deposited. A regionally developed regressive episode marks the end of Elbrook deposition at the end of the Middle Cambrian. This regression resulted in the deposition of widely developed restricted circulation dolomitic deposits of the Big Spring Station Member of the Conococheague Formation along with the contemporaneously deposited Gatesburg Formation of central Pennsylvania. Resubmergence of the platform was initiated during the early Late Cambrian with the expansion of extensive subtidal thrombolitic boundstone facies within the Zullinger Member of the Conococheague Formation. The vertical stacking of up to four of these thrombolite-dominated cycles records third-order transgressive episodes. These deepening events are separated by intervening shallowing episodes that produced thick intervals of ribbony and laminated mudcracked dolomite. The maximum deepening and submergence of the Great American Carbonate Bank came in the Early Ordovician with the deposition of the Stonehenge Limestone. The thick algal reefs of the Stonehenge's Funkstown Member reflect the increased water depth achieved during this depositional period. At the end of Stonehenge deposition, a regression occurred causing the platform to experience persistent and increased restrictions to circulation. This resulted in the deposition of the thick succession of meter-scale cycles of the Rockdale Run Formation in central Maryland and the Nittany Dolomite, and lower part of the Bellefonte Dolomite of the Nittany arch of central Pennsylvania (Figure 21).

This regressive phase culminated in regional exposure of the carbonate platform and a prolonged period of non-deposition that is known as the Knox unconformity. In Maryland, the magnitude of this lacuna is minimal because of increased local subsidence and continuous deposition. Thus, almost no gap in deposition has been identified within the Rockdale Run Formation and Pinesburg Station Dolomite (Brezinski et al., 1999).

Following the Knox exposure, the peritidal, cyclic style of deposition was reestablished and resulted in the deposition of the St. Paul Group. The vertical stacking of lithologies in the Row Park and New Market limestones represents transgressive and regressive facies of a third-order deepening event. This submergence reached its maximum deepening within the lower part of the Row Park

Limestone. Evidence of this event demonstrated in the Nittany arch region of central Pennsylvania with deposition of the equivalent Loysburg Formation. Shallow tidal-flat deposits of the New Market Limestone were bordered to the south and east by deep-water ramp deposits of the Lincolnshire Formation of Virginia. The St. Paul Group cycles are succeeded by deposition of ramp facies of the Chambersburg Formation in Maryland and the Edinburg Formation in Virginia. Carbonate deposition of the Great Valley carbonate succession was brought to an end with the progradation of deep-water clastic basinal deposits of the Martinsburg Formation.

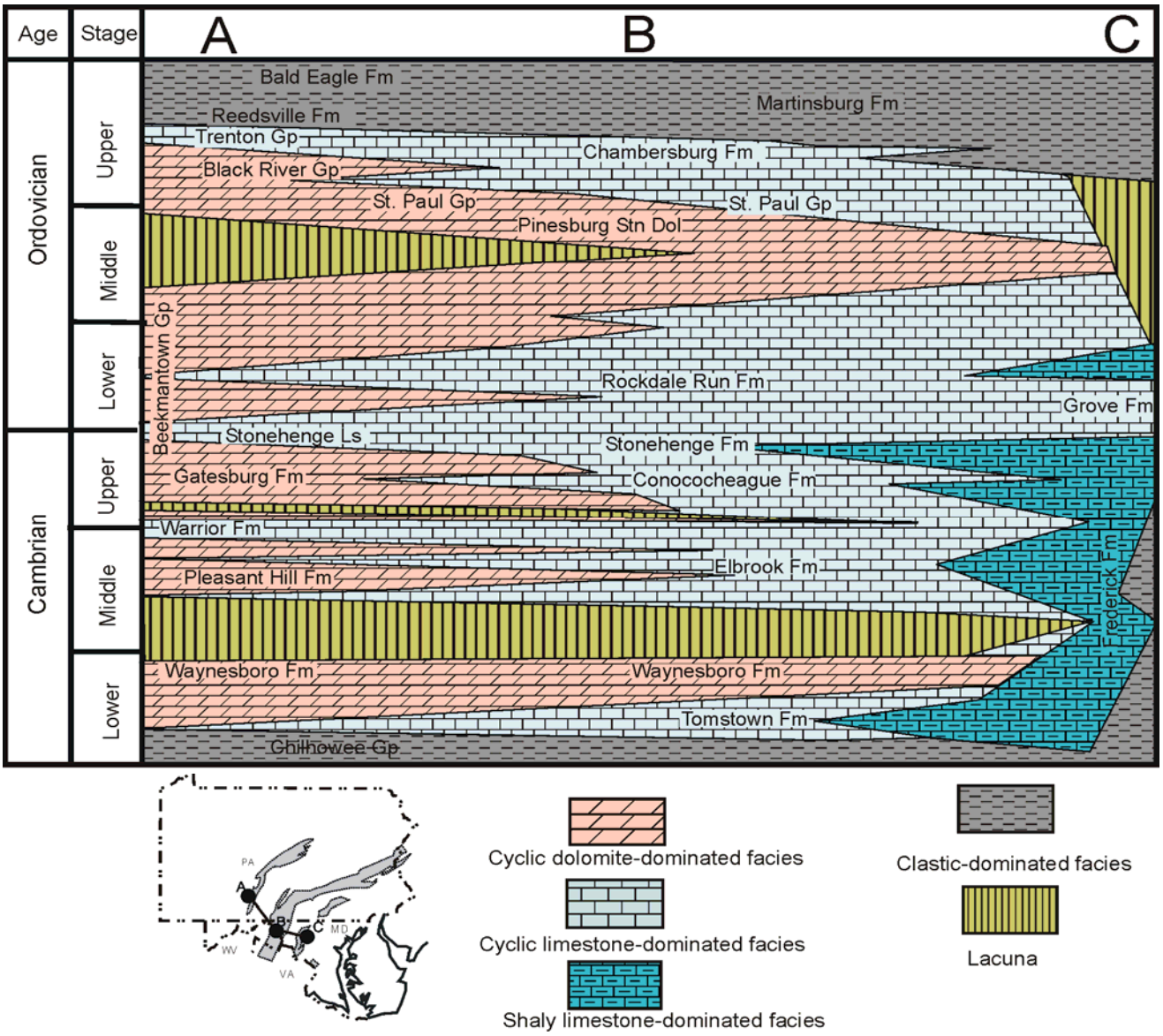

Figure 21.–Idealized facies relationships of Cambrian and Ordovician strata of the central Appalachian basin between the Nittany Arch of central Pennsylvania and the Frederick Valley of Maryland. No scale is implied, lateral relationships only.

STRUCTURES

The geologic structures (folds, faults, joints) of Maryland's Great Valley are complex, and appear to have been created through several episodes of deformation. The arrangement and distribution of the various carbonate units are the result of folds and faults produced mainly during the Alleghanian orogenic event. These structures also are important contributing factors in the development of karst systems in carbonate rocks of the Hagerstown Valley. Geologic cross-sections by Kulander and Dean (1986) have shown that there is an integral relationship between folding and faulting within the Great Valley. In Maryland, the entire Massanutten synclinorium and Blue Ridge anticlinorium, as well as most of the ancillary folding, can be attributed to movement along a large detachment fault (Figure 22). This detachment fault has been interpreted as having carried the entire Great Valley and South Mountain succession westward against the Ridge and Valley rocks. This fault comes to the surface as the North Mountain fault west of Clear Spring. Many of the subsidiary faults such as the Williamsport, Midway, and South Mountain faults are believed to originate along this basal detachment fault.

Folds

Folding is the most prominent geological structure within the Hagerstown Valley. Indeed, the entire Great Valley and adjacent Blue Ridge represent broad folds. Cloos (1947; 1971) showed that the entire Blue Ridge of Maryland represents a broad upfold that he termed the South Mountain anticlinorium (Figure 3). The South Mountain anticlinorium is overturned on its western limb (Cloos, 1958). This large fold is bordered to the west by a downfold that underlies the entire Hagerstown Valley, the Massanutten synclinorium (Figure 3). Cloos (1958) believed that these two structures were continuous with one another and were not broken by faults. The South Mountain-Massanutten folds are composite structures, and are made up of subsidiary folds of several different orders of magnitude. These smaller folds are overturned to recumbent on the overturned limbs of the South Mountain-Massanutten folds and many of their axial traces can be delineated and mapped (Figure 23).

Along the eastern margin of the Hagerstown Valley the overturned limb of the South Mountain anticlinorium has been thrust against the Tomstown Formation. Folds within the underlying Chilhowee Group strata are isoclinal and recumbent (Brezinski, 1992; Southworth and Brezinski, 1996). Folds within rocks in the eastern carbonate belt of the Massanutten synclinorium tend be overturned with axial planes that dip to the southeast (Brezinski, 1992, pl. 2). However, there are numerous folds in the outcrop belts of the Tomstown and Waynesboro formations where the axes are totally overturned and recumbent with the axial planes dipping to the northwest (Brezinski, 1992, pl. 1). The steepness of the axial planes for the overturned folds of the eastern outcrop belt tends to increase westward (Brezinski, 2009, 2013a, b); Brezinski and Bell, 2009). Thus, the orientation of the fold's axes in the eastern outcrop belt rotates from southeast dipping to vertical as one progresses from east to west.

Near the center of the Massanutten synclinorium, the fold axes become vertical and the fold limbs are steeply dipping, but the structures approach a symmetrical shape. In the western outcrop belt, the folds within the carbonate strata are broad and symmetrical.

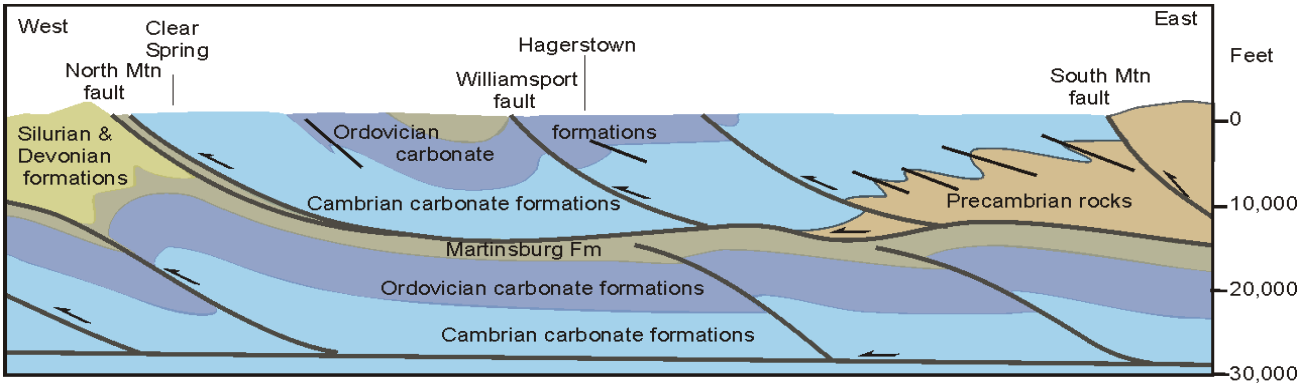

Figure 22.– Geologic cross-section of the Hagerstown Valley with interpreted relationship between folding and faulting. Modified from Kulander and Dean (1986, fig 6).

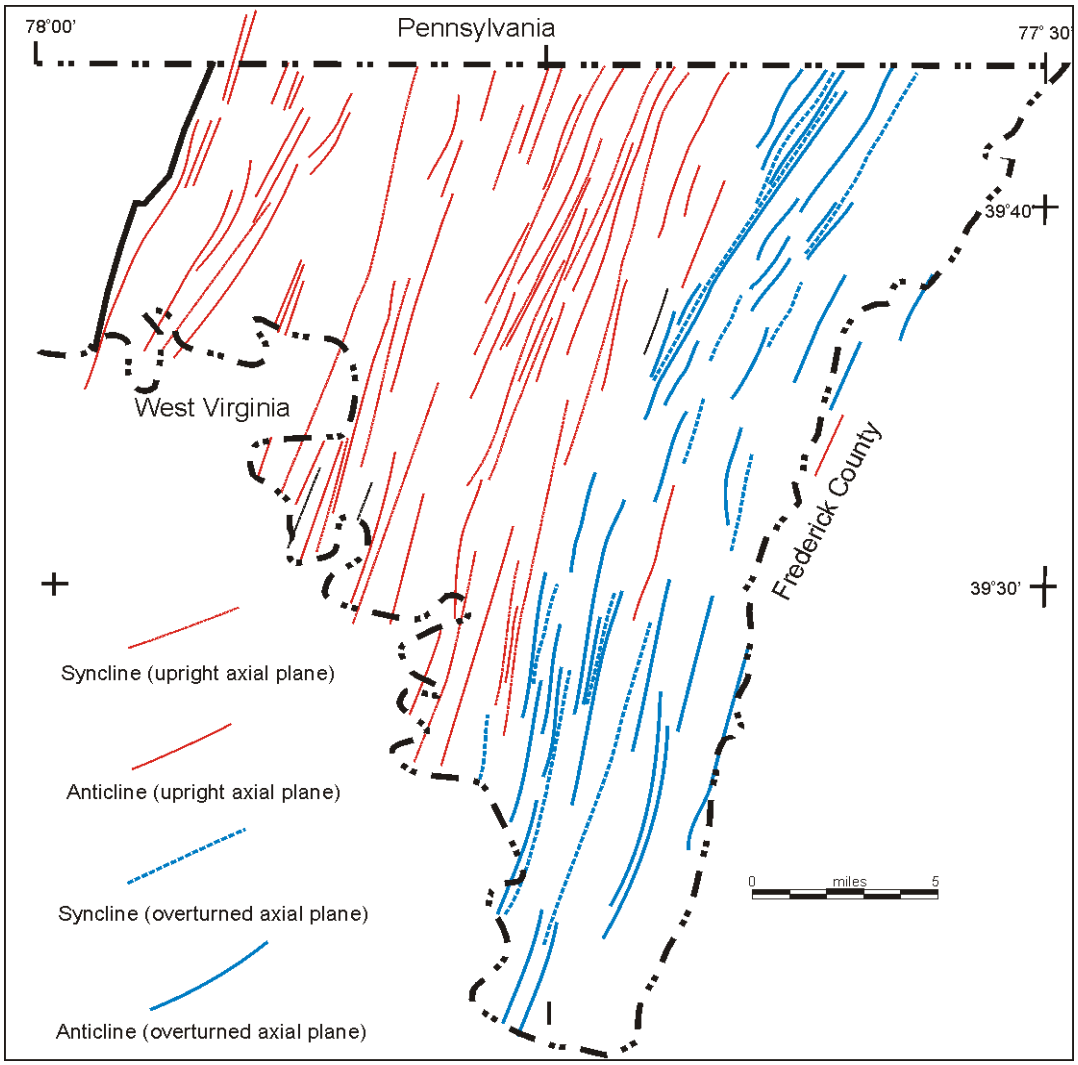

Figure 23.– Distribution of mappable fold axes within the Hagerstown Valley. Axes for the eastern Hagerstown Valley modified from Brezinski (2009, 2013a, b), Brezinski and Fauth (2009), and Brezinski and Bell (2009). Fold axes from western part of the valley modified from Sando (1957, pl. 2), Brezinski (2013a, b, 2014), and Brezinski and Glaser (2014).

The western boundary of the Hagerstown Valley is marked by an abrupt stratigraphic change that places gently folded Middle Cambrian Elbrook carbonates against highly folded Ordovician through Silurian clastic rocks of the Martinsburg, Juniata, and Tuscarora formations (Brezinski and Glaser, 2014). This change is marked by a regionally developed fault system that defines both the western edge of the Hagerstown Valley and the Massanutten Synclinorium.

Faults

Faults are fractures in rocks along which movement has taken place. These structures can be identified at various scales. Small faults, with movement measured in inches, are common in many outcrops of the Hagerstown Valley. Conversely, some of the larger faults are regional structures that have been interpreted to be the result of tens or even hundreds of miles of displacement (Figure 22). Regardless of size, faults tend to be associated with broken, fractured, and folded adjacent strata. That attribute, in conjunction with their linear character, provide conduits for long-distance groundwater flow and karst feature development.

Keedysville fault: The Keedysville marble bed at the base of the Bolivar Heights Member of the Tomstown Formation, has been interpreted as representing a fault surface (Brezinski, 1992; Brezinski et al., 1996). The interval can be traced for more than 60 miles along strike from Berryville, Virginia, to Glen Forney, Pennsylvania. At all locations this marble is lineated and parallel to

overlying and underlying bedding. Because there is no discernable stratigraphic offset, it is difficult to determine the level of stratigraphic throw. At several locations. it can be demonstrated that the marble has been folded along with the adjacent strata. This suggested to Brezinski et al. (1996) that this fault actually served as a detachment layer that separates the Cambrian and Ordovician carbonate succession from the underlying Chilhowee Group clastics. They also postulated that this fault may have been formed during the Taconic orogeny based upon multiple generations of foliation and folding (Brezinski et al., 1996).

During the course of this study no discernable karst influence was observed in association with this structure.

Beaver Creek fault: Brezinski (1992) has shown that numerous stratigraphic discontinuities are associated with the outcrop belt of the Waynesboro Formation (Figure 24A). These stratigraphic discontinuities are interpreted as representing a fault that coincided with the location of Beaver Creek, and which is termed the Beaver Creek fault (Brezinski, 1992, 2009; Brezinski and Bell, 2009; Brezinski and Fauth, 2009). The trace of the fault is very sinuous, indicating that it either has a very low angle, or has been gently folded. Because a single, low-angle fault cannot explain all of the observed discontinuous relationships, Brezinski (1992) proposed that the Beaver Creek fault may have been folded following emplacement. Besides the stratigraphic offsets, outcrop exposures reveal that a mylonitic marble interval developed at the top of the Tomstown Formation in conjunction with the formation of the Beaver Creek fault. In the Funkstown quadrangle, this fault is demonstrably mylonitic, and has been interpreted as a splay off the Keedysville detachment interval northwest of the town of Keedysville (Brezinski, 1992). If this interpretation is correct, then the Beaver Creek fault is also Ordovician in age (Taconic orogeny).

The apparent coincidence between the set of stratigraphic discontinuities associated with the Beaver Creek fault and the course of Beaver Creek itself indicates that this structure has influenced dissolution of rock to some extent. Furthermore, in the Smithsburg quadrangle, Brezinski and Fauth (2009) identified a number of springs along the fault's trace.

South Mountain fault system: Cloos (1941) showed that stratigraphic irregularities existed between the Chilhowee and Tomstown strata along the eastern boundary of the Hagerstown Valley. These stratigraphic anomalies juxtaposed overturned Chilhowee strata against the Tomstown Formation (Figure 24B). Brezinski (1992) interpreted these stratigraphic incongruities as a fault that he named the South Mountain fault (Brezinski, 2009; Brezinski and Bell, 2009; Brezinski and Fauth, 2009). The South Mountain fault can be traced southward from the Maryland-Pennsylvania State line near Penmar to Rohrersville. Southward from Rohrersville this structure coincides with a long-recognized structure that Cloos (1941) believed to be a normal fault. Southworth and Brezinski (1996) named this structure the Short Hill-South Mountain Fault. Kinematic indicators taken from core drilling that penetrated this fault near the town of Weverton, in the Harpers Ferry quadrangle, demonstrate that the fault dips gently to the east, and that the most recent movement of this fault is compressional. This is counterintuitive to the geologic relationship displayed by this fault that places younger Harpers Formation strata on older Precambrian basement gneisses. Thus, this fault is interpreted as a late Paleozoic thrust fault that places South Mountain against the Great Valley succession. However, from Rohrersville southward, this fault is interpreted as a reactivation of the early Paleozoic Rohrersville normal faulting (Southworth and Brezinski, 1996).

In the Smithsburg quadrangle, Brezinski and Fauth (2009) identified a line of springs along the South Mountain Fault. This suggests that this structure plays a significant part in the karst development in their easternmost part of the Hagerstown Valley.

Eakles Mills fault: Brezinski (1992) recognized a fault with a straight trace that passes through Eakles Mills, near Keedysville, and could be delineated northward into the Funkstown Quadrangle (Brezinski and Bell, 2009). Brezinski (1992) termed this structure the Eakles Mills fault. This structure can now be traced into Pennsylvania where it merges with the Antietam Cove Fault of Root (1968). This vertical fault is exposed within the eastern wall of the Benevola Quarry in the Funkstown quadrangle where the Dargan Member of the Tomstown is placed in contact with the Elbrook Formation (Figure 24C). The vertical fracture cleavage associated with this structure suggests that it is a brittle fracture and, thus, may be as young as Triassic.

This fault can be demonstrated to have significant impact on the karst development adjacent to its trace. The most significant effect is a line of springs that have been identified along the fault line.

Williamsport fault: Stose (1910) and Root (1968) identified a series of faults along the contact between the Ordovician carbonate rocks and the Martinsburg Formation in southern Franklin County, Pennsylvania. Geologic mapping in Maryland (Sando, 1957; Brezinski, 2013b, 2014) has shown there are stratigraphic irregularities that place folded strata of the Stonehenge Limestone through Chambersburg Formation on the east against the

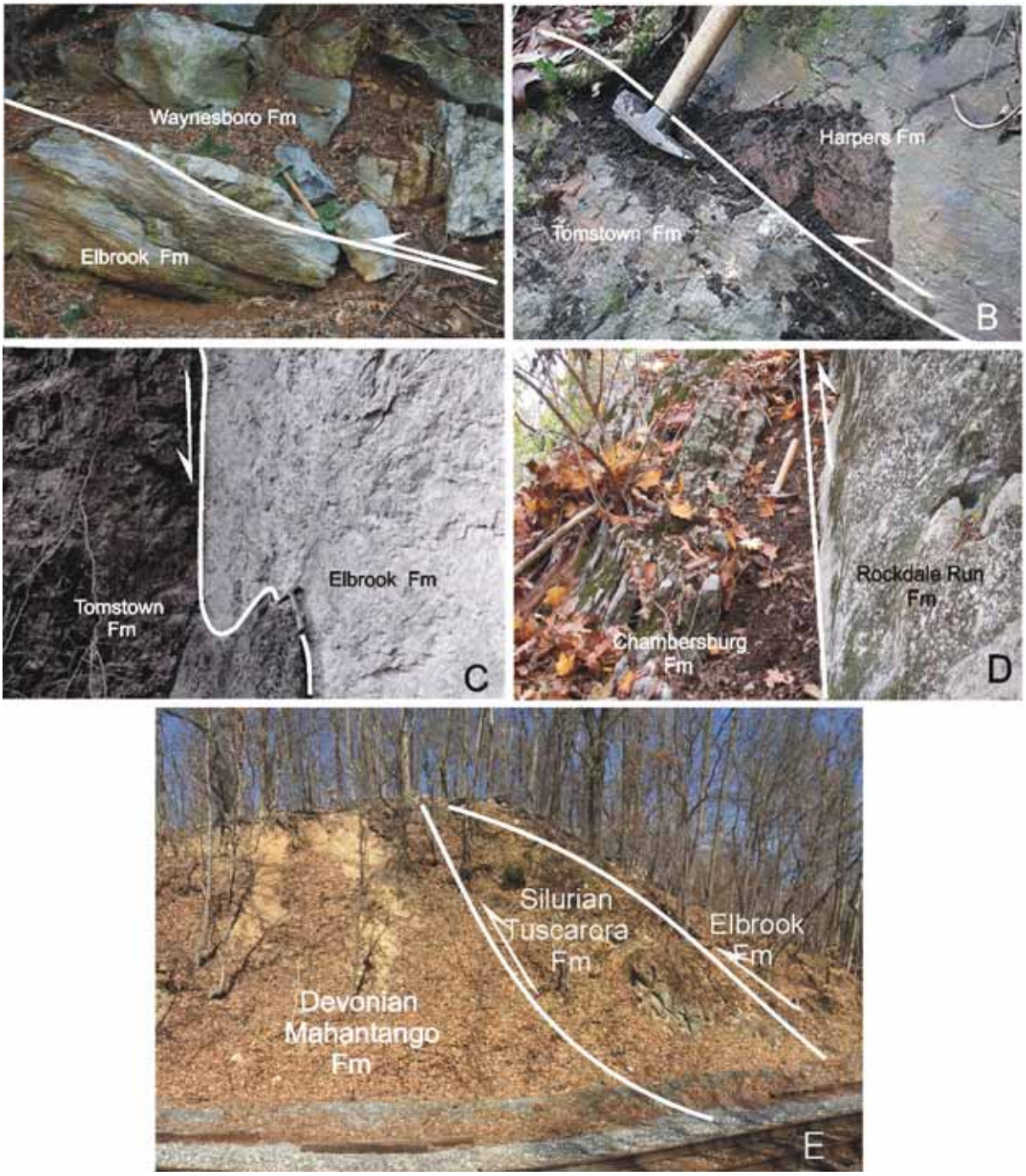

Figure 24.– Examples of faults exposed in the Hagerstown Valley. A, Beaver Creek fault, Wagners Crossroads. Cavetown Member of the Waynesboro Formation is thrust over the Elbrook Formation. B, South Mountain fault, Edgemont, Maryland. Phyllites of the Harpers Formation thrust over the Bolivar Heights Member of the Tomstown Formation. C, Eakles Mills fault at Benevola Quarry. Elbrook Formation is in fault contact with the Benevola Member of the Tomstown Formation. D, Williamsport fault along the C&O Canal. Steeply inclined fault plane places the Rockdale Run Formation against the Chambersburg Formation. E, North Mountain fault, McCoy's Ferry. Footwall rocks of the Middle Devonian Mahantango Formation are overridden by the Middle Cambrian Elbrook Formation. A slice of the Silurian Tuscarora Formation is caught between the two blocks.

Martinsburg Formation. The line of discontinuities passes through the town of Williamsport and, consequently, was named the Williamsport fault by Brezinski (2014). Where it crops out, this fault exhibits a dip of approximately 60° to the southeast (Figure 24D) and places Rockdale Run Formation dolomites against the Chambersburg and Martinsburg formations. Exposures along the C&O canal demonstrate that numerous subsidiary faults are associated with this structure (Figure 24D). This fault can be traced southward into West Virginia (Dean et al., 1987) where it merges with the Files Crossroad fault.

Halfway fault: East of the Williamsport fault is a structure that is evidenced by truncation of stratigraphic units and folds. This structure is suggested at the Potomac River by the folding and truncation of the Big Spring Station Member of the Conococheague Formation against younger strata of the Zullinger Member near Dam Four (Brezinski, 2014). As this structure is traced northward through Halfway, it juxtapose of various members of the Stonehenge Limestone against the Rockdale Run Formation (Brezinski, 2013b). It currently can be traced from the Potomac River into southern Franklin County, Pennsylvania (Root, 1968), where it merges with a number of smaller discontinuities. Because this structure exhibits only modest amounts of stratigraphic offset, it is interpreted to be of minor significance within the Great Valley succession.

North Mountain fault system: The western boundary of the Great Valley in Maryland is demarcated by a large fault or system of faults that is present at the eastern base of Fairview Mountain (Brezinski and Glaser, 2014). This fault system places the middle Cambrian Elbrook Formation in the hanging wall against a foot wall of the Martinsburg Formation, and locally, Silurian and Devonian strata on the footwall. This structure is a regional discontinuity that can be traced from Staunton Virginia into southern Pennsylvania (Stose, 1910). Kulander and Dean (1986) interpreted this system as the sole of a thrust sheet that includes the entire Great Valley succession and places it against younger Ordovician, Silurian, and Devonian strata (Kulander and Dean, 1986; Orndorff, 2012). Brezinski and Conkwright (2012) and Brezinski and Glaser (2014) interpreted this fault as a thrust and maintained that a number of closely spaced faults juxtaposed to Fairview Mountain are congruent splays related to this large structural discontinuity.

Cross-Strike faults: Several discontinuities appear to trend across the regional strike and truncate both stratigraphy and structures. These cross-strike faults appear to have developed very late in the deformational history of the area, inasmuch as they offset many of the large structures and have been interpreted as extensional features (Orndorff, 1992). These faults tend to exhibit stratigraphic offset of between 50 to 100 feet.

Where Interstate 70 crosses South Mountain, a structure trends subparallel to the highway. This structure truncates the Catoctin Formation and Chilhowee Group rocks of the Blue Ridge. Brezinski and Fauth (2009) recognized this structure and named it the I-70 fault, since it is subparallel to the highway. Along the same trend, there are recognizable offsets in the Tomstown, Waynesboro, and Elbrook formations. Although the relative directions of motion are not always consistent with that observed on South Mountain, these offsets are interpreted to represent the same cross-fault. The I-70 cross-fault is the largest cross-strike feature observed in this study.

Figure 25.– Outcrop joint patterns. A, Reticulate pattern of joints within a dolomitic layer in the Elbrook Formation. B, Dissolution along interconnected joints within the Stonehenge Limestone.

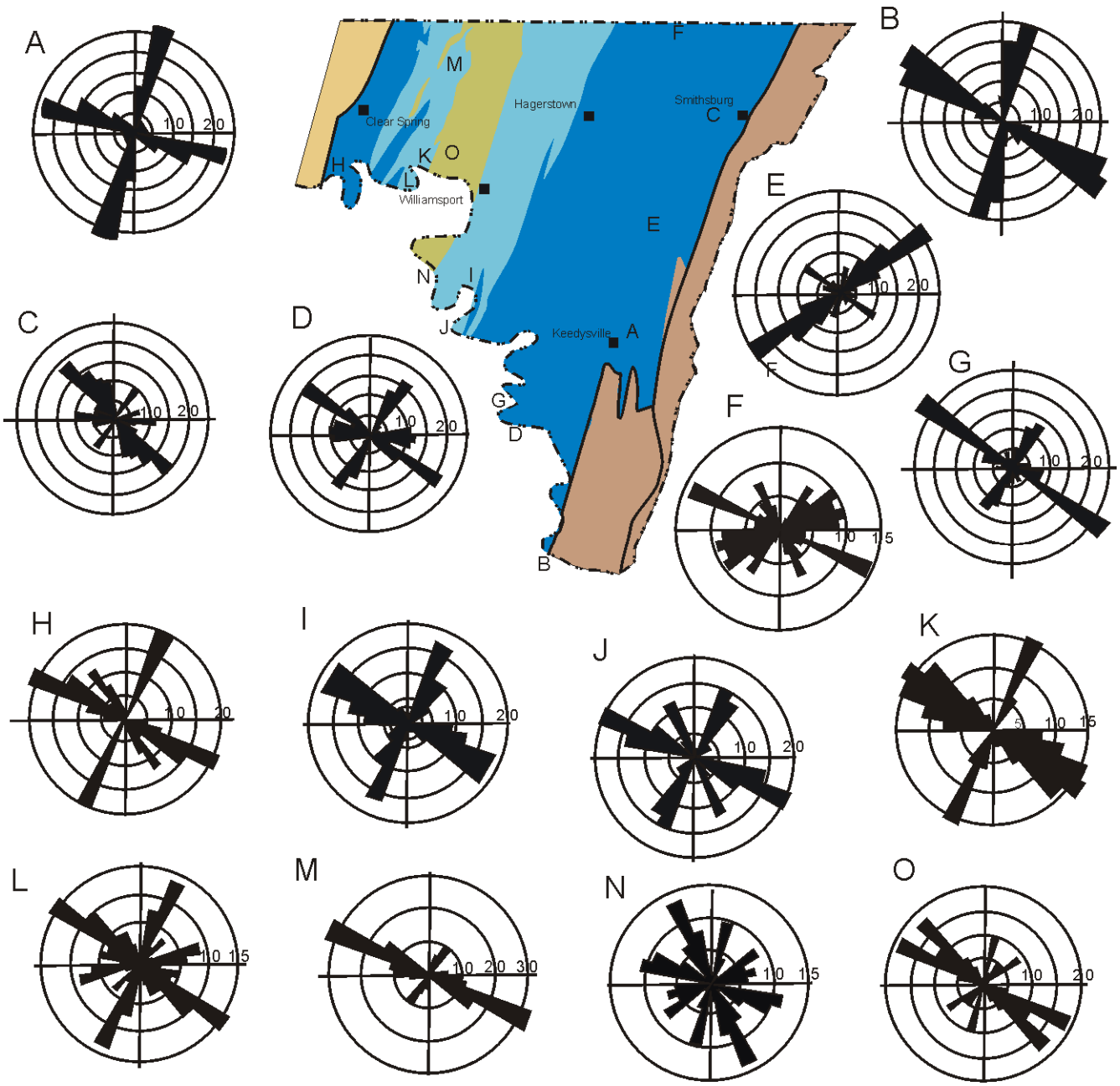

Figure 26.– Geologic and geographic variations in fracture plane orientation within strata of the Hagerstown Valley. A, Tomstown Formation, Bolivar Heights Member, Crystal Grottoes. N=120. B, Tomstown Formation, Bolivar Heights Member along C&O Canal at Fort Duncan. N=110. C, Waynesboro Formation, Cavetown quarry. N=103. D, Elbrook Formation, River Road, Shepherdstown, West Virginia. N=101. E, Elbrook Formation, Beaver Creek quarry, west pit. N=96. F, Elbrook-Conococheague contact, Maryland Route 60 at Pennsylvania State line. N=103. G, Lower part of the Conococheague Formation, C&O Canal, Snyders Landing. N=101. H, Conococheague Formation, C&O Canal, Four Locks. N=75. I, Stonehenge Limestone, Funkstown Member, McMahons Mill. N=124. J, Rockdale Run Formation, Big Slackwater area. N=99. K, Rockdale Run Formation, C&O Canal, milemarker 103. N=114. L, Pinesburg Station Dolomite, Pinesburg quarry and C&O Canal. N=112. M, St. Paul Group, Rockdale Quarry. N=52. N, Chambersburg Formation, C&O Canal, Potomac Sportsman's Club. N=79. O, Martinsburg Formation, lower member, Pinesburg. N=79.

Orndorff (1992) studied a smaller cross-strike fault along College Road near St. James, Maryland. Duigon (2001) noted a number of springs align with this fault.

Joints

Perhaps the most pervasive geologic structure in the Great Valley is joints. Joints are fractures that along which no perceptible movement has taken place. These fractures are present to varying degrees in all formations in the Hagerstown Valley (Figure 25). Their numbers and orientations tend to change in relationship to variations in rock composition or with respect to their proximity to faults or position on fold limbs. In general, those joints that are oriented perpendicular to fold axes are termed cross joints and those that lie parallel to axes are called strike joints. Joints tend to be an understudied type of structure, but they play an important role in the understanding of the deformation of sedimentary rocks. In karst areas, joints present interconnected fracture planes that offer avenues for interformational and intraformational waters to pass. This prevalent water flow causes dissolution and widening of the individual joint planes. The result is constant widening of the planes until they become sufficiently large enough to allow collapse of soils or other surficial coverings.

Figure 26 demonstrates the directional variability exhibited of joints within the different carbonate rock formations of the Hagerstown Valley. This figure illustrates that, at any single outcrop, the orientation of jointing is commonly dominated by a single direction of fracturing. However, a secondary, typically ancillary direction is commonly displayed normal to the dominant direction (Figure 26 A, B, D, G, H, I, K, L). Most commonly, the dominant set possesses a northwest strike with azimuth ranging from 280° to 310°. The second, usually less dominant, group of joints tends to have azimuths of 0° to 30°. There also are rare examples where there is no clearly dominant joint orientation (Figure 26 F, N).

A slightly different view of the joint orientations is obtained when the strikes of all joint surfaces measured during this study are assembled in a composite diagram (Figure 27). Rose diagrams of the azimuths of 2,009 joint surfaces measured during this study are portrayed using 2-degree (Figure 27A) and 5-degree (Figure 27B) petals. These rose diagrams clearly illustrate the dominant joint sets that pervade the rocks of the Hagerstown Valley. In Figure 27A the prominent northwest striking joints are at 293°, 300°, and 305°. In Figure 27B these individual sets are merged into the combined northwest petal that ranges from 290° to 310°. This is the dominant strike direction of jointing in the Great Valley of Maryland. The main fracture system is orientated normal to the structural strike of the South Mountain and Massanutten folds, suggesting that it represents extension normal to the main strain that formed the Great Valley in Maryland (Cloos, 1971).

In addition to the dominant northwest-striking joint sets, a secondary, northeast-striking, group of joints is evident. These fractures are dominated by sets striking at 25° and 32° (Figure 27A). These individual sets are more clearly evident in Figure 27B where their strike ranges from 25° to 35°. This set of fractures parallels the dominant direction of axial planar cleavage seen in subordinate folds of the Hagerstown Valley. Therefore, this group of fracture planes is interpreted as paralleling the axial plane of the Massanutten synclinorium (Cloos, 1971).

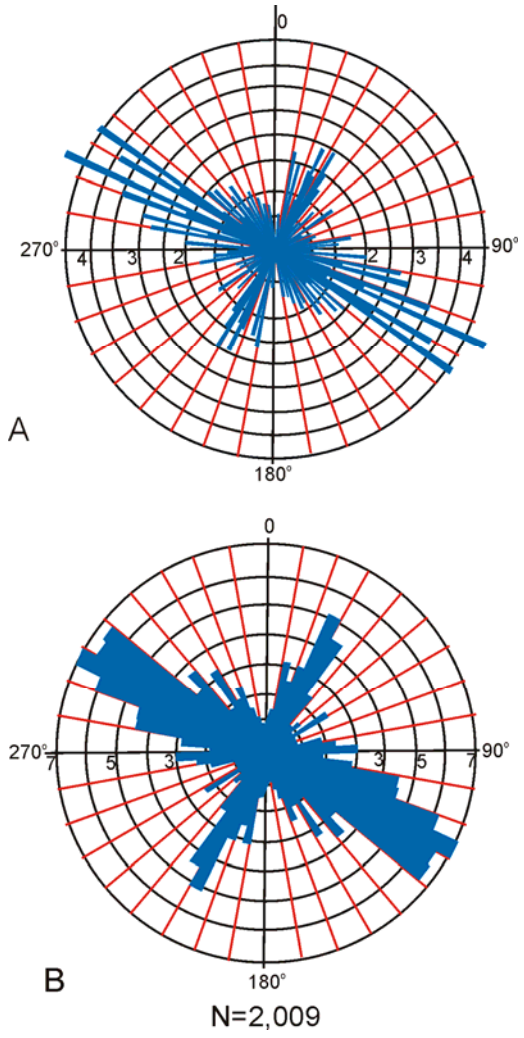

Figure 27.– Rose diagrams utilizing two- (A) and five-degree (B) petals for the strike azimuths of 2,009 joint surfaces measured within rocks of the Hagerstown Valley.

Beyond these two prominent striking sets of joints, there are ancillary sets of fractures that approach an east-west strike of 85° and 265°, and another set that varies from 315° to 340°. These sets are locally prominent at particular outcrops (Figure 26 D, J, N, respectively).

The main fracture systems observed in the Hagerstown Valley are parallel and perpendicular to the compressional and tensional stresses experienced during the creation of the Blue Ridge anticlinorium and Massanutten synclinorium. These stresses were developed during the Alleghanian orogeny, approximately 250 million years ago. An understanding of the prominence and pervasiveness of these rock fractures can lead to better prediction of subterranean water movement and, thus, better comprehension of the genesis of sinkholes and springs in the Hagerstown Valley.

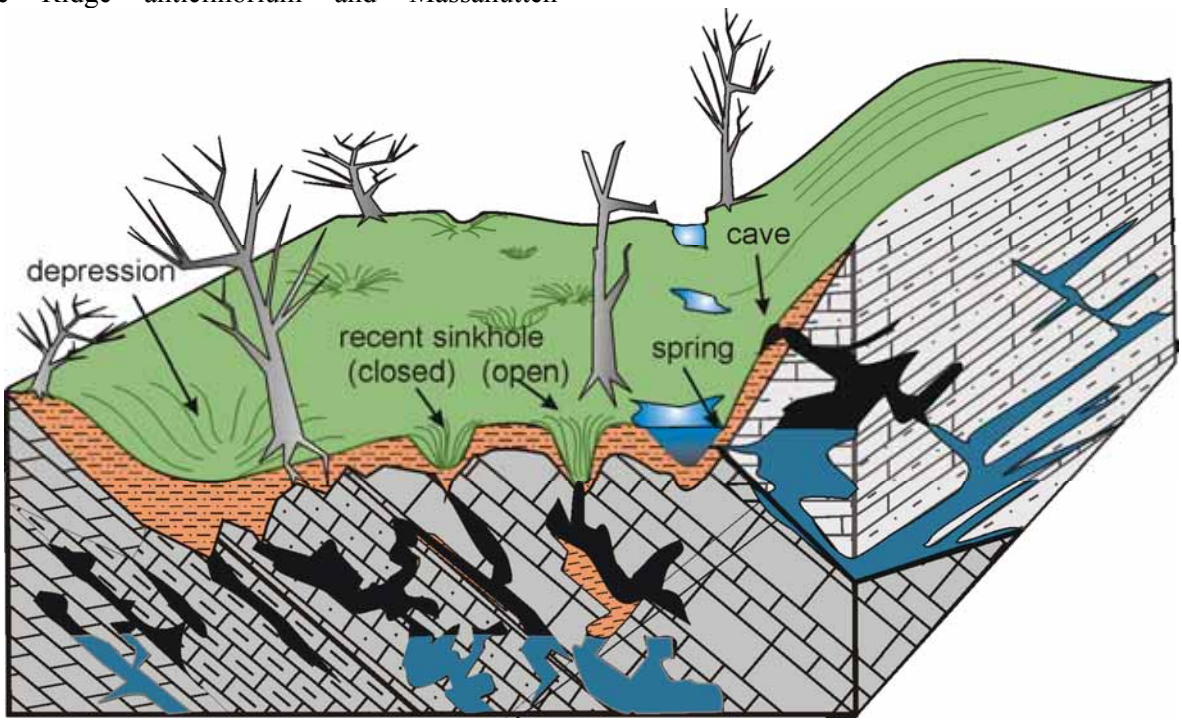

Figure 28.– Idealized karst and the types of features identified in this study.

KARST DEVELOPMENT IN THE HAGERSTOWN VALLEY

The stratigraphy and structure discussed above provide a generalized foundation that can help in understanding the variations in the make-up of the bedrock and aid in delineating karst feature distribution. The distribution, density, and types of karst features can be shown to be controlled by these variations in rock composition, texture, and fracturing. Without a well-defined geologic basis for comparison, it would be difficult to evaluate whether the distribution of karst features is related to geologic, topographic, hydrologic, or human-induced factors. The remainder of this report will discuss the identification and distribution of karst features, and the evaluation of whether their distribution, frequency, and dimensions are related to bedrock geology or one of these other factors. Four types of karst features were identified during the Hagerstown Valley study. These are: depressions, active sinkholes, springs, and caves (Figure 28). Closed depressions, or dolines, are by far the most common type of karst feature encountered. Depressions are low areas towards which the surrounding topography is inclined (Figure 29A). These depressions are typically bowl-shaped, but can be elongate. Depressions vary greatly, not only in their outline, but also in size. They can occur as small, shallow depressions as little as several yards across to broad indentations, more than 100 yards wide. Such large, shallow depressions tend to form in areas along the eastern and western margins of the Hagerstown Valley in areas covered by thick accumulations of colluvium. These large features appear to represent slow dissolution of the underlying bedrock. However, the thick cover of Quaternary deposits and soil produces a slowly subsiding bedrock-overburden interface. Examination of some smaller depressions shows that, through time, they have coalesced to form large depressions.

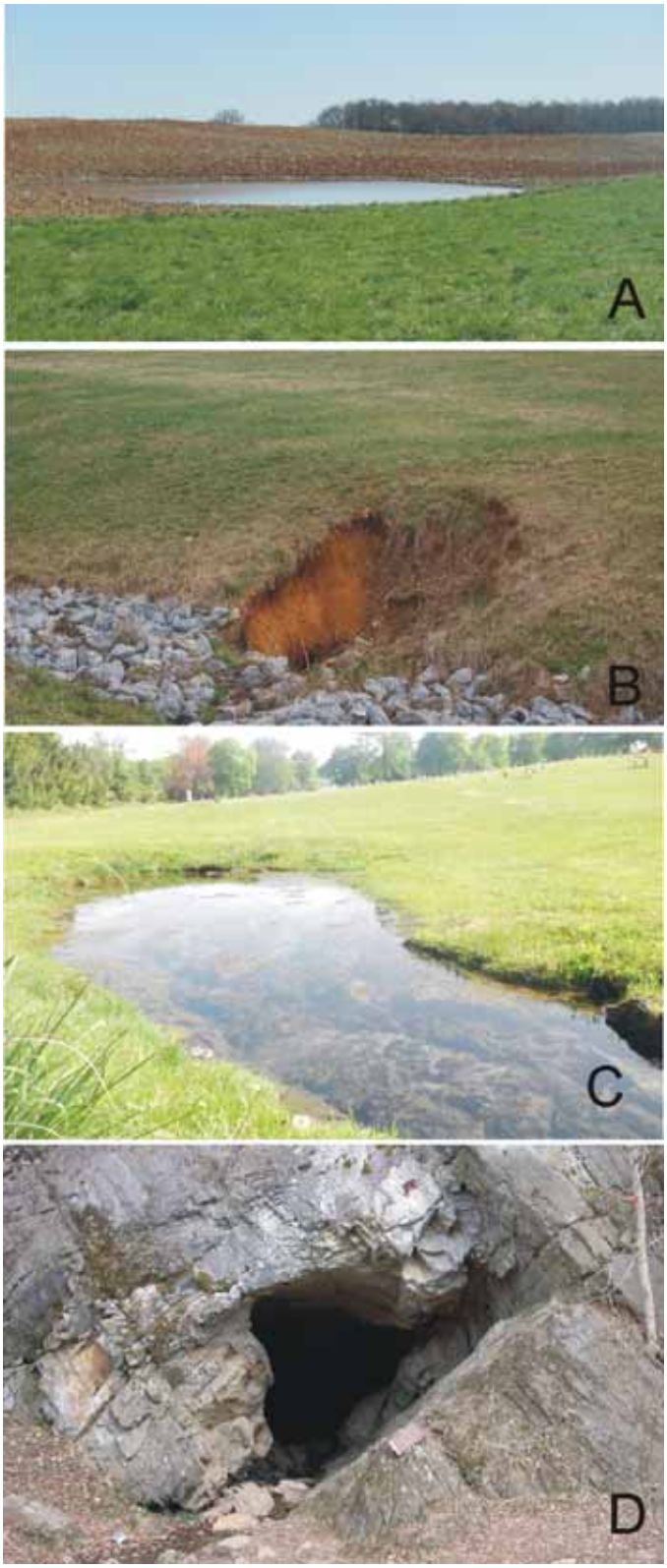

Figure 29.–Types of karst features identified and located in this study. A, Depressions. B, Active collapses. C, Karst springs. D, Caves.

The second category of karst features recognized in this study is active collapse sinkholes. As with closed depressions (i.e. dolines), active sinkholes can display a wide range of surficial features. The most common, and widely recognized, type of active sinkhole in the Hagerstown Valley exposes an open throat and occurs as clear gaping hole (Figure 29B). The active category also includes narrow, steep-sided depressions that lack an open throat, but are unvegetated, suggesting recent activity. Soil cover-collapses occur when soil bridges that covered an open or partially open subterranean void fail. Collapses that are known to have occurred in recent years and have been repaired also are included in this category. Lastly, swallowholes in streambeds wherein the stream starts subterranean flow, are considered as a specific type of active sinkhole.

The third category of karst features identified during the course of this study is karst springs (Figure 29C). While these are not one of the more common types of karst features, they represent an important component that helps shed light on movements of subterranean water and groundwater-surface water interaction.

Caves are the least common type of karst features, but generally are considered an important karst element (Figure 29D). Caves are open voids of varying size that are produced by subterranean groundwater flow and subsequent rocks dissolution. Caves that were encountered during geologic field work were located and noted. However, because these features have been exhaustively described by Franz and Slifer (1971), they were not examined extensively in this study. Consequently, cave occurrences within the current data matrix are probably underrepresented. The reader should be aware that the data set upon which this report is based does not represent a complete and exhaustive compilation of all karst features present in the Hagerstown Valley. It simply represents an unbiased sampling of karst data with respect to the geologic units.

The various types of karst features were identified from the above-described in conjunction with geologic field mapping efforts, and pictorially presented as a GIS layer on published geologic and karst maps of the Maryland portions of the Keedysville, Shepherdstown, Harpers Ferry, Charlestown, Funkstown, Myersville, Smithsburg, Hagerstown, Mason-Dixon, Williamsport, Clear Spring, and Hedgesville 7.5-minute quadrangles (Brezinski, 2009, 2013a, 2013b, 2014; Brezinski and Bell, 2009; Brezinski and Fauth, 2009; Brezinski and Glaser, 2014). These geographic areas were canvassed during

geologic field mapping, and definable karst features were precisely located and identified utilizing a Trimble GeoExplorer III® Global Positioning System (GPS) receiver. In some circumstances, features that could not be entered because of property permission constraints were located by offsetting to another location where the azimuth back to the feature could be determined, and the distance could be delineated by utilizing a laser range finder.

Once data were collected in the field, GPS files were post-processed. Post-processing is an office procedure whereby the locations identified by the field receiver are differentially corrected by comparing the exact position of the satellites in the constellation as recorded by the field receiver with the position of the satellites as recorded by a base station. The primary base station used in this study is the U.S. Geodetic Survey receiver at Hagerstown, Maryland. When that base station was not operating, a secondary station at Gaithersburg, Maryland or Richmond, Virginia was utilized. In some cases, poor field data quality, owing to an inadequate satellite constellation, produced files that could not be post-processed. In such cases, these data points were either used without being differentially corrected, or the sites were revisited to acquire new data. The *corrected* (post-processed) GPS files and their locations typically have a precision of less than 1 meter; however, those that were not corrected commonly have accuracy of 5 to 10 meters. While both of these levels of precision are insufficient for most surveying purposes, even the unprocessed files were considered of adequate resolution for the current study of 1:24,000 scale mapping, especially when one considers that some of the larger depressions were more than 200 feet in diameter. The karst feature locations were stored in the State Plane Coordinate System with a North American Datum (NAD) of 1983.

In addition to the geographic coordinates, data acquired at each location included the karst feature type, bedrock unit identification, presence or absence of Quaternary deposits that might cover the feature, and other possibly significant characteristics, such as location in a drainage lowland, drainage ditch, or storm water management reservoir.

Karst Feature Summary

Three thousand eight hundred and one karst features were identified and located in the ten quadrangles (or partial quadrangles) that comprise the Hagerstown Valley. This count of karst features does not represent a complete catalogue of all karst features present in the Hagerstown Valley. However, because most accessible areas were examined, the total can be considered a representative delineation of the features present.

Depressions are by far the most common feature recorded, making up nearly sixty six percent of all identified features (Figure 30). Active sinkholes comprised twenty-five percent of all features. Springs and cave entrances constituted nine percent and 0.5 percent of all karst features, respectively.

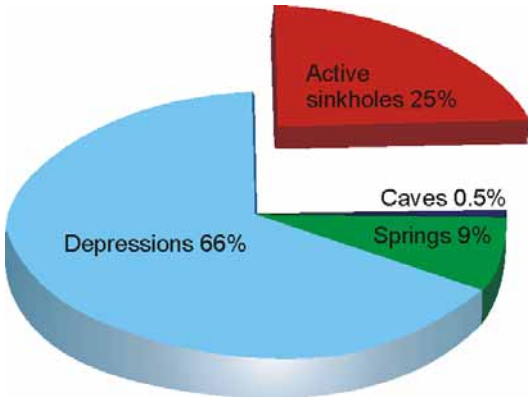

Figure 30.– Pie diagram summarizing the relative percentages of the different types of karst features identified during study of the Hagerstown Valley.

These percentages differ only modestly from those observed in the final results of the Frederick Valley karst terrain study (Brezinski, 2004a, fig. 26). Within the Frederick Valley, depressions were only slightly less abundant, constituting sixty-four percent of all karst features. Conversely, active sinkholes were more prevalent in the Frederick Valley, and made up slightly more than thirty-four percent of karst features. Springs were significantly less prominent in the Frederick Valley, representing 1.8 percent of karst features. As in the Frederick Valley, cave entrances in the Hagerstown Valley were so rare that they were considered statistically insignificant.

Karst Feature Distribution

The 3,801 features located during this study are not distributed evenly throughout the Hagerstown Valley. Although their distribution did not appear to be random, identifying proximate or possible reasons for their distribution is in some cases tenuous. Nonetheless, there are several statistically testable observations that indicate distributional relationships. For example, springs tend to occur along, but are not restricted to, major stream courses (Figure 31). Not only is this suggested by the distribution shown on Figure 31, but frequency distribution similar relationship (Figure 32). Furthermore, springs show a strong parallel distribution to mapped faults (Figure 32).

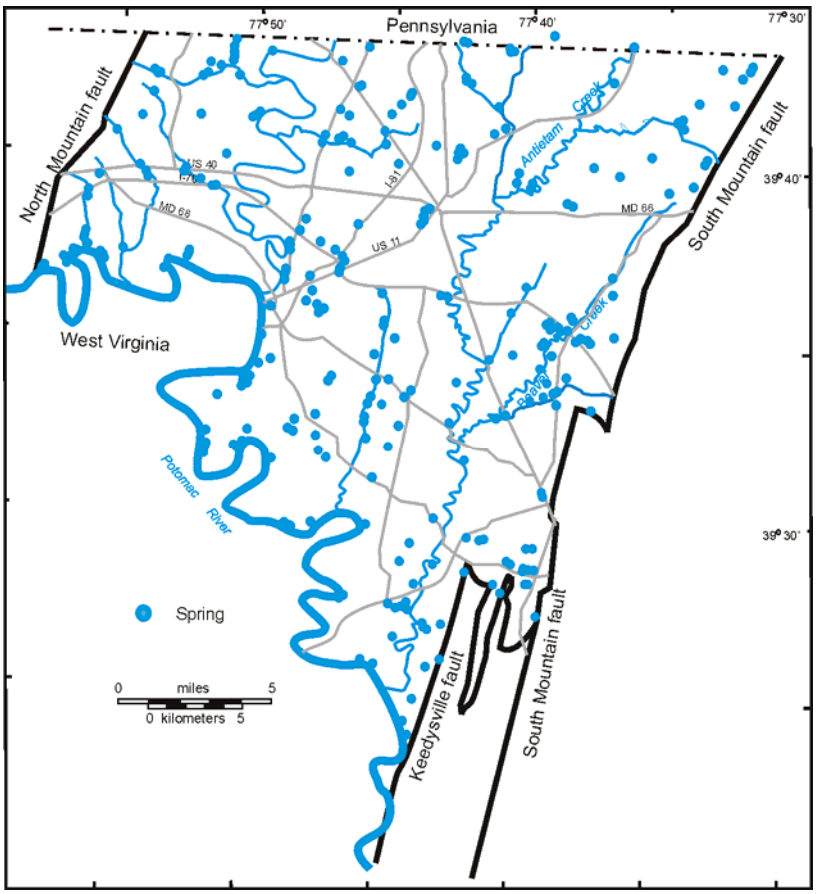

Figure 31.– Map of identified springs found in the Hagerstown Valley.

Depressions are the most common karst feature encountered during this study. Varying sizes of these features can be found throughout the Hagerstown Valley. However, there are several areas where depressions are clustered (Figure 33). A few areas of clustering are adjacent to the Potomac River and Conococheague Creek where the hydrologic gradient increases. The greatest grouping of depressions appears along the eastern and western margins of the Hagerstown Valley. Nearly 35% of all depressions are located near the eastern and western borders of the valley. These areas are covered by thick wedges of sandstone colluvium that are interpreted as having once covered the flanks of South Mountain on the eastern side of the valley and Fairview Mountain on the western side. This relationship is interpreted to be the result of intense dissolution in these areas. However, the thick colluvium appears to have clogged the karst system, inhibiting active sinkhole development.

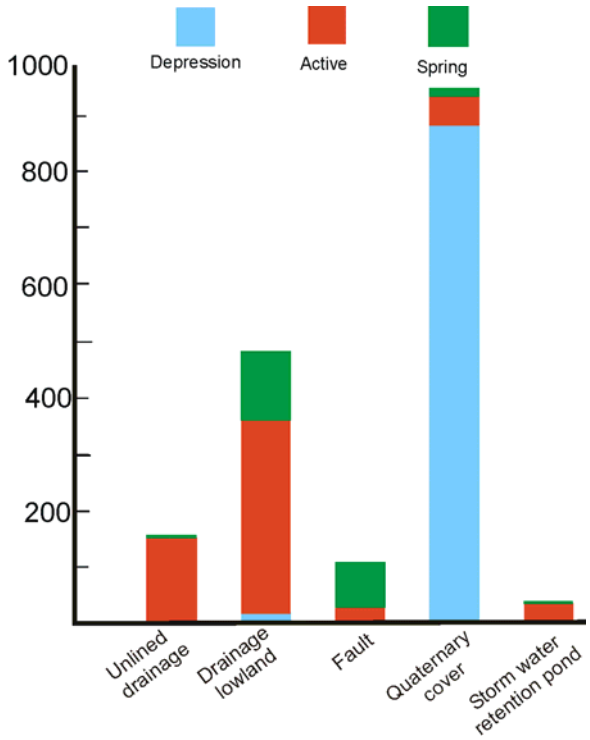

Figure 32.– Karst feature causation. A, Stacked bar chart of attributable causation to karst feature development in the Hagerstown Valley.

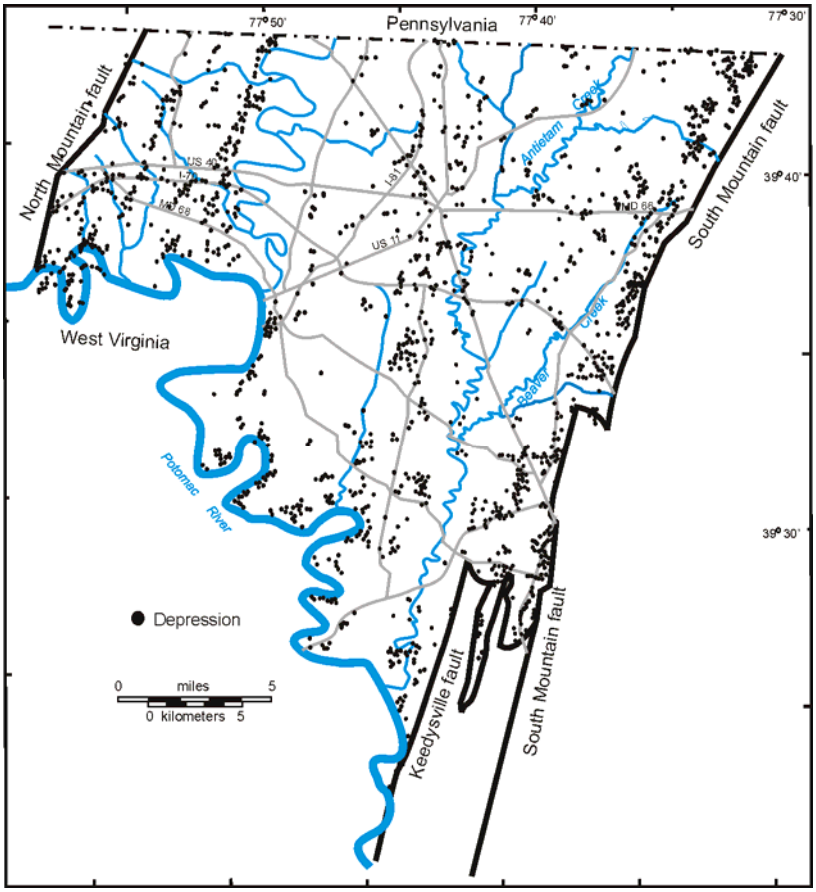

Figure 33.− Distribution of identified depressions in the Hagerstown Valley.

Active sinkholes are less common than depressions, but are important feature because of the potential life and property loss. Although active sinkholes can come in varying sizes, they tend to be small features only several meters wide and deep. Active sinkhole can be shown to be largely related to stream lowlands and unlined roadside drainage. They also tend to be more common adjacent to the Potomac River and Conococheague Creek (Figure 34).

Structure as a Factor in Karst Feature Distribution

A variety of stratigraphic and structural factors can be shown to contribute to the distribution, density, and type of karst features. Rock structures, both sedimentological and structural, are demonstrably important causative factors in karst development in the Hagerstown Valley. Several structural elements were evaluated to assess their effect on karst feature development and distribution.

Stratification: Changes in sediment size or composition can lead to weakness in rock strata. These changes are created by variations in depositional processes, such as energy level, temperature, or sea level height, and can produce differences in grain size, shape, and composition in the primary layers known as bedding or stratification. Planes of weaknesses are called partings, and can develop along these different layers. This type of fracture is often overlooked as an avenue of dissolution, but there are many examples where this is evident in the limestones and dolomites of the Hagerstown Valley. These narrow voids are especially important in folded strata where they may be widened or even closed by movement of fluids. During structural deformation such incompetent layers may amplify rock movement, folding, faulting, and fracturing, and consequently allow passage and dissolution by interstitial and intrastratal waters. These parting planes are enlarged further as solutions continue to pass through them. Thus, those units with abundant parting planes can provide increased potential for karst development (Figure 35A).

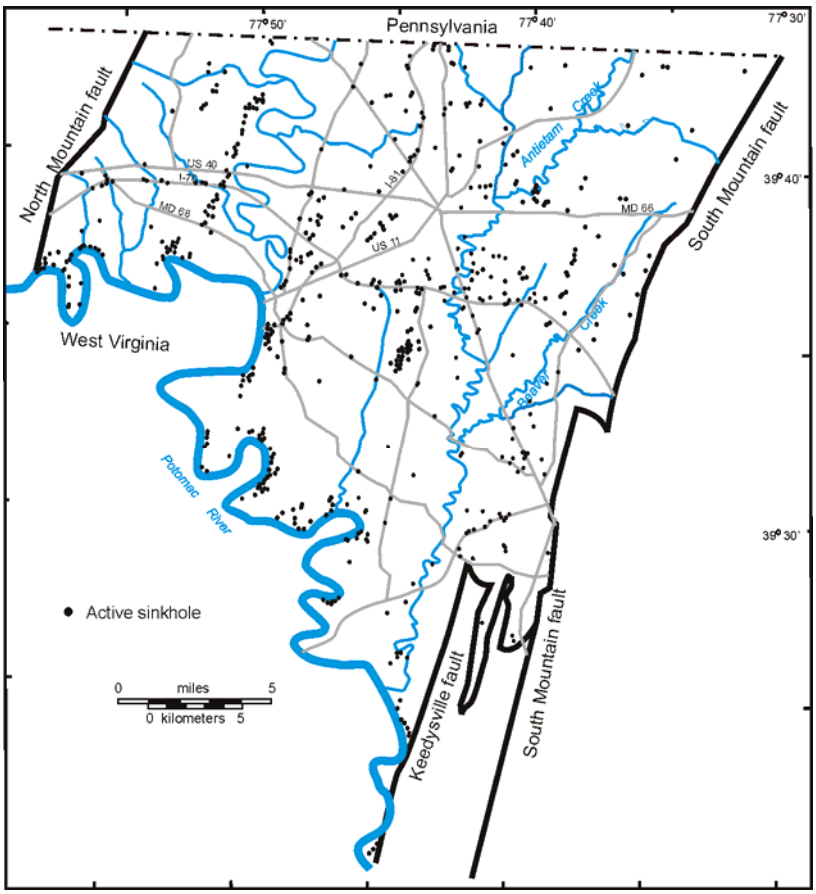

Figure 34.− Distribution of identified active collapse sinkholes in the Hagerstown Valley.

During this study, numerous cases of solution-widened fractures were observed and documented. Bedding dissolution can be one of the more prominent fracture systems that allow preferential dissolution. This means solution also can penetrate deep into the bedrock substrate. In many cases, particular strata such as those that are purer carbonate have higher levels of internal fracturing that preferentially dissolves (Figure 35 B, C).

One of the most prominent examples observed during this study is illustrated in a sketch made of an area along the C&O Canal in the Keedysville quadrangle (Figure 36). At this site, solution avenues tend to parallel bedding planes in the overturned bedding of the Bolivar Heights Member of the Tomstown Formation. A secondary solution system is recognized that trends perpendicular to the main fracture system, which in this case is the joint network.

Another case illustrative of preferred solution along stratification is the development of caves at Snyders Landing, near Sharpsburg (Figure 37). At this location, solution has persisted along a fractured dolomite interval within the Conococheague Formation. Numerous entryways are evident, and tend to follow the vertical stratification. Intersecting joint surfaces provide auxiliary and secondary passageways for the cave.

Figure 35.– Primary bedding and dissolution. A, Bedrock grikes with intervening soil-filled runnels in the St. Paul Group strata exposed in a pasture near Pinesburg. B, Dissolution of dolomite strata within the St. Paul Group. C, Bedding dissolution within the Rockdale Run Formation.

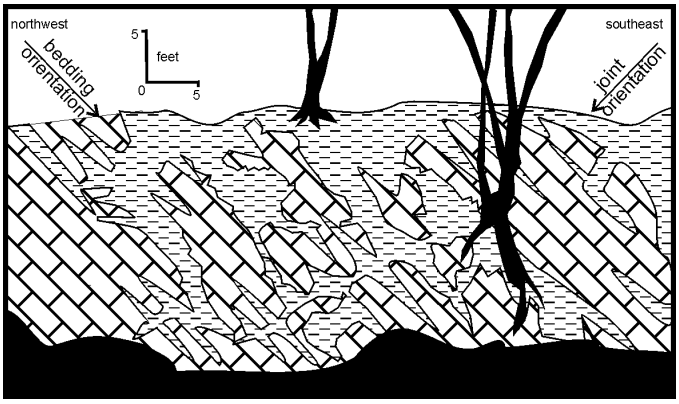

Figure 36.—Sketch of filled solution cavities within the thinly bedded Bolivar Heights Member of the Tomstown Formation along the C&O Canal National Historic Park at 65.3. Solution-filled cavities tend to parallel original limestone stratification (bedding) and, to a lesser extent, the intersecting joints.

Jointing: As discussed in the previous section and illustrated in Figure 25, joints pervade all rock units of the Hagerstown Valley. The prominence of joints and their susceptibility to dissolution vary from one bedrock formation to another and lithology. Joints that tend to produce the widest solution cavities appear to form within more massive units or in units composed of purer carbonate such as those containing thrombolitic layers (Figure 38A). Joints within thinly bedded or shaly carbonates commonly are narrow and discontinuous. Typically, outcrops display several different systems of joints that trend in different directions. The intersections of these fracture planes that are oriented in several different directions allow for the development of a network of dissolution. These fracture systems in conjunction with bedding planes produce a dissolution network that characterizes shallow bedrock in karst terrains. Where joints and cleavage or joints and stratification intersect, there are abundant opportunities for water to permeate and dissolve the surrounding rocks. These avenues are enlarged through time to produce a maze-like dissolution pattern. In cases where the soil is removed by erosion, the remnant limestone pinnacles clearly delineate the areas between joint planes (Figure 38B).

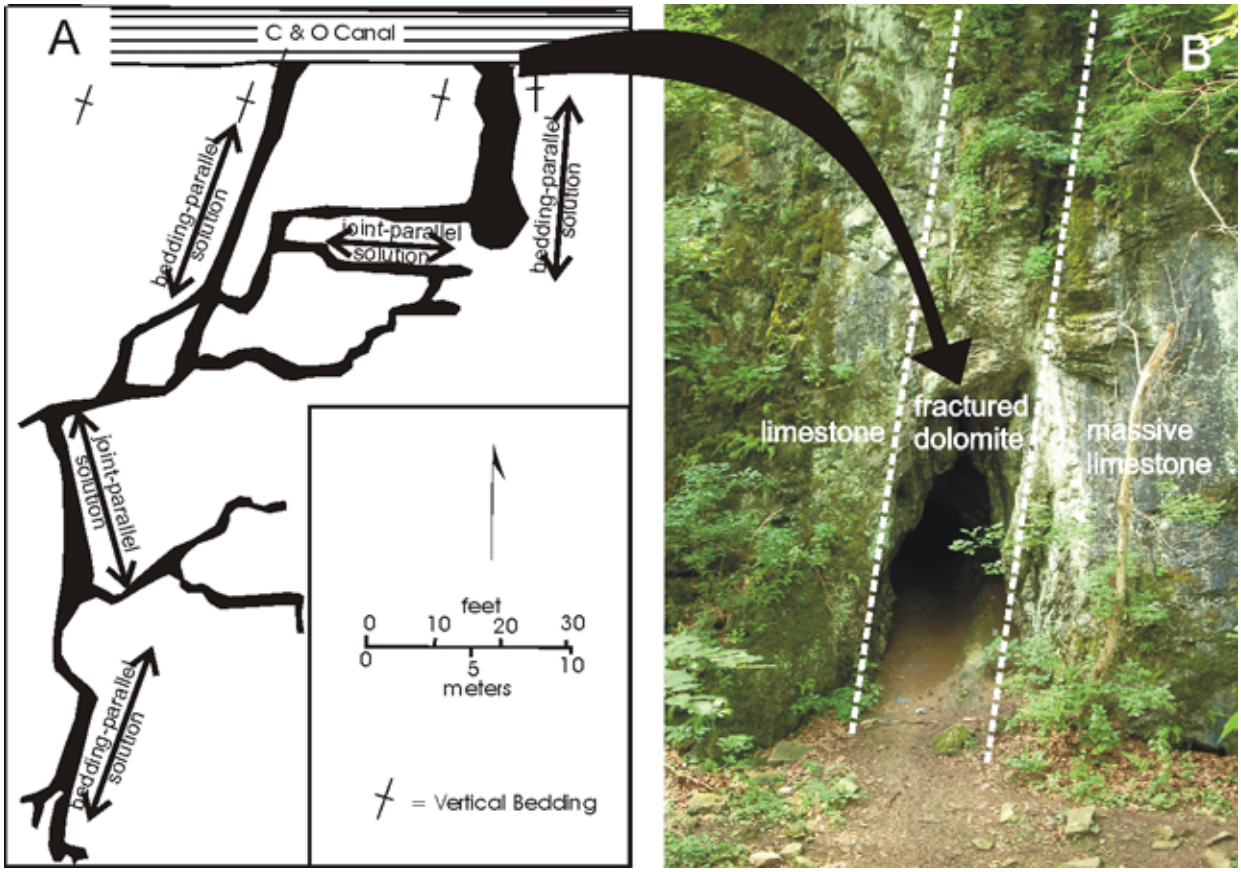

Figure 37.– A, Sketch of solution cavities of Snyders Landing Cave No. 2 from Franz and Slifer (1971). At this location main passageways of the cave parallel the vertical stratification, while side passages parallel the dominant joint system. B, Cave entrance illustrates compositional differences in vertically oriented stratification of the Conococheague Formation (white lines). Much of the cave is restricted to the highly fractured dolomite layer.

An excellent example of dissolution along intersecting joints or fractures is illustrated by the passageways present in the cave at Crystal Grottoes (Figure 39). This commercial cavern occurs in limestones of the Bolivar Heights Member of the Tomstown Formation. At this location, an overturned anticline governs the shape of this karst feature. The cavern has formed in nearly horizontal strata near the hinge of this fold (Brezinski, 2009). These rocks exhibit an intersecting network of fractures with one set oriented northwest and the other northeast. Two distinct directions of passageways roughly parallel the orientation of the two fracture sets. Dissolution has progressed along these two fracture directions and has created the rectilinear pattern of passages. The orientation of these fracture systems tends to parallel the Hagerstown Valley's prominent fracture directions. Consequently, the local folding and fracturing mimic that of the valley as a whole (Figure 27).

Although there is a strong tendency for solution to progress along conjugate fracture planes, sometimes one of the prominent fracture directions is preferentially dissolved. This may be due to bedding orientations, lithology, or other factors. Figures 39A and B demonstrate the common relationship where cavity orientations parallel the fracture plane orientations. However, in the rose diagram in Figure 40C, the solution cavities appear to be perpendicular to the dominant fracture direction. In Figure 40D the dominant fracture direction has few cavities developed along it, and most of the solution has taken place parallel to the direction of secondary fracture. Orndorff and Harlow (2002) have also showed the importance of the intersection of joint planes as conduits of solution in the Shenandoah Valley of Virginia.

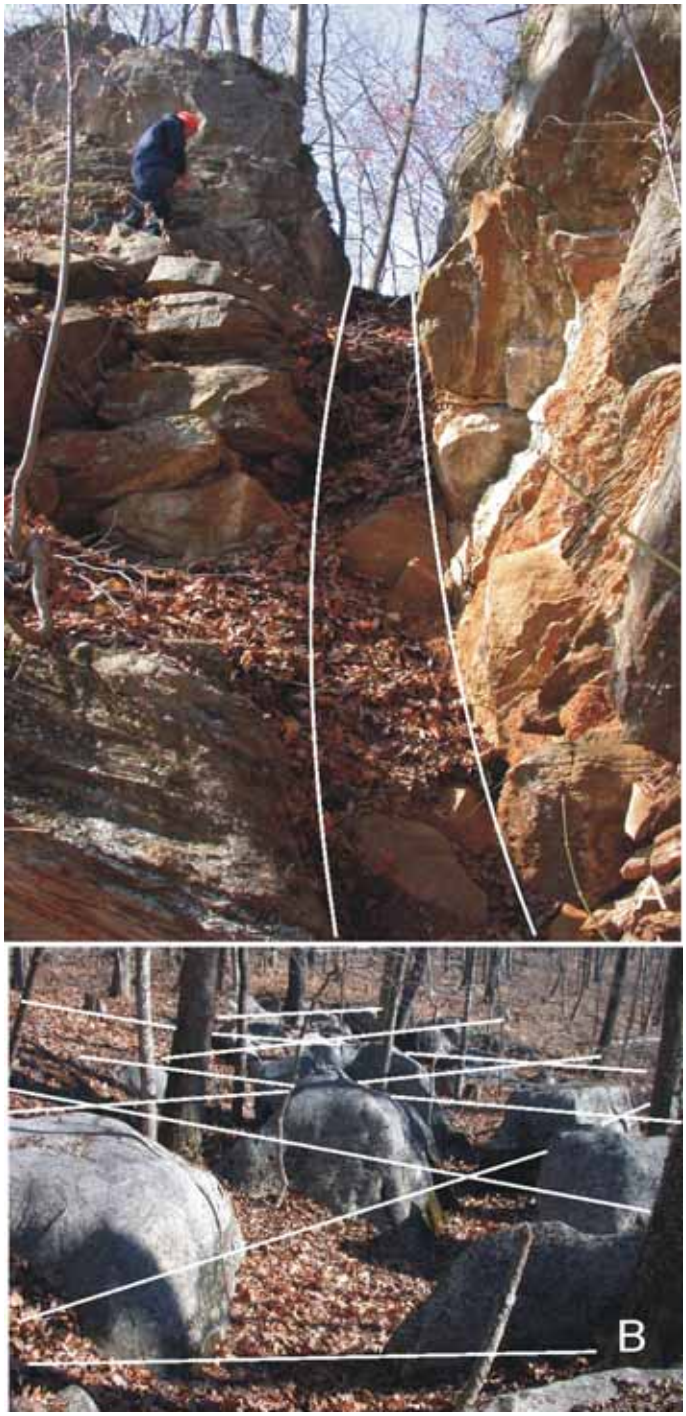

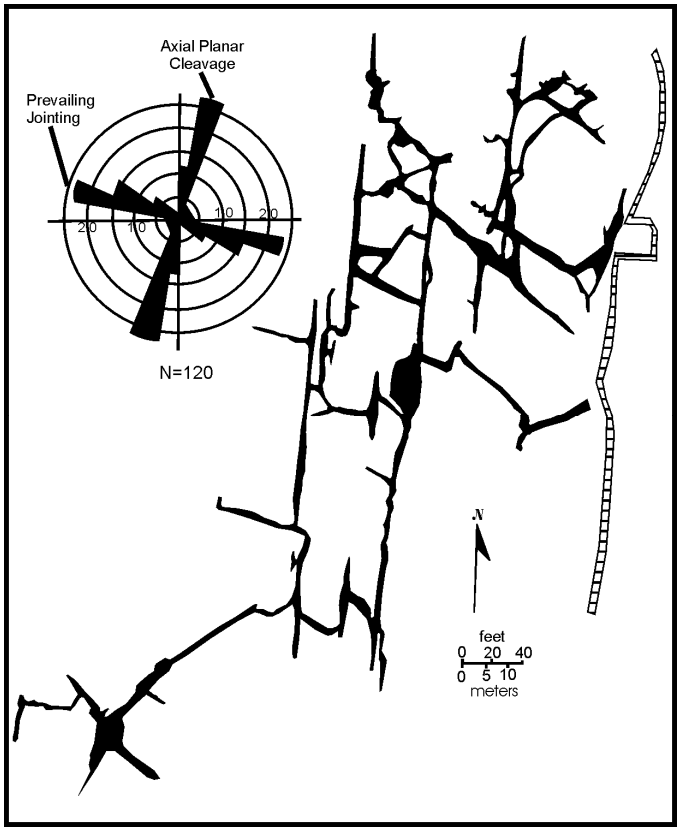

Figure 39– Sketch of the pattern of solution cavities that make up Crystal Grottoes (from Franz and Slifer, 1971). The rectilinear arrangement of passages tends to parallel the two dominant fracture systems; a west-northwest-trending joint system, and a north-northeast-trending alignment of axial planar cleavage. The joint rose shows results of 120 fractures measured in the vicinity of the cave. From Doctor et al. (2015).

Figure 38.– Pinnacles of limestone karst. A, Solution widened joint within thrombolitic interval of the Conococheague Formation. B, Joints (white lines) parallel widened solution areas that are now.

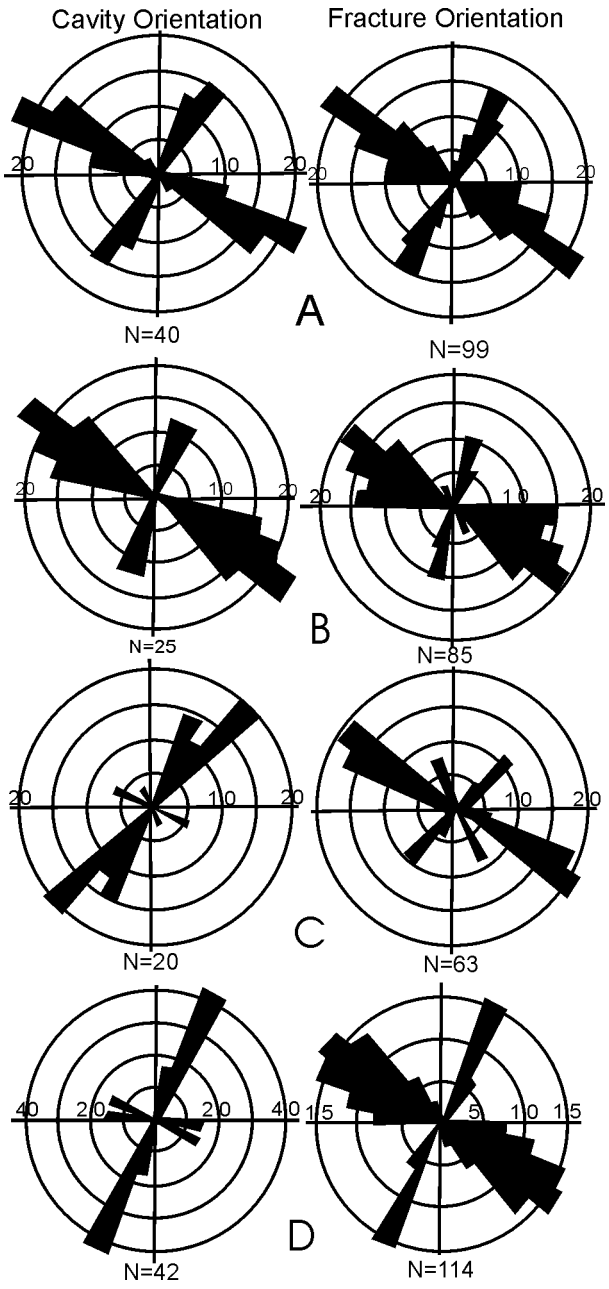

Figure 40.– Orientation of fracture and solution cavities. A, Rose diagrams of fracture and solution passageway orientations within the Shady Grove Member of the Conococheague Formation. B, Rose diagrams of fracture and solution passage orientations within the Funkstown Member of the Stonehenge Limestone. C, Rose diagrams of fracture and solution cavity orientations within the upper Elbrook Formation. D, Rose diagrams of fracture and solution cavity orientations within the Rockdale Run Formation.

Faults: Harrison et al. (2002) demonstrated the important of fault zones to karstification. Brezinski (2004, 2007) also noted that faulting had very little influence on karst development in the Frederick Valley. However, in the Great Valley various scales of faulting can be shown to play considerable roles in karst development (Doctor et al., 2008). These faults are interpreted as having a proximate effect on both the development and alignment of sinkholes and springs.

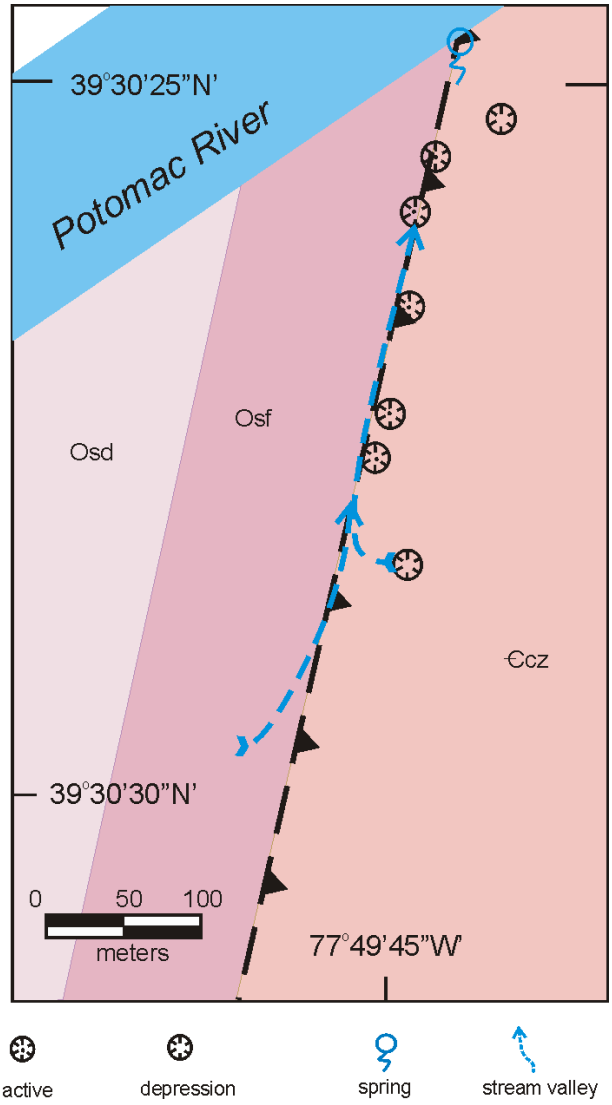

Figure 41.– Geologic sketch map of aligned sinkholes and blind valley along an unnamed fault near the Big Slackwater area of the C&O Canal. Ccz = Zullinger Member, Conococheague Formation; Ccs=Shady Grove Member, Conococheague Formation; Osd = Dam Five Member, Stonehenge Limestone; Osf = Funkstown Member, Stonehenge Limestone.

One example of fault-controlled sinkhole development was identified near the Big Slackwater area of the C&O Canal National Historical Park (Figure 41). At this location, a line of active sinkholes is present within a linear blind valley. This series of sinks ends at the foot of the valley and is interpreted to coincide with a fault contact between the Funkstown Member of the Stonehenge Limestone and the Shady Grove Member of the Conococheague Formation (Brezinski, 2014). This fault can be observed along the canal towpath, and very closely aligns with a small cave identified in the Potomac cliffs (Franz and Slifer, 1971). This unnamed fault is interpreted as having provided a conduit for groundwater movement that enlarged and produced the cover-collapse sinkholes, and perhaps the cave.

Another example of the influence of faulting on karst feature distribution was identified three miles south of Williamsport (Figure 42). At this location, drag along a splay of the Williamsport fault has created an overturned anticline in the Stonehenge Limestone with the Stoufferstown Member at its core. The interpreted fault contact places the Stoufferstown strata against Funkstown Member rocks (Brezinski, 2014). A north-flowing tributary to the Potomac River is superimposed along the fault and to a lesser degree, the fold's axis. The high hydraulic gradient, associated with the steep descent of the stream along the fault-controlled tributary, is marked by alternating active sinkholes that swallow the stream and springs that bring it back to the surface (Figure 42). The final spring brings the stream to the surface along the banks of the Potomac River and the C&O Canal towpath.

A third example of sinkhole and spring distribution associated with faulting was identified near the intersection of Rockdale Road, Cresspond Road, and Conococheague Creek in the Mason-Dixon Quadrangle (Brezinski, 2013b). In this area, cross-strike faults penetrate the Middle Ordovician carbonate units and place them in contact with the Martinsburg Formation along Cresspond Road (Figure 43). Sinkholes, both along Rockdale Road and Cresspond Road, are interpreted as being the main sources water flow that is conducted along these faults to the springs at the ponds.

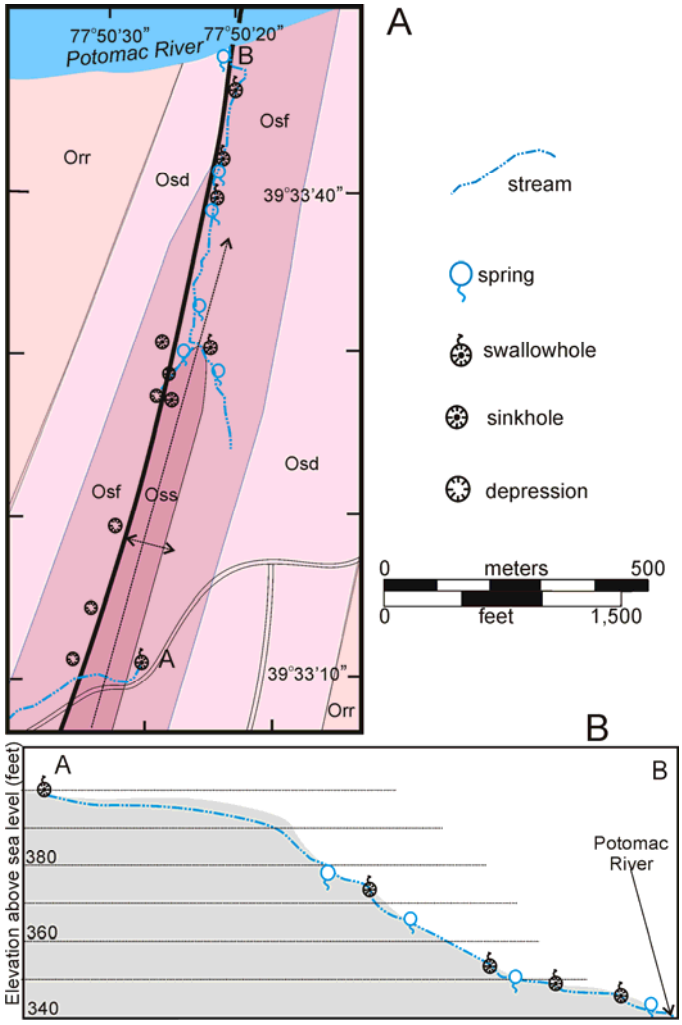

Figure 42.– A, Geologic sketch map of aligned sinkholes, swallowholes, and springs along an unnamed splay of the Williamsport fault, three miles south of Williamsport near C&O Canal milemarker 96.7. B, Cross-section of the stream's descent from the uplands to the Potomac River. Oss = Stoufferstown Member, Stonehenge Limestone; Osd = Dam Five Member, Stonehenge Limestone; Osf = Funkstown Member, Stonehenge Limestone; Orr = Rockdale Run Formation.

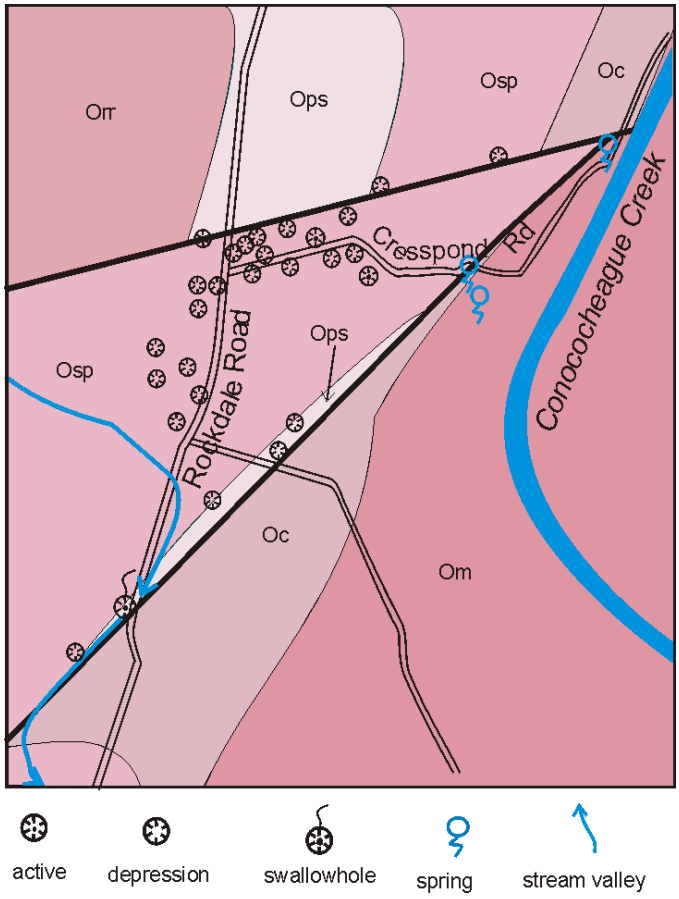

Figure 43.– Geologic sketch map of the distribution of swallowholes, sinkholes, depressions, and springs along a number of cross-strike faults at Cresspond Road. The swallowhole along Rockdale Road is interpreted as being the source for much of the water for the springs at Cress Ponds. Om=Martinsburg Formation; Oc=Chambersburg Formation; Osp=St. Paul Group undifferentiated; Ops=Pinesburg Station Dolomite; Orr=Rockdale Run Formation.

While examples of faults controlling sinkhole distribution tend to be very localized, numerous cases were identified where fault traces are interpreted to coincide with and partially control spring locations. Some instances of fault-controlled spring alignment are present along the South Mountain fault in the Smithsburg quadrangle (Brezinski and Fauth, 2009), adjacent to the Eakles Mills fault at Wagners Crossroads in the Funkstown quadrangle (Brezinski, 2009), and by the Williamsport fault near Williamsport (Brezinski, 2014).

Along the western base of South Mountain, in the Smithsburg quadrangle, a line of springs is observed to coincide with the mapped contact between the Harpers and Tomstown formations (Figure 44). This contact is interpreted as the South Mountain fault, a structural discontinuity that can be traced from Loudoun County, Virginia to Adams County, Pennsylvania (Southworth and Brezinski, 1996). In the Smithsburg quadrangle, fracturing associated with the faulting, as well as the placement of impermeable clastics of the Harpers Formation against the readily soluble Bolivar Heights Member of the Tomstown Formation, are interpreted as reasons for the alignment of a number of springs.

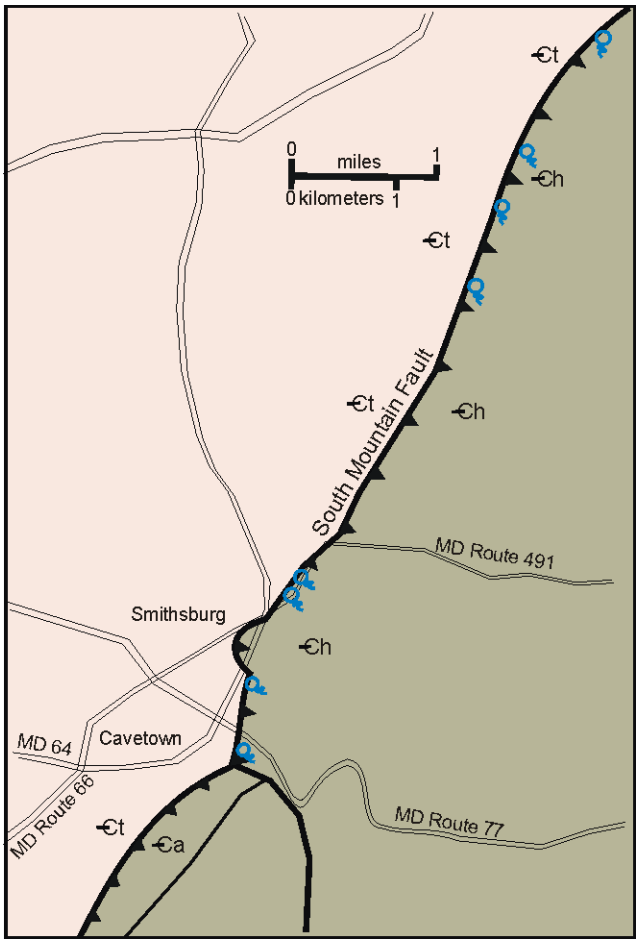

Figure 44.– Distribution of springs along the South Mountain fault in the Smithsburg quadrangle.

In addition to the line of springs identified along the South Mountain fault, an excellent case can be made for the occurrence of fault-controlled springs that coincide with the trace of the Eakles Mills fault in the Funkstown Quadrangle. Brezinski (1992) interpreted the Eakles Mills fault as a vertical structure displaying a well-developed vertical fracture cleavage. The fracturing and postulated solution is interpreted to have produced a line of springs in the vicinity of Doubs Mill at U.S. Route 40 (Brezinski and Bell, 2009). At this location, closely spaced springs appear to follow the mapped trace of the Eakles Mills fault

(Figure 45). At one location along the fault trace, artesian flow occurs in a line of closely spaced springs that exhibit a strong linearity with the adjacent stream (Figure 46).

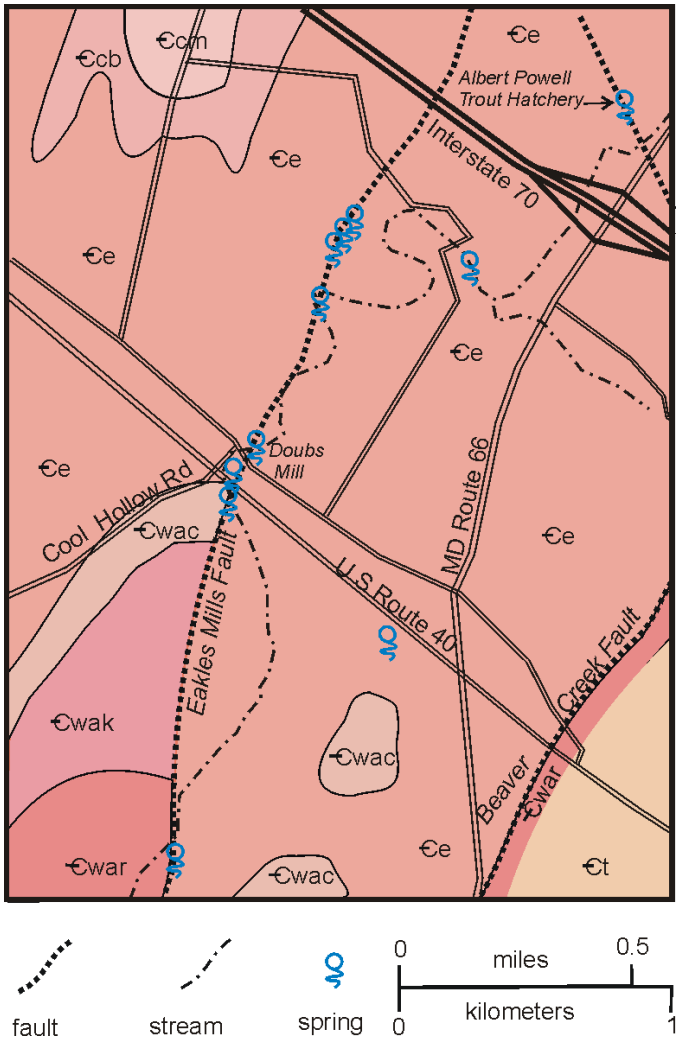

Figure 45.– Sketch map illustrating the distribution of springs along the Eakles Mills fault near Doubs Mill and U.S. Route 40.

Within the Hagerstown and adjacent Mason-Dixon quadrangles, a line of springs can be shown to coincide with the contacts between various members of the Stonehenge Limestone and Rockdale Run Formation and the Martinsburg Formation (Figure 47). Brezinski (2014) named this discontinuity the Williamsport fault. In the Williamsport quadrangle, the fracturing associated with the faulting as well as the placement of impermeable clastics of the Martinsburg Formation against the soluble Stonehenge Limestone and Rockdale Run Formation appear to have resulted in the development of closely-spaced springs and

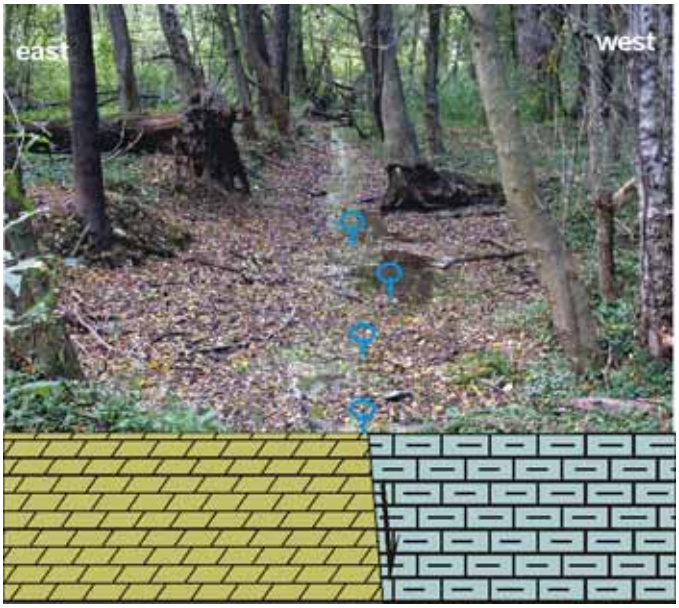

Figure 46.– Alignment of springs along the Eakles Mills fault north of Doubs Mill at U.S. 40. Note the linearity of the stream course. View is looking south.

seeps. Further to the north in the Mason-Dixon quadrangle, numerous springs, depressions, and swallowholes have formed near the trace of this fault.

Many small faults obliquely intersect the regional tectonic fabric. These localized cross-faults also are known for their propensity for spring development. Duigon (2001, fig. 18) has shown that the fracturing along small cross-faults may allow dissolution and permit the development of localized springs. Furthermore, Brezinski (2009) identified the large springs at the Albert Powell Trout Hatchery along I-70 as having formed along a large cross-strike fault (Figure 45).

Folds: In addition to the various types of fractures controlling the distribution of karst features, folding can be shown to play a role in the development of karst. The impact of folding on karst development has already been shown in the discussion of Crystal Grottoes. In that example, the cave has formed near the axis of a fold and many of the north-northeast-trending passageways can be attributed to dissolution along the fold's axial planar cleavage.

Another example of folding influencing karst development is evident in the Hagerstown City Park. The park occupies the trough of an overturned, northeast plunging syncline that exposes the Funkstown Member of the Stonehenge Limestone along the fold axis (Figure 48). The axial area also is occupied by a small lake that exposes numerous springs around its periphery. With the exception

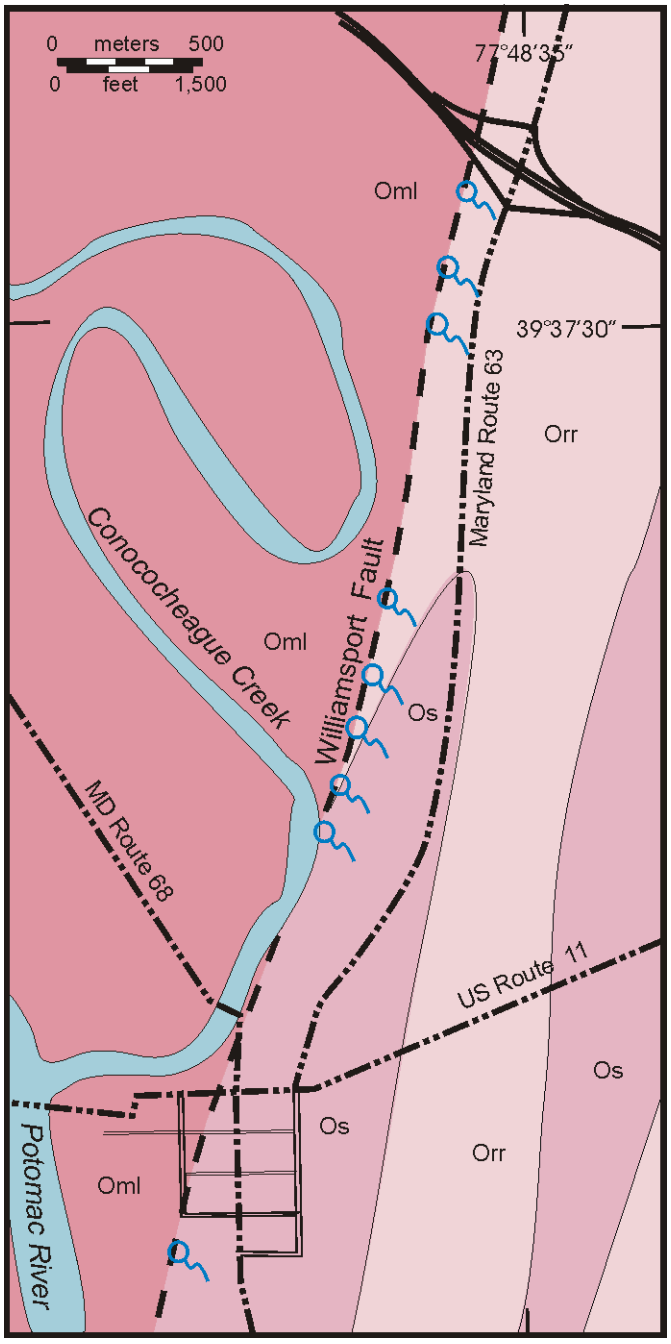

Figure 47.– Distribution of closely-spaced springs along the Williamsport fault at the contact between the Stonehenge Limestone and Rockdale Run Formation and the Martinsburg Formation near the town of Williamsport. Map modified from Brezinski (2014). Om=Martinsburg Formation; Os=Stonehenge Limestone; Orr=Rockdale Run Formation.

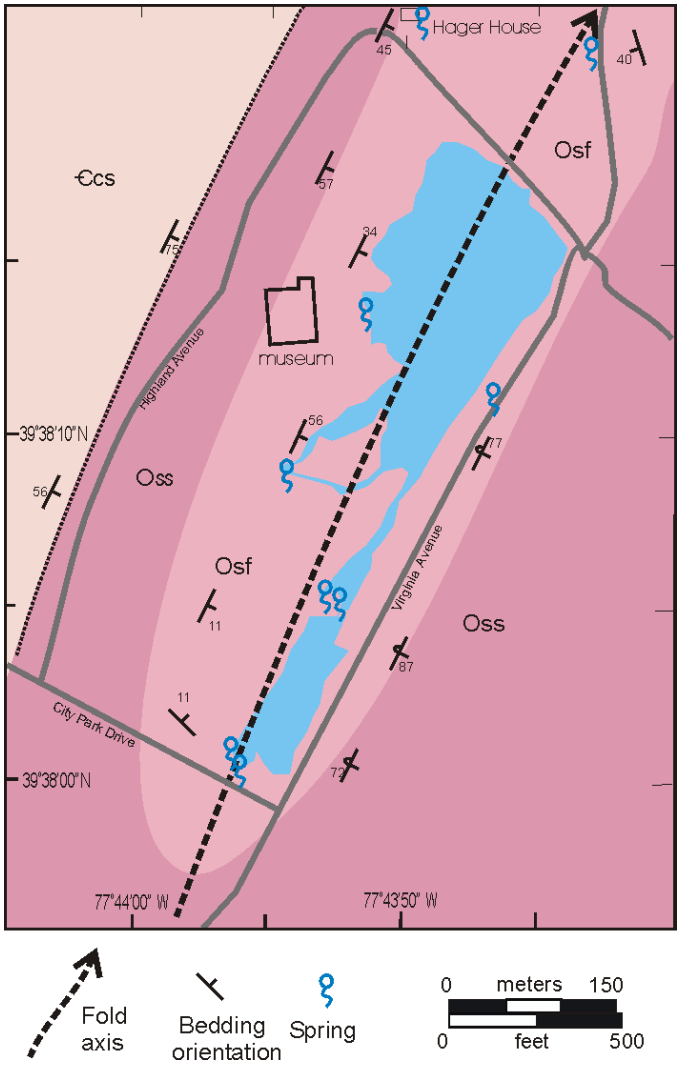

Figure 48.– Sketch map illustrating distribution of springs around the periphery of the lake in Hagerstown City Park. The distribution of the springs is interpreted as being controlled by the near centripedal drainage into the synclinal trough by the surrounding ground water. Map modified from Brezinski (2013a). Ccs=Shadygrove Member, Conococheague Formation; Oss=Stoufferstown Member, Stonehenge Limestone; Osf=Funkstown Member, Stonehenge Limestone.

of the southeast flank of the syncline, the structural dip within the Stoufferstown and Funkstown members of the Stonehenge is inclined towards the lake. The presence of the springs along the edge of the lake is interpreted not only to be the result of their position along the local water table, but the inclination of the Stonehenge strata funneling groundwater towards the synclinal trough (Figure 48).

A well-developed karst area is present between the Potomac River and Delinger Road, west of McMahon Mill

in the Williamsport quadrangle (Brezinski, 2014). This area is riddled with deep dolines, active sinkholes, and several blind valleys (Figure 49). All drainage appears to be subterranean insofar as stream flow from the north enters a swallowhole just south of Delinger Road. From this location southward to the Potomac River, no surface streams are present. The stream reappears at the mouth of a cave along the C&O Canal National Historical Park at the Potomac River.

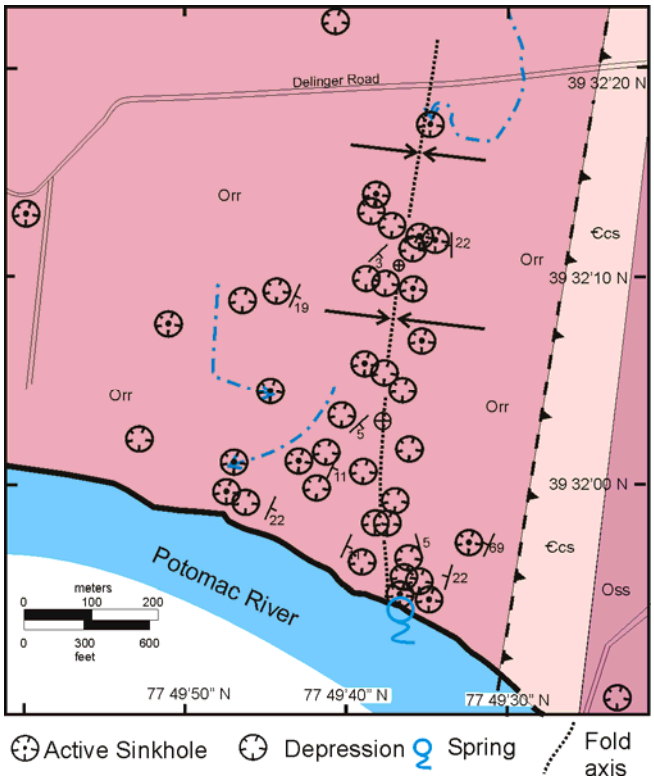

Figure 49.– Sketch map of a synclinal area within the Rockdale Run Formation west of Cedar Grove, Washington County, Maryland. Modified from Brezinski (2014). Dolines, blind valleys, and collapse sinkholes are concentrated near the axis of a broad syncline. Ccs=Shadygrove Member, Conococheague Formation; Oss=Stoufferstown Member, Stonehenge Limestone; Orr=Rockdale Run Formation.

The dissolution features in this area tend to be concentrated near the axis of a broad, gentle syncline within the Rockdale Run Formation (Figure 49). This structural factor, in conjunction steepened hydrologic gradient from a more than 50-foot drop in elevation between the swallowhole at Delinger Road and the spring at the Potomac River, is interpreted as playing a major part in the dissection of this area by dissolution. The fold is interpreted as concentrating and guiding subterranean flow down-dip towards the axis and then down plunge in the direction of the Potomac River. The blind valleys suggest that surface flow may once have been active, but now all flow occurs in the subsurface.

Topography and Relief as Factors in Karst Feature Distribution

Depressed Water Table: Wilson and Beck (1992) and Beck (1986) demonstrated the effect of increased sinkhole activity surrounding areas of a lowered potentiometric surface (i.e. water table). Orndorff and Goggin (1994) showed that entrenched streams increased local hydrologic gradient and is a major control in karst development over stratigraphy and structure in the Shenandoah Valley of Virginia. Brezinski (2004) demonstrated that sinkhole activity in southern Frederick City could be largely attributable to an increased hydrologic gradient created by a water table depressed by local quarry pumping. In the Hagerstown Valley there are several areas where active sinkhole density could be attributable to a water table is substantially lower than the surrounding land surface which in turn creates an increased hydrologic gradient. Unlike the Frederick example where the water table was depressed by activity of humans, in the Hagerstown Valley these areas tend to be concentrated along the main waterways such as the Potomac River and Conococheague Creek which have experience fluvial incision. The grouping of karst features where the water table is depressed can be seen on Figures 32 and 33. Clusters of active sinkholes are located within several areas in the bluffs of the Potomac River, and along the western edge of Conococheague Creek. All of these areas possess significant differences between the elevation of the local base level and that of the surrounding land surface. This difference varies between forty and seventy feet (Figure 50).

The relationship between the depressed level of the local water table and karst development is evident in cave distribution in the Hagerstown Valley. Franz and Slifer (1971, fig. 55) showed that many of the caves in Washington County, Maryland, tended to be concentrated along the Potomac River and Conococheague Creek. It is interpreted that the large differences between the elevation of the ground surface and the pool level of the Potomac River, which serves as the local base level, produce a sharp hydrologic gradient. This groundwater gradient facilitates in-cavity sediment movement adjacent to the river.

The influence of the topographic-hydrologic gradient on the number, depth, and character of karst features is shown in Figure 50. The area south of Interstate 81 near its crossing of the Potomac River lies within the

Stonehenge Limestone. The upland area east of the Potomac River has many steep-sided sinkholes. The only spring in the area is located along the local base level, beneath the C&O Canal towpath. The depth of each sinkhole was measured with a calibrated staff, and the karst features exhibits a general increase towards the west. This change in karst feature magnitude is attributed to a steepening in the topographic gradient westward which, in this case, is interpreted to be a proxy for the hydrologic gradient. The relationship between the depth of karst features and the topography is interpreted to result from increased removal of void-filling sediments in the direction of the Potomac River by a stronger hydrologic flow. The end result is deeper, steep-sided sinkholes.

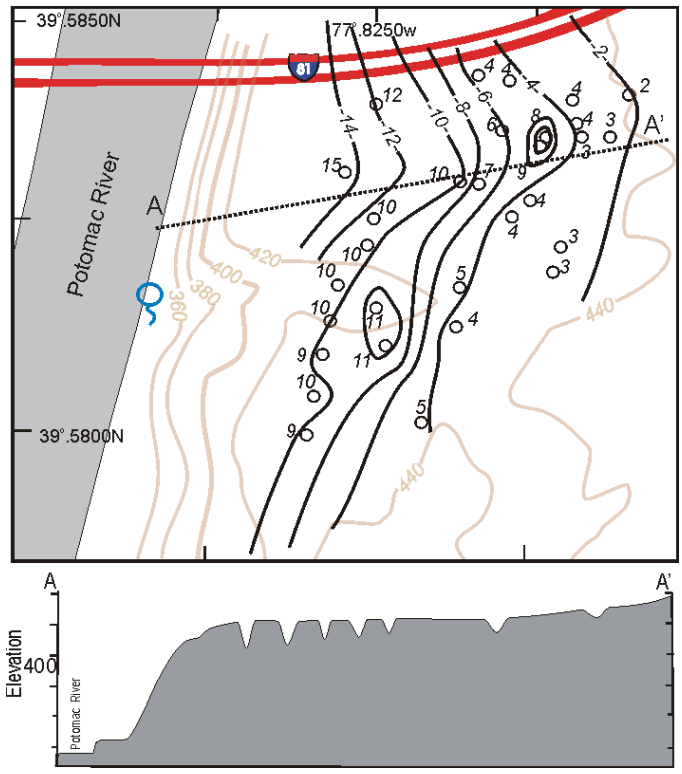

Figure 50.– Relationship between depression depth and relief as a proxy of hydrologic gradient along the Potomac River south of Williamsport, Maryland. Contours of depression depth lie subparallel to the increased topographic gradient near the river bluff. Topographic gradient in this case is considered a proxy for hydrologic gradient.

Surface drainage patterns: Brezinski (2004) showed that pre-urbanization drainage patterns depicted on historical topographic maps displayed a strong positive relationship with active sinkhole development in the Frederick Valley. Figure 32 illustrates that a similar relationship can be demonstrated in the Hagerstown Valley. As is typical of most karst terrains, the surface drainage of much of the Hagerstown Valley lacks abundant perennial streams other than the major trunk streams such as Antietam and Conococheague creeks. A dendritic drainage pattern is reflected more consistently by the topography than by the surface streams. In most cases, this pattern manifests itself as a series of swales, or ephemeral drainageways, that only contain running streams after heavy rain or snow melts. Under normal conditions, surface runoff moves to subterranean courses that transfer the water to the local base level. Notwithstanding the lack of surface streams, these drainageways reflect areas of increased water movement, both subterranean and surficial. Consequently, the underlying bedrock can exhibit indications of increased dissolution. The extra dissolution that is inferred to take place in these swales makes them prime areas for sinkhole development.

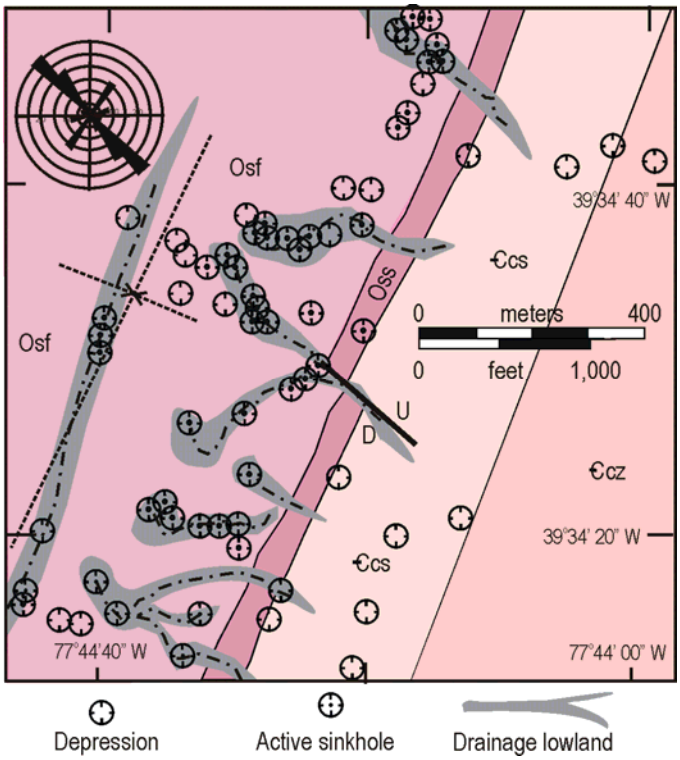

Figure 51.–Sketch map illustrating the relationship between sinkholes and drainage lowlands. Ephemeral stream valleys, which are interpreted to lie parallel to the main joint network, tend to be areas where sinkhole activity is concentrated. Modified from Brezinski and Bell (2009). Ccz=Zullinger Member, Conococheague Formation; Ccs=Shadygrove Member, Conococheague Formation; Oss=Stoufferstown Member, Stonehenge Limestone; Osf=Funkstown Member, Stonehenge Limestone.

One example where the relationship between drainage pattern and sinkhole activity can be illustrated is in the

Funkstown quadrangle. At this location, localized ephemeral streams and their lowlands parallel the prevailing joint system (Figure 51). These lowlands are sites where sinkhole activity has its greatest incidence. Not only do sinkholes concentrate along the ephemeral stream courses, but they occur in greater numbers within the Funkstown Member of the Stonehenge Limestone.

Another example where the relationship between topography and sinkhole activity can be illustrated occurs within the Conococheague Formation where it crops out south of Williamsport (Figure 52). In this case, three ephemeral streams drain into a large depression containing numerous active sinkholes. All of the active sinkholes in the area are either concentrated along the drainage lowlands that descend into the large depression or in the depression itself.

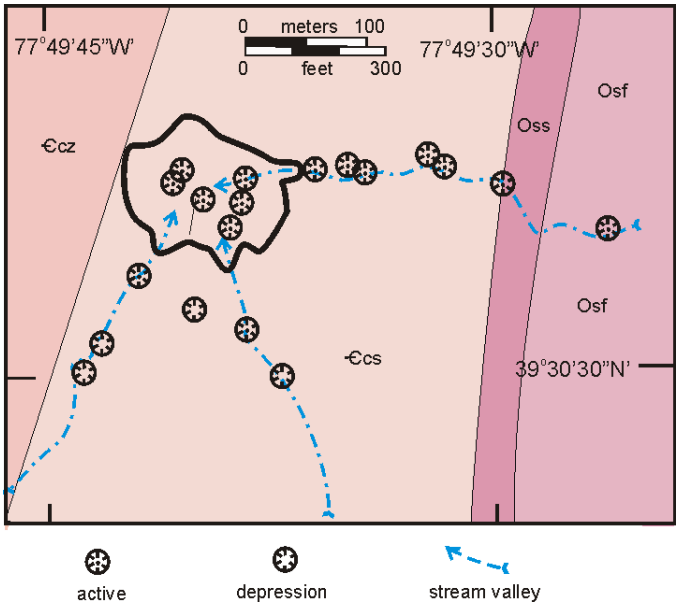

Figure 52.– Sketch map illustrating the alignment of active sinkholes along ephemeral streams that drain into a large depression south of Williamsport. Data from Brezinski (2014). Ccz=Zullinger Member, Conococheague Formation; Ccs=Shadygrove Member, Conococheague Formation; Oss=Stoufferstown Member, Stonehenge Limestone; Osf=Funkstown Member, Stonehenge Limestone.

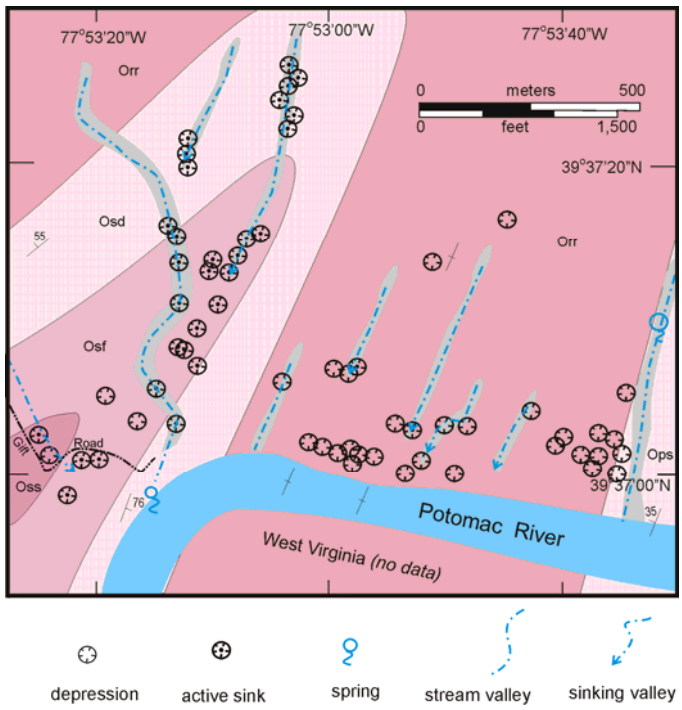

Figure 53.– Sketch map of sinkhole distribution and its relationship the stratigraphy, geologic structure, and topography in an area of the Hedgesville Quadrangle (Brezinski and Glaser, 2014). Karst features (including blind valleys) are distributed adjacent to the Potomac River and within the Funkstown Member of the Stonehenge Limestone. Oss=Stoufferstown Member, Stonehenge Limestone; Osf=Funkstown Member, Stonehenge Limestone; Osd=Dam Five Member, Stonehenge Limestone; Orr=Rockdale Run Formation; Ops=Pinesburg Station Dolomite.

An area that displays a variety of topographic factors that affect the formation of karst topography can be seen in Figure 53. In this area in the Hedgesville quadrangle, several folded Lower Ordovician carbonate units are exposed along the Potomac River (Figure 53). Local relief along the river is as much as 80 feet. This high relief within the outcrop belt of the Rockdale Run Formation is interpreted to contribute to the formation of a number of karst features including dolines, active sinkholes, and blind valleys. Figure 53 illustrates how the number and density of karst features progressively decrease northward away from the Potomac River. This presumably reflects a hydrologic gradient. Within the outcrop belt of the Funkstown Member of the Stonehenge Limestone, numerous active sinkholes are present, both within and outside of ephemeral stream valleys. Some ephemeral stream lowlands form blind valleys that are little more than merged active sinkholes and depressions. The drainage in

this area comes to the surface at a spring along the Potomac River.

Topography and the localized hydrologic gradient that it produces play a major role in sinkhole development in the Hagerstown Valley. The type and density of karst features produced also can be controlled by structural elements, as described previously, and lithologic factors.

Stratigraphy as a Factor In Karst Feature Distribution

A main working hypothesis of this study is that lithology, or rock composition, plays a significant role in controlling karst feature distribution. To test this postulate, it was necessary to precisely map the rock units in the Hagerstown Valley and then compare their outcrop pattern with karst feature distribution. Of paramount importance to the geologic mapping aspect of this study was the use of reliable stratigraphic units that are lithologically consistent and areally extensive enough that future workers could repeat the mapping without generating substantial differences. However, a point of diminishing returns had to be considered when subdividing the individual formations that produces karst features were within. Increasingly fine subdivisions have the potential to elucidate some previously unrecognized karst prone interval, but such units also tend to be geographically localized, and as such may provide insufficient numbers of karst features to be statistically significant. This is exemplified by subdivisions of the Waynesboro Formation. All members of this unit tend to yield statistically insignificant numbers of karst features. However, it can be shown, somewhat subjectively, that the Cavetown Member presents a significant potential for catastrophic karst development by way of cave development. The subdivisions described herein are meant to provide subsequent researchers a foundation for more site-specific studies and give them a stratigraphic starting point from which they can further subdivide units in more detail.

Not all carbonate units exhibit an equal susceptibility to karst development in the Hagerstown Valley stratigraphic succession. Although all of the carbonate units contained at least one type of karst feature, these features were not distributed evenly throughout the Hagerstown Valley geologic units. Table 1 summarizes the numbers and types of karst features found in each geologic formation.

Table 1 illustrates the variability of numbers and types of karst features observed and recorded between the various stratigraphic units. Figure 54 is a stacked bar chart that summarizes the relative number of karst features in the carbonate rock units of the Hagerstown Valley. From this portrayal of the data, it is clear that some units are more susceptible to the formation of depressions, such as the

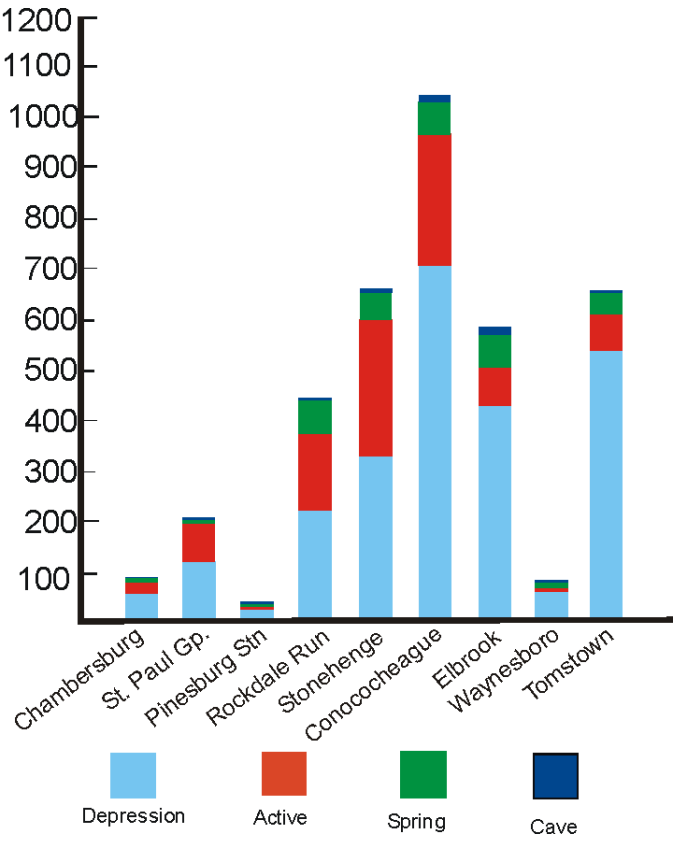

Figure 54.– Stacked bar chart of numbers of karst features in the Hagerstown Valley karst study.

Tomstown (82% of all features) or Elbrook (74% of all features) formations. Other units appear to be more prone to active sinkhole development, such as the Stonehenge Limestone (41% of all features) or St. Paul Group (36% of all features).

A different portrayal of this information is shown in Figure 55, where several inferences may be gained. Firstly, the Conococheague Formation and Stonehenge Limestone contain significant percentages of all three karst features- depressions, active sinkholes, and springs. These two formations contain more than half of all active sinkholes, and along with the Elbrook and Rockdale Run formations contain more than 75% of all springs. Lastly, the Chambersburg Formation, which Duigon (2001) considered the most sinkhole-prone unit in the Hagerstown Valley, contains only a minor percentage of any of the feature types. The outdated geologic mapping used by Duigon led to this erroneous conclusion. Current mapping identifies the main sinkhole-prone unit to be the St. Paul Group (Brezinski, 2013b; Brezinski and Glaser, 2014).

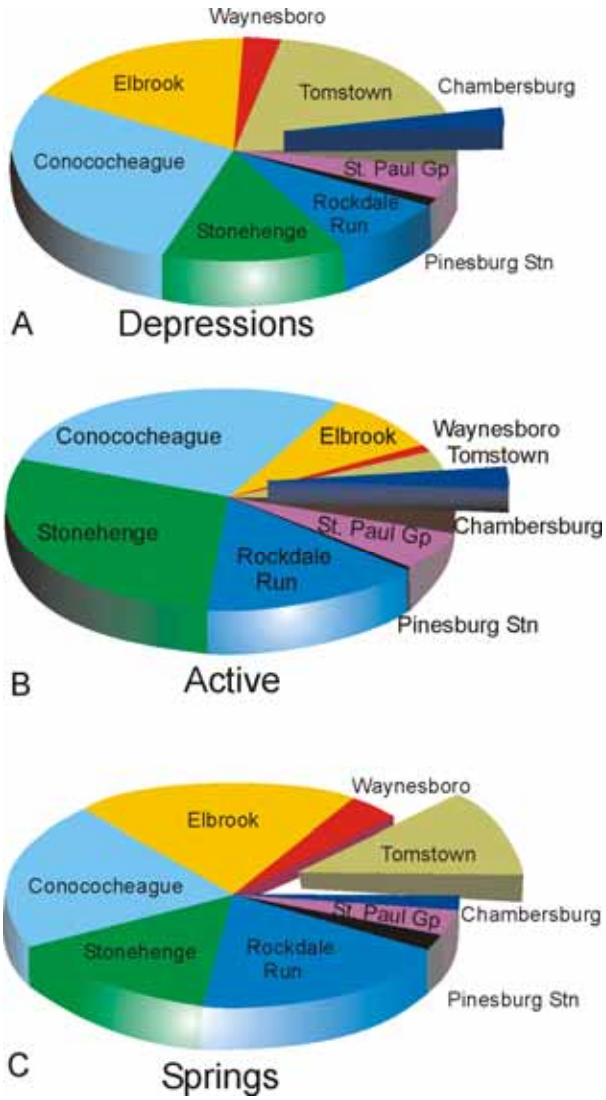

Figure 55.– Pie diagrams illustrating relative percentages of (A) depressions, (B) active sinkholes, and (C) springs identified during the Hagerstown Valley karst study.

Superficial examination of Table 1 and Figures 53 and 54 tends to confirm the *a priori* working hypothesis of this study that not all geologic units exhibit a consistent and predictable distribution or ratio of karst features.

Karst Susceptibility: Evaluation of karst feature distribution based on map patterns (Figures 30, 32, and 33), statistical graphs (Figure 55), or tabular data (Table 1) allows for generalizations to be drawn about the propensity for an outcrop area to develop karst features. For example, evaluating the total number of karst features present when within a formation, some units have a high number of features (e.g., Conococheague Formation). However, because that formation underlies such a large area in the Hagerstown Valley, a relatively low number features occur per square mile of exposure (Table 1). Some units have large outcrop areas and, therefore, have more area in which to develop karst features. This contrasts with some units that may have small outcrop areas (e.g., St. Paul Group) and moderately low numbers of karst features, but a very high number of features per square mile. A large number of features per unit area is a more clarifying metric of karst susceptibility than simply the raw number of features contained within that particular unit. More importantly, not all karst features should be considered equal in importance. With this in mind, units with relatively large numbers of springs (e.g., the Elbrook Formation) or depressions (e.g., the Tomstown Formation) should not be considered as more susceptible units than those with low numbers of springs or depressions (e.g., Chambersburg Formation), especially if those latter units have large numbers of active sinkholes. Knowing and understanding which units have high incidences of active sinkholes per unit area or the ratio of active sinkholes to depressions is much more illuminating than simply totaling the numbers of features per stratigraphic unit.

Brezinski (2004) presented karst distribution data for the carbonate rocks of the Frederick Valley. He found that a more important statistic was the ratio between active sinkholes and the total number of karst features present within a formation. Brezinski (2004) termed this ratio the "Karst Susceptibility Index" or KSI. The KSI ostensibly demonstrates the relative karst susceptibility of each stratigraphic unit. This ratio was presented in the form of:

$$KSI=(active/mile^2)/(number\ of\ features/mile^2),$$

or more simply

$$KSI=(no.\ active\ sinkholes)/(total\ no.\ features)$$

The KSI gives a relative value of the sensitivity of a particular rock unit to the development of karst features that is somewhat more quantitative than the raw data presented in Table 1.

When the KSI is compared to the raw numbers of karst features (Table 1), a somewhat different picture of susceptibility appears. Some units with large numbers of karst features (Tomstown and Elbrook formations) have comparatively low KSI's, while others with modest totals of features (Chambersburg Formation and St. Paul Group)

Formation	Area ($mi.^2$)	Dolines	Sinkholes	Springs	Caves	Total	KSI
Tomstown	28.679	550	76	41	1	668	0.11
Waynesboro	15.687	66	4	11	4	85	0.05
Elbrook	47.799	430	77	67	6	580	0.13
Conococheague	86.202	713	262	69	6	1050	0.25
Stonehenge	33.982	336	272	51	0	659	0.41
Rockdale Run	45.878	229	148	64	1	442	0.34
Pinesburg Stn	2.058	25	6	6	0	37	0.16
St Paul Gp	3.231	113	69	12	0	194	0.36
Chambersburg	3.226	56	24	6	0	86	0.28
Total	**267**	**2518**	**938**	**327**	**18**	**3801**	

Table 1. Compilation of numbers of karst features identified within each formation in the Hagerstown Valley.

have high KSI's. This is because the KSI emphasizes active sinkholes. Weighting the active sinkholes was done because they pose a greater risk for economic loss and personal injury than do depressions or springs, even though the former may have an important role in groundwater quality. Critical to this thinking was the recognition that large areas in the Hagerstown Valley are underlain by units such as the Tomstown and Elbrook formations. But, only rarely do these units experience catastrophic collapses. Conversely, the St. Paul Group has a relatively high number of catastrophic collapses recognized within its outcrop belt.

One caveat in the calculation of the KSI is the prerequisite that statistically significant numbers of features need to be identified. Otherwise, spurious calculations can potentially arise. This is exemplified by the low KSI of 0.05 for the Waynesboro Formation. While this index value would normally indicate a very low susceptibility, it should be noted that all karst features identified within this formation are contained within the Cavetown Member. Evaluation of this member suggests that it may have a significantly higher KSI than the formation as a whole. This is indicated by the development of substantial caves within this unit at the type section in the Cavetown quarry and at Mt. Aetna Cave.

The values of the KSI for each unit were plotted against the stratigraphic section of the Hagerstown Valley in Figure 56. In places on the section, the relative KSI was modified to correspond to changes in lithology that were identified subjectively as having either a higher or lower KSI than the formation as a whole. For instance, the Funkstown Member of the Stonehenge Limestone is demonstrably more susceptible to active sinkhole development than is the underlying Stoufferstown Member. This can be shown in the examples on Figures 50 and 52. In both of these cases, the Stonehenge Limestone contains many depressions and active sinkholes. However, it is the Funkstown Member that exhibits a high incidence rate and density of active sinkhole development.

The graphic portrayal of KSI values (Figure 56) can be utilized as a first approximation by planners, developers, and engineers for site-specific evaluation of areas within the Hagerstown Valley. It is clear that, at the formation level, the Stonehenge Limestone, St. Paul Group, and Chambersburg Formation are three of the most susceptible units to karst development in the Hagerstown Valley. Other highly susceptible units like the Conococheague or Rockdale Run formations exhibit only localized intervals of increased susceptibility. These highly susceptible intervals, not mappable at the 1:24,000 scale, exhibit very high dissolution characteristics, but their potentially high KSI is subdued or dampened by the surrounding intervals that have very low solubility potential. An example of this is the "oolitic unit" with the lower part of the Rockdale Run Formation, which is very soluble and produces a relatively large number of active sinkholes. However, it is sandwiched between intervals containing considerable amounts of insoluble chert and/or dolomite. These insoluble layers deter solution of the soluble units and provide support if cavities develop.

Intraformational solution produces a localized stratigraphic susceptibility. This phenomenon can be shown to occur. An example is illustrated in Figure 57 along the C&O Canal National Historical Park near mile marker 108.5. In this example, one thrombolite interval of the Conococheague Formation exposed along the towpath contains many soil-filled solution cavities.

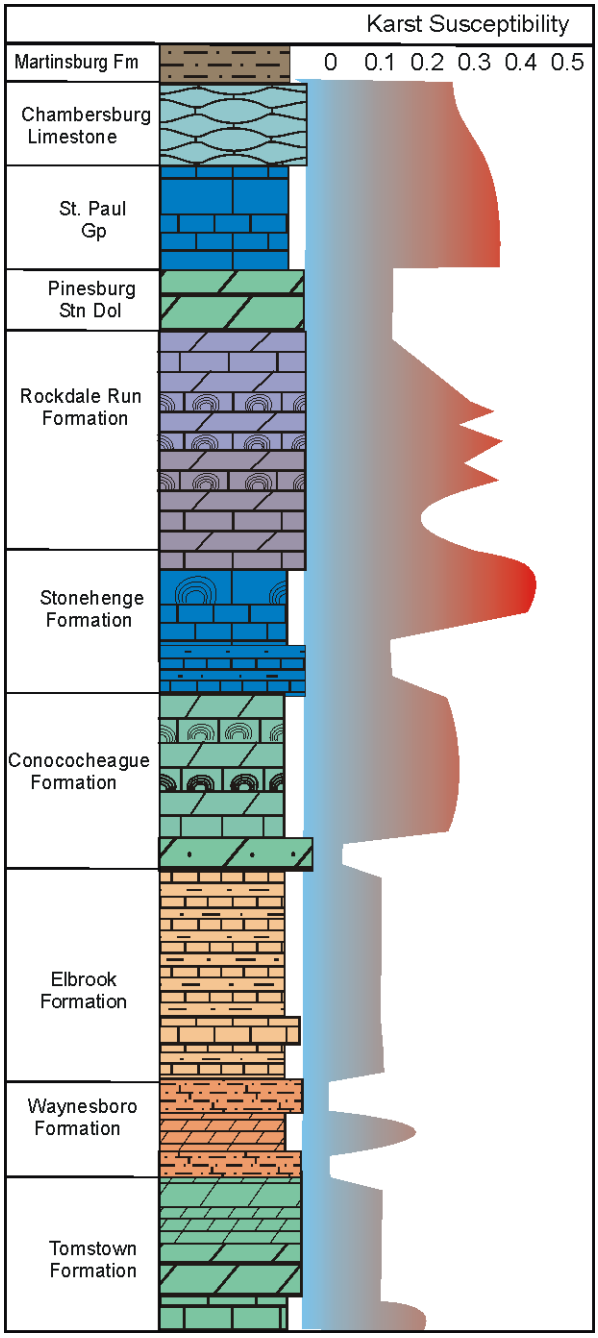

Figure 56.– Stratigraphic variation of karst susceptibility index (KSI) in the Hagerstown Valley of Washington County, Maryland.

This thrombolite interval can be traced northward along strike into an area containing a dense distribution of active sinkholes. Laminated dolomitic strata that exhibit very little evidence of karstification are juxtaposed on both side of this thrombolite intervals.

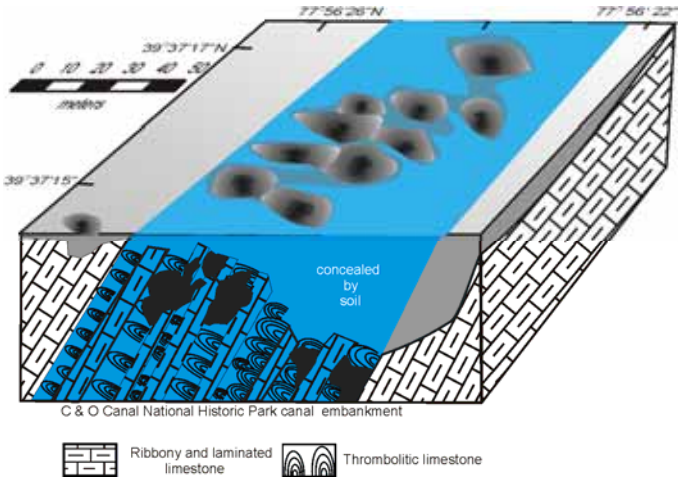

Figure 57.– Block diagram illustrating localized karst susceptibility of a thrombolitic interval of the Conococheague Formation along the C&O Canal National Historical Park near mile marker 108.5. Filled cavities along the canal can be traced along strike to an area containing a densely arranged number of active sinkholes.

Human Activity as a Factor in Karst Feature Distribution

While geologic and topographic factors have been shown above to play critical roles in the distribution and type of karst features, human activity can also be an important factor in karst development. In the Frederick Valley of Maryland, Brezinski (2007) demonstrated that areas of normally low incidence of sinkhole activity could become very active when impacted by things like urban development, quarrying, and highway construction. These activities can change the soil-bedrock-water table equilibrium that may have existed over long periods of time.

Storm Water Impoundments: Sinkhole formation was commonly observed in areas where new or relatively new storm water impoundment areas were constructed. This has been shown to be a common location for sinkhole development when these excavations are built in business parks or housing developments (Kochanov, 1999). These retention areas are constructed by stripping away the soil often exposing the underlying bedrock as well as soil-filled voids and inactive sinkholes. As these areas are filled with water during periods of high rainfall, the previously plugged solution cavities are opened by flushing of the enclosed sediments and soil. Furthermore, these ponds tend to be constructed along existing drainage lowland-areas that have been shown in previous sections to have a high potential for sinkhole development. Figure 58 illustrates several examples where these impoundments have become sites of unusually high sinkhole activity. At

the eastern edge of Williamsport a broad storm water retention facility has been constructed along an ephemeral stream within the Rockdale Run Formation (Figure 58A). Unremediated sinkholes have persisted and slightly grown in this catchment basin over the past half decade. A similar example is present within the Elbrook outcrop belt near Wagners Crossroads (Figure 58B). Perhaps the best example is located near St. James, where new housing developments have prompted the creation of two separate retention ponds along several ephemeral streams within the outcrop belt of the Funkstown Member of the Stonehenge Limestone (Figure 58C). The impoundment basins have been the location of numerous cover-collapse sinkholes (Figure 58D). Furthermore, the intervening stream lowland has been the site of greatly increased karst development including a large area of overlapping active sinkholes (Figure 58C). This is interpreted as the result of increased runoff coming from the impervious surfaces of streets, roofs, and driveways coming from the new housing development.

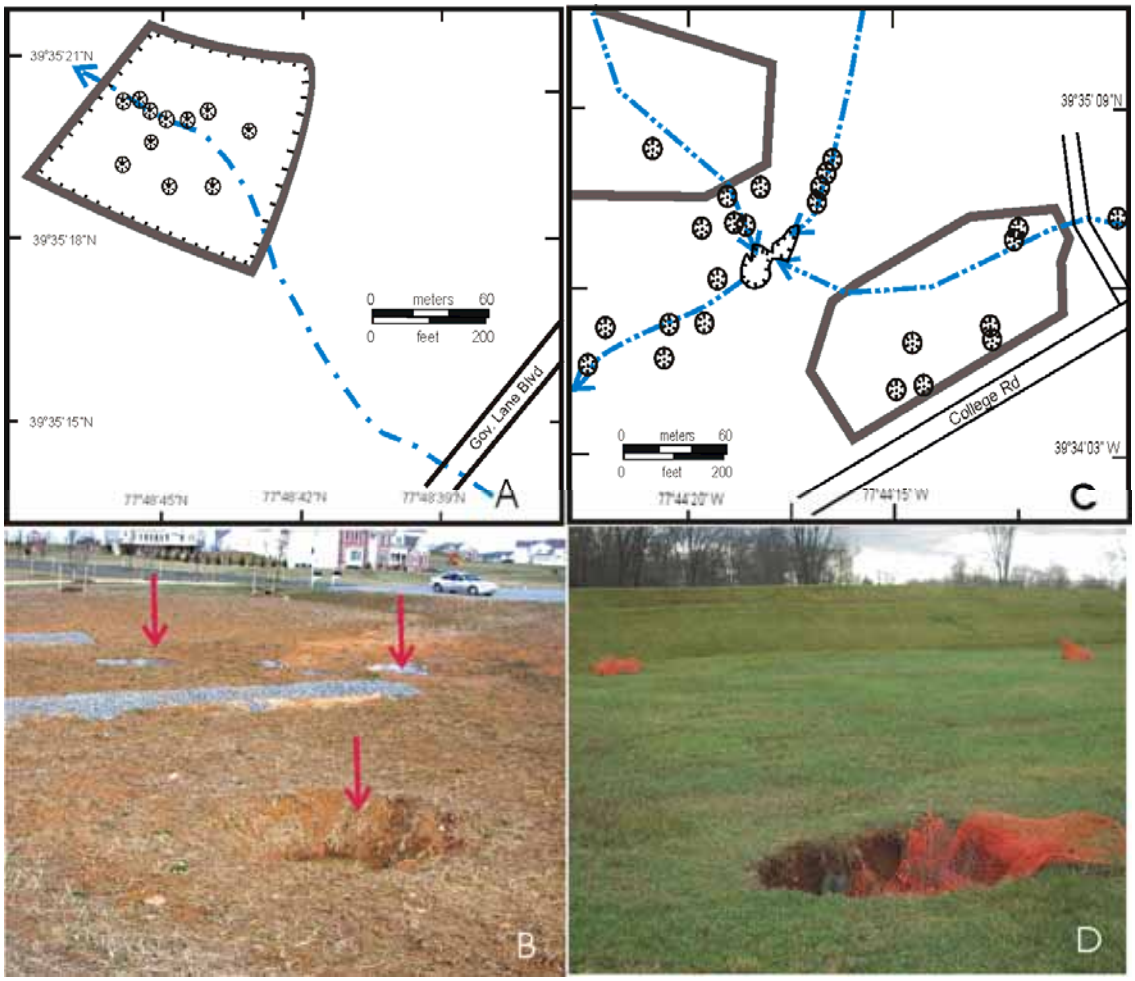

Figure 58.– Storm water impoundments. A, Retention facility is site of sinkhole activity east of Williamsport along Governors Lane Boulevard. B, Newly created retention is site of numerous sinkholes near Wagners Crossroad. Arrows mark active sinkholes. C, Storm water impoundments along ephemeral streams at a housing development along College Road, Funkstown. Note the high density of sinkhole activity in drainageways caused by increased runoff from the housing development. D, Southern impoundment shown in D. Active sinkholes are marked by safety fencing.

Unlined Drainage: A common site where sinkhole activity is found to occur in the Hagerstown Valley was along unlined drainage, especially along highways (Figure 59). Unlined roadside drainages, in a manner similar to storm water impoundments promote sinkhole activity. These excavations are constructed along highways by the removal of soil cover exposing filled solution cavities within the bedrock. During periods of high runoff, water tends to flush the filled cavities which result in the occurrence of catastrophic soil cover collapse sinkholes. Examples are illustrated in Figure 59. This type of cover-collapse sinkhole does not occur along the eastern and western borders of the Hagerstown Valley where thick, colluvial Quaternary deposits covers and conceal the bedrock.

Sinkholes related to unlined drainage are not restricted to roads and highways. Several examples were identified where cover-collapse sinkholes correspond to unlined drainages in housing developments where runoff was directed along yards and common areas (Figure 59C).

Quarry Dewatering: When quarrying of bedrock proceeds to a depth below the local water table, it typically necessitates removal of incoming groundwater through pumping. The outcome of this pumping is identical to that seen surrounding a water well, but on a much broader scale. The pumping of water inflowing at the level of the quarry floor creates a new, localized water table that is at a lower topographic level than the water table in surrounding areas. As a result, the groundwater flows towards the new, lower level. The altered hydrologic gradient allows subterranean voids that normally would be filled with sediment, to be flushed by water moving along the steepened gradient. This potential hazard in the vicinity of limestone quarries has long been recognized as the cause of many sinkhole problems witnessed in the Frederick area (Brezinski, 2004a, 2007). In the Hagerstown Valley this relationship was identified at two of the three active quarries. The incidence rates of active sinkholes surrounding these quarries vary greatly and were interpreted as resulting from differences in the composition and structure of the quarried rock unit.

Figure 60 illustrates a case of quarry dewatering and its local impact on the karst system. In 2005, quarrying operations in the Holcim Inc., Security quarry, just east of Hagerstown, intersected a cave located within the Conococheague Formation and produced a high level of water flowing into the quarry. Further study suggested that the cave may have developed near or along a previously unidentified thrust fault. Dye trace analysis of the surrounding area (Aley, 2007) determined that

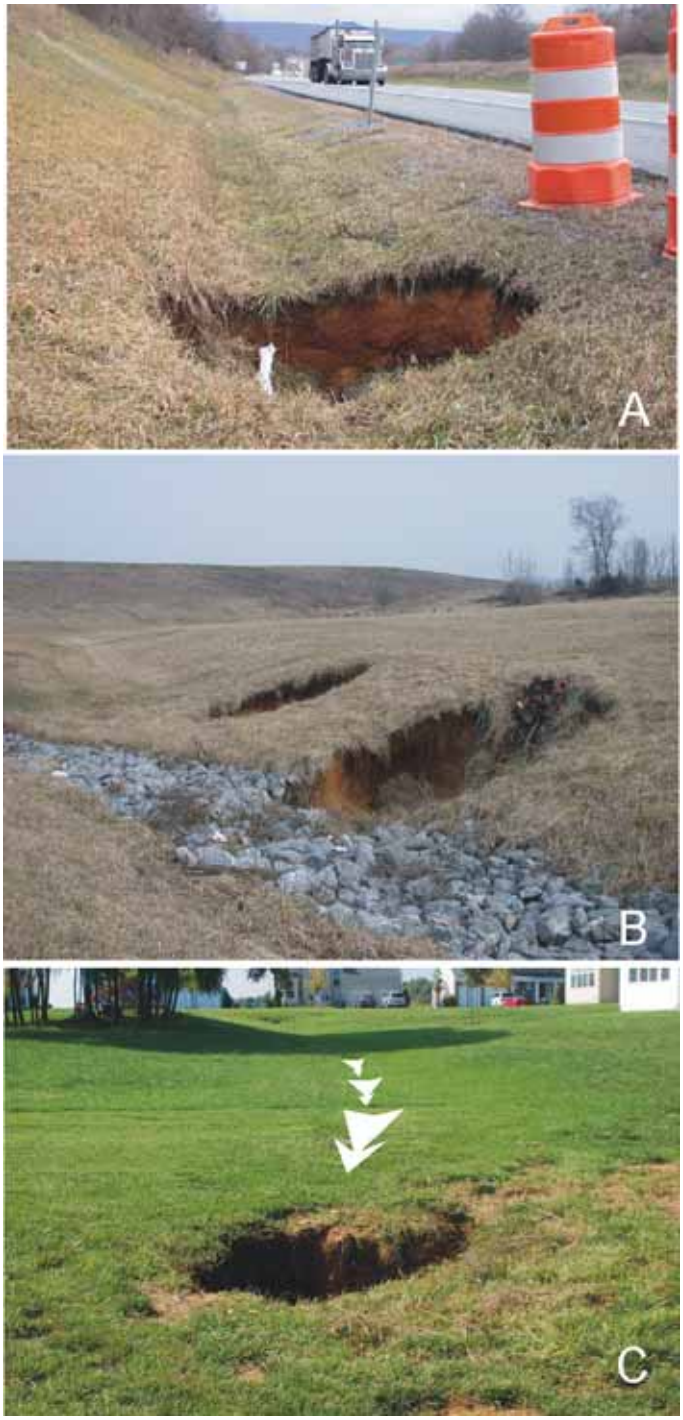

Figure 59.– Karst and unlined drainages. A, Cover-collapse sinkhole developed in the Elbrook Formation in unlined highway drainage along Interstate 70. B, Sinkhole along permeable drainage lining at the Hagerstown Airport. C, Active sinkhole developed in lawn drainage near Funkstown.

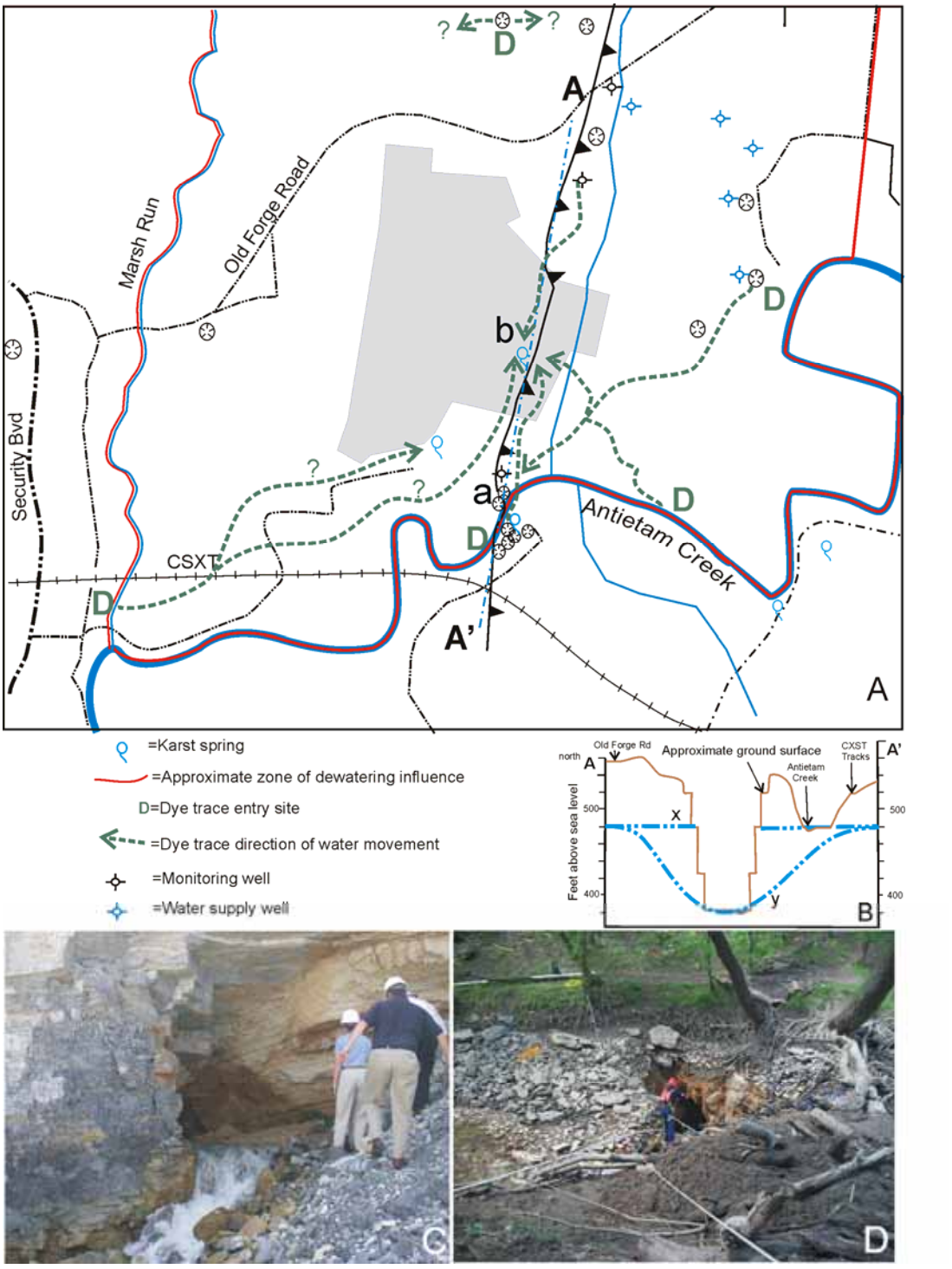

Figure 60.– Quarry dewatering and karst activation. A, Map of the area surrounding Security quarry (gray shaded area) and locations of interpreted fault, sinkholes and springs. Groundwater flow patterns based upon dye trace analysis of Aley (2007). B, Topographic profile along strike from A to A' illustrating interpreted pre-quarrying (x) and current (y) water table and resulting cone of depression. C, Catastrophic collapse sinkhole along the stream channel of Antietam Creek in April 2011. The sinkhole exposed in the stream channel is within a coffer dam during repair attempts (image courtesy of Greg Day, Maryland Department of Environment). D, Spring emerging from the cave opened in eastern face of the Security quarry in 2005.

groundwater flow was drawn towards the base of the quarry. Soon after the cave was breached, a spring to the south along Antietam Creek stopped flowing and several sinkholes formed in that area. In April 2011, a sinkhole opened in the channel of Antietam Creek. The inflowing waters presumably emptied into the quarry to the north. The working hypothesis is that when the cave and spring were opened in 2005, the water table, which was already depressed by quarrying, was presented with a direct avenue into the quarry. This was ostensibly accomplished by solution that was active along fracturing caused by the unnamed north-south oriented thrust fault. Further evidence of the fault's involvement is that sinkholes continue to develop to the south directly along the strike of the interpreted thrust fault.

The events along Antietam Creek are interpreted to be the result of both the depressed water table created by quarry dewatering, and by preferential dissolution that occurred along the fault. When the cave and spring along the eastern edge of the quarry were opened, a direct conduit was created to capture and direct groundwater from Antietam Creek directly into the quarry. With the increased hydrologic gradient of the water table, solution voids were flushed free of sediments and resulted in the continued sinkhole activity.

Since the opening of the sinkhole in the course of Antietam Creek, extensive grouting has served to largely impede water flow into the quarry. However, the locally lowered water table continues to spawn increased sinkhole activity along the banks of Antietam Creek.

Utilization of Findings for Site Specific Evaluation

Brezinski (2007, fig. 9) showed how multiple overlapping factors can impact both the incidence and density of sinkhole development in Maryland's Frederick Valley. He also identified several rock formations in the Frederick Valley that were highly susceptible to sinkhole formation (Brezinski, 2004a). Wherever these formations cropped out, sinkhole activity was higher than normal. Additionally, several areas were identified within the outcrop belts of these susceptible rock formations where catastrophic collapse sinkholes were extremely common. These highly active zones were located in areas where urban development had redirected the locations of surface streams. One particular area along Interstate 70 that was adjacent to an active quarry faced a confluence of geologic, topographic, and human factors that were conducive to karst feature development. As a result, the area experienced very high levels of cover-collapse sinkhole formation.

In the Hagerstown Valley, several formations also exhibit strong tendencies towards active sinkhole development, while others show only modest affinities (Table 1). However, sinkhole proclivity cannot exclusively be correlated to the bedrock unit alone. Other geologic factors contribute in controlling the type, number, and distribution of karst features. These geologic factors play varying roles in karst feature distribution, and rarely can karst activity at a particular location be unequivocally attributed to a single cause. In areas where various factors overlap, the greatest potential for catastrophic-collapse sinkholes occurs.

Understanding the influence of each variable with respect to location may have demonstrable implications in site evaluation during highway planning, construction, and maintenance, urban planning and development, or home purchase. Knowledge of the relative importance of these factors in any one area may be critical in engineering and site evaluation and selection. The nexus of these geologic and topographic factors in sinkhole development can produce a highly unstable karst regime and understanding their relative importance is critical to effective and safe site evaluation before any significant earthmoving activity begins.

In an effort to evaluate the Hagerstown Valley for prominent areas of likely karst development, a generalized map of potential aggregate causes was produced (Figure 61). This map was constructed by dividing the Hagerstown Valley into an approximately 1-mile square grid. For each square the number of karst factors was tallied. This methodology is based on and expanded from efforts of Shofner and Mills (2001) for the State of Tennessee. The work of Shofner and Mills was simply the compilation of karst depressions within blocks of 2.5′ of longitude and latitude. In this study, factors used for the tally included karst susceptibility of the bedrock units present, water table elevation in relation to topographic relief, presence of faults, and occurrence of thick Quaternary deposits of colluvium or terraces. For bedrock units, the factor value corresponded to their KSI number. Those units with a KSI below 2 were arbitrarily assigned a value of 1, those below 3 were given a value 2, and under 4 received a value of 3. Factor values of the bedrock KSI were then added to other identified complicating factors. Faults, Quaternary deposits, and topography and differential in the water table were each given factor values of 1. The factors for each square were totaled and are shaded according to their numerical values as shown in Figure 61.

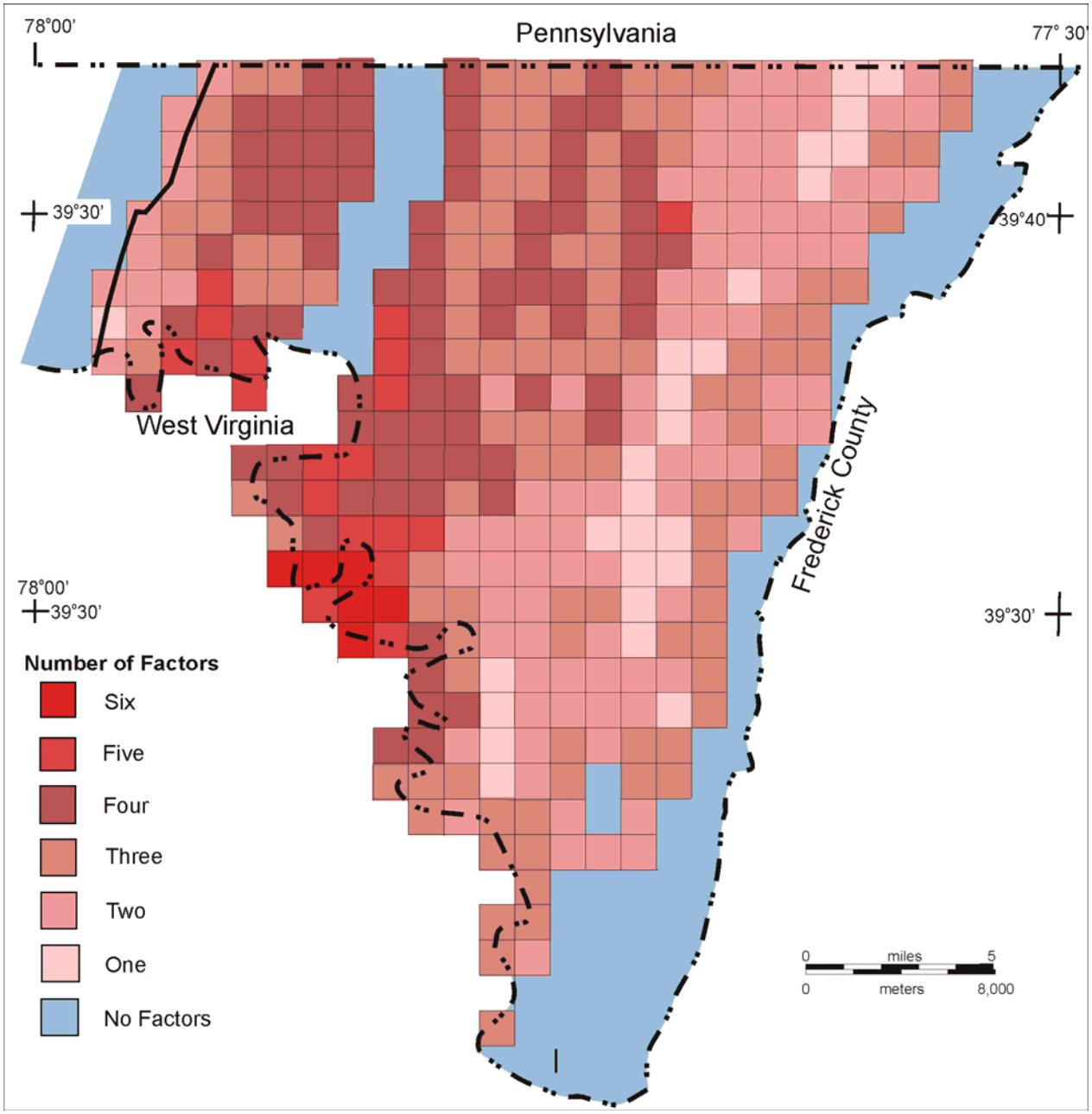

Figure 61.– Map of potential karst hazard factors. Karst factor numbers for each area block are based upon inherent geologic and topographic factors (see text).

The karst factor map illustrates two general patterns of change in karst risk factors. The first pattern is the trend from lower risk areas along the eastern and western edges of the valley to greater values toward the center. This pattern excludes the central belt of Martinsburg clastic rocks where no karst risks exist. This pattern can be attributed to the change from Cambrian carbonate rocks along the edges of the valley to the purer, more easily dissolved Ordovician carbonates near the center of the valley. The second pattern is the tendency for an increase in factors from north to south. This trend can be attributed to changes in the water table associated with the Potomac River. While there is a slightly increased level of karst factors associated with areas immediately adjacent to the Potomac River, the highest number of factors (six) was determined to be in areas adjacent to the Potomac River and near the center of the synclinorium.

At the scale examined, the karst hazards factor map can show only very general trends in locating potential karst problem areas. However, the same process can be

applied at virtually any scale. More detailed site analysis may reveal the complex interplay of each factor on a more site specific scale.

In summary, the geologic, topographic, and human activity factors that contribute to sinkhole formation, and that were identified during this study, can be utilized as a set of baseline characters for assessment in any highway improvement project, urban development effort and site evaluation. These characters provide a foundation upon which more detailed and localized site studies may be based. This information provides an underpinning that site developers can employ in identifying areas of high sinkhole susceptibility.

Living on Maryland's Great Valley Karst

Sherwood (2004) outlined several salient environmental concerns when living in areas underlain by karst in Maryland. Key among these concerns is the proximity of home septic and water well placement. Because areas underlain by carbonate rocks provide unfettered conduits for untreated sewage to migrate into underground aquifers, it is of paramount importance that water wells be placed as far from septic drain fields as possible. Furthermore, water wells in karst cutter areas (i.e., in topographic depressions) can have high water yields since they benefit from the centripetal drainage that they promote. However, they also present greater potential for entry of contaminants, such as lawn fertilizers, weed killers or sewage, into the potable water table (Figure 62A). These problems can be amplified on farms where there is a need for large amounts of drinking water for animals as well as a requirement to safely dispose of their waste. In these cases, it is crucial that all waste pits be lined and overflow very limited as these excavations present potential point sources of aquifer contaminants (Figure 62B).

Similar potential for contamination can be identified surrounding highway salt storage and distribution areas. Road surfaces are treated in winter with high levels of salt. However, large quantities of salt are stored year-round. Water wells located near one of these facilities or adjacent to roadways, can be more susceptible to contamination (Figure 62C).

Throughout the Hagerstown Valley, a common practice is to use steep-sided depressions or active sinkholes as a miniature landfill. These venues present exceptional opportunities for transferring surface waters into the water table (See previous sections of this report). This practice was determined to be widespread and numerous examples were identified during this study (Figure 62D). While this custom can, at times, be unsightly and relatively harmless (as illustrated in Figure 62D), when this method of disposal is used for such things as old tires, motor oil, or animal carcasses, it can present a serious contamination problem for local water usage.

The same bedrock characteristics that can make inhabiting karst regions dangerous, can also provide benefits to the inhabitants. Many of Maryland's highest yielding springs are found in the State's karst areas. The Department of Natural Resources' Albert Powell trout hatchery, on the eastern side of the valley, has a spring with high flow rate. This karst spring is located along a local fault (Figures 44, 61E). Another example of the benefits of karst can be observed along Cresspond Road north of Wilson. In this case, several high-yield springs provide sufficient water for watercress aquaculture. These springs are fed by several local cross-faults that have offset the carbonate rock units (Figure 62F).

In conclusion, homeowners, business owners, farmers, and travelers all should be aware of the potential dangers and benefits of living on or passing through karst regions. Because groundwater in karst terrains can travel fairly rapidly through the rock over great distances, a seemingly inconspicuous or innocuous spill of a pollutant can quickly find its way into the drinking water of a property owner miles away. It is vital that any such spill be reported to government officials and remediated immediately.

CONCLUSIONS

Brezinski (2004a) demonstrated the importance of understanding the distribution and interrelationship of geologic and human factors to the distribution of karst features of the Frederick Valley of Frederick County, Maryland. While geology and human factors can also be shown to play roles in karst development in the Hagerstown Valley, geologic factors currently appear to impact karst feature development much more than those created by humans (Figure 62). Understanding stratigraphy, structure, and topography is critical to understanding and predicting the type and density of karst features in Maryland's Great Valley. However, comparison of attributes assignable to active sinkhole development in the Hagerstown and Frederick valleys demonstrates that the impact of human activity in the latter greatly outweigh that in the former. In examining Figure 63 one can determine that 21% of all active sinkholes identified in the Hagerstown Valley resulted from human activity (unlined drainage (17%) and storm water impoundments (4%)). By contrast, 50% of the

Figure 62.– Living on Maryland's Great Valley karst. A, Home water supply well (circled) drilled in front-yard depression. B, Farm manure storage pit. C, Salt storage facility and runoff area. D, Active sinkholes employed as a trash dump. E, A high flow spring located along a large cross-fault, Albert Powell trout hatchery. F, Fault-related springs used for watercress agriculture, Cresspond Road at Conococheague Creek.

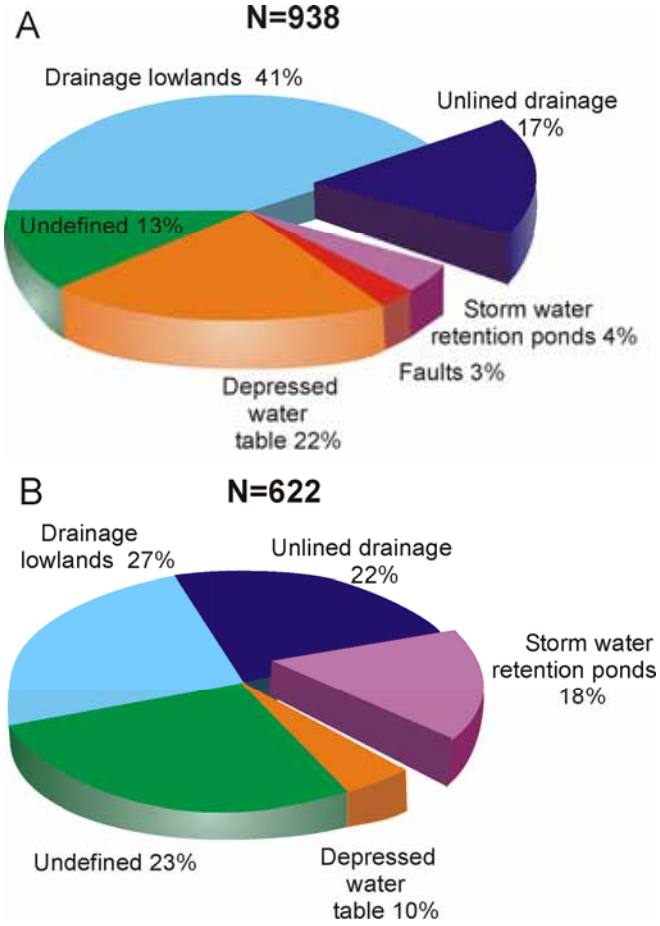

Figure 63.– Pie diagrams comparing probable proximate causes of active sinkhole formation between the Great Valley (A) and Frederick Valley (B) of Maryland. Frederick Valley data extracted from Brezinski (2001, 2001b, 2004b, 2004c, 2004d).

Frederick Valley's active sinkholes can be assigned to human causation (unlined drainage (22%), storm water impoundments (18%), and depressed water table 10%). In the Frederick Valley, depressed water table is assigned as a human activity, because nearly all sinkhole activity assigned to this factor were in areas surrounding active quarrying or development (Brezinski, 2007, figs. 9, 13, 14, 16). In the Hagerstown Valley, only several instances of sinkhole activity were determined to have resulted from quarrying (Figure 60). Depressed water table attribution to sinkhole formation was prominent in areas adjacent to the Potomac River and Conococheague and Antietam creeks (Figure 34). In comparing the two most important karst areas in the State of Maryland, the Hagerstown and Frederick valleys, human activity plays a more important role in the latter, while geology is more important in the understanding of sinkhole activity in the former. In coming years it is predicted that within the Hagerstown Valley, increased human activity and development will lead to increase sinkhole activation there.

ACKNOWLEDGEMENTS

This report is based upon geologic maps and geologic field mapping conducted during a cooperative study between the Maryland Geological Survey and the Maryland State Highway Administration's Office of Materials Technology (OMT) Project MD-14-SP009B4M. The support of SHA OMT personnel Rodney Wynn and Eric Dougherty is acknowledged and appreciated. Access to Holcim, Inc. Security quarry was provided by Thomas Newman and Victoria Mock. Heather Quinn, Robert Conkwright, and Elizabeth Sylvia of the Maryland Geological Survey were instrumental in preparing GIS-based geologic and karst maps upon which this report is based. Rebecca Kavage-Adams assembled the composite geology-karst map portrayed in Plate 1. The author thanks Carla Kertis and Randall Orndorff (U.S. Geological Survey), and Eric Dougherty (Maryland State Highway Administration) for helpful comments provided on earlier drafts of this report. The interpretations presented herein are solely those of the author.

REFERENCES

Aley, T., 2007, Delineation of the zone of influence for the St. Lawrence cement quarry, Hagerstown, Maryland. Ozark Underground Laboratory Water and Land Use Investigations, 33 p.

Bassler, R.S., 1919, The Cambrian and Ordovician deposits of Maryland: Maryland Geological Survey Systematic Report, 424 p.

Beck, B.F., 1986, A generalized genetic framework for the development of sinkholes and karst in Florida, U.S.A.: Environmental Geology Water Sciences, 8:5-18.

Bell, S.C., 1993, Geology of the Hagerstown Quadrangle, Washington County, Maryland: Maryland Geological Survey Geologic Map, scale 1:24,000.

Brezinski, D.K., 1992, Lithostratigraphy of the western Blue Ridge cover rocks in Maryland: Maryland Geological Survey Report of Investigations 55, 69 p.

Brezinski, D.K., 1996a, Stratigraphy of the Elbrook Formation (Middle to Upper Cambrian) in Maryland and adjacent states: Maryland Geological Survey, Special Publication 3, p. 165-186.

Brezinski, D.K., 1996b, Carbonate ramps and reefs: Paleozoic stratigraphy and paleontology of Western Maryland: Maryland Geological Survey Geologic Guidebook 6, North American Paleontological Convention VI, 25 p.

Brezinski, D.K. 2001, Karst features map of the Buckeystown Quadrangle, Frederick and Montgomery Counties, Maryland: Maryland Geological Survey, scale 1:24,000.

Brezinski, D.K., 2001b, Karst features map of the Maryland Portion of the Point of Rocks Quadrangle, Frederick County, Maryland: Maryland Geological Survey, scale 1:24,000.

Brezinski, D.K., 2004a, Stratigraphy of the Frederick Valley and its relationship to karst development: Maryland Geological Survey Report of Investigations 75, 101 p.

Brezinski, D.K., 2004b, Karst Features Map of the Frederick Quadrangle, Frederick County, Maryland: Maryland Geological Survey Geologic Map, scale 1:24,000.

Brezinski, D.K., 2004c, Karst Features Map of the Walkersville Quadrangle, Frederick County, Maryland: Maryland Geological Survey Geologic Map, scale 1:24,000.

Brezinski, D.K., 2004d, Karst Features Map of the Woodsboro Quadrangle, Frederick and Carroll Counties Maryland: Maryland Geological Survey Geologic Map, scale 1:24,000.

Brezinski, D. K., 2007, Geologic and anthropogenic factors influencing karst development in the Frederick region of Maryland: Environmental Geosciences, 14:41-38.

Brezinski, D.K., 2009, Geologic map of the Keedysville and parts of the Shepherdstown, Harpers Ferry, and Charlestown quadrangles, Washington and Frederick Counties, Maryland: Maryland Geological Survey Digital Geological Map K_SHCGEO2009.1, scale 1:24,000.

Brezinski, D.K., 2013a, Geologic and karst features map of the Hagerstown quadrangle, Maryland: Maryland Geological Survey Digital Geological Map HAGER2013.1, scale 1:24,000.

Brezinski, D.K., 2013b, Geologic and karst features map of the Mason-Dixon quadrangle, Maryland: Maryland Geological Survey Digital Geological Map MASON2013.1, scale 1:24,000.

Brezinski, D.K., 2014, Geologic and karst features map of the Williamsport quadrangle, Washington County, Maryland: Maryland Geological Survey Digital Geological Map WILLI2014.1, scale 1:24,000.

Brezinski, D.K., and Bell, S.C., 2009, Geologic Map of the Funkstown quadrangle, Washington County, Maryland: Maryland Geological Survey Digital Geological Map FUNKSGEO2009.1, scale 1:24,000.

Brezinski, D.K. and Bell, S.C., 2013, Geologic Map of the Hagerstown quadrangle, Washington County, Maryland: Maryland Geological Survey Digital Geological Map HAGERGEO2013.1, scale 1:24,000.

Brezinski, D.K., and Fauth, J.L., 2009, Geologic map of the Myersville and Maryland portion of the Smithsburg quadrangles, Washington and Frederick Counties, Maryland: Maryland Geological Survey Digital Geological Map MY_SM2009.1, scale 1:24,000.

Brezinski, D.K., and Conkwright, R.D., 2013. Geologic map of Garrett, Allegany, and western Washington Counties, Maryland: Maryland Geological Survey Geologic Map, version 1.1, scale 1:100,000.

Brezinski, D.K., and Glaser, J.D., 2014, Geologic map of the Clear Spring and Hedgesville quadrangles, Washington County, Maryland: Maryland Geological Survey Digital Geological Map CL_HE2014.1, scale 1:24,000.

Brezinski, D.K., Anderson, T.A, and Campbell, P., 1996, Evidence for a regional detachment at the base of the Great Valley sequence in the central Appalachians,

Maryland: Maryland Geological Survey Special Publication 3: 223-230.

Brezinski, D. K., Repetski, J.E., and Taylor, J.F., 1999, Stratigraphic and paleontologic record of the Sauk III regression in the central Appalachians, *in* Santucci, V.L. and McClelland, L., eds., National Park Service Paleontological Research: 4: 32-41.

Brezinski, D.K, Taylor, J.F., and Repetski, J.E., 2012, Sequential development of platform to off-platform facies of the great American carbonate bank in the central Appalachians, *in* J.R. Derby, J.R., Fritz, R.D., Longacre, S.A., Morgan, W.A., and Sternbach, C.A., eds., The Great American Carbonate Bank: The geology and economic resources of the Cambrian–Ordovician Sauk megasequence of Laurentia: AAPG Memoir 98, p. 383–420.

Brezinski, D.K., Taylor, J.F., Repetski, J.E., and Loch, J.D., 2015, Cambrian–Ordovician of the central Appalachians: Correlations and event stratigraphy of carbonate platform and adjacent deep-water deposits, *in* Brezinski, D.K., Halka, J.P., and Ortt, R.A., Jr., eds., Tripping from the Fall Line: Field Excursions for the GSA Annual Meeting, Baltimore, 2015: Geological Society of America Field Guide 40, p. 61–83.

Clarke, J.M., and Schuchert, C., 1899, The nomenclature of the New York series of geological formations: Science, 10:874-878

Cloos, E., 1941, Geologic Map of Washington County: Maryland Geological Survey, scale 1:62,500.

Cloos, E., 1947, Oolite deformation in the South Mountain fold, Maryland: Geological Society of America Bulletin, 58:843-918.

Cloos, E. 1958, Structural Geology of South Mountain and Appalachians in Maryland: Johns Hopkins University Studies in Geology 17, 85 p.

Cloos, E., 1971, Microtectonics of the western edge of the Blue Ridge Maryland and Virginia: Johns Hopkins University Studies in Geology 20, 234 p.

Dean, S.L., Kulander, B.R., and Lessing, P., 1987, Geology of the Hedgesville, Keedysville, Martinsburg, Shepherdstown, and Williamsport quadrangles, Berkley and Jefferson Counties, West Virginia: West Virginia Geological and Economic Survey, scale 1:24,000.

Demicco, R.V., 1985, Platform and off-platform carbonates of the Upper Cambrian of Western Maryland, USA: Sedimentology, 32:1-22.

Demicco, R.V., and Mitchell, R.W., 1982, Facies of the Great American Bank in the central Appalachians, *in* P.T. Little, ed., Central Appalachian Geology: Northeastern-Southeastern Sections of Geological Society of America, Fieldtrip Guidebooks, p. 171-266.

Doctor, D.H., Weary, D.J., Orndorff, R.C., Harlow, G.E., Jr., Kozar, M.D., and Nelms, D.L., 2008, Bedrock structural controls on the occurrence of sinkholes and springs in the northern Great Valley karst, Virginia and West Virginia, *in* Proceedings of the 11th Multidisciplinary Conference on Sinkholes and Engineering and Environmental Impacts of Karst, Tallahassee, Florida, 23–26 September: Carlsbad, New Mexico, National Cave and Karst Research Institute, p. 12–22.

Doctor, D.H., Weary, D.J., Brezinski, D.K., Orndorff, R.C., and Spangler, L.E., 2015, Karst of the Mid-Atlantic region in Maryland, West Virginia, and Virginia, *in* Brezinski, D.K., Halka, J.P., and Ortt, R.A., Jr., eds., Tripping from the Fall Line: Field Excursions for the GSA Annual Meeting, Baltimore, 2015: Geological Society of America Field Guide 40, p. 425–484.

Duigon, M.T., 2001, Karst hydrogeology of the Hagerstown Valley, Maryland: Maryland Geological Survey Report of Investigations 73, 128 p.

Edwards, J., 1978, Geologic map of Washington County: Maryland Geological Survey County Map, scale 1:62,500.

Epstein, J.B., Orndorff, R.C., and Rader, E.K., 1995, Middle Ordovician Stickley Run Member (new name) of the Martinsburg Formation, Shenandoah Valley, northern Virginia, *in* Stratigraphic Notes, 1994: U.S. Geological Survey Bulletin, 2135, p. 1-13.

Franz, R., and Slifer, D., 1971, Caves of Maryland: Maryland Geological Survey, Educational Series 3, 120 p..

Harrison, R.W., Newell, W.L., and Necdet, M., 2002, Structure and gensis: karstification along an active fault zone: U.S. Geological Survey Water Resources Investigation Report, 02-4174, p. 45-48.

Jennings, J.N., 1985, Karst Geomorphology: Basil Blackwell, New York, 293 p.

Keith, A., 1893, Chapter III, Geology, *in* G.H. Williams and W.R. Clark, Maryland: Its Resources, Industries, and Institutions: Maryland Geological Survey, p. 68.

Keith, A., 1894, The Harpers Ferry Folio: U.S. Geological Survey Atlas Folio 10, 5 p.

Kulander, B.R., and Dean, S.L. 1986, Structure and tectonics of cenral and southern Appalachian Valley and Ridge and Plateau provinces, West Virginia and Virginia: American Association of Petroleum Geologists Bulletin, 70:1674-1684.

Kochanov, W.E., 1999, Sinkholes in Pennsylvania: Pennsylvania Geological Survey (4^{th} Series) Educational Series 11, 33 p.

McBride, E., 1962. Flysch and and associated beds of the Martinsburg Formation (Ordovician), central Appalachians: Journal of Sedimentary Petrology, 32:39-91

Morgan, W.A., 2012, Sequence stratigraphy of the great American carbonate bank, *in* J.R. Derby, R.D. Fritz, S.A. Longacre, W.A. Morgan, and C.A. Sternbach, eds., The great American carbonate bank: The geology and economic resources of the Cambrian-Ordovician Sauk megasequence of Laurentia: AAPG Memoir 98, p. 37–82.

Mussman, W.J., and Read J.F., 1986, Sedimentology and development of a passive-to convergent-margin unconformity: Middle Ordovician Knox unconformity, Virginia Appalachians: Geological Society of America Bulletin, 97:282–295.

Neuman, R.B., 1951, St. Paul Group: A revision of the "Stones River" Group of Maryland and adjacent states: Geological Society of America Bulletin, 62:267-324.

Nickelson, R.P., 1956, Geology of the Blue Ridge near Harpers Ferry, West Virginia: Geological Society of America Bulletin, 67:239-270.

Nutter, L.J., 1973, Hydrogeology of the carbonate rocks, Frederick and Hagerstown Valleys, Maryland: Maryland Geological Survey Report of Investigations 19, 70 p.

Orndorff, R.C., 1992, Tectonic significance of cross-strike faults in the central Appalachian Great Valley of Maryland and West Virginia: Southeastern Geology, vol. 32, no. 4, p. 197-214.

Orndorff, R.C., 2012, Fold-to-fault progression of a major thrust zone revealed in horses of the North Mountain fault zone, Virginia and West Virginia, USA: Journal of Geological Research, v. 2012, article 294093, 13 p.

Orndorff, R.C., and Goggin, K.E., 1994. Sinkholes and karst related features of the Shenandoah Valley of the Winchester 30X60 minute quadrangle, Virginia and West Virginia: U.S. Geological Survey, Miscellaneous Field Studies Map, MF 2262, scale 1:100,000

Orndorff, R.C., and Harlow, G.E., 2002. Geohydrologic framework of the northern Shenandoah Valley carbonate aquifer system: U.S. Geological Survey Water Resources Investigation Report, 02-4174, p. 81-89.

Palmer, A.R., and James, N.P., 1979, The Hawke Bay event: A circum-Iapetus regression near the Lower Middle Cambrian Boundary, *in* Wones, D.R., ed., The Caleodonides in the U.S.A.: Virginia Polytechnic Institute and State University Memoir 2 Pp. 15-19.

Rader, E.K., and Read, J.F., 1989, Early Paleozoic continental shelf to basin transition, northern Virginia: 28th International Geological Congress fieldtrip guidebook T221: American Geophysical Union, Washington, D.C., 9 p.

Reger, J.P., and Cleaves, E.T., 2008, Physiographic map of Maryland: Maryland Geological Survey, scale 1:250,000.

Ryder, R.T., Harris, A.G., and Repetski, J.E., 1992, Stratigraphic framework of Cambrian and Ordovician rocks in the central Appalachian Basin from Medina County, Ohio, through southwestern and south-central Pennsylvania to Hampshire County, West Virginia: U.S. Geological Survey Bulletin 1839-K, 32 p.

Read, J.F., 1989, Controls on Evolution of Cambrian-Ordovician passive margin, U.S. Appalachians, *in* P.D. Crevello, J.F. Read, J.F. Sarg, and J.L. Wilson, eds., Controls on Carbonate Platform and Basin Development: SEPM Special Paper 44, p. 147-165.

Root, S.I., 1968, Geology and Mineral Resources of Southeastern Franklin County, Pennsylvania: Pennsylvania Topographic and Geologic Survey (4th series), Atlas 119, 118p.

Sando, W.J., 1956, Nomenclature of Lower Ordovician rocks of Washington County, Maryland: Geological Society of America Bulletin, 67:935-938.

Sando, W.J., 1957, Beekmantown Group (Lower Ordovician) of Maryland: Geological Society of America Memoir 68, 161 p.

Sando, W.J., 1958, Lower Ordovician section near Chambersburg, Pennsylvania: Geological Society of America Bulletin, 69:837-854.

Sherwood, T., 2004, Karst and sinkholes in western Maryland: Western Maryland Resource Conservation and Development Council Users Guide, 21 p.

Shofner, G.A., and Mills, H.H., 2001, A simple map index of karstification and its relationship to sinkhole and cave distribution in Tennessee: Journal of Cave and Karst Studies 63:67-75.

Stose, G.W., 1906, Sedimentary rocks of South Mountain, Pennsylvania: Journal of Geology, 14:201-220.

Stose, G.W., 1908, Cambro-Ordovician limestones of the Appalachian Valley in southern Pennsylvania: Journal of Geology, 16:698-714.

Stose, G.W. 1910, Mercersburg-Chambersburg Folio: U.S. Geological Survey Atlas Folio, 144 p.

Southworth, S, and Brezinski, D.K., 1996, Geology of the Harpers Ferry Quadrangle, Virginia, Maryland, and West Virginia: U.S. Geological Survey Bulletin, 2123, 33 p, 1996.

Taylor, J.F., Repetski, J.E., and Orndorff, R.C., 1992, The Stonehenge Transgression: A rapid submergence of the central Appalachian platform in the early Ordovician, *in* B.D. Webby and J.F. Laurie eds.,

Global Perspectives on Ordovician geology: Balkema, p. 409-418.
Taylor, J. F., Brezinski, D.K., and Durika, N.J., 1997, The Lower to Middle Cambrian transition in the central Appalachian region (abs.): Proceedings and Abstracts of the 2nd International Trilobite Conference, p. 48.
Wilson, J.L., 1952, Upper Cambrian stratigraphy in the central Appalachians: Geological Society of America Bulletin, 63:275-322.
Wilson, W.L., and Beck, B.R., 1992, Hydrologic factors affecting new sinkhole development in the Orlando area, Florida: Ground Water, 30:918-930.
Woodward, H.P., 1949, The Cambrian System in West Virginia: West Virginia Geological Report, v.20, 317 p.

APPENDIX I - Measured Stratigraphic Sections

(See Plate 1 for section locations)

Section 1

Section along CSX railroad tracks, and the Potomac River at the northern end of Bolivar Heights, Jefferson County, West Virginia. Section begins near the base of the Tomstown Formation, and is the type section of the Bolivar Heights Member. Section re-measured and modified from Brezinski (1992). 39°20′60″ N, 77°45′21″ W.

Thickness (feet) unit	total	
Tomstown Formation		
Bolivar Heights Member		
45.0	45.0	White, laminated marble with tan, dolomitic laminae (Keedyville marble bed).
2.0	47.0	Medium gray, platy limestone.
19.0	66.0	Interbedded, laminated, dark gray limestone and dark yellowish orange dolomite.
12.0	78.0	Dark gray, platy limestone.
3.0	81.0	Medium gray, shaly limestone.
8.0	89.0	Dark gray, laminated limestone with continuous beds.
0.5	89.5	Dark gray dolomite.
12.0	101.5	Medium to dark gray, laminated limestone.
2.0	103.5	Medium gray, platy limestone (sheared).
31.0	134.5	Dark gray, laminated to ribbony limestone with a few rounded, dolomitic burrows.
24.0	158.5	Dark gray, very thin-bedded limestone with distorted, brownish gray burrows.
5.5	164.0	Dark gray, thin-bedded limestone.
7.0	171.0	Dark gray, thin-bedded, bioturbated limestone.
8.0	179.0	Dark gray, laminated limestone with a few dolomitic burrows.
4.0	183.0	Dark gray, very thin-bedded limestone with abundant dolomitic burrows.
6.0	189.0	Dark gray, moderate yellowish brown-weathering, dolomitic, bioturbated limestone.
3.0	192.0	Dark gray, laminated, burrowed limestone.
27.0	219.0	Dark gray, burrow-mottled limestone with tan laminations.
Fort Duncan Member		
20.0	239.0	Dark gray, thick-bedded, bioturbated dolomite.
5.0	244.0	Covered.
147.0	391.0	Dark gray, thick-bedded, bioturbated, coarse-grained dolomite.
55.0	446.0	Covered.
Benevola Member		
20.0	466.0	Light gray, fractured, aphanitic dolomite.
65.0	531.0	Covered. Section moved to riverbank.
40.0	571.0	Light gray, massive dolomite.
Dargan Member		
250.0	821.0	Covered.
25.0	846.0	Light to medium gray, medium-bedded, bioturbated dolomite.
10.0	856.0	Light gray, coarse-grained dolomite.
45.0	901.0	Covered.
9.0	910.0	Dark gray, bioturbated dolomite.
10.0	920.0	Covered.
47.0	967.0	Medium to dark gray, coarse-grained, ribbony dolomite with numerous bioturbated beds.
25.0	992.0	Covered.
50.0	1042.0	Dark gray, medium-bedded, coarse-grained, bioturbated dolomite, rippled and ribbony.
3.0	1045.0	Dark gray, laminated dolomite.
9.0	1054.0	Medium gray, coarse-grained, bioturbated dolomite.
2.0	1056.0	Dark gray, ripple-laminated dolomite.
5.0	1059.0	Medium gray, bioturbated dolomite.
12.0	1071.0	Covered.
3.0	1074.0	Medium gray, cross-bedded, oolitic dolomite.
16.0	1090.0	Dark gray, bioturbated dolomite.
7.0	1097.0	Covered.
5.0	1102.0	Dark gray, laminated dolomite with sharp (hard ground) upper surface.
14.0	1116.0	Interbedded, dark gray, laminated, and bioturbated dolomite. Contains several oolitic beds.
15.0	1131.0	Dark gray, medium-bedded, bioturbated dolomite.
10.0	1141.0	Interbedded, dark gray, laminated limestone and dolomite.
27.0	1168.0	Interbedded, dark gray, laminated limestone and bioturbated dolomite.

Section 2

Section along C&O Canal and Lime Kiln Road, 1 mile northwest of Dargan, Washington County, Maryland. Section begins along canal in core of fold that exposes upper strata of Bolivar Heights Member of the Tomstown Formation. This is the type section of the Dargan Member. 39°23′19″ N, 77°43′59″ W.

Thickness (feet) unit	total	
Tomstown Formation		
Bolivar Heights Member		
48.0	48.0	Dark gray, impure limestone with tan, dolomitic stringers.
6.0	54.0	Covered.
16.0	70.0	Dark gray, burrowed limestone with dolomitic stringers.
3.0	73.0	Covered.
Fort Duncan Member		
7.0	80.0	Dark gray, thick-bedded, knotty dolomite.
11.0	91.0	Covered.
10.0	101.0	Dark gray, knotty dolomite.
4.0	105.0	Medium gray limestone.
7.0	112.0	Olive-black, knotty dolomite.
2.0	114.0	Dark gray, knotty dolomite with limestone interbeds.
210.0	324.0	Dark gray, medium- to thick-bedded, coarsed-grained, knotty dolomite.
Benevola Member		
10.0	334.0	Covered. Ccontinued on Lime Kiln Road.
45.0	379.0	Medium to light gray, granular, massive dolomite.
37.0	416.0	Very light gray, massive dolomite.
1.0	417.0	Brownish gray, bioturbated dolomite.
6.0	423.0	Brownish gray, laminated dolomite.
5.0	428.0	Covered.
6.0	434.0	Dark gray, bioturbated dolomite, thick-bedded at top.
2.0	436.0	Dark gray, ribbony dolomite.
25.0	461.0	Medium gray, medium-bedded dolomite, locally bioturbated.
3.0	464.0	Covered.
55.0	519.0	Very light gray, massive to thick-bedded dolomite; some indications of cross-bedding.
Dargan Member		
1.0	520.0	Medium gray, laminated dolomite.
3.0	523.0	Light gray, coarse-grained dolomite.
4.0	527.0	Dark gray, laminated, stromatolitic dolomite.
3.0	530.0	Dark gray dolomite.
7.0	537.0	Dark gray, stromatolitic dolomite.
3.0	540.0	Dark gray, thin-bedded dolomite.
5.0	545.0	Medium gray, laminated dolomite.
6.0	551.0	Medium gray, bioturbated dolomite.
3.0	554.0	Dark gray, laminated, algal dolomite.
1.0	555.0	Medium gray dolomite.
1.0	556.0	Medium gray, bioturbated dolomite.
3.0	559.0	Medium gray, laminated dolomite.
17.0	576.0	Medium gray, medium-bedded, bioturbated dolomite.
1.0	577.0	Dark gray, laminated dolomite.
3.0	580.0	Dark gray dolomite.
3.0	583.0	Dark gray, bioturbated dolomite.
4.0	587.0	Medium gray, bioturbated dolomite.
6.0	593.0	Medium gray, stromatolitic dolomite.
3.0	596.0	Medium gray, medium-bedded dolomite.
2.0	598.0	Medium gray, stromatolitic dolomite.
3.0	601.0	Medium gray, medium-bedded, bioturbated dolomite.
3.0	604.0	Covered.
4.0	608.0	Medium gray, laminated dolomite.
3.0	611.0	Covered.
15.0	626.0	Dark gray, laminated dolomite.
12.0	638.0	Dark gray, medium-bedded, bioturbated dolomite.
3.0	641.0	Dark gray, laminated dolomite.
3.0	644.0	Covered.
11.0	655.0	Dark gray, massive, coarse-grained, bioturbated dolomite.
25.0	680.0	Covered.
4.0	684.0	Medium gray, laminated dolomite.
10.0	694.0	Covered.
3.0	697.0	Medium gray dolomite.
5.0	702.0	Dark gray, laminated, vuggy dolomite.
6.0	708.0	Medium gray, thin-bedded, stylolitic limestone.
5.0	713.0	Very light gray, coarse-grained dolomite.
3.0	716.0	Light gray, laminated dolomite.
3.0	719.0	Medium gray, medium-bedded, bioturbated dolomite.
2.0	721.0	Covered.
10.0	731.0	Medium gray, laminated dolomite.
3.0	734.0	Medium gray, bioturbated dolomite.
2.0	736.0	Medium gray dolomite.
1.0	737.0	Dark gray, bioturbated dolomite.
1.0	738.0	Medium gray, laminated dolomite.
2.0	740.0	Dark gray, bioturbated dolomite.
12.0	752.0	Interbedded, medium gray, tan-weathering dolomite, and dark gray,

		laminated, stromatolitic limestone.
5.0	757.0	Dark gray, laminated limestone.
3.0	760.0	Medium gray, dense limestone.
3.0	763.0	Medium gray, laminated limestone.
10.0	773.0	Interbedded, dark gray, ribbony limestone, and algal, laminated dolomite.
2.0	775.0	Tan, argillaceous dolomite.
4.0	779.0	Medium gray, laminated limestone.
1.0	780.0	Tan, laminated dolomite.
7.0	787.0	Dark gray, laminated limestone, with grainstone interbeds.
3.0	790.0	Dark gray, sheared limestone.
4.0	794.0	Covered.
3.0	797.0	Dark gray, laminated limestone.
4.0	801.0	Covered.
1.5	802.5	Tan, laminated dolomite.
5.0	807.5	Dark gray, crinkle-laminated limestone.
2.0	809.5	Tan, argillaceous dolomite.
1.0	810.5	Dark gray, stromatolitic limestone.
2.0	812.5	Tan dolomite.
10.0	822.5	Dark gray, laminated dolomite.
25.0	847.5	Covered.
2.0	849.5	Tan dolomite.
7.0	856.5	Dark gray, laminated limestone.
2.0	858.5	Tan dolomite.
13.0	871.5	Dark gray, cherty limestone; chert black in color.
17.0	888.5	Interbedded, medium gray, cherty limestone and tan, laminated dolomite to dolomitic limestone.

Section 3

Section along abandoned Western Maryland railroad cut-off at Red Run Creek, south of Wayne Heights, Franklin County, Pennsylvania. Section begins in the Dargan Member, Tomstown Formation, and is the type section of the Red Run Member of the Waynesboro Formation. 39°43′59″ N, 77°33′ 03″ W

Thickness (feet) unit	total	
Tomstown Formation		
Dargan Member		
20.0	20.0	Dark gray, bioturbated dolomite.
7.0	27.0	Tan, laminated dolomite.
3.0	30.0	Tan, shaly dolomite.
7.0	37.0	Medium gray, ribbony dolomite.
15.0	52.0	Dark gray, silty limestone.
7.0	59.0	Covered.
5.0	64.0	Dark gray, dolomite.
3.0	67.0	Tan, laminated dolomite.
Waynesboro Formation		
Red Run Member		
3.0	3.0	Olive-gray, calcareous shale.
10.0	13.0	Medium gray, laminated, sandy dolomite.
3.0	16.0	Dark gray dolomite.
11.0	27.0	Dark gray, medium-bedded dolomite with sandy stringers.
12.0	39.0	Covered.
4.0	43.0	Medium gray, medium-bedded, sandy dolomite, weathering tan.
2.0	45.0	Covered.
2.0	47.0	Medium gray, sandy dolomite.
4.0	51.0	Olive-gray, calcareous shale.
7.0	58.0	Light gray, calcareous, medium-bedded sandstone with purple laminations at top.
4.0	62.0	Interbedded, medium gray and tan dolomite.
6.0	68.0	Covered.
5.0	73.0	Medium gray, tan weathering, dolomitic sandstone.
3.0	76.0	Tan, sandy, ribbony dolomite.
3.0	79.0	Covered.
15.0	94.0	Interbedded, tan, dolomitic sandstone, sandy, ribbony dolomite, and very dark-red shale.
3.0	97.0	Medium gray, medium-bedded, medium-grained, calcareous sandstone.
5.0	102.0	Tan, laminated, medium-grained sandstone.
7.0	109.0	Covered.
25.0	134.0	Interbedded, medium gray, sandy limestone, and olive-gray, calcareous, sandy shale.
Cavetown Member		
30.0	164.0	Dark gray, folded, sandy limestone.
10.0	174.0	Dark gray, massive limestone.
15.0	189.0	Covered.
21.0	210.0	Dark gray, massive, dolomitic limestone.
350.0	560.0	Covered. Thickness estimated by pacing.
17.0	577.0	Dark gray, bioturbated, massive dolomite.
120.0	697.0	Covered (thickness estimated by pacing).
Chewsville Member		
15.0	712.0	Dusky red, silty shale and sandy siltstone.
50.0	762.0	Covered.
3.0	765.0	Interbedded, dusky red shale, and grayish pink sandstone.
2.0	767.0	Covered.
6.0	773.0	Interbedded, light gray, medium-grained, cross-laminated sandstone, and rusty red,

		silty shale.
3.0	776.0	Covered.
2.0	778.0	Very light gray, medium-grained, flaser-bedded sandstone.
7.0	785.0	Interbedded, olive-gray, shaly limestone and shaly, sandy limestone.
3.0	788.0	Brown, calcareous sandstone.
11.0	799.0	Medium gray, oolitic limestone.

Section 4

Section of Waynesboro Formation exposed along the north and east walls of Beaver Creek Quarry, 1 mile south of Mt. Aetna, Washington County, Maryland. Section begins in the Cavetown Member on the northwest corner of quarry. 39°35′35″ N, 77°37′41″ W.

Thickness (feet)		
unit	total	
Waynesboro Formation		
Cavetown Member		
0.5	0.5	Olive-gray, calcareous shale.
1.0	1.5	Tan, argillaceous dolomite.
13.0	14.5	Interbedded, olive, calcareous shale and laminated, dolomitic limestone.
5.0	19.5	Dark gray, bioturbated dolomite.
3.5	23.0	Medium gray, laminated, dolomitic marble.
6.0	29.0	Medium gray dolomite.
19.0	48.0	Dark gray, massive, bioturbated dolomite.
3.0	51.0	Dark gray, laminated limestone.
12.0	63.0	Medium-dark gray, medium-bedded limestone with thin, shaly interbeds.
7.0	70.0	Medium gray, bioturbated dolomite.
1.0	71.0	Thin-bedded limestone.
15.0	86.0	Dark gray, thick-bedded, bioturbated, dolomitic limestone.
2.0	88.0	Dark gray, thin-bedded limestone.
3.0	91.0	Light gray, cross-bedded dolomite.
3.0	94.0	Interbedded, light gray dolomite and black, siliceous dolomite.
1.0	95.0	Dark gray, laminated limestone.
12.0	107.0	Dark gray, thin-bedded, ribbony dolomite.
2.0	109.0	Light gray, dolomite.
6.0	115.0	Dark gray, thin-bedded dolomite.
4.0	119.0	Thinly interbedded, dark gray limestone and olive, calcareous shale.
5.0	124.0	Dark gray, medium-bedded limestone.
2.0	126.0	Interbedded, dark gray limestone and shale.
5.0	131.0	Medium gray, medium-bedded dolomite.
6.0	137.0	Dark gray, thin-bedded limestone and olive shale.
21.0	158.0	Medium to dark gray, thin- to medium-bedded dolomite with thin, shaly partings.
1.0	159.0	Olive, calcareous shale.
3.0	162.0	Very light gray, bioturbated dolomite.
4.0	166.0	Medium gray, bioturbated dolomite.
14.0	180.0	Medium to dark gray, laminated to thin-bedded limestone to dolomitic limestone.
4.0	184.0	Tan, laminated dolomite.
10.0	194.0	Tan to light gray, thin-bedded, argillaceous limestone.
11.0	205.0	Dark gray, medium-bedded dolomite to dolomitic limestone.
3.0	208.0	Thinly interbedded, dark gray limestone and calcareous shale.
5.0	213.0	Dark gray, argillaceous limestone.
2.0	215.0	Dark gray, shaly, laminated limestone.
10.0	225.0	Dark gray, massive, bioturbated dolomite.
15.0	240.0	Dark gray, thin-bedded dolomite.
50.0	290.0	Fractured, dark gray dolomite, Probable fault zone, thickness in question.
7.0	297.0	Dark gray, thin- to medium-bedded limestone.
Chewsville Member		
7.0	304.0	Tan to medium gray, dolomitic shale.
2.0	306.0	Tan, argillaceous dolomite.
10.0	316.0	Olive-gray shale with tan, dolomitic interbeds and red-brown siltstone at top.
3.0	319.0	Tan, argillaceous dolomite.
5.0	324.0	Medium gray, argillaceous limestone.
10.0	334.0	Olive-gray shale with tan dolomite interbeds.
6.0	340.0	Interbedded, tan dolomite and gray, sandy limestone.
3.0	343.0	Interbedded, red-brown, sandy siltstone and fine-grained sandstone.

Section 5

Section in upper part of the Waynesboro Formation along CSXT railroad tracks, 1.0 mile east of Chewsville, Washington County, Maryland. Section begins near the base of the Chewsville Member of the Waynesboro. This is the type section of the Chewsville Member. 39°38′51″ N, 77°36′58″ W.

Thickness (feet)		
unit	total	
Waynesboro Formation		
Chewsville Member		
5.0	5.0	Interbedded, dusky red, sandy siltstone

		and light gray, medium-grained sandstone with *Skolithos* burrows.
2.0	7.0	Dark reddish brown, sandy siltstone.
6.0	13.0	Covered.
3.0	16.0	Moderate reddish brown, silty, calcareous, fine-grained sandstone.
16.0	32.0	Covered.
4.0	36.0	Dusky red, silty shale to mudstone.
4.0	40.0	Light-brown, laminated to thinly cross-laminated, sandy, dolomitic limestone.
2.0	42.0	Moderate red, sandy siltstone with *Rusophycus* burrows.
2.0	44.0	Moderate reddish brown, sandy dolomite.
2.5	46.5	Pale reddish brown, very fine-grained, calcareous sandstone.
6.0	52.5	Covered.
2.5	55.0	Interbedded, moderate red, cross-bedded sandstone, and dusky red and olive-gray shale.
2.0	57.0	Interlaminated, olive-gray and dusky red, sandy siltstone with fine-grained sandstone lenses.
1.5	58.5	Olive-gray shale.
6.5	65.0	Interbedded, pale-reddish to reddish brown, laminated, sandy dolomite to calcareous sandstone.
2.0	67.0	Very light gray, medium-grained, well-sorted, platy sandstone.
5.0	72.0	Interbedded, dusky red, sandy siltstone and cross-laminated, grayish pink sandstone.
1.0	73.0	Grayish red sandstone.
7.0	80.0	Olive-gray to medium gray, shaly limestone to calcareous shale.
1.0	81.0	Medium gray, shaly dolomite.
1.0	82.0	Tan weathering, laminated, silty dolomite.
5.0	87.0	Tan-weathering, medium gray, medium-bedded, fine-grained sandstone with reddish shale partings.
2.0	89.0	Interbedded, dusky red and olive-gray, calcareous shale.
5.0	94.0	Interbedded, dusky red siltstone to mudstone and grayish-pink, medium-grained sandstone.
9.0	103.0	Covered.
7.0	110.0	Olive-gray to medium gray, laminated to ribbony, sandy limestone and dolomitic limestone.
5.0	115.0	Covered.
6.0	121.0	Medium gray, tan-weathering, stromatolitic dolomite.
5.0	126.0	Olive-gray shale with dusky red siltstone interbeds.
6.0	132.0	Medium gray, silty sandstone.
3.0	135.0	Light gray, tan-weathering, cross-bedded sandstone.
4.0	139.0	Covered.
2.0	141.0	Tan, sandy dolomite.
2.0	143.0	Olive-gray, dolomitic, medium-grained sandstone.
10.0	153.0	Thinly interbedded, dusky red and olive-gray siltstone and grayish pink sandstone.

Section 6

Section along the C&O Canal National Historical Park, and adjacent CSXT railroad tracks east of McCoys Ferry, Washington County, Maryland. Section begins approximately 100 yards east of milemarker 110. 39°36′33″ N, 77°58′05″ W.

Thickness (feet)		
unit	total	
		Elbrook Formation
		lower member
15.0	15.0	Interbedded, tan, laminated and fractured, gray dolomite.
110.0	125.0	Covered.
24.0	149.0	Interbedded, bioturbated, dolomite and laminated, algal dolomite.
42.0	191.0	Covered.
37.0	228.0	Thinly interbedded, medium gray to dark gray, argillaceous, lime mudstone and tan dolomite. Appears knotty on weathered surface, also contains some red, silty layers.
7.0	235.0	Thin-bedded, argillaceous, fractured dolomite.
11.0	246.0	Interbedded, medium gray, bioturbated, dolomitic, lime mudstone and tan, fractured dolomite.
3.0	249.0	Medium gray to tan, fractured, ribbony dolomite.
20.0	269.0	Dark gray, thick-bedded, bioturbated, mottled, dolomitic lime mudstone. Appears similar to Fort Duncan Member of Tomstown.
12.0	281.0	Covered.
6.0	287.0	Medium gray, fractured, dolomitic, lime mudstone.
120.0	407.0	Covered. Stream valley.
32.0	439.0	Interbedded, dark gray, thrombolitic, lime mudstone and medium gray dolomite.

7.0	446.0	Covered.
1.0	447.0	Dark gray, laminated, dolomitic, lime mudstone.
5.0	452.0	Covered.
2.0	454.0	Tan, laminated dolomite.
2.5	456.5	Medium gray, bioturbated dolomite.
2.0	458.5	Tan, ribbony dolomite.
1.5	460.0	Covered.
8.0	468.0	Tan, laminated, fractured dolomite.
1.0	469.0	Medium gray, dolomitic, lime mudstone.
5.0	474.0	Medium gray to grayish brown, fractured limestone.
10.0	484.0	Tan, laminated, platy dolomite.
27.0	511.0	Covered.
5.5	516.5	Medium gray, knotty dolomite.
3.0	519.5	Tan to light gray dolomite.
9.0	528.5	Covered.
1.0	529.5	Light gray, bioturbated, lime mudstone.
16.0	545.5	Covered.
6.0	551.5	Medium gray, bioturbated, dolomitic, lime mudstone.
2.0	553.5	Covered.
6.0	559.5	Medium gray, tan-weathering, fractured dolomite.
1.0	560.5	Dark gray, medium-bedded, lime mudstone.
46.0	606.5	Covered.
9.5	616.0	Dark gray, bioturbated, vuggy, lime mudstone.
4.0	620.0	Dark gray, thin-bedded, lime mudstone.
3.0	623.0	Dark gray, bioturbated, dolomitic, lime mudstone.
2.0	625.0	Reddish brown, silty shale to dolomitic shale.
1.0	626.0	Dark gray, bioturbated, dolomitic, lime mudstone.
12.0	638.0	Covered.
5.0	643.0	Tan, shaly dolomite.
4.0	647.0	Dark gray, bioturbated, lime mudstone.
13.0	660.0	Covered.
7.0	667.0	Tan dolomite, laminated at the base.
9.0	676.0	Light gray, lime mudstone.
1.0	677.0	Light brownish gray dolomite.
3.0	680.0	Tan, shaly dolomite.
9.0	689.0	Covered.
2.0	691.0	Tan, laminated, platy dolomite.
5.0	696.0	Tan to light gray, platy dolomite.
29.0	725.0	Interbedded, tan, platy dolomite and medium-bedded, laminated, mudcracked dolomite.
12.0	737.0	Covered.
3.0	740.0	Tan, shaly, platy dolomite.
1.0	741.0	Light gray, dolomitic, lime mudstone.
5.0	746.0	Tan, laminated dolomite.
10.0	756.0	Interbedded, tan, platy dolomite and gray, laminated dolomite.
40.0	796.0	Covered.
3.0	799.0	Light gray, dolomitic, lime mudstone.
2.0	801.0	Tan, laminated dolomite
4.0	805.0	Covered.
5.0	810.0	Tan, shaly, platy dolomite.
4.0	814.0	Light gray, laminated dolomite.
1.0	815.0	Tan dolomite.
3.0	818.0	Medium gray, stromatolitic, lime mudstone.
3.0	821.0	Light gray, laminated dolomite.
2.0	823.0	Covered.
1.5	824.5	Tan, laminated dolomite.
2.5	827.0	Light gray, thrombolitic, lime mudstone.
5.0	832.0	Covered.
5.5	837.5	Medium gray, very thin-bedded, lime mudstone.
2.5	840.0	Tan, knotty dolomite.
1.0	841.0	Tan, laminated dolomite.
2.0	843.0	Medium gray, thin-bedded, lumpy, lime mudstone.
3.5	846.5	Tan, laminated, argillaceous dolomite.
3.0	849.5	Covered.
2.5	852.0	Medium gray, vuggy, lime mudstone with weathered, dolomitic burrows.
2.0	854.0	Tan, platy, argillaceous dolomite.
3.5	857.5	Dark gray, bioturbated, lime mudstone with tan, dolomitic burrow fillings.
2.0	859.5	Tan, platy, argillaceous dolomite.
5.0	864.5	Tan, laminated, fractured dolomite.

middle member

16.0	880.5	Dark gray, thin to nodular bedded, bioturbated, lime mudstone with thin, tan, dolomitic partings.
2.5	883.0	Thinly interbedded, shaly, lime mudstone with thin, dolomitic laminations.
5.0	888.0	Interbedded, dark gray, lime mudstone with reddish, argillaceous laminations and shaly, gray dolomite.
1.0	889.0	Tan to light grayish brown dolomite, with small, lime mudstone nodules.
5.0	894.0	Dark gray, bioturbated, argillaceous, lime mudstone.
3.0	897.0	Covered.
4.0	901.0	Light gray, laminated dolomite.
32.0	933.0	Dark gray, argillaceous, bioturbated,

		nodular-bedded, lime mudstone with thin, shaly interbeds that are <2.0 inches thick.
12.0	945.0	Tan-weathering, medium gray, argillaceous, lime mudstone.
upper member		
10.0	955.0	Tan, thick-bedded, laminated, lumpy dolomite.
6.0	961.0	Covered.
4.0	965.0	Tan, laminated, argillaceous dolomite.
1.0	966.0	Light gray, dolomitic,, lime mudstone.
12.0	978.0	Tan weathering, light gray, argillaceous, laminated, dolomitic, lime mudstone to dolomite.
3.0	981.0	Covered.
4.0	985.0	Tan-weathering, medium-bedded, laminated dolomite.
16.0	1001.0	Covered.
20.0	1021.0	Interbedded, tan, laminated dolomite, and light gray, lumpy-bedded, lime mudstone.
5.0	1026.0	Medium gray, lime wackestone, intraclastic at the base.
4.0	1030.0	Covered.
3.0	1033.0	Dark gray, argillaceous, stromatolitic, lime mudstone.
2.0	1035.0	Tan to light gray, argillaceous, lime packstone, with recrystallized ooids.
12.0	1047.0	Medium to dark gray, argillaceous, bioturbated, lumpy, lime mudstone becoming tan, dolomitic at top.
10.0	1057.0	Tan, shaly, lumpy, dolomitic, lime mudstone.
15.0	1072.0	Interbedded, dark gray, thin-bedded, lime mudstone with shaly partings and medium gray, stromatolitic, lime mudstone.
20.0	1092.0	Covered.
7.0	1099.0	Medium gray, bioturbated, lime mudstone.
1.0	1100.0	Covered.
1.5	1101.5	Tan, laminated, argillaceous, platy dolomite.
5.0	1106.5	Medium gray, stromatolitic, lime mudstone.
22.0	1128.5	Covered.
6.5	1135.0	Tan, laminated dolomite.
14.0	1149.0	Covered.
8.0	1157.0	Tan, laminated, fractured dolomite.
30.0	1187.0	Covered. Shallow stream valley.
11.0	1198.0	Interbedded, tan, laminated, argillaceous dolomite and fractured, tan to light gray dolomite.
18.0	1216.0	Covered.
5.0	1221.0	Dark gray, ribbony, lime mudstone with tan laminations at top.
2.0	1223.0	Tan, laminated, argillaceous, dolomitic, lime mudstone.
6.0	1229.0	Covered.
11.0	1240.0	Tan, laminated dolomite.
2.0	1242.0	Dark gray, bioturbated dolomite.
9.0	1251.0	Covered.
5.0	1256.0	Tan and reddish, platy, ribbony dolomite.
3.0	1259.0	Medium gray, thrombolitic lime mudstone with tan, laminated dolomite cap.
5.0	1264.0	Tan-weathering, fractured dolomite.
2.0	1266.0	Ribbony dolomite.
3.0	1269.0	Dark gray, bioturbated, lime mudstone.
30.0	1299.0	Covered.
2.5	1301.5	Dark gray, thrombolitic, thin-bedded, lime mudstone.
2.0	1303.5	Dark gray, ribbony dolomite.
2.0	1305.5	Tan, thrombolitic, lime mudstone.
1.0	1306.5	Medium gray, laminated, lime mudstone.
12.0	1318.5	Tan, platy, argillaceous dolomite, medium-bedded and laminated at top.
1.5	1320.0	Light gray, thrombolitic, lime mudstone.
4.0	1324.0	Covered.
14.0	1338.0	Interbedded, tan, laminated, sandy, argillaceous dolomite and platy, tan, mudcracked dolomite, mostly covered.
3.0	1341.0	Tan, mudcracked, argillaceous dolomite
1.5	1342.5	Tan, platy, argillaceous dolomite.
2.5	1345.0	Tan, laminated dolomite.
1.0	1346.0	Light gray, stromatolitic, lime mudstone.
2.0	1348.0	Tan, platy, dolomite.
5.0	1353.0	Tan, argillaceous dolomite, laminated at top.
1.0	1354.0	Tan, platy, argillaceous, dolomite
1.0	1355.0	Thinly interbedded, dark gray, lime mudstone and tan, dolomitic laminae.
23.0	1378.0	Covered.
1.5	1379.5	Medium gray, thrombolitic lime mudstone.
2.5	1382.0	Thinly interbedded, dark gray, lime mudstone, and tan, ribbony dolomite.
2.0	1384.0	Thinly, laminated dolomite.
2.5	1386.5	Tan, platy, argillaceous dolomite.
3.0	1389.5	Covered.

2.0	1391.5	Dark gray, bioturbated, lime mudstone.
19.5	1411.0	Covered.
2.0	1413.0	Dark gray, bioturbated, lime mudstone.
7.5	1420.5	Interbedded, dark gray, lime mudstone, and tan, laminated dolomite.
5.0	1425.5	Tan, argillaceous, dolomitic, lime mudtone.
2.0	1427.5	Medium to dark gray, bioturbated, lime mudstone.
5.0	1432.5	Covered.
6.0	1438.5	Light gray, bioturbated and ribbony, lime mudstone.
2.0	1440.5	Dark gray, thrombolitic, lime mudstone.
1.0	1441.5	Dark gray, oolitic, lime packstone capped by thrombolitic, lime mudstone.
3.5	1445.0	Tan, laminated dolomite.
2.0	1447.0	Medium gray, bioturbated, lime mudstone.
5.5	1452.5	Tan, laminated, shaly dolomite.
6.0	1458.5	Covered.
4.0	1462.5	Light gray, thrombolitic dolomite.
1.0	1463.5	Medium gray, thrombolitic, lime mudstone.
4.0	1467.5	Covered.
4.0	1471.5	Medium gray, sandy, oolitic, lime packstone.
2.0	1473.5	Dark gray, stromatolitic, lime mudstone.
1.0	1474.5	Tan, laminated, argillaceous dolomite.
3.0	1477.5	Covered.
1.0	1478.5	Light gray, laminated dolomite.
8.0	1486.5	Dark gray, bioturbated, lime wackestone.
4.0	1490.5	Medium gray, stromatolitic, lime mudstone.
2.0	1492.5	Medium gray, bioturbated, lime wackestone.
3.0	1495.5	Tan to light gray, laminated, argillaceous dolomite.
10.0	1505.5	Medium to dark gray, bioturbated, sandy, oolitic, dolomitic limestone.
3.0	1508.5	Tan, argillaceous, laminated dolomite.
1.0	1509.5	Medium gray, thrombolitic, lime mudstone, stromatolitic at top.
4.5	1514.0	Tan to light gray, laminated dolomite.
2.5	1516.5	Medium gray, thrombolitic, lime mudstone.
3.0	1519.5	Tan-weathering, dark gray, laminated dolomite.
7.5	1527.0	Tan to medium gray, ribbony dolomite.
2.0	1529.0	Covered.
6.0	1535.0	Dark gray, bioturbated, stromatolitic, lime mudstone.
2.5	1537.5	Dark gray, oolitic, lime packstone.
5.5	1543.0	Dark gray, thrombolitic, oolitic, lime wackestone.
4.0	1547.0	Dark gray, tan weathering, dolomitic lime mudstone.
6.5	1553.5	Tan, platy, argillaceous dolomite.
1.0	1554.5	Tan, thrombolitic dolomite.
6.5	1561.0	Dark gray, thrombolitic, lime mudstone, stromatolitic at top.
1.0	1562.0	Dark gray, intraclastic, lime packstone.
3.0	1565.0	Thinly interbedded, tan, platy dolomite and stromatolitic, lime mudstone.
1.0	1566.0	Medium gray dolomite.
1.5	1567.5	Medium gray, lime mudstone, platy at top.
1.0	1568.5	Dark gray, thrombolitic, lime mudstone.
2.0	1570.5	Dark gray, laminated, lime mudstone.
2.0	1572.5	Tan weathering, ribbony dolomite.
5.0	1577.5	Tan, platy dolomite.
4.5	1582.0	Interbedded, laminated, lime mudstone, and stromatolitic, lime mudstone.
1.0	1583.0	Light gray dolomite.
3.0	1586.0	Dark gray, thrombolitic, lime mudstone.
1.0	1587.0	Tan, platy, argillaceous dolomite.
1.0	1588.0	Light gray, argillaceous dolomite.
1.0	1589.0	Dark gray, nodular-bedded, argillaceous, lime wackestone.
3.0	1592.0	Dark gray, laminated, dolomitic, lime mudstone. Folded.
4.0	1596.0	Covered.
1.0	1597.0	Tan-weathering, dark gray, laminated dolomite.
2.0	1599.0	Covered.
1.0	1600.0	Dark gray, stromatolitic, lime mudstone.
3.0	1603.0	Interbedded, dark gray, dolomitic, lime mudstone and platy, dark gray dolomite.
5.0	1608.0	Thinly interbedded, dark gray, lime wackestone, and tan, laminated dolomite.
3.0	1611.0	Dark gray, thrombolitic, lime mudstone, stromatolitic at top.
4.0	1615.0	Dark gray, bioturbated, dolomitic, lime wackestone.
1.0	1616.0	Tan, laminated, argillaceous dolomite.
5.0	1621.0	Dark gray, thrombolitic, lime mudstone, stromatolitic at top.
5.0	1626.0	Tan to medium gray, laminated dolomite.
15.0	1641.0	Covered.
10.0	1651.0	Dark gray, bioturbated, thrombolitic limestone.
3.0	1654.0	Dark gray, laminated dolomite.

9.0	1663.0	Covered.
4.0	1667.0	Dark gray, argillaceous, dolomitic limestone.
45.0	1712.0	Covered. Stream valley.
3.0	1715.0	Dark gray, thrombolitic, lime mudstone.
10.0	1725.0	Interbedded, dark gray, laminated dolomite and bioturbated, dolomitic limestone.
1.0	1726.0	Medium gray, thrombolitic, lime mudstone.
5.0	1731.0	Dark gray, lime wackestone.
1.0	1732.0	Dark gray, lime mudstone.
4.0	1736.0	Dark gray, laminated dolomite.
5.0	1741.0	Thinly interbedded, dark gray, thrombolitic, lime mudstone, and tan, laminated dolomite.
2.0	1743.0	Dark gray, laminated dolomite.
2.0	1745.0	Covered.
3.0	1748.0	Dark gray, thrombolitic, lime mudstone.
3.0	1751.0	Covered.
2.5	1753.5	Thinly interbedded, dark gray, lime mudstone, with tan dolomite partings.
4.0	1757.5	Covered.
3.5	1761.0	Tan, laminated dolomite.
5.0	1766.0	Dark gray, ribbony, lime mudstone.
5.0	1771.0	Dark gray, thin-bedded, lime mudstone, with tan, dolomitic partings.
3.0	1774.0	Dark gray, tan-weathering, laminated dolomite.
25.0	1799.0	Interbedded, dark gray, ribbony, lime mudstone, and dark gray, laminated, dolomitic, lime mudstone.
3.0	1802.0	Dark gray, ribbony, lime mudstone, with tan, dolomitic partings.
1.5	1803.5	Covered.
2.0	1805.5	Medium gray, laminated dolomite.
5.0	1810.5	Dark gray, ribbony, lime mudstone.
4.5	1815.0	Interbedded, ribbony, lime mudstone, and tan, shaly dolomite.
2.0	1817.0	Medium gray, tan-weathering dolomite.
1.0	1818.0	Medium gray, laminated, dolomitic, lime mudstone.
3.0	1821.0	Dark gray, tan-weathering, laminated dolomite.
2.0	1823.0	Dark gray, lime mudstone with tan, dolomitic partings.
5.5	1828.5	Covered.
2.0	1830.5	Tan, laminated, shaly dolomite.
3.0	1833.5	Tan-weathering, dark gray, dolomitic, lime mudstone.
2.0	1835.5	Dark gray, stromatolitic, lime mudstone.
17.0	1852.5	Dark gray, knotty, bioturbated dolomite, with thin layers of laminated dolomite.
2.0	1854.5	Dark gray, bioturbated, thrombolitic, lime mudstone.
3.5	1858.0	Covered.
2.5	1860.5	Medium gray, tan-weathering, fractured dolomite.
1.5	1862.0	Light gray, tan-weathering, laminated dolomite.
2.5	1864.5	Covered.
1.0	1865.5	Dark gray, dolomitic, lime mudstone.
2.0	1867.5	Tan, shaly, platy dolomite.
4.0	1871.5	Thinly interbedded, tan, laminated dolomite and laminated gray dolomite.
2.5	1874.0	Dark gray, very thin-bedded, lime mudstone.
2.5	1876.5	Tan to yellowish weathering, shaly dolomite.
1.5	1878.0	Tan, platy, laminated dolomite.
1.0	1879.0	Covered.
5.0	1884.0	Tan-weathering, gray dolomite.
2.0	1886.0	Covered.
2.5	1888.5	Tan weathering, medium gray, dolomite.
3.0	1891.5	Dark gray, lumpy, argillaceous, lime wackestone.
2.0	1893.5	Tan, laminated dolomite.
3.0	1896.5	Dark gray, argillaceous, thin-bedded, lime mudstone.
4.0	1900.5	Covered.
3.5	1904.0	Dark gray, ribbony, lime mudstone.
2.0	1906.0	Dark gray, stromatolitic, lime mudstone.
2.5	1908.5	Covered.
3.5	1912.0	Dark gray, bioturbated, argillaceous dolomite.
11.0	1923.0	Interbedded, dark gray, stromatolitic, lime mudstone and thrombolitic, lime mudstone.
3.0	1926.0	Covered.
22.0	1948.0	Interbedded, dark gray, thrombolitic, lime mudstone, stromatolitic at top, and ribbony, dolomitic, lime mudstone.
1.0	1949.0	Tan, laminated dolomite.
3.0	1952.0	Covered.
3.5	1955.5	Dark gray, thrombolitic, lime mudstone, laminated at top.
1.5	1957.0	Tan, laminated dolomite.
1.0	1958.0	Dark gray, ribbony, lime mudstone.
9.0	1967.0	Interbedded, dark gray, stromatolitic, lime mudstone, and shaly, ribbony, lime mudstone.
0.5	1967.5	Tan, laminated dolomite.
7.0	1974.5	Interbedded, ribbony, lime mudstone and bioturbated, lime mudstone.

15.0	1989.5	Covered.
5.5	1995.0	Dark gray, dolomitic, lime wackestone.
6.5	2001.5	Dark gray, thrombolitic, lime mudstone and interbedded, ribbony, lime mudstone.
2.0	2003.5	Tan, stromatolitic, dolomitic, lime mudstone.
3.0	2006.5	Tan, laminated dolomite.
6.0	2012.5	Interbedded, dark gray, thrombolitic, lime mudstone and tan, ribbony dolomite.
5.5	2018.0	Covered.
2.0	2020.0	Dark gray, thrombolitic, lime mudstone.
2.0	2022.0	Dark gray, platy, lime mudstone.
2.5	2024.5	Tan-weathering, gray, fractured dolomite.
4.0	2028.5	Covered.
4.0	2032.5	Dark gray, platy, ribbony, lime mudstone.
1.5	2034.0	Tan, laminated dolomite.
2.5	2036.5	Dark gray, thin-bedded lime mudstone, platy at top.
3.0	2039.5	Dark gray, buff weathering, fractured dolomite.
7.5	2047.0	Medium gray, medium-bedded, dolomitic lime mudstone with a few thin thrombolitic intervals.
2.0	2049.0	Tan, laminated dolomite.
3.5	2052.5	Dark gray, stromatolitic, lime mudstone.
1.0	2053.5	Tan, laminated dolomite.
1.5	2055.0	Dark gray, stromatolitic, lime mudstone.
27.0	2082.0	Dark gray, medium-bedded, dolomitic lime mudstone interbedded with gray, laminated dolomite.
1.0	2083.0	Dark gray, lumpy-bedded, lime wackestone.
2.5	2085.5	Covered.
3.5	2089.0	Dark gray dolomite.
3.5	2092.5	Covered.
4.5	2097.0	Dark gray, intraclastic, thrombolitic, lime packstone.
3.5	2100.5	Dark gray, ribbony, lime mudstone with tan dolomite stringers.
2.5	2103.0	Light gray, fractured dolomite.
150.0	2253.0	Covered. Stream valley.
3.0	2256.0	Dark gray, lumpy, bioturbated, lime wackestone.
6.0	2262.0	Medium gray, medium-bedded dolomite.
2.0	2264.0	Dark gray, ribbony, dolomitic, lime mudstone.
1.0	2256.0	Dark gray, sandy dolomite.
40.0	2296.0	Covered.
2.0	2298.0	Medium gray, laminated dolomite.
15.0	2313.0	Covered.
3.0	2316.0	Dark gray, ribbony, lime mudstone with tan, dolomitic partings.
10.0	2326.0	Covered.
11.0	2337.0	Dark gray, ribbony, dolomite with gray laminated interbeds.
6.0	2343.0	Dark gray, thrombolitic, lime mudstone.
24.0	2367.0	Interbedded, medium to thick bedded, medium gray, laminated dolomite and ribbony dolomite.
3.0	2370.0	Dark gray, thrombolitic, lime mudstone.
22.0	2392.0	Interbedded, bioturbated ,dolomitic lime mudstone, and stromatolitic dolomitic Liam mudstone.
24.0	2416.0	Covered. Fence line.
6.0	2422.0	Dark gray, thrombolitic, lime mudstone.
9.0	2431.0	Dark gray, medium-bedded, ribbony, lime mudstone and laminated, dolomitic, lime mudstone.
5.0	2435.0	Covered.
1.5	2436.5	Medium gray, sandy, dolomitic, lime wackestone.
10.0	2446.5	Interbedded, dark gray, sandy, lime wackestone and laminated dolomite.
2.5	2449.0	Dark gray, shaly, lime grainstone-packstone.
3.0	2452.0	Dark gray, thrombolitic, lime wackestone.
2.0	2456.0	Medium gray, laminated, dolomitic, lime mudstone.
2.0	2458.0	Dark gray, ribbony, limey dolomite.
1.0	2459.0	Medium gray, ribbony dolomite.
5.0	2464.0	Medium gray, laminated to ribbony dolomite.
2.0	2466.0	Dark gray, fractured, laminated dolomite.
7.0	2473.0	Covered.
2.0	2475.0	Dark gray, intraclastic, lime packstone.
1.5	2476.5	Dark gray, ribbony, dolomitic, lime mudstone.
3.0	2479.5	Interbedded, ribbony dolomite and lime mudstone.
2.0	2481.5	Covered.
2.0	2483.5	Dark gray, ribbony, lime mudstone.
5.0	2488.5	Dark gray, ribbony dolomite.

Conococheague Formation

Big Spring Station Member

5.5	5.5	Tan to light brown, cross-bedded, calcareous, fine-grained sandstone.

2.0	7.5	Tan, laminated dolomite.
1.0	8.5	Dark gray, sandy, lime wackestone.
6.0	14.5	Tan, thin-bedded, calcareous, fine-grained sandstone.
2.0	16.5	Tan, laminated dolomite.
6.0	22.5	Medium gray, ribbony and laminated, dolomite.
2.5	25.0	Medium gray, thrombolitic, dolomitic, lime mudstone.
3.0	28.0	Dark gray, ribbony dolomite.
1.0	29.0	Medium gray, lime mudstone.
5.5	34.5	Medium gray, ribbony dolomite.
1.5	36.0	Medium gray, sandy, lime packstone.
3.0	39.0	Tan, laminated dolomite.
3.0	42.0	Dark gray, lumpy dolomite.
2.0	44.0	Medium gray, laminated dolomite.
35.0	79.0	Interbedded, medium gray, ribbony dolomite and tan, laminated dolomite with few intervals of dolomitic thrombolites.

Section 7

Section of the upper part of the Elbrook Formation and Conococheague Formation along the C&O Canal National Historical Park, east from milemarker 108. Section begins in the upper member of the Elbrook Formation and continues to the Lockhouse at Two Locks. 39°37′13″ N, 77°56′02″ W.

Thickness (feet) unit	total	
Elbrook Formation		
35.0	35.0	Interbedded, laminated, dolomitic limestone and tan dolomite.
12.0	47.0	Covered.
7.0	54.0	Dark gray, thrombolitic limestone.
87.0	141.0	Interbedded, medium gray, medium-bedded, lime wackestone and tan to gray, laminated, dolomitic, lime mudstone.
Conococheague Formation		
Big Spring Station Member		
4.5	4.5	Thinly interbedded, tan dolomite and cross-bedded, quartz sandstone.
1.1	5.6	Tan, blocky, dolomitic mudstone.
3.0	8.6	Light gray, laminated, dolomitic limestone.
6.0	14.6	Interbedded, laminated limestone and tan, dolomitic limestone.
2.4	17.0	Dark gray, thrombolitic, dolomitic limestone.
2.0	19.0	Tan, blocky dolomite
2.0	21.0	Light gray, bioturbated, dolomitic limestone.
3.0	24.0	Tan, laminated dolomite.
3.0	27.0	Covered.
3.5	30.5	Medium gray, bioturbated, dolomitic limestone.
11.0	41.5	Interbedded, tan dolomite and bioturbated, dolomitic limestone.
3.0	44.5	Covered.
5.0	49.5	Light gray to tan dolomite.
3.0	52.5	Tan, cross-bedded, dolomitic sandstone.
2.0	54.5	Medium gray, laminated, dolomitic limestone.
3.5	58.0	Tan, blocky dolomite.
7.0	65.0	Interbedded, ribbony, limestone and tan dolomite.
45.0	110.0	Interbedded, dark gray, dolomitic limestone and tan to gray, medium-bedded limestone.
45.0	155.0	Covered.
4.0	159.0	Tan, bioturbated dolomite.
1.4	160.4	Tan, blocky dolomite.
2.5	162.9	Light gray, thin-bedded, calcareous sandstone.
2.0	164.9	Covered.
3.0	167.9	Light gray to tan, blocky dolomite.
20.0	187.9	Covered.
70.1	258.0	Interbedded, medium-bedded, dark gray, bioturbated, dolomitic limestone, and laminated, dolomitic limestone, and a few tan, laminated dolomites.
Zullinger Member		
4.0	262.0	Medium gray, prism-cracked, laminated, dolomitic limestone.
7.0	269.0	Medium gray, thrombolitic limestone with oolitic cap (trilobites).
2.0	271.0	Dark gray, dolomitic limestone.
3.0	274.0	Dark gray, thrombolitic limestone.
11.0	285.0	Medium gray, thin-bedded to laminated limestone.
3.5	288.5	Medium gray, thrombolitic limestone.
10.0	298.5	Mostly covered.
9.0	307.5	Dark gray, thrombolitic lime mudstone (3-6 feet thick), with wispy partings of cherty limestone.
2.0	309.5	Thin-bedded, lime mudstone with tan, dolomitic partings.
6.0	315.5	Dark gray, thrombolitic, lime mudstone.
6.5	319.0	Medium gray, thin-bedded, lime

		packstone-grainstone.
5.5	325.5	Dark gray, thrombolitic lime mudstone.
3.0	328.5	Dark gray, platy, laminated, dolomitic limestone.
20.0	348.5	Dark gray, thrombolitic lime mudstone. Trilobites, *Buttsia, Drabia*.
7.0	355.5	Dark gray, ribbony and laminated lime mudstone
5.5	361.0	Dark gray, thrombolitic, lime mudstone.
4.5	365.5	Light gray to tan, laminated dolomite.
15.0	380.5	Ribbony lime mudstone with tan dolomitic partings, locally intraclastic.
4.5	385.0	Dark gray, thrombolitic limestone.
32.0	417.0	Interbedded, laminated, and ribbony, medium gray limestone with wispy and few intraclastic beds.
5.0	422.0	Dark gray, thrombolitic and stromatolitic lime mudstone.
7.0	429.0	Medium gray, laminated lime mudstone.
1.5	430.5	Medium gray, stromatolitic lime mudstone.
1.3	431.8	Medium gray lime mudstone.
1.8	433.6	Medium gray, medium-bedded, lime mudstone.
2.0	435.6	Dark gray, ribbony, lime mudstone
7.0	442.6	Dark gray, massive, thrombolitic, lime mudstone, medium-bedded at top.
15.0	457.6	Medium gray, ribbony lime mudstone.
1.5	459.0	Dark gray, lime wackestone.
10.0	469.0	Dark gray, laminated to ribbony, lime mudstone with dolomitic interbeds and partings and prism-cracked.
2.0	471.0	Dark gray, thrombolitic lime mudstone ribbony at top.
3.0	474.0	Dark gray, laminated to ribbony, lime mudstone.
3.0	477.0	Tan, laminated dolomite.
2.0	479.0	Dark gray, thrombolitic, lime mudstone.
20.0	499.0	Interbedded, ribbony, lime mudstone with thin, tan, dolomitic partings.
15.0	514.0	Interbedded, dark gray, ribbony, lime mudstone.
1.0	515.0	Tan, blocky, laminated dolomite.
2.0	517.0	Medium gray, medium-bedded grainstone-packstone.
5.0	522.0	Dark gray, ribbony, lime mudstone with thin, intraclast beds.
4.0	526.0	Interbedded, tan, laminated dolomite and ribbony, gray, lime mudstone.
1.5	527.5	Medium gray, intraclastic grainstone.
38.0	565.5	Interbedded, dark gray, ribbony, lime mudstone with tan, laminated dolomite
		partings, and several thin, intraclastic packstone intervals.
1.0	566.5	Light gray, intraclastic, lime packstone.
2.0	568.5	Dark gray, platy, argillaceous, lime mudstone.
2.0	570.5	Tan, blocky, laminated dolomite.
2.5	573.0	Thinly interbedded, light gray, lime mudstone and tan, laminated dolomite.
4.0	577.0	Medium gray, thrombolitic, lime mudstone, thin-bedded at top, with tan, dolomitic partings.
28.5	605.5	Thinly interbedded, dark gray, ribbony, lime mudstone with black, argillaceous partings.
1.5	607.0	Dark gray, dolomite with shaly, platy, upper surface.
37.0	644.0	Interbedded, dark gray, ribbony, dolomitic, lime mudstone and tan dolomite, with abundant mudcracks.
6.5	650.5	Dark gray, thin-bedded, laminated and ribbony, lime mudstone-wackestone.
2.5	653.0	Dark gray, dolomitic thrombolite.
2.0	655.0	Tan, laminated dolomite.
4.0	659.0	Medium gray, thrombolitic lime mudstone with intraclastic cap.
3.0	662.0	Dark gray, laminated, lime wackestone.
7.0	669.0	Dark gray, ribbony and laminated, lime mudstone.
4.5	673.5	Dark gray, thrombolitic, lime mudstone.
3.0	676.5	Dark gray, laminated, argillaceous, lime wackestone.
9.0	685.5	Medium gray, medium-bedded, lime wackestone.
5.0	690.5	Dark gray, thrombolitic, lime mudstone.
1.5	692.0	Medium gray, ribbony, laminated dolomite.
1.5	693.5	Medium gray, stromatolitic, lime mudstone.
1.5	695.0	Medium gray, ribbony, lime wackestone.
1.0	696.0	Medium gray, medium-bedded, lime mudstone.
3.0	699.0	Dark gray, thrombolitic, lime mudstone.
1.0	700.0	Tan, laminated dolomite.
2.0	702.0	Dark gray, thrombolitic, lime mudstone.
4.0	706.0	Dark gray, ribbony, lime mudstone, with tan, dolomitic partings.
10.0	716.0	Dark gray, thrombolitic, lime mudstone.
6.0	722.0	Tan, blocky dolomite.
6.0	728.0	Massive, dark gray, thrombolitic, lime mudstone.
2.0	730.0	Light gray, intraclastic grainstone.

10.0	740.0	Light gray, medium-bedded, lime wackestone, mostly covered.
17.0	757.0	Dark gray, ribbony, lime mudstone.
6.0	763.0	Covered.
10.0	773.0	Medium gray, medium-bedded, ribbony and laminated lime mudstone.
11.0	784.0	Covered.
4.0	788.0	Dark gray, thin- to medium-bedded, lime mudstone.
2.0	790.0	Tan, laminated dolomite.
29.0	819.0	Interbedded, dark gray, ribbony, lime mudstone, and thin-bedded, lime mudstone.
56.0	875.0	Interbedded, medium-bedded, lime mudstone-wackestone and ribbony, lime mudstone, with a few grainstone-packstone layers.
5.0	880.0	Tan, blocky, laminated dolomite, ribbony at top.
12.0	892.0	Dark gray, ribbony, lime mudstone, with tan, dolomitic partings.
15.0	907.0	Covered.
7.0	914.0	Medium gray, laminated, lime mudstone.
23.0	937.0	Interbedded, dark gray, ribbony, lime mudstone and thin-bedded, lime packstone-grainstone.
1.5.	938.5	Tan, blocky fractured, dolomite.
2.5	941.0	Light gray, laminated, lime mudstone.
5.0	946.0	Dark gray, ribbony, lime mudstone with tan, dolomitic partings.
5.5	951.5	Interbedded, thickly and thinly laminated, dark gray, lime mudstone.
7.0	958.5	Interbedded, medium gray, oolitic, lime grainstone, and light gray, laminated, lime mudstone.
67.0	1025.5	Interbedded, medium gray, laminated, lime wackestone and ribbony, lime mudstone with a few grainstone interbeds <1.0 foot thick.
10.0	1035.5	Dark gray, ribbony, lime mudstone**.**
35.0	1070.5	Interbedded, medium gray, ribbony, lime mudstone and platy-bedded, argillaceous, laminated, lime mudstone with a few thin thrombolite intervals <1.0 foot thick.
7.0	1077.5	Massive, medium gray, thrombolitic, lime mudstone.
21.0	1098.5	Interbedded, medium gray, laminated and ribbony, lime wackestone-mudstone.
2.0	1100.5	Medium gray, laminated dolomitic lime mudstone.
35.0	1135.5	Interbedded, medium gray, laminated and ribbony, lime mudstone with a few cross bedded grainstone-packstone intervals.
5.0	1140.5	Medium gray, oolitic, intraclastic, packstone-grainstone.
15.0	1155.5	Dark gray, very thin-bedded, lime mudstone, lumpy-bedded at top.
5.0	1160.5	Medium gray, cross-bedded, oolitic, lime grainstone with trilobite fragments.
2.0	1162.5	Medium gray, thrombolitic, lime mudstone with trilobites.
23.0	1185.5	Interbedded, medium gray, laminated, dolomitic, lime mudstone, and ribbony, lime mudstone and thin-bedded, thrombolitic lime mudstone.
27.0	1212.5	Covered.
23.5	1236.0	Interbedded, medium gray, ribbony, mudcracked, thin-bedded, lime mudstone and thrombolitic, lime mudstone (thrombolites typically <1.0 foot thick.).
11.0	1247.0	Interbedded, dark gray, medium-bedded, grainstone-packstone and laminated, dolomitic, lime mudstone.
10.0	1257.0	Thinly interbedded, laminated, dolomitic, lime mudstone and thin-bedded, lime mudstone.
26.0	1283.0	Covered.
12.0	1295.0	Interbedded, tan, laminated dolomite and medium gray, thrombolitic, lime mudstone.
3.0	1298.0	Medium gray, thrombolitic, lime mudstone
22.0	1320.0	Thinly interbedded, dark gray, ribbony, lime mudstone, and laminated, tan dolomite.
33.0	1353.0	Interbedded, medium gray, ribbony, shaly, lime mudstone and medium-bedded, lime wackestone and intraclastic packstone.
22.0	1375.0	Covered. Swale east of rock pinnacle.
5.0	1380.0	Medium gray, thick-bedded, sandy grainstone.
6.0	1386.0	Medium gray, ribbony, lime wackestone.
9.0	1395.0	Light gray, thrombolitic, lime mudstone, with laminated grainstone at the top.
9.0	1404.0	Interbedded, dark gray, laminated, lime mudstone and ribbony, bioturbated, lime wackestone.

2.0	1406.0	Medium gray, bioturbated packstone-grainstone.
15.0	1421.0	interbedded, medium gray, lime grainstone and laminated, lime mudstone.
10.0	1431.0	Covered.
45.0	1476.0	Interbedded, thin-bedded, bioturbated, lime mudstone and thin, thrombolitic interval (<1.0 feet).
5.0	1481.0	Interbedded, thinly laminated, lime mudstone and bioturbated, lime mudstone.
2.0	1483.0	Light gray, thrombolitic, lime mudstone.
12.5	1495.5	Dark gray, medium-bedded, oolitic, lime grainstone with thin, ribbony interbeds.
7.5	1503.0	Medium gray, ribbony, lime mudstone.
2.0	1505.0	Medium gray, thrombolitic, lime mudstone.
3.0	1508.0	Dark gray, medium-bedded, lime grainstone.
19.0	1527.0	Interbedded, medium-bedded- lime grainstone, laminated, dolomitic, lime mudstone and thrombolitic, lime mudstone.
9.0	1536.0	Covered.
52.0	1588.0	Interbedded, laminated, lime mudstone and thin-bedded mudstone with thin, stromatolitic intervals.

Section 8

Section along the C&O Canal National Historic Park from milemarker 83.5 to milemarker 83.3 Section begins near the top of the Big Springs Station Member of the Conococheague Formation and proceeds eastward. 39°29′34″ N, 77°48′36″ W.

Thickness (feet) unit	total	
Conococheague Formation		
Big Spring Station Member		
3.0	3.0	Thrombolitic, lime mudstone.
3.0	6.0	Tan, laminated dolomite.
4.0	10.0	Tan, fractured dolomite.
3.0	13.0	Covered.
6.0	19.0	Tan, fractured dolomite.
2.0	21.0	Medium gray, ribbony, lime mudstone.
1.0	22.0	Tan, laminated dolomite.
4.0	26.0	Medium gray, fractured, dolomitic limestone.
4.0	30.0	Tan, laminated dolomite.
3.0	33.0	Gray, ribbony, lime mudstone.
5.0	38.0	Gray, ribbony, lime mudstone.
6.0	44.0	Tan, laminated dolomite.
1.0	45.0	Gray, ribbony, lime mudstone.
5.0	50.0	Tan, laminated dolomite.
6.0	56.0	Tan dolomite, mostly covered.
Zullinger Member		
6.0	62.0	Light gray, thrombolitic, lime mudstone, with laminated, lime mudstone flanking beds.
1.0	63.0	Light gray, laminated, lime mudstone.
3.0	66.0	Covered.
4.0	70.0	Tan, laminated, fractured dolomite.
3.0	73.0	Light gray, thrombolitic, lime mudstone.
7.0	80.0	Tan, ribbony to laminated dolomite.
2.0	82.0	Light gray, ribbony, lime mudstone.
3.0	85.0	Tan, laminated dolomite.
7.0	92.0	Covered.
6.0	98.0	Light gray, thrombolitic, lime mudstone.
4.0	102.0	Light gray, ribbony, dolomitic, lime mudstone.
5.0	107.0	Tan, laminated dolomite.
5.0	112.0	Light gray, thrombolitic, lime mudstone.
8.0	120.0	Tan, ribbony to laminated dolomite.
5.0	125.0	Light gray, thrombolitic, lime mudstone.
4.0	129.0	Tan, laminated dolomite.
4.0	133.0	Light gray, ribbony, lime mudstone.
2.0	135.0	Medium gray, thrombolitic limestone with oolitic capstone containing trilobites.
2.0	137.0	Medium gray to tan, ribbony, dolomitic limestone.
4.0	141.0	Light gray, thrombolitic limestone.
2.0	143.0	Medium gray, ribbony, lime mudstone.
2.0	145.0	Tan to gray-brown, ribbony, lime mudstone.
5.0	150.0	Light gray, thrombolitic, lime mudstone.
1.0	151.0	Tan, laminated dolomite.
2.0	153.0	Tan, thrombolitic dolomitic, lime mudstone.
1.0	154.0	Tan, ribbony dolomite.
4.0	158.0	Light gray, thrombolitic, lime mudstone.
3.0	161.0	Medium gray, ribbony, lime mudstone.
2.0	163.0	Covered.
7.0	170.0	Light gray, thrombolitic, lime mudstone, ribbony at top.
2.0	172.0	Tan, fractured dolomite.
4.0	173.0	Light gray, thrombolitic, lime mudstone (west side of gully).
7.0	180.0	Covered (gully).
4.0	184.0	Light gray, thrombolitic, lime mudstone.
2.0	186.0	Covered.

1.0	187.0	Tan, laminated dolomite.
4.0	191.0	Light gray, thrombolitic lime mudstone.
5.0	196.0	Tan laminated dolomite.
4.0	200.0	Covered.
4.0	204.0	Medium gray, thrombolitic, lime mudstone.
3.0	207.0	Tan, laminated dolomite.
4.0	211.0	Light gray, stromatolitic, lime mudstone.
25.0	236.0	Medium to light gray, ribbony, lime mudstone with thin intervals of thrombolitic, lime mudstone.
5.0	241.0	Medium gray, thrombolitic, lime mudstone.
4.0	246.0	Covered.
5.0	251.0	Light gray, thrombolitic, lime mudstone.
2.0	253.0	Light gray, ribbony ,lime mudstone.
2.0	255.0	Tan, laminated, dolomite.
1.0	256.0	Light gray, thrombolitic, lime mudstone.
2.0	258.0	Light gray, laminated, dolimitic limestone.
3.0	261.0	Light gray, thrombolitic, lime mudstone.
2.0	263.0	Tan, blocky, laminated dolomite.
4.0	267.0	Medium gray, thrombolitic, lime mudstone, thin-bedded at top.
2.0	269.0	Tan, blocky, laminated dolomite.
4.0	271.0	Medium gray, thrombolitic, lime mudstone.
1.0	278.0	Tan, blocky, laminated dolomite.
4.0	282.0	Light gray, thrombolitic lime mudstone.
2.0	284.0	Tan laminated dolomite.
2.0	286.0	Light gray, thrombolitic, lime mudstone.
2.0	288.0	Tan laminated dolomite.
2.0	290.0	Light gray, thrombolitic, lime mudstone.
6.0	296.0	Light gray, laminated, lime mudstone with tan dolomite at top.
4.0	300.0	Light gray, thrombolitic, lime mudstone.
12.0	312.0	Light gray, ribbony, lime mudstone, with thin layers (<1.0 feet) of thrombolitic, lime mudstone.
5.0	317.0	Light gray, thrombolitic, lime mudstone.
4.0	321.0	Medium gray, thin-bedded, to ribbony, lime mudstone.
1.0	322.0	Tan, laminated dolomite.
3.0	325.0	Light gray, laminated dolomite.
5.0	330.0	Tan, laminated dolomite.
3.0	335.0	Light gray, laminated, lime mudstone.
2.0	337.0	Tan, laminated dolomite.
5.0	342.0	Light gray, laminated, dolomitic, lime mudstone.
5.0	345.0	Tan, laminated dolomite.
3.0	348.0	Covered.
3.0	351.0	Light gray, thrombolitic, lime mudstone.
70.0	421.0	Covered.
3.0	424.0	Tan, fractured dolomite
4.0	428.0	Covered.
3.0	431.0	Light gray, ribbony, lime mudstone.
10.0	441.0	Interbedded, ribbony, lime mudstone and thrombolites.
4.0	445.0	Covered.
13.0	458.0	Light gray, thrombolitic, lime mudstone, ribbony interbeds.
2.0	460.0	Covered.
5.0	465.0	Light gray, thrombolitic, lime mudstone.
3.0	468.0	Covered.
2.0	470.0	Tan, laminated dolomite.
1.0	471.0	Light gray thrombolite.
3.0	474.0	Tan laminated dolomite.
10.0	484.0	Light gray, thrombolitic, lime mudstone.
2.0	486.0	Light gray, ribbony, lime mudstone.
5.0	491.0	Tan, laminated dolomite.
2.0	493.0	Tan, shaly dolomite.
3.0	496.0	Tan, laminated dolomite.
4.0	500.0	Light gray, thrombolitic, lime mudstone.
3.0	503.0	Light gray ribbony, lime mudstone.
2.0	505.0	Tan, laminated dolomite.
15.0	520.0	Light gray, ribbony, lime mudstone with thin (<1.0 foot thick) thrombolites.
3.0	523.0	Covered.
3.0	526.0	Light gray, thrombolitic, lime mudstone.
20.0	546.0	Light gray, ribbony and laminated, lime mudstone.
23.0	569.0	Covered.
3.0	572.0	Tan, laminated dolomite.
8.0	580.0	Light gray, laminated, ribbony, lime mudstone.
1.0	581.0	Tan, laminated dolomite.
1.0	582.0	Light gray, laminated, lime mudstone.
4.0	586.0	Tan, laminated dolomite.
3.0	589.0	Light gray, thrombolitic, lime mudstone.
2.0	591.0	Tan, laminated dolomite.
2.0	593.0	Light gray, thrombolitic, lime mudstone.
4.0	597.0	Tan, laminated dolomite.
11.0	608.0	Light gray, ribbony, lime mudstone with thin, thrombolite layers.
2.0	610.0	Tan, laminated, shaly dolomite.
5.0	615.0	Light gray, ribbony, lime mudstone.
1.0	616.0	Tan, laminated dolomite.
6.0	621.0	Light gray, ribbony, lime mudstone.
2.0	623.0	Tan, laminated dolomite.
6.0	629.0	Medium to light gray thrombolite.
4.0	633.0	Tan, laminated dolomite.
4.0	637.0	Covered.
50.0	687.0	Interbedded, light gray, ribbony, lime

		mudstone, and thin, tan dolomite. Top at Dam Four cave.
67.0	754.0	Interbedded, light gray, ribbony and thrombolitic, lime mudstone and tan, laminated dolomite.
36.0	790.0	Interbedded, tan, fractured and laminated dolomite.
22.0	812.0	Tan, fractured dolomite with thin, laminated, dolomitic interbeds and thin thrombolites at base.
6.0	818.0	Covered.
9.0	827.0	Tan, massive dolomite.
3.0	830.0	Covered.
6.0	836.0	Tan, massive dolomite.
1.0	837.0	Light gray, thrombolitic, lime mudstone.
7.0	844.0	Tan, massive dolomite with thin, laminated intervals.
3.0	847.0	Light gray, thrombolitic, lime mudstone.
1.0	848.0	Tan, laminated dolomite.
3.0	851.0	Light gray, thrombolitic, lime mudstone.
7.0	858.0	Covered.
3.0	861.0	Light gray to tan, fractured dolomite.
12.0	873.0	Light gray, thrombolitic, lime mudstone.
6.0	879.0	Light gray to tan, thrombolitic dolomite.
4.0	883.0	Covered.
42.0	925.0	Interbedded, light gray, ribbony, lime mudstone and thin, thrombolite beds, and tan, laminated and fractured dolomite.
12.0	937.0	Interbedded, laminated, lime mudstone and laminated dolomite.
9.0	946.0	Light gray, massive, thrombolitic, lime mudstone.
42.0	988.0	Interbedded, gray, ribbony and thin, thrombolitic, lime mudstone and tan, laminated dolomite.
9.0	997.0	Covered.
12.0	1009.0	Gray, ribbony and thin-bedded, lime mudstone.
3.0	1012.0	Tan, sandy dolomite.
8.0	1020	Light gray brown, ribbony, lime mudstone.
1.0	1021.0	Tan dolomite.
15.0	1036.0	Light gray, ribbony and laminated lime mudstone.
4.0	1040.0	Gray, blocky, dolomitic, lime mudstone.
21.0	1061.0	Interbedded, gray-brown, ribbony, lime mudstone with thin, thrombolitic layers.
5.0	1066.0	Light gray-brown, thrombolitic, lime mudstone.
6.0	1072.0	Gray, laminated, lime mudstone.
22.0	1094.0	Interbedded, light grayish brown, ribbony, lime mudstone, with thin, tan, thrombolitic, dolomite layers.
15.00	1109.0	Gray, ribbony, lime mudstone with thin thrombolites.
35.0	1144.0	Interbedded, ribbony and laminated, lime mudstone.
31.0	1175.0	Interbedded, ribbony, lime mudstone with thin, thrombolitic layers and a few,thin, tan, dolomitic layers.
24.0	1199.0	Grayish brown, ribbony, lime mudstone.
19.0	1218.0	Interbedded, ribbony and thrombolitic, lime mudstone.
5.0	1223.0	Grayish brown, thrombolitic, lime mudstone.
5.0	1228.0	Covered.
4.0	1232.0	Gray, ribbony, lime mudstone.
60.0	1292.0	Covered (stream valley).
18.0	1310.0	Light gray, ribbony, lime mudstone.
59.0	1369.0	Interbedded, light gray-brown, ribbony, lime mudstone with thin thrombolites and tan, laminated dolomite.
15.0	1384.0	Light grayish brown, thin-bedded to ribbony, lime mudstone.
16.0	1400.0	Covered.
57.0	1457.0	Interbedded, ribbony, lime mudstone and thombolitic, lime mudstone and tan, laminated dolomite.
8.0	1465.0	Covered.
4.0	1469.0	Thin-bedded, lime mudstone.
9.0	1478.0	Covered.
20.0	1498.0	Light grayish brown, laminated and intraclastic, lime mudstone.
4.0	1502.0	Gray, thrombolitic, lime mudstone.
4.0	1506.0	Light gray, intraclastic and thrombolitic, lime packstone to mudstone.
7.0	1513.0	Covered.
11.0	1524.0	Light grayish brown, ribbony, lime mudstone.
21.0	1545.0	Interbedded, ribbony and thrombolitic, lime mudstone. Base of thrombolite.
23.0	1568.0	Light gray, thick-bedded, thrombolitic, lime mudstone.
12.0	1580.0	Covered.
3.0	1583.0	Light gray, ribbony, lime mudstone.
2.0	1585.0	Covered.
3.0	1588.0	Gray, thrombolitic, lime mudstone.
1.0	1589.0	Covered.
9.0	1598.0	Light gray, massive thrombolite.
2.0	1600.0	Covered.
4.0	1604.0	Light gray, massive thrombolite.
1.0	1605.0	Tan, shaly dolomite.
6.0	1611.0	Covered.

3.0	1614.0	Light gray, ribbony, lime mudstone.
8.0	1622.0	Covered.
9.0	1631.0	Thinly interbedded, light gray, ribbony and thrombolitic, lime mudstone.
95.0	1726.0	Covered.
5.0	1731.0	Light gray, thrombolitic, lime mudstone.
5.0	1736.0	Light gray, ribbony, lime mudstone.
3.0	1739.0	Covered.
5.0	1744.0	Light gray, ribbon and laminated, lime mudstone.
3.0	1747.0	Covered.
8.0	1755.0	Light gray, massive, thrombolitic, lime mudstone.
5.0	1760.0	Grayish brown, ribbony, lime mudstone.
2.0	1762.0	Gray, thrombolitic, lime mudstone.
2.0	1764.0	Covered.
7.0	1771.0	Light gray, massive, thrombolitic, lime mudstone.
1.0	1772.0	Tan, fractured dolomite.
4.0	1776.0	Covered.
4.0	1780.0	Light gray, thrombolitic, lime mudstone.
7.0	1787.0	Grayish brown, ribbony to laminated, lime mudstone.
12.0	1799.0	Light gray, thrombolitic, lime mudstone.
29.0	1828.0	Interbedded, ribbony, lime mudstone to laminated limestone.
1.0	1829.0	Intraclastic, lime grainstone.
12.0	1841.0	Light gray, ribbony, lime wackestone.
4.0	1845.0	Light gray, thrombolitic, lime mudstone.
9.0	1854.0	Grayish brown, ribbony, lime wackestone.
4.0	1858.0	Light gray, thrombolitic, lime mudstone.
5.0	1863.0	Covered. Base of thrombolite interval.
15.0	1878.0	Grayish brown, massive, thrombolitic, lime mudstone.
6.0	1884.0	Gray, ribbony, lime mudstone.
5.0	1889.0	Light gray, thrombolitic, lime mudstone.
5.0	1894.0	Light gray, ribbony, lime mudstone.
11.0	1905.0	Light grayish brown, massive, thrombolitic, lime mudstone.
5.0	1910.0	Covered.
5.0	1915.0	Light gray, thrombolitic, lime mudstone. (*Plethopeltus*)
10.0	1925.0	Covered.
48.0	1973.0	Interbedded, grayish brown, ribbony, lime mudstone and thin, thrombolitic beds.
33.0	2006.0	Covered.
5.0	2011.0	Light gray, thrombolitic, lime mudstone.
3.0	2014.0	Covered.
6.0	2020.0	Light gray, thrombolitic, lime mudstone.
4.0	2024.0	Covered.
6.0	2030.0	Grayish brown, massive, thrombolitic, lime mudstone.
11.0	2041.0	Light gray, laminated lime mudsotne.
6.0	2047.0	Covered.
8.0	2055.0	Light gray, ribbony, lime mudstone with thin, thrombolite layers.
10.0	2065.0	Covered.
51.0	2116.0	Interbedded, gray, laminated, lime mudstone and thin, thrombolitic, lime mudstone.
37.0	2153.0	Covered.
8.0	2161.0	Gray, massive, thrombolitic, lime mudstone.
20.0	2181.0	Interbedded, gray, ribbony, lime mudstone, and thin thrombolites.

Section 9

Section along the C&O Canal National Historic Park towpath that begins at Lock 46 within the Shady Grove Member of the Conococheague Formation and proceeds eastward towards Dam Number Five, and ends in the basal Rockdale Run Formation. This is the type section of the Dam Five Member. 39°36′55″ N, 77°55′36″ W.

Thickness (feet) unit	total	
Conococheague Formation		
Shady Grove Member		
3.0	3.0	Tan, laminated dolomite.
3.0	6.0	Gray, ribbony limestone.
2.0	8.0	Gray, thrombolitic limestone.
20.0	28.0	Covered.
4.0	32.0	Gray, thrombolitic limestone.
6.0	38.0	Gray, ribbony, lime mudstone.
4.0	42.0	Covered.
3.0	45.0	Light gray, thrombolitic, lime mudstone.
1.0	46.0	Tan, laminated dolomite.
3.0	49.0	Covered.
2.0	51.0	Gray, laminated, lime mudstone.
2.0	53.0	Light gray, intraclastic grainstone, grades upward into packstone.
2.0	55.0	Gray, ribbony, lime mudstone.
5.0	60.0	Gray, bioturbated, thin-bedded, lime mudstone.
1.0	61.0	Tan dolomite, mostly covered.
2.0	63.0	Tan, bioturbated dolomite.
5.0	68.0	Light gray, thin-bedded, lime mudstone.
2.0	70.0	Tan, sandy dolomite.
3.0	73.0	Light gray, ribbony, lime mudstone, sandy at top.
8.0	81.0	Gray, ribbony to laminated, lime

		mudstone.
2.0	83.0	Covered.
6.0	89.0	Gray, ribbony, lime mudstone.
1.0	90.0	Tan, laminated dolomite.
4.0	94.0	Light gray, ribbony, lime mudstone.
1.0	95.0	Tan, laminated dolomite.
5.0	100.0	Light gray, laminated, platy lime mudstone.
1.0	101.0	Covered.
1.0	102.0	Tan, laminated dolomite.
2.0	104.0	Light gray, sandy, lime grainstone.
10.0	114.0	Covered.
1.0	115.0	Medium gray to tan, ribbony to laminated, lime mudstone.
3.0	118.0	Light gray, thrombolitic limestone.
3.0	121.0	Tan, laminated dolomite.

Stonehenge Limestone

Stoufferstown Member

6.0	6.0	Medium gray, ribbony to platy, lime mudstone.
9.0	15.0	Covered.
3.0	19.0	Tan, bioturbated dolomite.
4.0	23.0	Gray, ribbony, lime mudstone.
1.0	24.0	Gray, thrombolitic, lime mudstone.
3.0	28.0	Light gray, ribbony, dolomitic lime mudstone.
1.0	29.0	Medium gray, thrombolitic, lime mudstone.
2.0	31.0	Covered.
7.0	38.0	Light gray, ribbony, lime mudstone.
2.0	40.0	Gray dolomite.
3.0	43.0	Light gray, thrombolitic, lime mudstone.
3.0	46.0	Gray, thin-bedded, lime mudstone.
2.0	48.0	Covered.
3.0	51.0	Gray, thin-bedded, platy, lime mudstone.
2.0	53.0	Light gray, thrombolitic, lime mudstone, with black, chert nodules.
5.0	58.0	Gray, ribbony, lime mudstone.
9.0	67.0	Medium gray, thin-bedded, lime mudstone (quarry above canal).
10.0	77.0	Gray, ribbony, lime mudstone.
1.0	78.0	Light gray, thrombolitic, lime mudstone.
16.0	94.0	Medium to light gray, ribbony lime mudstone .
59.0	153.0	Covered.
16.0	169.0	Gray, ribbony, lime mudstone, thin-bedded at top.
1.0	170.0	Gray, medium-bedded, lime mudstone.
2.0	172.0	Covered.
2.0	174.0	Gray, thin-bedded, lime grainstone.

Funkstown Member

10.0	184.0	Gray, massive, thrombolitic, lime boundstone.
3.0	187.0	Gray, ribbony, lime mudstone.
3.0	190.0	Covered.
2.0	192.0	Gray, thin-bedded, lime mudstone
12.0	204.0	Gray, massive, thrombolitic, lime boundstone.
6.0	210.0	Medium gray, ribbony to thin-bedded, lime mudstone.
26.0	236.0	Medium gray, thrombolitic, lime boundstone.
4.0	240.0	Medium gray, ribbony, lime mudstone.
18.0	258.0	Covered.
3.0	261.0	Medium gray, ribbony, lime mudstone.
16.0	277.0	Medium gray, massive, thrombolitic, lime boundstone.
2.0	279.0	Covered.
7.0	286.0	Medium gray, massive, thrombolitic, lime boundstone.
4.0	290.0	Medium gray, medium-bedded to ribbony, lime mudstone, grainstone at top.
7.0	297.0	Gray, massive, thrombolitic, lime boundstone.
6.0	303.0	Covered.
16.0	319.0	Medium gray, thrombolitic, lime mudstone, stromatolitic at top.
21.0	340.0	Covered.
8.0	348.0	Medium gray, medium-bedded, lime mudstone. Black chert at top.
7.0	355.0	Covered.
4.0	359.0	Medium gray, thrombolitic, lime boundstone.
9.0	368.0	Gray, ribbony to laminated, lime mudstone.
2.0	370.0	Covered.
7.0	377.0	Medium gray, thrombolitic, lime boundstone.
9.0	386.0	Covered.
3.0	389.0	Medium gray, thrombolitic, lime boundstone.
25.0	414.0	Medium gray, ribbony, lime mudstone.
36.0	450.0	Medium gray, ribbony to laminated, lime mudstone with thin (<1.0 foot) thrombolitic beds and interbeds of intraclastic grainstone.
3.0	453.0	Medium gray, thrombolitic, lime boundstone.
4.0	457.0	Gray, thin-bedded to ribbony, lime mudstone.

1.0	458.0	Tan dolomite.
5.0	463.0	Medium gray, bioturbated and ribbony, lime mudstone.
7.0	470.0	Medium gray, thrombolitic, lime boundstone.
6.0	476.0	Medium gray, thin-bedded to ribbony, lime mudstone.
1.0	477.0	Tan dolomite.
5.0	482.0	Gray, blocky, thrombolitic, lime boundstone.
11.0	493.0	Medium gray, medium-bedded to ribbony, lime mudstone with thin, dolomite beds and lenses.
16.0	509.0	Medium gray, massive, thrombolitic, lime boundstone, with black, chert nodules at top.
2.0	511.0	Tan, laminated dolomite.
2.0	513.0	Light gray, thrombolitic- lime boundstone.
4.0	517.0	Medium gray, thin-bedded, bioturbated lime mudstone.
5.0	522.0	Medium gray, thrombolitic, lime boundstone, with ribbony interbeds and tan dolomite at top.

Dam Five Member (type section)

6.0	528.0	Medium gray, ribbony, lime mudstone with shaly partings.
27.0	555.0	Medium gray, thin- to medium-bedded, ribbony, lime mudstone with few, thin, thrombolitic beds.
1.0	556.0	Light gray, laminated dolomite.
2.0	558.0	Medium gray, laminated, lime mudstone with black chert nodules.
3.0	561.0	Medium gray, thrombolitic, lime boundstone.
1.0	562.0	Tan to light gray, laminated dolomite with black, chert nodules at top.
2.0	564.0	Medium gray, ribbony to laminated, dolomitic, lime mudstone.
1.0	565.0	Tan, laminated dolomite.
12.0	577.0	Interbedded, gray, laminated, lime mudstone and thin (< 1.0 foot), thrombolitic, lime boundstone.
5.0	582.0	Medium gray, medium-bedded, lime grainstone, oolitic at top.
14.0	596.0	Medium gray, thin-bedded to ribbony, lime mudstone.
2.0	598.0	Medium gray, oolitic, lime packstone.
12.0	610.0	Interbedded, medium gray, ribbony, lime mudstone, and medium-bedded, lime grainstone.
2.0	612.0	Tan, laminated, dolomitic, lime mudstone.
5.0	617.0	Gray, massive, oolitic, lime grainstone.
6.0	623.0	Medium gray, medium-bedded, lime grainstone.
7.0	630.0	Medium gray, ribbony, lime mudstone with dolomitic partings.
14.0	644.0	Medium gray, medium-bedded, lime grainstone.
5.0	649.0	Medium gray, thin- to ribbony-bedded, lime mudstone.
9.0	658.0	Medium gray, medium-bedded, oolitic, lime grainstone.
1.0	659.0	Tan, laminated dolomite.
3.0	662.0	Light gray, oolitic, lime grainstone.
7.0	669.0	Medium gray, medium-bedded, lime packstone, with grainstone layers.
6.0	675.0	Medium gray, ribbony, lime mudstone with tan, dolomitic partings and black, chert nodules.
61.0	736.0	Medium dark gray, ribbony, lime mudstone, with siliceous, dolomite partings.
9.0	745.0	Medium gray, medium-bedded to ribbony, lime mudstone.
5.0	750.0	Gray, ribbony, lime mudstone.
29.0	779.0	Medium dark gray, ribbony, lime mudstone with thin layers of oolitic, lime grainstone.
7.0	786.0	Medium gray, thin-bedded, lime mudstone.
3.0	789.0	Tan, laminated, shaly dolomite.
5.0	794.0	Covered.
1.0	795.0	Medium gray dolomite.
5.0	800.0	Covered.
3.0	803.0	Medium gray, medium-bedded, lime grainstone.
5.0	808.0	Light gray, medium-bedded, lime mudstone.
1.0	809.0	Light gray, laminated dolomite.
10.0	819.0	Light gray, medium-bedded, oolitic, lime grainstone.
1.0	820.0	Covered.
11.0	831.0	Medium gray, medium- to thin-bedded, lime grainstone.
1.0	832.0	Medium gray, ribbony, lime mudstone.
13.0	845.0	Medium gray, medium- to ribbony-bedded, lime mudstone.

Rockdale Run Formation

2.0	2.0	Covered.
2.0	4.0	Medium gray, thrombolitic, lime

		boundstone.
1.0	5.0	Tan, laminated dolomite.
2.0	7.0	Medium gray, thrombolitic, lime boundstone.
1.0	8.0	Tan, laminated dolomite.
3.0	11.0	Medium gray, lime mudstone.
2.0	13.0	Medium gray, laminated, dolomitic, lime mudstone.
2.0	15.0	Medium gray, thrombolitic, lime boundstone.
4.0	19.0	Covered.
1.0	20.0	Tan, laminated dolomite.

Section 10

Section in the Stonehenge Limestone along northern boundary of Funkstown, Washington County, Maryland. Section begins in the upper Conococheague Formation along the north bank of Antietam Creek and continues eastward along creek and tributary valley. Re-measured from Sando (1957), section 12. This is the type section of the Funkstown Member. 39°36′59″ N, 77°42′17″ W.

Thickness (feet) unit	total	
Conococheague Formation		
45.0	45.0	Medium gray, medium-bedded to ribbony, lime mudstone.
5.0	50.0	Covered.
34.0	84.0	Medium gray, medium-bedded to ribbony, lime mudstone containing a few, thin, thrombolite layers.
5.0	89.0	Covered.
Stonehenge Limestone		
Stoufferstown Member		
19.0	19.0	Dark gray, thin-bedded, ribbony, siliceous limestone.
17.0	36.0	Dark gray, massive, thrombolitic, lime boundstone.
97.0	133.0	Dark gray, thin-bedded, ribbony, siliceous limestone.
8.0	141.0	Covered.
13.0	154.0	Dark gray, thin-bedded, ribbony, siliceous limestone, weathers to tan, fractured, calcareous, shale chips.
9.0	163.0	Covered.
Funkstown Member (type secton)		
35.0	35.0	Medium gray, light gray-weathering, massive, thrombolitic, lime boundstone.
15.0	50.0	Medium gray, medium-bedded, thrombolitic, lime boundstone.
6.0	56.0	Medium to dark gray, ribbony, lime mudstone with tan, siliceous partings.
35.0	91.0	Covered, stream valley.
12.0	103.0	Medium to dark gray, massive, thrombolitic, lime boundstone.
3.0	106.0	Medium to dark gray, ribbony, lime mudstone with tan, siliceous partings.
16.0	122.0	Covered.
9.0	131.0	Medium gray, massive, thrombolitic, lime boundstone.
5.0	136.0	Medium to dark gray, ribbony, lime mudstone with tan, siliceous partings.
13.0	149.0	Medium gray, medium-bedded, thrombolitic, lime boundstone.
7.0	156.0	Medium gray, ribbony, lime mudstone
25.0	181.0	Dark gray, massive, thrombolitic, lime boundstone.
3.0	184.0	Medium gray, ribbony, lime mudstone.
25.0	209.0	Dark gray, massive, thrombolitic, lime mudstone.
42.0	251.0	Medium to dark gray, thick-bedded to massive, thrombolitic, lime mudstone. Poorly exposed.
10.0	261.0	Covered.
10.0	271.0	Medium to dark gray, massive, thrombolitic, lime mudstone.
11.0	282.0	Medium gray, thinly-bedded to ribbony, lime wackestone to mudstone.
27.0	309.0	Covered.
7.0	316.0	Medium to dark gray, massive, thrombolitic, lime mudstone boundstone.
3.0	319.0	Medium gray, ribbony lime wackestone to packstone.
5.0	324.0	Medium dark gray, thick-bedded, thrombolitic, lime boundstone.
30.0	354.0	Covered.
Dam Five Member		
25.0	25.0	Medium gray, thin to medium-bedded, lime wackestone to packstone.

Section 11

Section progressing west to east in the upper part of the Stonehenge Limestone through basal strata of the Martinsburg Formation along the C&O Canal National Historical Park. Section begins at east end of parking area at end of Gift Road at approximately milemarker 103.1. Much of this section is the same as measured by Sando (1957), section 1. 39°36′59″ N, 77°53′15″ W.

Thickness (feet) unit	total	
Stonehenge Limestone Dam Five Member		
5.0	5.0	Medium gray, light gray-weathering, massive, thrombolitic, lime boundstone.
3.0	8.0	Medium gray, thin- to medium-bedded, lime mudstone.
4.0	12.0	Medium gray, gray-weathering, massive, thrombolitic, lime boundstone, nodular at top.
30.0	42.0	Medium gray, thin- to medium-bedded, ribbony, lime mudstone.
1.0	43.0	Tan, laminated dolomite.
90.0.	133.0	Medium gray, light gray-weathering, massive, thrombolitic, lime boundstone with thin, thrombolite beds, < 3.0 feet thick.
2.0	135.0	Tan, fractured dolomite.
11.0	146.0	Medium gray, ribbony, lime mudstone.
4.0	150.0	Medium gray, massive, thrombolitic, lime boundstone.
5.0	155.0	Medium gray, ribbony, lime mudstone.
3.0	158.0	Medium light gray thrombolitic, lime mudstone.
6.0	164.0	Medium light gray, ribbony, lime mudstone.
27.0	191.0	Covered.
5.0	196.0	Medium gray, thin-bedded, lime packstone.
2.0	198.0	Tan, laminated dolomite.
9.0	207.0	Medium gray, medium-bedded, lime wackestone-packstone.
15.0	222.0	Covered.
3.0	225.0	Medium gray, thrombolitic, lime boundstone.
12.0	237.0	Medium gray, thin-bedded, lime wackestone.
1.0	238.0	Tan, fractured dolomite.
20.0	258.0	Medium gray, medium-bedded to ribbony, lime wackestone-packstone.
Rockdale Run Formation		
2.0	2.0	Light gray, fractured dolomite.
3.0	5.0	Medium gray, thrombolitic, lime boundstone.
2.0	7.0	Light gray, fractured dolomite.
4.0	11.0	Medium gray, thick-bedded, lime mudstone-wackestone.
3.0	14.0	Tan, laminated dolomite.
2.0	16.0	Light gray, thin-bedded, lime mudstone.
3.0	19.0	Light gray to tan, laminated dolomite.
2.0	21.0	Light gray, thin-bedded, lime mudstone.
4.0	25.0	Light gray, fractured dolomite.
6.0	31.0	Light gray, massive, thrombolitic, lime boundstone.
5.0	36.0	Light gray, medium-bedded, lime mudstone.
7.0	40.0	Covered.
3.0	43.0	Light gray, thrombolitic, lime boundstone.
5.0	48.0	Tan, laminated, fractured dolomite.
6.0	54.0	Medium gray, thin-bedded, lime mudstone.
5.0	59.0	Tan, fractured dolomite.
4.0	61.0	Covered.
5.0	66.0	Medium gray, massive, thrombolitic, lime boundstone.
2.0	68.0	Light gray, thin-bedded, lime mudstone.
1.0	69.0	Tan dolomite.
3.0	72.0	Tan, laminated dolomite. Surveyors stake.
5.0	77.0	Medium gray, thrombolitic, lime boundstone.
75.0	152.0	Covered. Stream valley. Milemarker 103.
4.0	156.0	Medium gray, medium-bedded, lime mudstone.
3.0	159.0	Tan dolomite.
3.0	162.0	Medium gray, lime mudstone.
5.0	167.0	Covered.
5.0	172.0	Medium gray, thrombolitic, lime boundstone.
18.0	190.0	Covered.
5.0	195.0	Tan, fractured dolomite.
6.0	201.0	Light gray, ribbony, lime mudstone.
36.0	237.0	Covered.
5.0	242.0	Medium gray, medium-bedded, thrombolitic, lime boundstone.
2.0	244.0	Tan, laminated dolomite.
17.0	461.0	Medium gray, thin-bedded to ribbony, lime mudstone-wackestone.
6.0	467.0	Tan, fractured dolomite.
2.0	469.0	Light gray, ribbony, lime mudstone.
1.0	470.0	Covered.
16.0	486.0	Medium gray, thin-bedded to ribbony, oolitic, lime packstone.
2.0	488.0	Tan, fractured dolomite.
6.0	494.0	Massive, oolitic, lime packstone.
3.0	497.0	Medium gray, fractured dolomite.
3.0	500.0	Light gray, oolitic, lime packstone.
5.0	505.0	Light gray, laminated dolomite.
3.0	508.0	Light gray, ribbony lime wackestone,

		thrombolitic at top.
2.0	510.0	Tan, laminated dolomite.
5.0	515.0	Light gray, thrombolitic, lime boundstone.
2.0	517.0	Light gray, laminated, lime mudstone.
6.0	523.0	Light gray, ribbony, lime mudstone.
3.0	526.0	Light gray, laminated dolomite.
6.0	532.0	Covered. Swale.
1.0	533.0	Light gray, laminated, lime mudstone.
4.0	537.0	Light gray, thrombolitic, lime boundstone.
55.0	592.0	Interbedded, medium gray, thrombolitic boundstone and ribbony, lime mudstone.
2.0	594.0	Covered.
27.0	621.0	Medium gray, ribbony, lime mudstone with thin layers of thrombolitic, lime boundstone.
4.0	625.0	Tan to light gray, laminated dolomite.
15.0	640.0	Interbedded, light gray, ribbony, lime mudstone and thin, thrombolitic, lime boundstone.
3.0	643.0	Light gray, laminated dolomite.
15.0	658.0	Interbedded, medium gray, thrombolitic, lime boundstone and ribbony and laminated, lime mudstone.
3.0	661.0	Light gray, laminated dolomite.
5.0	666.0	Light gray, thin-bedded, lime mudstone.
7.0	673.0	Medium gray, thrombolitic, lime boundstone.
1.0	674.0	Tan, laminated dolomite.
16.0	690.0	Medium gray, ribbony limestone.
15.0	705.0	Medium gray, thin-bedded, cherty, lime mudstone.
2.0	707.0	Tan, laminated dolomite.
2.0	709.0	Light gray, thrombolitic, lime boundstone.
2.0	711.0	Light gray, laminated, lime mudstone.
30.0	741.0	Interbedded, medium gray, cherty, lime mudstone, and light gray, laminated, dolomite.
7.0	748.0	Medium gray, ribbony, lime mudstone-wackestone.
3.0	751.0	Light gray, fractured dolomite.
12.0	763.0	Light gray, ribbony, lime mudstone.
1.0	764.0	Tan, laminated dolomite.
13.0	777.0	Interbedded, medium gray, ribbony limestone, and tan, laminated dolomite.
135.0	912.0	Interbedded, medium gray, ribbony, lime mudstone with thin (<1.0 feet), thrombolitic boundstone and light gray to tan, laminated dolomite.
1.0	913.0	Covered.
60.0	973.0	Medium gray, medium- to thin-bedded, lime mudstone with a few, thin, thrombolite intervals.
25.0	998.0	Medium gray, thin-bedded, lime mudstone.
2.0	1000.0	Light gray, laminated dolomite.
12.0	1012.0	Medium gray, ribbony, lime mudstone.
3.0	1015.0	Tan, laminated dolomite.
12.0	1027.0	Medium gray, thin-bedded to ribbony lime mudstone.
2.0	1029.0	Light gray to tan, laminated dolomite.
6.0	1035.0	Medium gray, thrombolitic, lime boundstone, ribbony at top.
3.0	1038.0	Light gray to tan, laminated dolomite.
60.0	1098.0	Medium gray, thin-bedded to ribbony, lime mudstone with thrombolitic boundstone interbeds.
10.0	1108.0	Medium gray, thin-bedded, lime mudstone.
5.0	1113.0	Tan, fractured dolomite.
3.0	1116.0	Medium gray, medium-bedded, lime mudstone.
22.0	1138.0	Covered.
8.0	1146.0	Tan, laminated, mudcracked dolomite.
5.0	1151.0	Medium gray, medium-bedded, lime mudstone.
2.0	1153.0	Tan, laminated dolomite.
3.0	1156.0	Medium gray, medium-bedded dolomite.
4.0	1160.0	Tan, laminated dolomite.
85.0	1245.0	Medium gray, medium-bedded, lime mudstone to wackestone with a few burrowed beds. Axemann Limestone equivalent strata.
3.0	1248.0	Medium gray, nodular-bedded, lime mudstone.
5.0	1253.0	Tan, laminated dolomite.
7.0	1260.0	Light gray, ribbony, lime mudstone.
4.0	1264.0	Tan, laminated dolomite.
94.0	1358.0	Medium gray, medium-bedded to ribbony limestone with a few, thin, bioturbated and thrombolitic layers.
25.0	1383.0	Covered. Old sinkhole with surveyors stake.
15.0	1398.0	Medium gray, thin-bedded, lime mudstone.
11.0	1409.0	Covered.
6.0	1415.0	Tan, laminated dolomite.
7.0	1422.0	Medium gray, thin-bedded limestone.
5.0	1427.0	Tan, laminated dolomite.
3.0	1430.0	Tan, thrombolitic, lime boundstone.
2.0	1432.0	Tan, laminated dolomite.

11.0	1443.0	Light gray, thin-bedded limestone.
2.0	1445.0	Tan, laminated dolomite.
3.0	1448.0	Medium gray, thrombolitic, lime boundstone with chert nodules.
20.0	1468.0	Interbedded, light gray limestone and tan, laminated dolomite.
8.0	1476.0	Tan dolomite.
67.0	1543.0	Interbedded, light gray, thin-bedded, lime mudstone and light gray to tan, fractured dolomite. Cave above canal.
42.0	1585.0	Interbedded, tan to light gray dolomite with thin layers of gray limestone.
6.0	1591.0	Covered.
6.0	1597.0	Light gray, fractured dolomite.
3.0	1600.0	Tan, fractured dolomite.
16.0	1616.0	Medium gray, medium-bedded limestone, thrombolitic at top.
6.0	1622.0	Tan, fractured, laminated dolomite.
4.0	1626.0	Medium gray, thin-bedded, lime mudstone.
5.0	1631.0	Tan, laminated dolomite.
7.0	1638.0	Light gray, fractured, thin-bedded limestone.
16.0	1654.0	Covered.
7.0	1661.0	Tan, fractured dolomite.
3.0	1664.0	Gray, thin-bedded, dolomitic limestone.
5.0	1669.0	Light gray, fractured dolomite.
8.0	1677.0	Light gray, thrombolitic, lime boundstone.
3.0	1680.0	Light gray, fractured dolomite.
3.0	1683.0	Light gray, fractured, dolomitic limestone.
3.0	1686.0	Covered.
5.0	1691.0	Light gray, thrombolitic, lime boundstone.
1.0	1692.0	Tan, laminated dolomite.
4.0	1696.0	Light gray, thrombolitic, lime boundstone.
1.0	1697.0	Tan, laminated dolomite.
7.0	1704.0	Covered.
2.0	1706.0	Light gray, thrombolitic, lime boundstone.

Dolomite member

3.0	1709.0	Tan, fractured, laminated dolomite.
5.0	1714.0	Light gray, fractured, thrombolitic dolomite.
6.0	1720.0	Tan, fractured dolomite.
3.0	1723.0	Light gray, ribbony dolomite.
4.0	1727.0	Light gray, fractured dolomite.
1.0	1728.0	Light gray, thrombolitic dolomite.
30.0	1758.0	Light gray, fractured dolomite.
2.0	1760.0	Light gray, dolomitic limestone.
20.0	1780.0	Light gray, medium-bedded, bioturbated, thrombolitic dolomite.
5.0	1785.0	Tan, fractured dolomite.
40.0	1825.0	Medium gray, medium- to thick-bedded, bioturbated dolomite.
8.0	1833.0	Covered.
12.0	1845.0	Medium gray, medium-bedded dolomite.
5.0	1850.0	Tan, fractured dolomite.
35.0	1885.0	Medium gray, medium-bedded dolomite.
20.0	1905.0	Light gray, highly fractured dolomite.
10.0	1915.0	Light gray, thin-bedded dolomite.
3.0	1918.0	Covered.
2.0	1920.0	Light gray, laminated dolomite.
2.0	1922.0	Light gray, thrombolitic dolomite.
5.0	1927.0	Light gray, laminated dolomite.
5.0	1932.0	Light gray, bioturbated and thrombolitic dolomite.
5.0	1937.0	Tan, fractured dolomite.
3.0	1940.0	Medium gray, ribbony, lime wackestone.
1.0	1941.0	Tan fractured dolomite.
6.0	1947.0	Medium gray, thrombolitic, lime boundstone.
3.0	1950.0	Medium gray, laminated, lime mudstone.
4.0	1954.0	Light gray, thrombolitic, lime boundstone.
12.0	1966.0	Light gray, fractured dolomite.
2.0	1968.0	Light gray, lime mudstone.
2.0	1970.0	Light gray, laminated, lime mudstone.
5.0	1975.0	Medium gray, thin-bedded, lime mudstone.
1.0	1976.0	Medium gray dolomite.
13.0	1989.0	Medium gray, massive, thrombolitic, lime boundstone.
5.0	1994.0	Light gray, thin-bedded to laminated, lime mudstone.
7.0	2001.0	Light gray, massive, thrombolitic, lime boundstone.
2.0	2003.0	Tan, fractured dolomite.
5.0	2008.0	Covered.
55.0	2063.0	Interbedded, light gray, thrombolitic, lime boundstone and tan, laminated dolomite.
12.0	2075.0	Covered.
13.0	2088.0	Light gray, thin-bedded dolomite.
9.0	2097.0	Medium gray, thrombolitic, lime boundstone, ribbony at top.
40.0	2137.0	Interbedded, medium gray, massive,

		thrombolitic, lime boundstone, and light gray dolomite.
5.0	2142.0	Medium gray, thrombolitic dolomite.
6.0	2148.0	Light gray, fractured dolomite.
3.0	2151.0	Covered.
30.0	2181.0	Interbedded, medium gray, dolomitic, lime wackestone and massive, fractured dolomite.
8.0	2189.0	Medium gray, thrombolitic, lime boundstone.
6.0	2195.0	Tan, laminated, fractured dolomite.
7.0	2202.0	Dark gray, thrombolitic dolomite.
35.0	2237.0	Covered.
8.0	2245.0	Medium gray, thrombolitic, lime boundstone.
2.0	2247.0	Medium gray, lime grainstone.
6.0	2253.0	Medium gray, thin-bedded, lime mudstone.
2.0	2255.0	Light gray, laminated, lime mudstone.
6.0	2261.0	Medium gray, medium-bedded to ribbony, lime mudstone.
3.0	2264.0	Medium gray, medium-bedded, thrombolitic, lime boundstone, ribbony at top.
6.0	2270.0	Medium gray, fractured dolomite.
8.0	2278.0	Medium gray, medium-bedded dolomite.
16.0	2294.0	Medium gray, medium-bedded, fractured dolomite with chert nodules at top.
7.0	2301.0	Medium gray, ribbony, dolomitic, lime mudstone.

Pinesburg Station Dolomite

6.0	6.0	Tan, fractured dolomite.
4.0	10.0	Light gray, fractured dolomite.
7.0	17.0	Medium gray, fractured dolomite.
90.0	107.0	Interbedded, medium gray, medium- to thick-bedded, fractured and lumpy dolomite.
27.0	134.0	Covered.
35.0	169.0	Light gray, medium-bedded, locally laminated dolomite.
100.0	269.0	Covered.
25.0	294.0	Light gray, medium-bedded, fractured dolomite.
3.0	297.0	Covered.
2.0	299.0	Light gray, fractured dolomite.
5.0	304.0	Covered.
51.0	355.0	Interbedded, medium gray, medium-bedded dolomite and laminated dolomite.
5.0	360.0	Covered.
44.0	404.0	Medium to light gray, thick-bedded, fractured dolomite.
17.0	421.0	Light gray, medium-bedded, fractured dolomite.
3.0	424.0	Light gray, laminated dolomite.
7.0	431.0	Light gray, fractured dolomite.
5.0	436.0	Light gray, medium-bedded dolomite.
1.0	437.0	Light gray, nodular dolomite.

St. Paul Group

Row Park Limestone

43.0	43.0	Medium light gray, massive, fenestral, lime mudstone.
12.0	55.0	Light gray, medium-bedded, dolomitic limestone.
5.0	60.0	Light gray, massive, dolomitic, lime mudstone.
3.0	63.0	Light gray, tan, fractured dolomite.
3.0	66.0	Light gray, massive, lime mudstone.
5.0	71.0	Light gray, ribbony to laminated limestone.
11.0	82.0	Light gray, ribbony, lime mudstone.
15.0	97.0	Interbedded, light gray, fractured dolomite and laminated to ribbony, lime mudstone.
1.0	98.0	Tan dolomite.
27.0	125.0	Light gray, massive, fenestral, lime mudstone with few interbeds of ribbony, lime mudstone.
9.0	134.0	Light gray, fenestral, lime mudstone.

New Market Limestone

33.0	33.0	Light gray, ribbony and laminated, lime mudstone.
90.0	123.0	Interbedded, light gray, ribbony to laminated, lime mudstone and stromatolitic, lime boundstone and tan, laminated dolomite.
82.0	205.0	Interbedded, light gray, thick-bedded, fenestral, lime mudstone and massive, medium-bedded, fossiliferous, lime mudstone and stromatolitic boundstone, and tan, laminated dolomite.
25.0	230.0	Dove white to light gray, thick-bedded to massive, dolomitic mudstone.

Chambersburg Formation

39.0	39.0	Medium to dark gray, thin- to nodular-bedded, argillaceous, lime mudstone.
10.0	49.0	Dark gray, argillaceous, thin- to nodular bedded, lime mudstone.

30.0	79.0	Mostly covered. Probable *Echinosphaerites* beds.
25.0	104.0	Dark gray, nodular-bedded, lime mudstone.
23.0	127.0	Dark gray, thin-bedded, lime mudstone.
27.0	154.0	Dark gray, thin- to wavy-bedded, lime mudstone.
38.0	192.0	Dark gray, medium- to thick-bedded, lime mudstone.
99.0	291.0	Dark gray, thin- to wavy-bedded, lime mudstone.

Martinsburg Formation

7.0	7.0	Dark gray, calcareous, cleaved shale. Fault likely at contact.

Section 12

Section in the upper part of the Rockdale Run Formation through Chambersburg Formation along the north side of westbound Interstate 70 at Cedar Ridge Road. Section begins along the guard rail on the north side of the eastbound lane west of Cedar Ridge Road. 39°39′05″ N, 77°51′42″ W.

Thickness (feet) unit	total	

Rockdale Run Formation

4.0	4.0	Medium gray, bioturbated, dolomitic lime mudstone.
5.0	9.0	Medium gray, vuggy limestone.
2.0	11.0	Covered.
5.0	16.0	Dark gray, bioturbated, lime mudstone.
2.0	18.0	Light gray, laminated, lime mudstone.
6.0	24.0	Medium gray, bioturbated, lime mudstone.
2.0	26.0	Tan, fractured dolomite.
3.0	29.0	Light gray, ribbony, lime mudstone.
1.0	30.0	Tan, fractured dolomite.
5.0	35.0	Light gray, thin-bedded, lime mudstone.
2.0	37.0	Medium gray, dolomitic, lime mudstone.
4.0	41.0	Medium gray, thrombolitic, lime mudstone.
2.0	43.0	Medium gray, laminated, dolomitic limestone.
4.0	47.0	Medium gray, bioturbated, lime mudstone.
2.0	49.0	Medium gray dolomitic limestone.
2.0	51.0	Tan, fractured dolomite.
5.0	56.0	Medium gray, bioturbated dolomite.
6.0	62.0	Light gray, fractured dolomite.
2.0	64.0	Light gray, bioturbated dolomite.
2.0	66.0	Light gray, laminated, dolomitic limestone.
3.0	69.0	Tan, fractured dolomite.
3.0	72.0	Medium gray, bioturbated, dolomitic limestone.
6.0	78.0	Medium gray, bioturbated lime mudstone.
3.0	81.0	Medium gray, lime mudstone with coral fragments.
1.0	82.0	Medium gray, laminated dolomite.
3.0	85.0	Medium gray, medium-bedded, lime mudstone.
6.0	91.0	Light gray, medium-bedded, dolomitic lime mudstone.
8.0	99.0	Medium grayish brown, bioturbated, vuggy, lime mudstone.
1.0	100.0	Light gray, laminated, lime mudstone.
3.0	103.0	Light gray, thrombolitic, lime mudstone.
3.0	106.0	Medium gray, medium-bedded, lime mudstone.
4.0	110.0	Dark gray, shaly, lime mudstone.
3.0	113.0	Light gray, bioturbated and laminated dolomite.
1.0	114.0	Light gray, intraclastic, lime packstone.

Pinesburg Station Dolomite

5.0	5.0	Medium gray dolomite.
2.0	7.0	Medium gray, laminated dolomite.
3.0	10.0	Medium gray, bioturbated dolomite.
2.0	12.0	Light gray, laminated dolomite.
6.0	18.0	Medium gray, medium-bedded dolomite.
14.0	32.0	Medium gray, fractured dolomite.
6.0	38.0	Medium gray, medium-bedded, fractured dolomite.
5.0	43.0	Medium gray, laminated dolomite.
3.0	46.0	Medium gray, medium-bedded dolomite.
3.0	49.0	Medium grayish brown, laminated dolomite.
6.0	55.0	Medium gray, bioturbated dolomite.
8.0	63.0	Medium gray dolomite.
3.0	66.0	Tan, laminated dolomite.
14.0	80.0	Interbedded, medium gray, bioturbated, thrombolitic and laminated dolomite.
6.0	86.0	Tan flowstone (sinkhole).
16.0	102.0	Interbedded, light gray, bioturbated and laminated dolomite.
6.0	108.0	Medium grayish brown, ribbony dolomite with abundant chert nodules.
24.0	132.0	Light gray, medium-bedded, fractured

		dolomite.
5.0	137.0	Medium gray, laminated to ribbony dolomite.
25.0	162.0	Interbedded, light gray, bioturbated and laminated dolomite.
1.0	163.0	Tan, laminated dolomite.
3.0	166.0	Dark gray, ribbony dolomite.
18.0	184.0	Light gray, fractured dolomite.
6.0	190.0	Light grayish brown, ribbony dolomite.
22.0	212.0	Interbedded, medium gray, bioturbated and laminated dolomite. Mostly covered.
3.0	215.0	Tan to grayish brown dolomite.
36.0	251.0	Interbedded, light gray, bioturbated dolomite and medium gray, fractured dolomite.
6.0	257.0	Tan, fractured dolomite.
2.0	259.0	Medium gray, bioturbated dolomite.
3.0	262.0	Medium gray, ribbony dolomite, laminated at top.
12.0	274.0	Light gray, fractured dolomite.
3.0	277.0	Medium gray, medium-bedded dolomite.
8.0	285.0	Medium gray, thick-bedded, thrombolitic and laminated dolomite.
3.0	288.0	Medium gray, medium-bedded dolomite.
3.0	291.0	Medium to light gray, medium-bedded dolomite.
8.0	299.0	Medium gray, thick-bedded, bioturbated dolomite.
2.0	301.0	Light gray, fractured dolomite.
13.0	314.0	Light gray, fractured dolomite.
6.0	320.0	Light gray, medium-bedded dolomite.
St. Paul Group		
Row Park Limestone		
114.0	114.0	Light gray, massive, fenestral, lime mudstone with thin layers of intraclastic packstone.
13.0	127.0	Light gray, lime mudstone with intraclastic layers.
92.0	219.0	Medium light gray, medium-bedded, lime mudstone with intraclastic, lime packstone layers
11.0	230.0	Medium dark gray, bioturbated, lime wackestone to mudstone.
New Market Limestone		
18.0	18.0	Medium gray, medium-bedded, bioturbated and fenestral, lime mudstone and thin beds of tan, bioturbated dolomite.
2.0	20.0	Tan, fractured, laminated dolomite.
2.0	22.0	Light gray, fenestral, lime mudstone.
3.0	25.0	Tan, laminated, dolomitic limestone.
22.0	47.0	Medium gray, thick-bedded, bioturbated, locally fenestral, lime mudstone.
2.0	49.0	Tan, laminated dolomite.
3.0	52.0	Light gray, massive, fenestral and bioturbated, lime mudstone.
5.0	57.0	Medium gray, medium-bedded, intraclastic, lime mudstone-packstone.
4.0	61.0	Tan, laminated dolomite.
3.0	64.0	Medium gray, intraclastic, lime wackestone-packstone.
6.0	70.0	Medium gray, bioturbated and intraclastic,lime mudstone.
32.0	102.0	Medium gray, medium-bedded, lime mudstone interbedded with light gray, laminated dolomite.
124.0	226.0	Interbedded, medium-bedded, medium grayish brown, bioturbated, lime mudstone and tan dolomite.
25.0	251.0	Medium gray, medium-bedded, lime mudstone with brecciated layers.
22.0	273.0	Medium gray, thick-bedded, lime mudstone, with a few layers of fenestral fabric.
Chambersburg Formation		
13.0	13.0	Medium gray, medium- to thin-bedded, argillaceous, lime mudstone.
32.0	45.0	Medium dark gray, argillaceous thin- to lumpy-bedded, lime wackestone.
35.0	80.0	Dark gray, shaly, nodular-bedded, lime wackestone. *Echinoshaerites* beds.
70.0	150.0	Dark gray, thin-bedded, lime mudstone.
15.0	165.0	Dark gray, medium-bedded, argillaceous, lime mudstone.
15.0	180.0	Dark gray, medium- to thick-bedded, bioturbated, lime mudstone.
13.0	193.0	Dark gray, medium-bedded, lime mudstone with wispy, clay partings.
21.0	214.0	Medium gray, medium-bedded, lime mudstone.
35.0	249.0	Medium to dark gray, thick-bedded, bioturbated, lime wackestone.
23.0	272.0	Dark gray, medium-bedded, bioturbated, lime wackestone.
15.0	287.0	Dark gray, nodular-bedded, argillaceous, lime wackestone, shaly at top.

4.0	291.0	Dark gray, argillaceous, lime mudstone.	8.0	324.0	Covered.
25.0	316.0	Dark gray, medium-bedded, lime mudstone.	33.0	357.0	Dark gray, thin-bedded, lime mudstone.

APPENDIX II - Glossary of geologic terms used

Alleghanian - Referring to the mountain building episode that created the Appalachian Mountains, circa 250 Mya.

Alluvium - A sedimentary deposit left by a stream, stream channel, or floodplain.

Anticline - A convex upward bend in rock, the central part of which contains the oldest section of rock.

Anticlinorium - A broad upward bend in the Earth's crust made up of a series of anticlines and synclines, that, taken together, has the general outline of an arch.

Argillaceous - Containing significant amounts of clay.

Artesian - Movement of spring water to the surface due to natural pressure from overlying rock.

Bedding - Original or depositional layering in sedimentary rocks. Also called stratification.

Bedrock - Solid rock that underlies unconsolidated material, such as soil.

Biohermal - An organic buildup preserved in rock that produces local relief with adjacent strata.

Bioturbation - The destruction of layering in strata by movement of biota in the soft sediment.

Blind valley - A karst valley whose stream flows and terminates into a sinkhole.

Boundstone - A limestone composed of organically bound components (e.g., thrombolite, stromatolite).

Breccia - A clastic rock composed of particles more than 2 millimeters in diameter and marked by the angularity of its component grains and rock fragments.

Carbonate - One of several minerals containing one central carbon atom with strong covalent bonds to three oxygen atoms and typically having ionic bonds to one or more positive ions.

Carbonate rock - An easily dissolvable, sedimentary rock composed primarily of minerals such as dolomite or calcite.

Cave - A naturally formed void or opening beneath the surface of the Earth, formed by dissolution of carbonate bedrock.

Chert - A fine-grained rock made of microcrystalline quartz.

Colluvium - A sedimentary deposit formed by the movement of unconsolidated material down steep slopes.

Clastic rock - A sedimentary rock composed of fragments of pre-existing rocks.

Cross-bedding - The arrangement of sedimentary beds tilted at different angles to each other, indicating that the beds were deposited by flowing wind or water.

Cleavage - The tendency of certain minerals to break along distinct planes in their crystal structures where the bonds are weakest. Cleavage is tested by striking or hammering a mineral, and is classified by the number of surfaces it produces and the angles between adjacent surfaces.

Conglomerate - A clastic rock composed of particles more than 2 millimeters in diameter and marked by the roundness of its component grains and rock fragments.

Doline - A bowl or funnel shaped closed depression formed from the dissolving of underlying bedrock. Equivalent to a depression of this report.

Dolomite - A carbonate rock made up of more than 50 percent of the mineral calcium-magnesium carbonate $CaMg(CO_3)_2$.

Dolostone - A carbonate rock composed primarily of dolomite.

Fault - A fracture dividing a rock into two sections that have visibly moved relative to each other.

Fenestral - A fine-grained limestone containing irregularly shaped, calcite-filled, voids several millimeters in diameter.

Ferruginous - A rock rich in iron minerals.

Fold - A bend that develops in an initially horizontal layer of rock, usually caused by plastic deformation. Folds occur most frequently in sedimentary rocks.

Foliation - The arrangement of a set of minerals in parallel, sheet-like layers that lie perpendicular to the flattened plane of a rock. Occurs in metamorphic rocks on which directed pressure has been exerted.

Fracture - A crack or break in rock.

Grainstone - A limestone composed of carbonate grains or sand-sized clasts.

Graywacke - A sandstone composed of fragments of preexisting rocks.

Grike - A fracture or fissure along which dissolving of limestone occurs.

Intraclast - A limestone clast that has been broken by depositional processes.

Interbedded - Alternations of layers of rock with beds of a different kind of rock.

Joint - A fracture in rock where no visible movement has taken place.

Karst - A topography characterized by caves, sinkholes, disappearing streams, and underground drainage. Karst forms when groundwater dissolves pockets of limestone, dolomite, or gypsum in bedrock.

Lacuna - A gap in deposition, formation, or time.

Limestone - A sedimentary rock composed primarily of calcium carbonate. Some 10% to 15% of all sedimentary rocks are limestones.

Lithology - Referring to the composition and character of a

specific rock type.

Marble - A recrystallized and metamorphosed limestone or dolomite.

Orogeny - An episode of mountain building or deformation.

Oolitic - Pertaining to a rock that consists of carbonate grains that have concentric layers of growth.

Packstone - A limestone composed of a mixture of lime mud and carbonate grains.

Phyllite - A fine grained rock formed by the metamorphism of shale.

Quartzarenite - A sandstone composed of more than 95% quartz grains.

Quartzite - An extremely durable, nonfoliated metamorphic rock derived from pure sandstone and consisting primarily of quartz.

Ribbony - Referring to thin limestone strata typically less than 1 cm in thickness and resembling ribbons.

Runnel - A groove or channel through which groundwater flows.

Sandstone - A clastic sedimentary rock composed of particles that range in diameter from 1/16 millimeter to 2 millimeters in diameter. Sandstones make up about 25% of all sedimentary rocks.

Shale - A clastic sedimentary rock composed of clay particles.

Siliciclastic - Referring to a rock composed of clasts made of quartz.

Sinkhole - An open, circular, or funnel-shaped depression in the ground that forms when soluble rocks dissolve.

Spring - A location or zone where groundwater discharges to the surface.

Strata - An individual layer of a sedimentary rock.

Stratigraphic - Referring to the study of multiple strata.

Stromatolite - A dome-shaped layered limestone deposit formed by photosynthesizing colonial algae.

Swallowhole - An opening within a stream channel that directs stream flow to the underground.

Syncline - A concave fold in rock, or fold that bends downward, whose central part contains the youngest section of rock.

Synclinorium - A regional series of synclines and anticlines grouped together that have the general outline of a trough.

Thrombolite - An algal form similar to a stromatolite that has a clotted, rather than a laminated, structure.

Tuff - A fine-grained clastic rock of volcanic rock fragments.

Wackestone - A limestone composed of mostly mud with a few scattered carbonate grains.

APPENDIX III - Plate 1-Geologic and karst map of the Hagerstown Valley.

The attached geologic and karst map of the Hagerstown Valley is a compilation of the 1:24,000 scale geologic mapping conducted during this study.

A message to Maryland's citizens

The Maryland Department of Natural Resources (DNR) seeks to balance the preservation and enhancement of the living and physical resources of the state with prudent extraction and utilization policies that benefit the citizens of Maryland. This publication provides information that will increase your understanding of how DNR strives to reach that goal through the earth science assessments conducted by the Maryland Geological Survey.

MARYLAND DEPARTMENT OF NATURAL RESOURCES
Resource Assessment Service
Tawes State Office Building
580 Taylor Avenue
Annapolis, Maryland 21401
Toll free in Maryland: 1-877-620-8DNR
Out of State call: 1-410-260-8021
TTY users: Call via the Maryland Relay
Internet Address: www.dnr.Maryland.gov

MARYLAND GEOLOGICAL SURVEY
2300 St. Paul Street
Baltimore, Maryland 21218
Telephone Contact Information: 410-554-5500
Internet Address: www.mgs.md.gov

DNR Publication Number: 12-053118-73

2018

77° 50’ 77° 40’ 77° 30’ 39° 40’ 39° 30’ 39° 20’

PENNSYLVANIA

WEST VIRGINIA

North Mountain Fault

South Mountain Fault

Keedysville Fault

US 40 US 11 I-81 I-70 MD 58 MD 60 MD 64 MD 66 MD 68 MD 55 MD 34

Map Location

Quadrangles Covered by Map

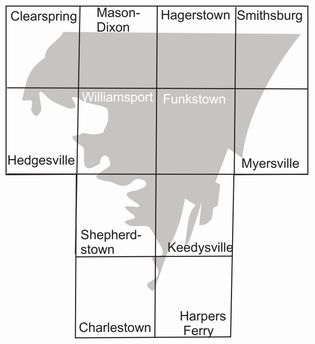

Maryland Geological Survey
Report of Investigations 86

Appendix III-Plate 1
Geologic and Karst Features Map of the Hagerstown Valley, Washington County, Maryland

by
David K. Brezinski
2018

Geologic Quadrangle assembly by
Robert D. Conkwright and Rebecca Kavage Adams

0 miles 5
0 kilometers 5

Description of Bedrock Units

Diabase
Dark gray, medium-grained, diabase. Weathers to rusty, red-brown subspheroidal boulders.

Martinsburg Formation

upper member
Medium gray, silty shale, interbedded with light gray, thin-to medium-bedded sandstone.

lower member
Predominately medium to dark gray, fissile shale with thin siltstone interbeds. Dark gray to black shale at base.

Chambersburg Formation
Medium to dark gray, nodular- to medium-bedded, fossiliferous limestone.

St. Paul Group (undivided)
Massive, light gray, fenestral, lime mudstone overlain by interbedded, medium to light gray, medium-bedded, stromatolitic limestone and laminated dolomitic limestone.

Pinesburg Station Dolomite
Medium to light gray, medium-bedded, highly fractured dolomite interbedded with light gray to tan laminated dolomite.

Rockdale Run Formation
Interbedded and cyclic limestone and dolomite, changing upsection into dominantly dolomitic limestone and dolomite.

Stonehenge Limestone

Dam Five Member
Medium to medium dark gray, medium-bedded, ribbony and oolitic, lime mudstone to packstone.

Funkstown Member
Massive, medium gray, algal lime boundstone, interbedded with medium gray, thinly bedded to ribbony, lime wackestone to lime packstone.

Stoufferstown Member
Dark gray, argillaceous, thinly bedded to ribbony, lime mudstone with thin beds of flat-pebble lime grainstone to conglomerate and hummocky, discontinuous, thin beds of laminated limestone.

Conococheague Formation

Shadygrove Member
Interbedded, medium to light gray, ribbony, cherty lime mudstone with flaggy to platy beds, and arenaceous grainstone.

Zullinger Member
Cyclically bedded, medium to dark gray, thrombolitic limestone and gray, ribbony and laminated limestone and tan, laminated dolomite.

Big Spring Station Member
Tan, massive, sandy dolomite interbedded with tan to light gray, fractured and laminated dolomite.

Elbrook Formation
Interbedded tan, thin- to thick-bedded limestone and dolomite at base, medium-bedded, dark gray limestone in the middle and cyclic, dark gray thrombolitic limestone and dolomitic limestone in the upper part.

Waynesboro Formation

Chewsville Member
Reddish brown to chocolate-brown, silty shale, siltstone, and silty fine-grained sandstone, interbedded with white, calcareous, *Skolithos*-burrowed sandstone beds and tan to buff, medium-bedded, sandy dolostone.

Cavetown Member
Medium- to thick-bedded, medium-to coarse-grained, intraclastic grainstone; tan, laminated dolostone and dolomitic limestone; and medium-gray, oolitic, lime grainstone, ribbony carbonates, and burrow-mottled dolomitic limestone.

Red Run Member
Interbedded, tan-weathering, punky, fine-grained sandstones; green-gray shale; gray sandy limestone; and laminated dolostone.

Tomstown Formation

Dargan Member
Interbedded medium to thick-bedded cyclic dark-gray, bioturbated dolomite dolomite and ribbony and algal limestone.

Benevola Member
Light-gray to white, massive to poorly bedded, highly fractured, sugary dolomite.

Fort Duncan Member
Medium- to dark-gray, thick-bedded, mottled dolomite with white, void-filling, sparry dolomite.

Bolivar Heights Member
Very light gray, sheared, laminated, dolomitic marble at its base overlain by thin- to medium-bedded, dark-gray, ribbony, burrow-mottled, lime mudstone.

Jurassic: Jd

Ordovician: Omu, Oml, Oc, Osp, Ops, Orr, Osd, Osf, Oss

Cambrian: Ccs, Ccz, Ccb, Ce, Cwac, Cwak, Cwar, Ctd, Ctb, Ctf, Ctbh

Karst depression

Active sinkhole

Spring

(29) Measured stratigraphic section (Appendix I)

Numbered highway

Data Use and Limitations

This map is a compilation of 1:24,000 digital geologic and karst maps released by the Maryland Geological Survey. The reader is directed to those publications for precise data location and origination. Published map employed in this compilation included: Brezinski (2009, 2013a, 2013b, 2014); Brezinski and Bell (2009); Brezinski and Fauth (2009), and Brezinski and Glaser (2014). These data represents results of data collection by the Department of Natural Resources, Maryland Geological Survey activity supported by the Maryland State Highway Administration, Office of Materials Technology, and the U. S. Geological Survey, National Cooperative Geologic Mapping Program. The views and conclusions contained in this document are those of the author and should not be interpreted as necessarily representing the official policies, either expressed or implied, of the U. S. Government. Field mapping was partially funded as a research grant by the Maryland State Highway Administration, Office of Materials Technology, and the U. S. Geological Survey, National Cooperative Geologic Mapping Program. The views and conclusions contained in this document are those of the author and should not be interpreted as necessarily representing the official policies, either expressed or implied, of the U. S. Government. The individual geologic maps upon which this map was compiled were created in digital form by Elizabeth Sylvia and Robert Conkwright of the Maryland Geological Survey.

REFERENCES

Brezinski, D.K., 2009, Geologic map of the Keedysville and parts of the Shepherdstown, Harpers Ferry, and Charlestown quadrangles, Washington and Frederick Counties, Maryland: Maryland Geological Survey Digital Geological Map K_SHCGEO2009.1, scale 1:24,000.

Brezinski, D.K., 2013a, Geologic and karst features map of the Hagerstown quadrangle, Maryland: Maryland Geological Survey Digital Geological Map HAGER2013.1, scale 1:24,000.

Brezinski, D.K., 2013b, Geologic and karst features map of the Mason-Dixon quadrangle, Maryland: Maryland Geological Survey Digital Geological Map MASON2013.1, scale 1:24,000.

Brezinski, D.K., 2014, Geologic and karst features map of the Williamsport quadrangle, Washington County, Maryland: Maryland Geological Survey Digital Geological Map WILL2014.1, scale 1:24,000.

Brezinski, D.K., and Bell, S.C., 2009, Geologic Map of the Funkstown quadrangle, Washington County, Maryland: Maryland Geological Survey Digital Geological Map FUNKSGEO2009.1, scale 1:24,000.

Brezinski, D.K., and Fauth, J.L., 2009, Geologic map of the Myersville and Maryland portion of the Smithsburg quadrangles, Washington and Frederick Counties, Maryland: Maryland Geological Survey Digital Geological Map MY_SM2009.1, scale 1:24,000.

Brezinski, D.K., and Glaser, J.D., 2014, Geologic map of the Clear Spring and Hedgesville quadrangles, Washington County, Maryland: Maryland Geological Survey Digital Geological Map CL_HE2014.1, scale 1:24,000.

High angle reverse fauls
(Rectangles on upthrown side)

Thrust fault
(Sawteeth on upthrown side)

Generic fault
U D
D=Downthrown side
U=Upthrown side